FLEXURAL-SHEAR RESISTANCE OF PRESTRESSED CONCRETE MEMBERS WITHOUT SHEAR REINFORCEMENT
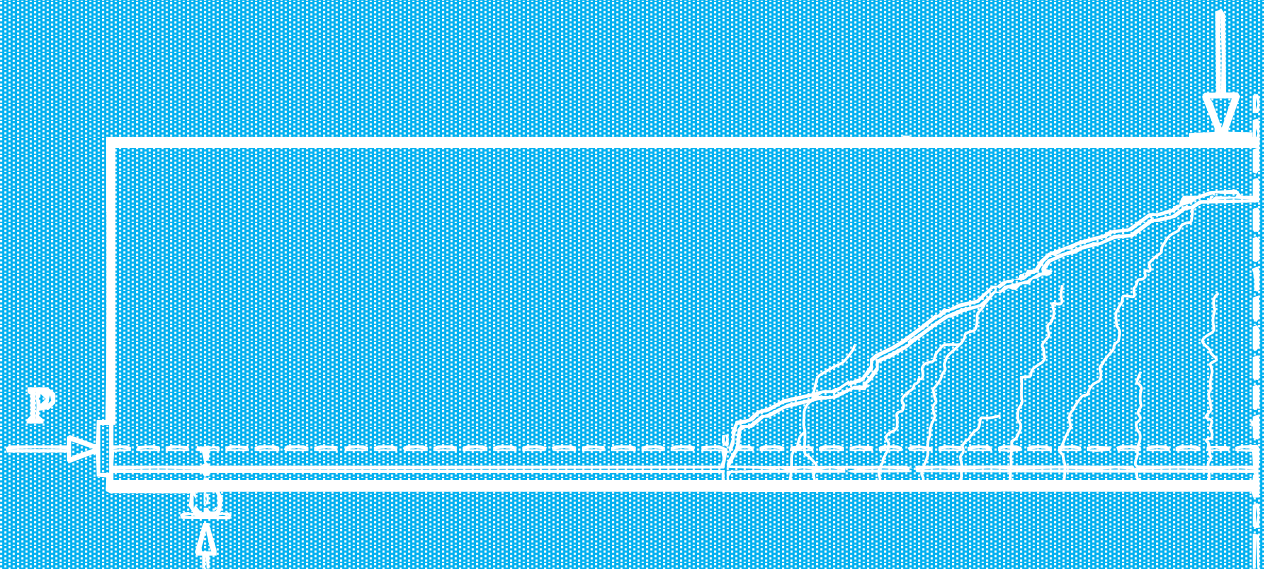
Andrés Germán Vallejos Balladares

2022

TUDelft
Delft University of Technology

Flexural-shear resistance of prestressed concrete members without shear reinforcement

By

A.G. Vallejos Balladares

in partial fulfillment of the requirements for the degree of

Master of Science
in Civil Engineering
Master Track: Structural Engineering

at the Delft University of Technology,
to be defended publicly on Monday March 21st, 2022

An electronic version of this thesis is available at http://repository.tudelft.nl/.

TUDelft

Abstract

To calculate the flexural-shear resistance of prestressed concrete members without shear reinforcement, a method based on Critical Shear Crack Theory (CSCT) has been presented for the new Eurocode (prEN1992). Two alternatives provided in draft 7/2020 (prEN1, prEN2) are the starting point given, and two other alternatives are proposed for analysis by this thesis (prEN3, prEN4). These alternatives and other design codes were evaluated based on the concepts involved, assumptions made, and the results obtained compared with experimental results.

The research started by compiling basic concepts handled by empirical (ACI318-19 or EC2), MCFT-based (AASHTO-LRFD), and CSCT-based (prEN1992) approaches for the calculation of the flexural-shear resistance of members without shear reinforcement. Experimental results of slender prestressed concrete beams without shear reinforcement were collected from the ACI-DAfStb-PC/2015 database, and these tests were classified into subsets according to the relevant criteria used in the different design codes such as type of shear failure or cross-section shape. Subset 1 groups rectangular and I/T shaped beams with flexural-shear failure. Subset 2 retains the rectangular beams from subset 1, and subset 3 filters the tests from subset 2, applying conditions checking for anchorage or flexural failures. In addition, different critical locations were assumed, some according to design code suggestions $(x_r = d \ or \ x_r = a - d)$, and others according to an assumption based on test results $(x_r = 0.65a)$.

The comparative evaluation results of the flexural-shear strength estimated by the different design codes with the experimental results were made for the 3 subsets and 3 critical locations defined. From this data set, the critical location $x_r = a - d$ was chosen as the appropriate based on a general evaluation of the precision acquired by the approaches and the higher flexural stresses present. Then the data for the 3 subsets at this location are captured and presented in a range from lowest to highest from here on.

Based on the results, it was concluded that AASHTO-LRFD and prEN1 are the most precise approaches with COV less than 0.25. However, AASHTO-LRFD tends to obtain very conservative results. ACI318-19M has the worst performance in terms of precision with COV in the range of 0.29 to 0.45, its approximate method tends to get results below the desired level of safety, and its detailed method tends to be more conservative. EC2 achieves a regular precision with COV between 0.28 and 0.31, the linearized alternative for the new Eurocode (prEN2) obtains similar COV values ending up with a regular precision as well, and both approaches have a good level of safety.

To improve prEN2, new alternatives (prEN3 and prEN4) were derived based on the linearization of the main failure criterion of the CSCT. Of the alternatives, prEN4 was the most precise (COV=0.25-0.26) with a good level of safety, recognizing that this alternative correctly applies the concept of prestressing as preload and incorporates the effect of the normal loads on the shear strength with a direct relationship dependent on the ratio d/a_{cs}, where $a_{cs} = |M_{Ed}/V_{Ed}|$. Finally, all approaches were tested in terms of usability in design cases for simply supported and continuous slab decks, concluding that prEN4 has a significant advantage in usability since it is an expression similar to the one used in the current EC2, and also obtains results that are on the safe side compared with a more precise approach like prEN1.

Alternative 4 (prEN4) is an approach with good accuracy and safety level, and can incorporate the effect of prestress on shear resistance straightforwardly and consistently, complying with the main assumptions of the CSCT and the assumption of prestressing as a preload indicated for the Eurocodes, thus incorporating only the influence of normal loads applied to the neutral axis to contribute to the shear resistance. prEN4 is also an approach that has been shown to capture the influence of all parameters considered to obtain a reliable estimation of the flexural-shear resistance; therefore, it is recommended to consider it as a potential alternative for a handy and reliable calculation of the flexural-shear resistance of beams without shear reinforcement.

Acknowledgements

Sow a thought and you reap an action;
sow an act and you reap a habit;
sow a habit and you reap a character;
sow a character and you reap a destiny

— *Ralph Waldo Emerson*

This work would not have been possible without the valuable guidance of the assessment committee members, led by Yuguang, who guided and supported me in the toughest moments completing this work. Eva, Gerrie, and Max, with their experience and exceptional knowledge, pushed me to improve this work and helped me to visualize my mistakes. Thank you all very much for your time invested and patience during all this time.

As this document marks the end of a stage, I would like to conclude by first thanking my friend, the carpenter, for the many lessons. To my family, to whom I owe everything. Victoria, despite the distance, I carried you with me every day, hoping to pave your way. I will also be forever grateful to my parents, who are my unconditional support all the time. None of this would have been possible without the help and trust they gave me from the beginning. Also, thanks to my sisters and family members who were looking out for me during this time.

I do not want to finish without mentioning my friends with whom I shared beautiful moments. This experience was complemented by the particularities of the people I have met from different cultures and mindsets. I will always remember them fondly and hope that everyone can find true happiness in life by discovering their place and purpose in this world and enjoying the wonderful journey we call life.

When wealth is lost, nothing is lost;
when health is lost, something is lost;
when character is lost, all is lost.

— *Billy Graham*

CONTENTS

1 INTRODUCTION

Research of the failure of prestressed concrete beams without shear reinforcement has given rise to a wide variety of proposals that are the subject of ongoing debate since, for the time being, there is no universally accepted method to compute the shear strength/capacity of reinforced and prestressed concrete members without shear reinforcement. The difficulty of this problem is immersed in the heterogeneous structure of concrete, a multiphase granular material formed by irregularly shaped aggregate particles of various sizes, embedded in hardened cement paste. This heterogeneous structure causes the concrete to deform non-linear and time-dependently under sustained loading [1].

Over time, shear resistance of concrete was estimated employing semi-empirical expressions that today may not be well adapted to commonly used structural configurations. Most of the design codes used have calibrated their analytical models from a database of mainly simply supported beam tests with point loads, which may not represent the structural configurations commonly used today. Furthermore, incorporating the effect of prestressed forces in the proposed expressions is sought in a theoretically justified manner.

In recent years, by implementing modern measurement techniques in experiments, e.g., the digital image correlation (DIC) technique, it has been possible to advance in the study of the topic and investigate the process of failure and phenomena. Several mechanical models proposed and successfully applied lead code provisions, although there is still no agreement on the phenomena and parameters governing the shear capacity, in part due to different interpretations.

The influence of prestressing, and other parameters such as beam height, aggregate size, longitudinal reinforcement ratio, and other parameters are being investigated to determine their role and contribution to shear strength [2]. For this purpose, efforts are being made to increment the available experimental tests on prestressed beams with different setups.

At the moment, there are different theories such as the Critical Shear Crack Theory (CSCT) and Modified Compression Field Theory (MCFT) that are currently being used in design codes to calculate with a physical-based background the shear strength of members without shear reinforcement. For the proposal for the new Eurocode, CSCT based approaches are being generated to improve the current empirical method used. Nevertheless, it is necessary to have simple formulations uniform for prestressed and non-prestressed concrete members, then the straightforward inclusion of prestressed effect on shear resistance calculation will be investigated in the present document.

1.1 BACKGROUND

Design evaluation of shear resistance depends on the application or non-application of shear reinforcement in prestressed concrete elements. There are theories based on equilibrium like strut-and-tie models and stress fields applied when shear reinforcement is present. Conversely, shear resistance for a prestressed concrete element without shear reinforcement provided in shear design codes has been empirically derived or validated, differing from each other depending on the parameters considered.

The current Eurocode (EN1992-1-1:2004) design procedure is based on expressions derived empirically from tests (simply supported beams under point loads typically), which makes it unsafe when it is applied outside the ranges for which the parameters were calibrated. The current approach does not take into account the influence of aggregate interlock, the effect of shear span-

to-effective depth ratio, underestimates the influence of the size effect, and considers linearly (addition of $k_1\sigma_{cp}$) the effect of prestressing over the shear resistance of concrete.

In recent decades, theories such as the critical shear crack theory (CSCT) or the modified compressive field theory (MCFT) have emerged, which have benefited the upgrading of design codes from empirical models to approaches based on physical models that logically represent the mechanics of failure. However, there is currently no generally accepted theory or physical model that explains the response of elements without shear reinforcement.

The critical shear crack theory estimates the crack width as a function of the longitudinal strain of reinforcement in the shear critical region, which provides the basis for evaluating the shear resistance of members without shear reinforcement. Recent research demonstrates the potential applicability of this theory in the design equations for standards applied to the design of concrete structures. For this reason, this theory is the proposed basis to be used for the second generation of the Eurocode. Current Swiss code SIA 262 is based on the CSCT failure criterion and other standards like AASHTO LRFD and CSA based their formulation on a general theory as the modified compression field theory (MCFT) with good results in its implementation to practical cases.

With the trend in the scientific community exposed, the applicability of the approaches based on the CSCT will be evaluated, and the influence of normal forces or its effect on some important parameters like the longitudinal reinforcement strain will be assessed. The presence of prestressing force in beams is common, and the effect of design codes modification on current structures has to be evaluated in the same way once there is a clear picture of the practical formulation that can be applied as a standard. The results of different proposals to consider the influence of prestressed forces will be assessed, comparing them with experimental results from the "*Deutscher Ausschuß für Stahlbeton (DAfStb H.617): ACI-DAfStb Shear databases 2015*" [3].

It should be noted in the same way that these types of changes in the current regulations could leave some structures marked as unsafe. Therefore, the impact on the security of the new proposals must be evaluated to take preventive measures or warn on time about risky situations. Last but not least, the usability of the proposed design method should be rated according to its simplicity, range of application, necessary parameters, and versatility.

1.2 AIM OF THE STUDY

Research question and scope

- **Research question**
  *How can **prestressing force influence** be taken into account to estimate the **flexural-shear resistance** of **members without shear reinforcement** straightforwardly, with an approach based on **Critical Shear Crack Theory (CSCT)**?*

According to the issues mentioned before and the research question presented, the following objectives should be accomplished:

- Develop the theory related to the mechanical model for shear transfer in flexural-cracked prestressed concrete members and review the application of the Critical Shear Crack Theory (CSCT) and Modified Compression Field Theory (MCFT) for this problem.

- Remark the primary assumptions made within the CSCT to analyze the influence of normal forces in the scope of the CSCT.

- Evaluation and development of the shear design of members without shear reinforcement subjected to prestressing loads according to current standards such as ACI, AASHTO-LRFD, and Eurocode.

- Evaluate the provided design procedure proposed for the 2nd generation of Eurocode in terms of usability, and explore improvements based on a coherent assumptions and simplifications based on theory and experimental results.

- Assess the design method proposed in typical case studies and estimate possible consequences of the proposal on current structures.

1.3 OUTLINE OF THE STUDY

The methodology to be pursued starts with the literature review of two theories that will underpin this study and are comparable, the CSCT and MCFT theories. At the level of design models, the most commonly used design codes such as ACI, AASHTO, and Eurocodes will be compared with the experimental database from ACI-DAfStb for prestressed beams without shear reinforcement with a focus on the results obtained for the proposal made for the new Eurocode.

It is necessary to classify and present some information related to the experimental database; then, one chapter will be dedicated to this purpose.

The comparison results will show specific indicators regarding the performance of the new Eurocode proposal concerning the experimental results and the other design codes. The aim is to identify the best performances for the case of prestressed beams without shear reinforcement and point out the points where improvements can be made in the new proposal for the Eurocode in terms of usability, precision, accuracy and consistent derivation based on theory. Usability will be evaluated by applying the different design codes in practical cases.

Figure 1-1 Structure of the methodology

2 LITERATURE REVIEW

2.1 SHEAR FAILURE OF PRESTRESSED CONCRETE MEMBERS WITHOUT SHEAR REINFORCEMENT

Although there is no consistent definition of shear capacity in prestressed and reinforced concrete beams without shear reinforcement, despite the initiatives carried out the last years, its phenomenological definition is accepted as a brittle failure with diagonal cracks developing in the span.

Shear cracks are generated depending on the magnitude of the principal tensile stresses within the beam cross-section. These principal stresses depend on the applied external forces and the prestress force applied in the case of prestressed beams. In case of straight tendons, the influence of the compressive force (N) introduced by prestress reduces the tensile flexural stresses ($f_x = f_i - N$), and in case of curved tendons the vertical shear caused by external loads is reduced if the vertical component of prestressing force acts in the opposite direction.

The orientation of the principal stresses and their magnitude along the beam height changes as a function of the resulting shear and flexural stresses acting on the beam after prestressing (scheme of analysis in Figure 2-1). The different configurations that can occur due to cross-section shape, prestressing force magnitude, web width, etc. lead to different types of cracks and failure modes that will be detailed in the following sections.

Figure 2-1 Principal stresses, and resulting shear and flexural stresses acting on beam after prestressing [4]

It is worth mentioning that most beams contain stirrups, but not in all cases these stirrups are considered effective shear reinforcement. This "nonconforming shear reinforcement" is considered as such because it does not meet the various design requirements and its contribution to the shear resistance is neglected. Therefore the beam is considered without stirrups for analysis [5], hence the non-shear-reinforcement case is important for assessment.

2.1.1 Types of cracks for beams without shear reinforcement

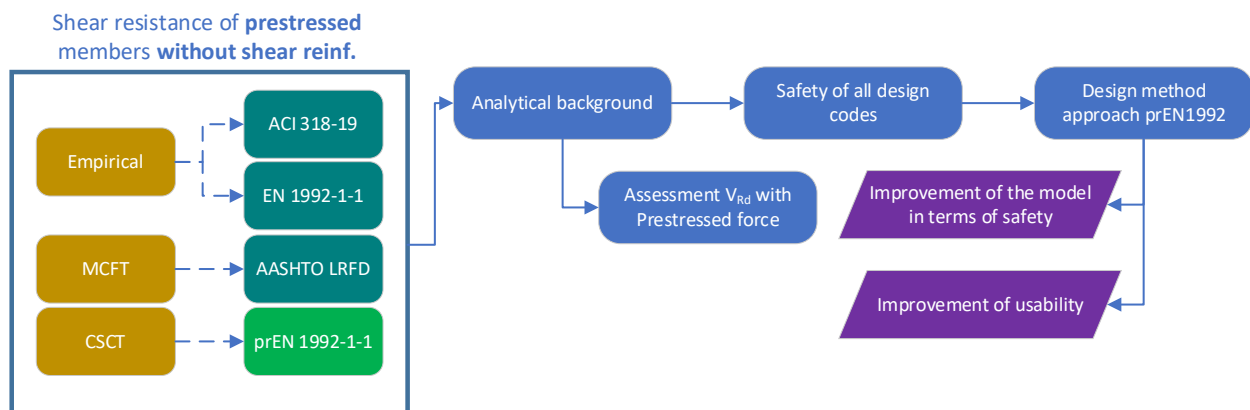For beams without shear reinforcement three types of cracks are defined as follow and are shown in Figure 2-2 [4].

- ***Flexural cracks***, which develop almost perpendicular to the longitudinal axis of the beam. These appear in regions with small shear stresses and dominant flexural stresses which are almost equal to a horizontal principal stress. The initial cracks widen and extend deeper toward the neutral axis and beyond with the increment in deflection of the beam.

- ***Flexural-shear cracks*** start as fine vertical flexural cracks on the tensioned fibers of the cross-section in regions with high flexural and shear stresses. These cracks rotate their inclination as they approach the centroidal axis of the beam where the highest shear stresses occur. This is caused by the rotation of the direction of the principal stresses influenced by the increasing shear stresses near the centroidal axis (Figure 2-1).
  In literature one can find different denominations of a flexural-shear crack like critical inclined crack, inclined flexural crack or critical shear crack, but all of them are pointing to the same thing. Also different authors have varied definitions for this type of cracks, like e.g. definition given by [6], a flexural crack with two secondary branches, one approaching the support at the level of the reinforcement in tension and the other approaching the point of maximum rotation in the compression zone.

- ***Web-shear (shear-tension) cracks*** are assumed to occur in regions not cracked by flexural stresses (without flexural cracks). These cracks initiate in the web when the principal tensile stress is equal to the maximum tensile strength of the concrete. This type of crack does not depend on the formation of flexural cracks in the tensioned fibers and the related type of failure is the most brittle one. These cracks usually appear in regions subjected to high shear and low bending, like e.g. in continuous prestressed concrete beams near points of contraflexure [7].
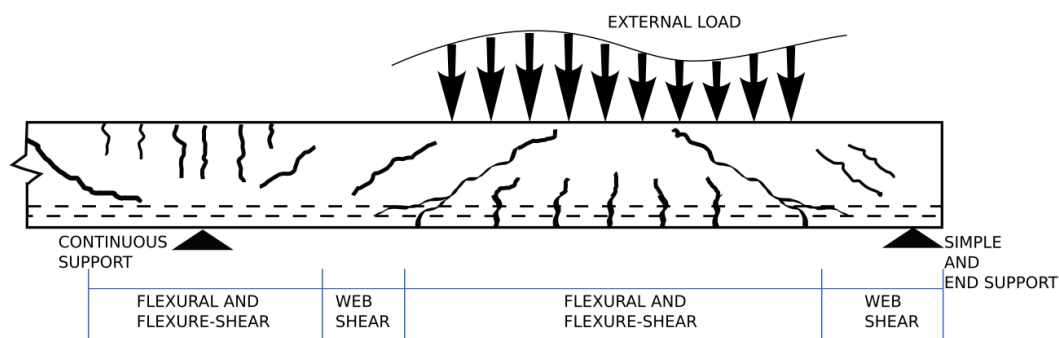

Figure 2-2 Types of cracks [4].

2.1.2 Shear failure modes in prestressed concrete members without shear reinforcement

Flexure-shear failure, shear-compression failure and shear-tension failure are considered the main shear failure modes for members considered without shear reinforcement, and these are going to guide the classification of the experimental database from ACI-DAfStb [3] afterwards.

Flexural-shear failure is related to the type of crack called equal; the dominant load transfer mechanism consists of variable internal forces acting over a constant lever arm. This failure mode is dominant in beams with large spans and the maximum shear forces related to its load transfer mechanism are usually lower than those found with the other load transfer mechanisms.

Shear-compression failure is the most violent and erratic mode of failure with several failure mechanisms, one can observe crushing of the concrete before failure. It occurs when the beam fails by crushing of the concrete at or near the top of the flexural-shear crack, a zone with high concentrated compression stresses. A characteristic of a shear-compression failure is that the load is carried mainly by direct compression struts, a common case when the flexural-shear crack arises close to the support when point loads are located close to supports. Within the load transfer mechanism formed in this case, the shear transfer action of the aggregate interlocking

has a minor contribution and this allow the load being transmitted by direct compression struts (more information about shear-transfer actions in section 2.2)

Last two failure modes are dependent on the development of the flexural-shear crack, and it is not always possible to predict whether the failure mode may be flexural-shear or shear-compression, the difference between these two failure modes is usually substantial [6].

To distinguish in some way members subjected to shear-compression failures from those more susceptible to flexural-shear failure the ratio between the shear span-to-effective depth ratio a/d and the shear slenderness M/Vd can be used [6], with the help of the "Kani's valley" explained in section 2.2.5.

Shear-tension failure is related with the called "diagonal tension cracks" that are known in this document as shear-tension cracks. Already mentioned the origin of this failure mode in the definition of the related type of crack, it can be added that the anchorage and bond conditions that usually occur in the region close to the support for prestressed concrete beams increase the likelihood of this type of failure. Beams with I or T cross-section are more susceptible than rectangular beams when they have thin webs that concentrate shear stresses in the web. Three types of failure initiated by a shear-tension crack can be distinguished (i) failure due to a single crack that tends to develop from the support to the point of loading (ii) failure due to the formation of multiple shear-tension cracks (web distortion) and (iii) failure due to the formation of multiple shear-tension cracks (web distortion) followed by crushing of the compression flange below the point of loading [5].

Other classifications can be found in literature, according to [8] shear failures can be subdivided in two categories, failure by shear-compression and failure by distress in the web. Distinguished according to whether or not the specimen loses its bearing capacity when the critical inclined crack occurs.

In case of members with shear reinforcement, another important shear failure occurs when the compressive strut fails in compression, failure identified as diagonal compression shear failure due to high compressive forces concentrated in thin webs mainly.

With the theory developed up to this point, as a summary, the different failure modes for *prestressed concrete members without shear reinforcement* can be grouped according to the type of crack and moment-shear ratio related, as is shown in the following Figure 2-1.

Table 2-1 Failure mode of members without shear reinforcement, related with type of cracks and moment-shear ratio

Failure mode	Type of crack	Moment-shear ratio
Shear-tension failure	Diagonal tension crack (shear-tension crack)	Low moment / High shear
Flexural-shear failure	Flexural-shear crack	High moment / High shear
Shear-compression failure		

It may also be desirable to detail other observations that better report the damage suffered by the beam until failure during the experiments, to consider other factors in the beam failure mechanism. For example, if the beam shows signs of horizontal shear damage, such as sliding shear failure at the interface between the web and flange in tension. Or, damage in the anchorage zone, representing damage in the prestress transfer lengths, such as strand slip or failure of the bond between the concrete and the strands. These observations are important for I-beams especially, where according to the aforementioned, certain group of tests can be selected to analyze particular types of failures.

2.2 SHEAR-TRANSFER ACTIONS FOR FLEXURAL SHEAR

Analysis of reinforced concrete beams without shear reinforcement can be done with the theory of elasticity prior to crack development. But for after cracking case it is more complicated, some approaches estimate the shear strength on the basis of the concrete tensile strength, others on the basis of fracture mechanics concepts, a number based on the upper-bound theorem of limit analysis with some modifications to account for the presence of concrete cracking, and some approaches account for various potential shear-transfer actions like the Critical Shear Crack Theory [9]. Although the shear-transfer actions, strain and size effects are taken into account in different manners within the different models the design expressions consider similar parameters with equal influences at the end [10].

The shear-transfer actions will be studied in detail one by one in subsections of section 2.2, and can be seen in their relative position within a reinforced concrete beam with bottom longitudinal reinforcement in the free body diagrams of Figure 2-3 and Figure 2-4. Depending on the location, shape and kinematics of the critical shear crack leading to failure the contribution of the different shear-transfer actions may vary. Once flexural cracks propagate from the tensioned fibers toward the centroidal axis some shear-transfer actions can develop [11], [9]. These shear-transfer actions are commonly classified into beam shear-transfer actions and arching action, being shear resistance in most of the cases the combination of these two mechanisms. Beam shear-transfer actions as compression zone capacity (cantilever action), aggregate interlock, dowel action and residual tensile strength of concrete, allow varying the force in the flexural reinforcement and carrying shear keeping constant the lever arm between the tension and compression chord. Conversely, arching action (section 2.2.5) allows carrying shear keeping constant the force in the flexural reinforcement [12].

It is observed, and explained later in section 2.2.5, that arching action is the dominant shear-transfer action for one-way slabs or beams with limited shear span-to-effective depth ratio ($a/d<2.5$), members with unbonded longitudinal reinforcement, and prestressed members having large compressive normal forces. On the other hand, beam shear-transfer actions are known to predominate in the case of slender members without shear reinforcement, although the scientific community disagrees on the predominant shear-transfer action and the phenomena governing the shear capacity [9].

To prove the last statement, Taylor was one of the first to calculate the contribution of each of the shear-transfer actions to the shear capacity of a slender cracked concrete member without shear reinforcement. He concluded in this study that the contribution of the aggregate interlock is predominant carrying 35% to 50% of the total shear force applied in the section, the contribution of the dowel action varies between 15% to 25% and the compression zone carries between 20 to 40% of the total shear force. The only detail that was not considered in Taylor's study was the residual tensile strength of concrete contribution [12].
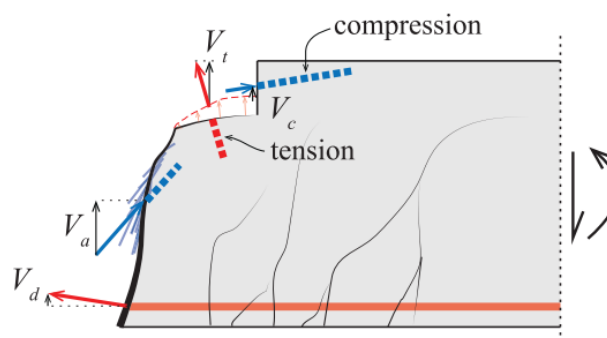

Figure 2-3 Potential shear-transfer actions for reinf. concrete elements without shear reinforcement: Aggregate interlock (V_a), residual tensile strength (V_t), contribution of inclination of compression chord (V_c), and dowel action of longitudinal reinf. (V_d) [13]
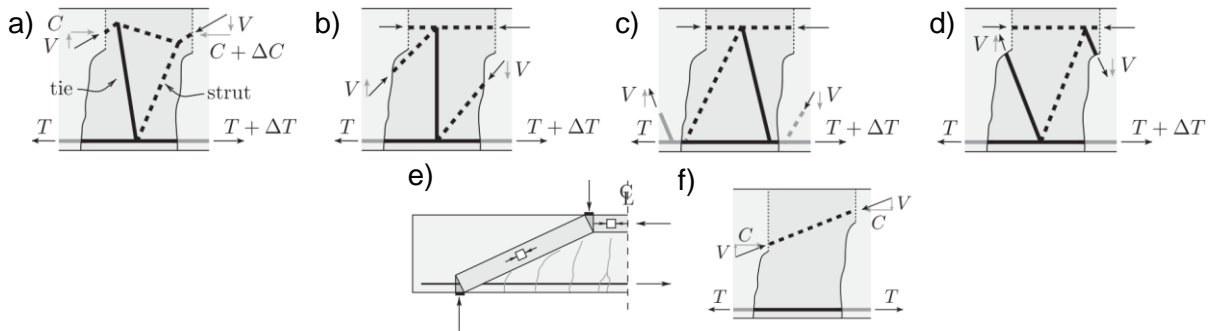
Figure 2-4 Strut and tie models (tensile force – solid lines, compressive force – dashed lines) for shear-transfer actions: (a) compression zone capacity; (b) aggregate interlock; (c) dowel action; (d) residual tensile strength of concrete; (e-f) arching action [10].

The work developed by Taylor applies to reinforced concrete beams and is helpful to have an initial look, but for the case study of this document, it is necessary to analyze the shear behavior of post-tensioned concrete beams. Understanding the work done by P. Huber ([14], [15]) can give some guidelines of what happens. First, the prestressing results in the addition of the vertical component of the prestressing force (V_p), and the vertical component of the additional tensile force (ΔV_p) in inclined tendons due to applied loads. The value of ΔV_p depends on the crack width, and the total contribution of the vertical component of the prestressing force depends on the tendon's angle of inclination.

According to the test results on post-tensioned beams without shear reinforcement, shear-transfer actions like of aggregate interlock (V_a) and residual tensile strength (V_t) are negligible because the critical shear crack is quite wide, and minimal crack sliding occurs. The prestressing force in the principal stress directions causes the crack angle to be reduced, thus reducing the influence of V_a from 35% to 50% for reinforced concrete members to practically zero for prestressed concrete members. The residual tensile strength (V_t) contribution is not relevant because it was observed that the length over which residual tensile stresses are transmitted is too short. The dowel action's contribution (V_d) depends on the effective width between the individual longitudinal bars, and its contribution varies between 5% to 20%, being too small in regions near end supports. The contribution of the compressive zone (V_{cc}) is important for post-tensioned beams due to the relevance of the arching action. The contribution of V_{cc} of the total shear capacity is between 25% and 60%, with high contribution for regions near intermediate supports for continuous beams. Finally, the contribution of the vertical components of the prestressing force $(V_p + \Delta V_p)$, depends on the effective prestress force applied and the inclination of the harped tendons, noting a collaboration in a range between 3-16% of the total shear force.
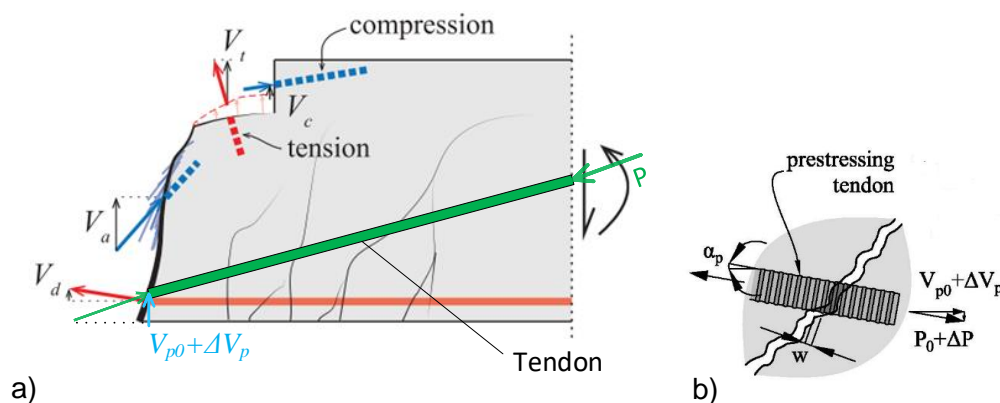

Figure 2-5 a) Free-body diagram of the possible shear-transfer actions acting in a post-tensioned beam b) Breakdown or detail of the vertical component of prestressing force [14]

2.2.1 Compression zone capacity (Cantilever action)

The first observation was made by Kani [16], noting that the formation of flexural cracks transformed the reinforced concrete beam into a comb-like structure (Figure 2-6). The area in compression related to the comb backbone, and the area in tension treated as the "concrete teeth", each tooth separated from each other by the flexural cracks. With this analogy, the stresses in the compressive zone increase rapidly during the bending process due to the decrease of its area as a result of cracking. With cracks, the shear stress is supported by the inclined compression chord, and its strength is limited by the development of the vertical flexural crack into a quasi-horizontal crack, which disables the tension tie of the tooth [10].

Figure 2-6 Comb-like structure defined by Kani [12]

The contribution of the compression zone to the shear resistance depends on the depth of the uncracked concrete (c), the most important parameter in this case. The evaluation of the depth of the compression zone can be done by using sectional analysis considering force equilibrium and strain compatibility conditions of the cross-section (Figure 2-7).

Figure 2-7 Strain and stress distribution of a prestressed concrete beam [17]

Because the depth of the compression zone is small for slender members without axial compression, most codes neglect its effect on shear capacity. For slender prestressed beams, the capacity of the compression zone mostly depends on its depth and the capacity of the concrete in compression. This is because the prestressing force reduces the inclination of the cracks, increases the depth of the compression zone, and generates a higher compressive force that must be transmitted [18].

2.2.2 Aggregate interlock

Aggregate interlock refers to the ability to transfer shear force between the two faces of concrete separated by a crack through contact between the aggregates and the opposite face. Its mechanism is related to the way cracks form in concrete, since the strength of the hardened cement paste is lower than that of the aggregate particles in most cases, the cracks intersect the cement paste but border the edges of the aggregate particles. The mechanism is then formed by the aggregate particles extending from one side of the crack, "interlocking" with the opposite side to resist shear displacement.

Experiments conducted in the past have shown that the shear forces across cracks induce normal and tangential displacements that generate normal and shear stresses between the crack faces. Based on these observations, Walraven [19] concluded the existence of an interrelation between crack width, crack slip, normal and shear stresses. It was also highlighted and clearly demonstrated the relevance of aggregate interlocking to the shear resistance of a cracked beam. Experiments reported by Walraven [19] demonstrate the plastic behavior in general of the aggregate interlocking due to the plastic behavior of the cement paste in compression and friction.

Furthermore, failure of the aggregate interlock cannot produce the sudden opening of an inclined crack from an existing flexural crack. This can be only possible when lateral confinement on the crack is released (dowel action) to cause a sudden loss of aggregate interlock [6].

The strength of this shear-transfer action depends on the crack opening (w) and the relative slip of the crack (δ) as shown in Figure 2-8, with contact stresses developed in normal and tangential direction as shown in Figure 2-4-b. The crack opening, the roughness of the contact surface (influenced by the aggregate size and shape of the crack) and the degree of slip (δ) between the lips of the crack are the factors that limit the strength of the aggregate interlocking [10].
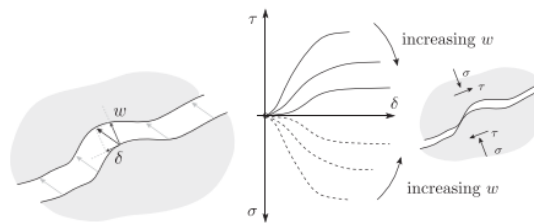
Figure 2-8 Aggregate interlock: (a) kinematics of a shear crack with relative components of opening (w) and slip (δ); and (b) contact stresses [12]

2.2.3 Dowel action

It is the ability of the longitudinal bars to transfer forces perpendicular to their axis. Longitudinal bars can act as dowels between the lips of a crack to transfer shear forces, an action that is efficient where spalling cracks cannot develop in concrete (short-span beams where critical shear crack develops near bearing plate or when it develops through the compression reinforcement). In case spalling cracks can develop parallel to the longitudinal reinforcement (Figure 2-4-c) as in case of slender beams without shear reinforcement, the dowel action decreases and it is even negligible. Therefore, it can be concluded, for members without shear reinforcement, that the dowel capacity decreases as the strain in the longitudinal reinforcement increases [10].

Available experimental investigations identified that the bar diameter, the tensile strength of concrete, the concrete cover, the net width and the strains in the longitudinal reinforcement bars are the main parameters governing the dowel action. Nevertheless, there is no consensus on the relative importance or influence of each parameter on the dowel capacity, in this way, there are several proposed models that consider different parameters in a particular way [12].

2.2.4 Residual tensile strength of concrete

Once the concrete cracks, it allows a certain amount of tensile stresses to be transferred across the cracks, and tension ties develop through them. The residual tensile stresses at the crack tip of the critical shear crack transfer the shear forces, this crack tip is located in the so-called fracture process zone (FPZ) in which a crack can transfer stresses until it reaches a certain maximum width [10] (< 0.1 mm. [20]).

The softening behavior that the concrete exhibits once it cracks was firstly measured by Evans and Marathe [21], who highlighted the importance of understanding the stress-strain curves for concrete elements subject to tension loads to obtain more information about the mode of failure of concrete and the phenomenon of redistribution of stresses in certain regions.

The Fictitious Crack Model developed by Hillerborg [22] to study the behaviour of concrete in tension is used commonly in fracture mechanics. It assumed that at certain peak load within a narrow zone of micro-cracks the strains start to localize (process zone, point 1, Figure 2-9). Once micro-cracks grow, a crack develops but stress transfer is still possible through the crack (points 2-3, Figure 2-9). Concrete has no capacity to transfer stresses once crack opening is larger than the limit width (point 3, Figure 2-9).
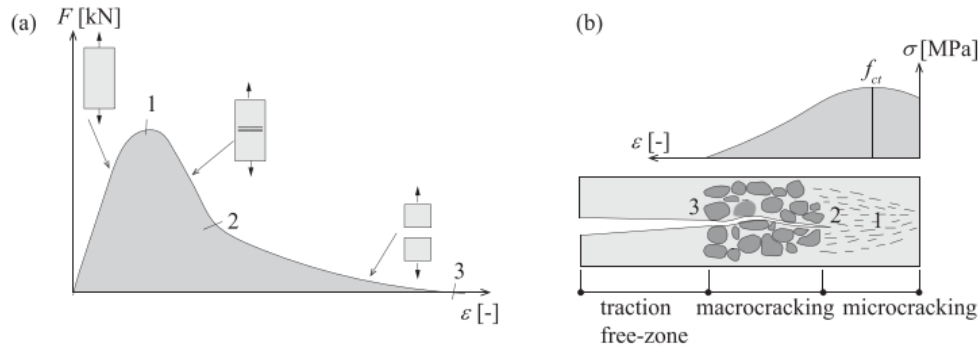
Figure 2-9 (a) Tensile load-deformation response of a concrete specimen; (b) illustration of the fracture process zone around the tip of the crack: micro-cracks (1-2), micro-cracks merge into a macrocrack in the softening region after the tensile peak [12]

2.2.5 Arching action

Arching action refers to the compressive force that is transmitted directly from the point of application of the external force to the support. In contrast to the last 4 beam shear-transfer actions that allow variation in the force for the tension reinforcement according to the bending moment, in this case it is assumed a constant force in the flexural reinforcement and shear is carried by an inclined compression strut as shown in Figure 2-4-e [12].

The plasticity-based arching action was found in agreement with observed test results for short-span members. In case of slender beams without shear reinforcement, flexural cracks potentially develop across the theoretical compressive strut limiting its strength, resulting in a plastic solution that overestimates the actual strength. This influence of the slenderness on the governing shear-transfer actions can be presented with the "Kani's valley" shown in Figure 2-10. Arching action governs for deep beam and the shear carried is equal to the plastic strength. For slenderness between $(\gamma_1 < \gamma < \gamma_2)$ cracks penetrate within the strut reducing its capacity. For larger slenderness $(\gamma > \gamma_2)$ the arching action develops in combination with the other shear-transfer actions, the members fail again in bending now that beam shear-transfer actions offer enough shear strength.
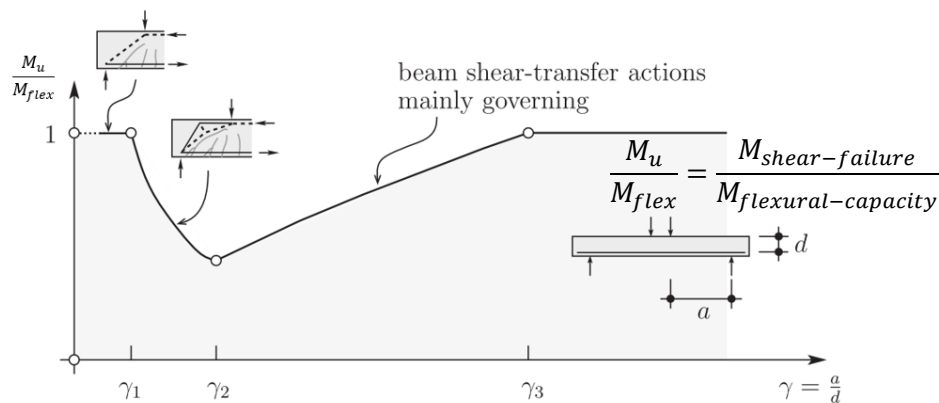

Figure 2-10 Kani's valley: governing shear transfer actions as function of shear span-to-effective depth ratio [23]

The analog truss that models the concrete behavior will be influenced by introducing a compressive strut from the prestressing force applied on the lateral face of the beam, close to the

support. For straight tendons, the truss develops from the point of application of the point load to the intersection point between the vertical and horizontal guidelines formed by the reaction force of the support and the applied prestressing force (Figure 2-11-right). In the case of curved tendons, the inclination of the strut will be less (Figure 2-11-left), and the vertical component of the prestressing force can reduce the acting shear force if it acts in the opposite direction of the applied external load [24].
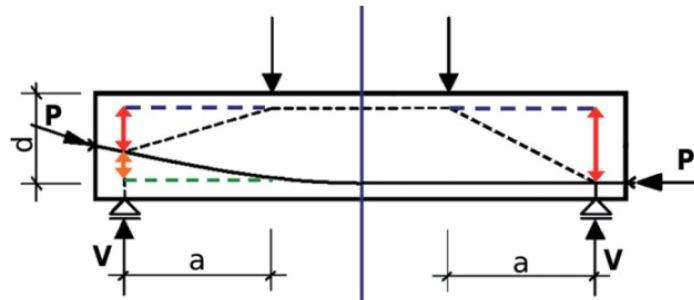
Figure 2-11 Influence of prestress force on analogous truss [24]

The ties formed near support and prestressing introduction points suggest the formation of cracks in this region. Furthermore, the introduction of compressive stresses influences the mechanism of flexural-shear failure reducing the width of the flexural cracks and increasing the compression zone height. Consequently, the compressive struts carry high compressive forces, and the arching action tends to dominate for higher ranges of shear slenderness.

2.2.6 Parameters influencing shear resistance of prestressed concrete

Certain parameters have been identified as having a significant influence on the contributions of the shear resistance mechanisms. *The one with more influence are going to be treated in detail below.*

1. **Concrete strength**

   The governing parameter for most design codes is the tensile strength of the concrete, which governs the crack width and the ability to transfer shear forces. In design codes is common to relate the concrete tensile strength with concrete compressive strength (f_c) which is the main information about concrete obtained in common practice. Some codes as Eurocode correlates the tensile strength of concrete with $f_c^{1/3}$, whereas ACI318-19 adopt relations with $f_c^{1/2}$, the differences seem to be negligible although has been demonstrated that $f_c^{1/2}$ is the most appropriate [11].

   The shear strength of members without shear reinforcement is strongly dependent on this parameter, on the critical shear crack width and on shear crack plane roughness as reflected in CSCT described in section 2.3.1. [18].

   The strength of concrete is directly related with the height of the compression zone and the shear-transfer mechanism described in section 2.2.1 (Compression zone capacity). The higher the compressive strength of the concrete, the lower the necessary height of the compression zone required to reach equilibrium.

   In case of high strength concrete, as the cement paste matrix becomes stronger than aggregates the crack results in a straight crack through the aggregates instead of a rough crack along the surface of the aggregates, thus for this reason the aggregate interlocking capacity could decrease.

2. **Longitudinal reinforcement ratio**

   In this case the Kani's shear failure valley will be mentioned again, referring to the "valley of diagonal failure" diagram shown in Figure 2-12 where it is plotted for different longitudinal reinforcement ratios ($\rho_l = A_s/A_c$). As it can be seen, the valley decreases with lower percentages of reinforcement and practically disappears with percentages lower

than 0.6% in case of steel with $f_y = 400\ MPa$. This indicates that as the longitudinal reinforcement decreases so does the dowel action, because the strains increase in the longitudinal reinforcement bars, reconfirming again what was said at the end of section 2.2.3.
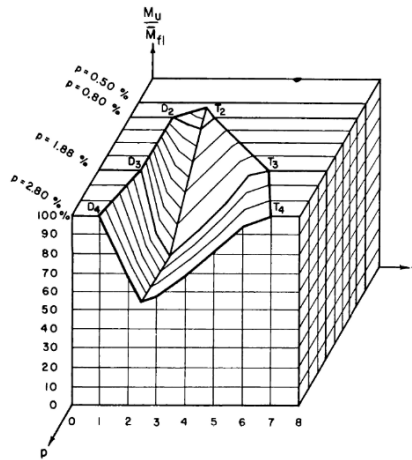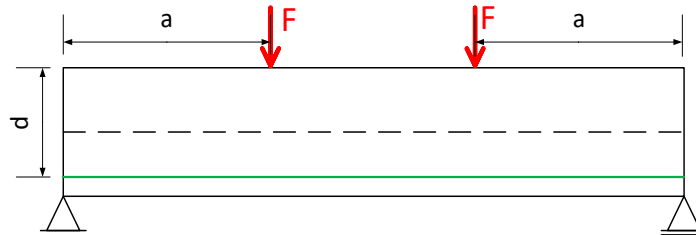

Figure 2-12 Kani's shear failure valley, shear strength as function of a/d and ρ_l (reinforcement ratio)

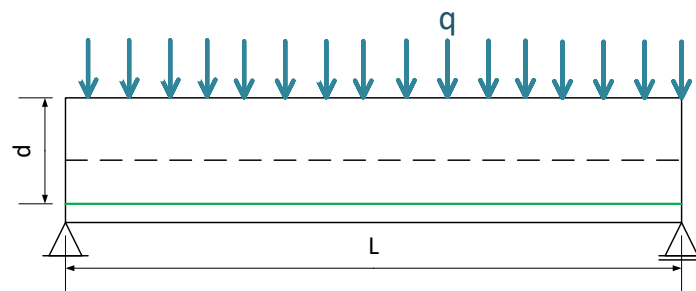3. **Shear span-to-effective depth ratio**

   It is the moment-shear-ratio in relation to the depth of the beam (M/Vd) that can be expressed for different load cases as follow

   o For simple supported members under concentrated loads

$$\lambda = \frac{M}{V \cdot d} = \frac{V \cdot a}{V \cdot d} = \frac{a}{d}$$

   o For simple supported members under distributed loads

$$\lambda = \frac{M}{V \cdot d} = \frac{q \cdot \dfrac{l^2}{8}}{q \cdot \dfrac{l}{2} \cdot d} = \frac{l}{4d} = \frac{a_{eq}}{d} \; ; with\ a_{eq} = \frac{l}{4}$$

This parameter is important for shear strength of slabs or rectangular beams. For members subject to a concentrated load with a/d between 2 and 5, the bending moment is usually the lowest with a relative high shear force. In case of shear span-to-effective depth ratio below 2.5, part of the shear force can be transferred to the support by direct compressive struts (arching action). This may give a parameter to distinguish the failure modes mentioned in section 2.1.2.

In the case of prestressing beams, the compressive forces introduced to the beam favor the arching action's influence and increase the flexural failure capacity of the beam. Then some researchers suggest modifying the range of shear slenderness (a/d) as a function of the prestressing force, incrementing the values stated for reinforced concrete beams due to the influence of the prestressing force into the failure mechanism [25].

4. **Size effect**

   Again Kani, with his work "How safe are our large reinforced concrete beams?" [26], was the first to address this concern and concluded that for reinforced concrete beams without shear reinforcement, the shear resistance decreases with increasing size of the member. Nowadays codes such as ACI318-19 and Eurocode are aware of this into their models. The ACI318-19 code considering its effect for now only for axially stressed beams and not for prestressed beams.

5. **Normal/prestress force**

   In case of prestress force, the effect is positive for the shear capacity because it is going to reduce the width of the shear cracks and increase the height of the uncracked compressive zone. But it is necessary to limit the prestressing forces added because at some point the member can behave in a brittle way. The opposite happens if there are normal forces in tension as it increases the crack width and reduces the shear capacity of the beam.

   To analyze these facts in detail, a simple example might help to illustrate this point.

   Concrete is analyzed before it cracks linearly and elastically, and the beam shear strength depends on the combination of concrete and steel reinforcement for shear integrity, which indicates that concrete must crack to engage the reinforcement. In the same way as non-prestressed concrete beams, prestressed concrete beams rely upon forming a plastic truss when the cracks transfer shear stresses through a series of strut and ties.

   Let's assume a case of a simply supported beam with a concentrated load at midspan and a prestress force at the centroid as shown in Figure 2-13 below.
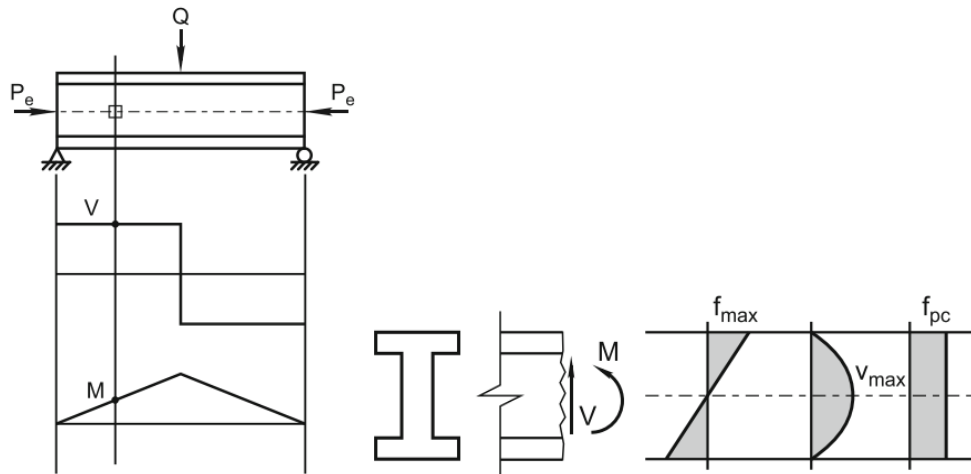

Figure 2-13 Shear and moment diagram for example, with stresses calculated at cross-section analyzed

Assuming the cross-section to analyze in between one support and the point load, and assuming that the concrete remains linear elastic, then the stresses can be calculated as follow:

The flexural stress is equal to

$$f_b = \frac{M \cdot c}{I_g} \ [MPa]$$

Where M is the bending moment, c is the distance of the cross-section analyzed, and I is the second moment of inertia of the cross-section.

The shear stress is equal to

$$\tau = \frac{V \cdot Q}{I_g \cdot t} \ [MPa]$$

Where V is the shear force, Q is the first moment of inertia of the section above the point of interest, and t is the thickness of the section at the location analyzed.

The prestress is equal to

$$f_{pc} = \frac{P_e}{A_c}$$

Where P_e is the effective prestress force applied, and A_c is the area of the cross-section.

Then, the stresses acting at the section's neutral axis can be analyzed using Mohr's circle. If the stresses are computed at their principal orientation, for non-prestressed beams, one finds that the main orientation is at 45 degrees from the beam axis, which matches the crack that would form in the web under this stress state. And if one applies a force in compression the main orientation and crack angle consequently will be reduced as shown in the following Figure 2-14 and as is going to be explained analytically in the next paragraphs.
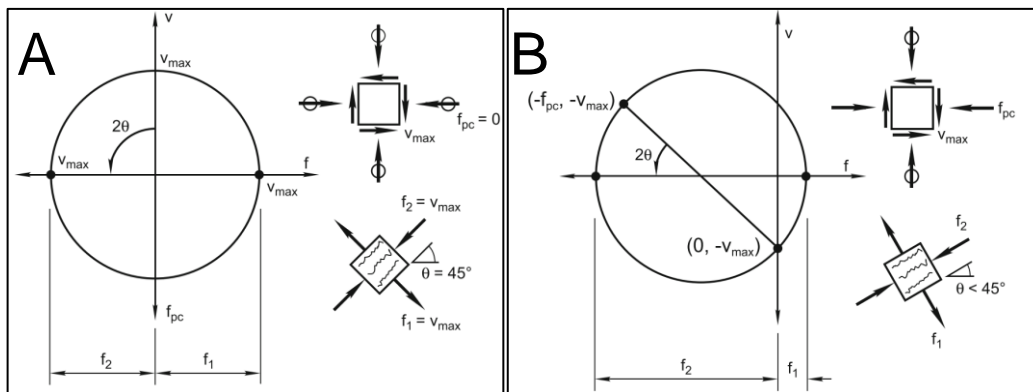
Figure 2-14 Principal stresses at neutral axis for a beam with (A) a prestress force equal zero (B) prestressing

Analyzing the shear stress as a function of the prestress force with the equation stated below and assuming the principal tensile stress equal to the tensile strength of concrete, a plot illustrating the effect of prestress in the cracking formation at the web of the beam can be generated and is shown in Figure 2-15. Based on this graph, when the prestress force is zero, the principal tensile stress equals the applied shear stress. However, the shear required to reach the principal tensile stress increases in the same proportion when prestress force is applied. Consequently, prestress has a positive effect preventing the crack formation increasing their strength.

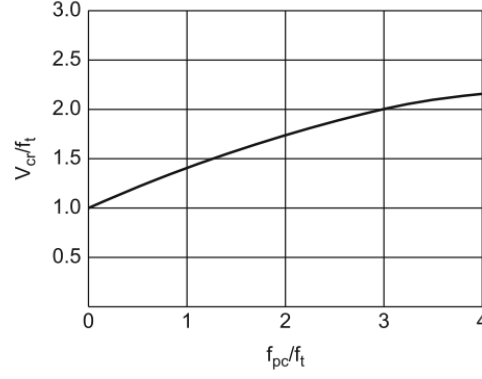$$\frac{\tau}{f_1} = \sqrt{1 + f_{pc}/f_1} \rightarrow \frac{V_{cr}}{f_t} = \sqrt{1 + f_{pc}/f_t}$$

Figure 2-15 Shear stress required for cracking as function of the prestress force applied

Now, to extend the analysis to the effect of prestress on the principal angle and estimate the effect that prestressing might have on the shear crack angle, the equation of the principal angle as function of the prestress and principal tensile strength can be derived as follow.

$$\tau^2 = \left(\frac{f_{pc}}{2} + f_1\right)^2 - \left(\frac{f_{pc}}{2}\right)^2 \; with \; \tau = \left(\frac{f_{pc}}{2} + f_1\right) \cdot \sin(2\Theta)$$

$$Expanding: \left(\frac{f_{pc}}{2} + f_1\right)^2 - \left(\frac{f_{pc}}{2}\right)^2 = \left(\frac{f_{pc}}{2} + f_1\right)^2 \cdot \sin^2(2\Theta)$$

$$simplifying: 1 - \frac{\left(\frac{f_{pc}}{2}\right)^2}{\left(\frac{f_{pc}}{2} + f_1\right)^2} = \sin^2(2\Theta) \rightarrow \cos^2(2\Theta) = \left[\frac{\frac{f_{pc}}{2}}{\frac{f_{pc}}{2} + f_1}\right]^2$$

$$Finally: \Theta_{cr} = \frac{1}{2}\cos^{-1}\left[\frac{\frac{f_{pc}}{f_1}}{\frac{f_{pc}}{f_1} + 2}\right] \tag{[Eq. 2-5]}$$

The plot of this expression in Figure 2-16, assuming the principal tensile stress equal to the concrete tensile strength, illustrates the effect of prestressing on principal angle. When the prestressing is zero the crack angle theoretically forms at 45 degrees. Then the prestressing is applied this angle is reduced, for example when the prestressing added is twice the tensile strength of concrete the crack angle is theoretically at 30 degrees from the longitudinal beam axis.
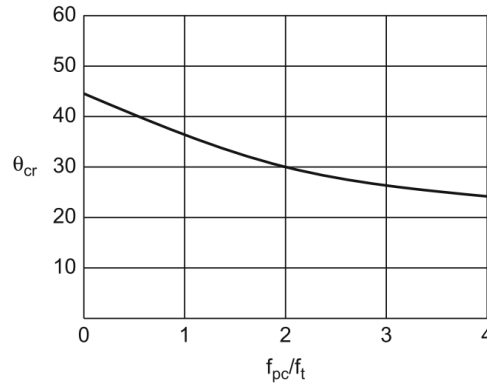

Figure 2-16 Variation of the principal angle as function of the applied prestressing

2.3 SHEAR STRENGTH MODELS

As an introduction, a classification of the different models used to determine the shear strength can be mentioned. Starting with the *empirical models*, derived from regression analysis of test data, without putting too much emphasis on the mechanics of the problem. Next*, tooth or comb models* can be mentioned with the model by Kani [16] leading them with his comprehensive mechanical model explaining the flexural-shear failure. Other proposed models are *based on the capacity of the compression zone, based on fracture mechanics, based on plasticity theory and based on longitudinal strains* [27].

Models based on longitudinal strains are of particular interest to discuss in detail, they relate the shear capacity directly to the longitudinal reinforcement strain. Shear models that lead design codes today are based on the Modified Compression Field Theory [28] and the Critical Shear Crack Theory [9]. Both address the shear-transfer mechanisms as function of the longitudinal strain, a unique parameter, and consider both the high influence of the aggregate size and concrete compressive strength in the roughness of the critical crack, hence, in the aggregate interlock of the section subjected to shear [11].

2.3.1 Critical Shear Crack Theory (CSCT)

The CSCT provides a rational basis for evaluating the shear and punching strength of elements without shear reinforcement, based on the estimation of crack width in the critical shear region. This theory is strongly dependent on the critical shear crack width and on its roughness, this dependency is expressed by [Eq. 2-6], where f_c is the concrete compressive strength, w the critical shear crack width, and d_g is the maximum aggregate size [9].

$$\frac{V_R}{bd} = \sqrt{f_c}\, f(w, d_g)$$

For this theory the following hypotheses are accepted [9]:

- Depending on the load configuration the shear strength is verified in a section where the width of the critical shear crack can be represented by the resultant strain at a depth *0.6d* from the compression face (Figure 2-17)
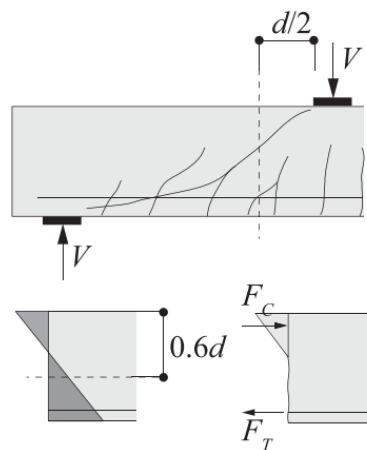

Figure 2-17 Critical Shear Crack Theory (CSCT) assumptions: control section and reference fibre for strain [9].

- The product of the longitudinal strain in the control depth ε times the effective depth of the element *d* is proportional to the critical crack width ($w \propto \varepsilon d$), although, this is only valid for rectangular cross-section without skin reinforcement in the side faces.
  The longitudinal strain is evaluated assuming a linear elastic behavior in compression for concrete (neglecting its tensile strength, Figure 2-17-b) and assuming that plane sections remain plane too. If no axial force is applied, like prestress force, the strain can be derived

based on the bending moment *M* in the critical section at the level of the control depth defined as follows.

$$\varepsilon = \frac{M}{bd\rho E_s \left(d - \frac{c}{3}\right)} \cdot \frac{0.6d - c}{d - c}$$

[Eq. 2-7]

Width: $c = d\rho \frac{E_s}{E_c}\left(\sqrt{1 + \frac{2E_c}{\rho E_s}} - 1\right)$

Modulus of elasticity of concrete: $E_c \approx 10,000\, f_c^{1/3}\, [MPa]$
Longitudinal reinforcement ratio: $\rho = A_s/A_c$

Considering the influence of the critical crack with, the aggregate size and the concrete compressive strength an analytical expression was proposed as follow to evaluate the shear strength.

$$\frac{V_R}{bd\sqrt{f_c}} = \frac{1}{3 \cdot \left(1 + 120\frac{\varepsilon d}{16 + d_g}\right)}\ [MPa, mm]$$

[Eq. 2-8]

Based on the above, the main assumption of the CSCT theory states that the shear strength depends on the member geometry (width *b* times effective depth *d*), the square root of the compressive strength of concrete f_c, the critical shear crack opening *w* and its roughness ($d_g + 16\,mm$). Other assumptions can be consulted in detail in [10], [29], and the summary of the most important ones is as follows [13]

1. Development of the critical shear crack (shape, location, and kinematics) governs the shear strength.
2. The center of rotation used to describe the relative displacement of the bodies separated by the critical shear crack is assumed to be located at the crack tip. The crack opening and sliding profile is variable along the crack height and it is governed by the crack kinematics.
3. Shear forces can potentially be carried by various shear-transfer actions like *aggregate interlock* due to crack sliding, *dowel action* of the longitudinal reinforcement crossing the crack, *residual tensile strength* of cracked concrete and the inclined *compression chord*.
4. On the basis of equilibrium, kinematics and fundamental constitutive laws of materials, the amount of shear transferred by each potential shear transfer action can be calculated.
5. When the sum of all potential shear-transfer actions (see Figure 2-3) equals the shear demand, failure occurs. The capacity of the free-body defined by the critical shear crack to transfer shear forces can be defined as: $V_R = V_{agg} + V_{Res} + V_{Dowel} + V_{Compr}$ (Refer to Figure 2-18)

The critical shear crack can be assumed to be characterized by a bilinear shape (Figure 2-18) and to develop at the location of minimum strength. An iterative calculation of the strength is necessary to determine the location of the critical shear crack x_A, and there are three potential positions initially ($x_A = d, x_A = 0.5a, x_A = a - d$) for reinforced concrete members [30]. The location of the critical crack in the case of prestressed beams is expected to be influenced by the stress incorporated in the cross-section, decreasing the crack angle and bringing it closer to the points of static or geometric discontinuity.
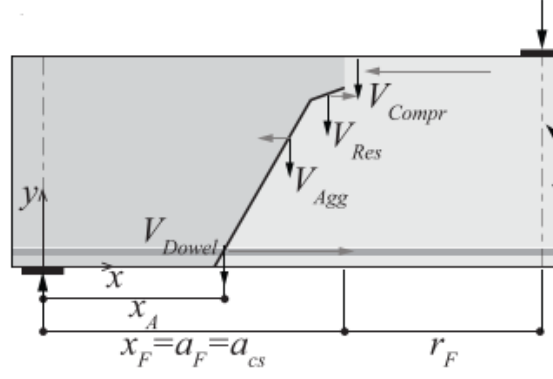
Figure 2-18 Rigid body equilibrium and internal forces [12]

2.3.2 Modified Compression Field Theory (MCFT)

Developed by Vecchio and Collins [28], this mechanical model of MCFT is based on the assumption that aggregate interlock is the main shear-transfer action. It considers cracked concrete as a unique orthotropic material and gives it its own constitutive relationship. In addition to taking into account local stress conditions at the crack surface, stresses and strains are treated as average values based on a rotating smeared crack model. This allows the crack direction to be reoriented according to the response of the material and the loading condition.

An important assumption in the MCFT is that the directions of the principal stress and principal strain in the concrete remain coincident. The MCFT is formulated using three sets of equations: equilibrium (global-average stresses and local-stresses at cracks), compatibility (deformation of concrete and reinforcement assumed identical, or perfect bond assumed), and constitutive relationships (stress-strain relationships for concrete and reinforcement) [31].

The MCFT considers the stresses transmitted across the critical crack, and the ability of the crack to transmit shear stresses is assumed to be dependent of the crack width w, the maximum aggregate size d_g and the concrete strength f_c. This shear transferred through the crack is limited by the following expression based on the aggregate interlock experiments performed by Walraven [19].

$$\frac{V_c}{bd} \leq \frac{0.18\sqrt{f_c}}{0.31 + \dfrac{24w}{d_g + 16}} \; [MPa, mm]$$

[Eq. 2-9]

Where d_g is the maximum aggregate size in millimeters, w the crack width in millimeters and the concrete compressive stress f_c in MPa. The crack width should be the average over the crack surface, it can be estimated by the product of the principal tensile strain and the crack spacing ($w = \varepsilon_1 \cdot s_\theta$)

For the development of this theory the initial problem to be solved was the determination of how the three in-plane stresses (f_x, f_y, v_{xy}) are related to the three in-plane strains ($\epsilon_x, \epsilon_y, \gamma_{xy}$). For the elaboration of the solution the following additional assumptions were applied [31].
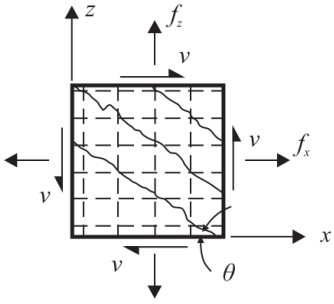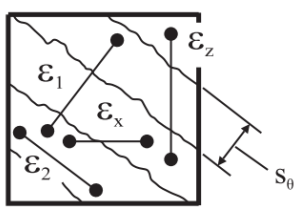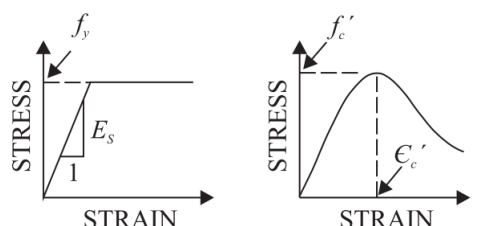
- The influence of loading history is not considered. Stress and strain considered in terms of average values over areas/distances large enough to include several cracks.
- Longitudinal and transverse reinforcing assumed to be uniformly distributed.
- Tensile stresses/strains will be treated as positive quantities and compressive stresses/strains as negative quantities.
- Deformed element edges remain straight and parallel.

Perhaps one of the advantages of the MCFT is that it was easier to interpret the results obtained to support the model, because it was developed by testing reinforced concrete elements in pure shear using a membrane element test instead of the traditional shear test where a simply supported beam is subjected to one or two point loads.

Comparing the principal stress in the concrete, f_2, with its corresponding strain, ε_2, was inferred that diagonally cracked concrete was weaker and softer than the same concrete in a standard cylinder test. This difference found depends on the magnitude of the coexisting principal tensile strain, ε_1, as it increases the difference in responses increase too. Furthermore, it was found that even after extensive cracking of the element, Mohr's circle for average stresses could predictably and consistently show the principal tensile stresses in the concrete, f_1. Taking into account these tensile stresses in cracked concrete modified the previous compression field theory and allowed the MCFT to predict the behavior of elements with and without shear reinforcement [32].

A summary of the equilibrium equations, geometric conditions and stress-strain relationships used in the MCFT is presented in the following Table 2-2.

Table 2-2 Modified Compression Field Theory equilibrium equations, geometric conditions and stress-strain relationships [32]

Equilibrium:	Geometric conditions:	Stress-strain relationships:
Average stresses 1. $f_x = \rho_x f_{sx} + f_1 - v\cot(\theta)$ 2. $f_z = \rho_z f_{sz} + f_1 - v\tan(\theta)$ 3. $v = \dfrac{f_1 + f_2}{\tan(\theta) + \cot(\theta)}$	**Average Strains** 6. $\tan^2(\theta) = \dfrac{\varepsilon_x + \varepsilon_2}{\varepsilon_z + \varepsilon_2}$ 7. $\varepsilon_1 = \varepsilon_x + \varepsilon_z + \varepsilon_2$ 8. $\gamma_{xz} = 2(\varepsilon_x + \varepsilon_2)\cot(\theta)$	**Reinforcement** 11. $f_{sx} = E_s \varepsilon_x \le f_{yx}$ 12. $f_{sz} = E_s \varepsilon_z \le f_{yz}$ **Concrete** 13. $f_2 = \dfrac{f_c'}{0.8 + 170\varepsilon_1} \cdot \left[2 \cdot \dfrac{\varepsilon_2}{\varepsilon_c'} - \left(\dfrac{\varepsilon_2}{\varepsilon_c'}\right)^2\right]$
Stresses at cracks 4. $f_{s.xcr} = \dfrac{f_x + +v\cot(\theta) + v_{ci}\cot(\theta)}{\rho_x}$ 5. $f_{s.zcr} = \dfrac{f_z + +v\tan(\theta) + v_{ci}\tan(\theta)}{\rho_z}$	**Crack widths** 9. $w = s_\theta \varepsilon_1$ 10. $s_\theta = \dfrac{1}{\frac{\sin(\theta)}{s_x} + \frac{\cos(\theta)}{s_z}}$	14. $f_1 = \dfrac{0.33\sqrt{f_c'}}{1 + \sqrt{500\varepsilon_1}} \; MPa$ **Shear stress on crack** 15. $v_{ci} \le \dfrac{0.18\sqrt{f_c'}}{0.31 + \frac{24w}{a_g + 16}} \; MPa, mm$

2.4 CODE PROVISIONS FOR SHEAR RESISTANCE OF PRESTRESSED MEMBERS

Design code models are a simplified version of the scientific or mechanical models, e.g. for estimation of the shear strength of concrete the Swiss Code SIA 262:2013 [33] uses a simplified version of the CSCT and the CSA A23.3:04 [34] of the MCFT. Then design code models can be said that are the representation of the current knowledge, proposing expressions that attempt to balance factors such as accuracy, precision, ease of use, and safety. Conversely, purely

mechanical models focus on the accuracy and precision of their predictions based on scientific explanations [11].

Design codes used usually have different approaches in the calculation of the shear resistance of prestressed members without shear reinforcement due to different assumptions made or failure mechanisms considered. Four relevant design codes will be evaluated for this document, Eurocode 2 [35], American Concrete Institute [36], American Association of State Highway and Transportation Officials AASHO-LRFD [37] and Eurocode 2 draft 2020-11 [38].

The ACI, AASHTO LRFD, Eurocode 2 and the new Eurocode 2 draft take into account the three types of failure mentioned in section 2.1.2 [18] and these are summarized in the following Table 2-3.

Table 2-3 Failure modes in the different design codes

Code	Flexural-shear failure	Shear-tension failure	Shear behaviour in discontinuity regions (shear compression)
Eurocode 2	Regions cracked in bending	Regions uncracked in bending	Strut-and-tie model
ACI	Flexure-shear strength V_{ci}	Web-shear strength V_{cw}	Strut-and-tie model
AASHTO LRFD	General approach		Strut-and-tie model
Proposal Eurocode 2	General approach		Design with strut-and-tie models and stress fields

Most models describe flexural-shear failures, then accuracy of models for members subjected to shear-compression failures is unknown. When the flexural-shear crack arises close to the support, e.g., when concentrated loads are placed at a distance less than $2.5 \cdot d$, the aggregate interlock has a minor contribution [18].

It should be noted that some approaches refer to the characteristic concrete compressive strength f_{ck} (Eurocodes) and others to the specified compressive strength of concrete f_c' (ACI318-19 and AASHTO-LRFD). The conversion relationship between f_{ck} and f_c' is specified in section 4.1.2 to get comparable values between design codes applied in Europe and America. It is also worth mentioning that for the comparison of the different approaches with the experimental results, it is necessary to use the mean compressive strength of concrete $f_{cm.cyl}$ instead of the design value usually specified in the design codes.

2.4.1 Eurocode 2: Design of concrete structures (EN 1992-1-1)
This design code distinguishes beams that do or do not require shear reinforcement. In case of members without shear reinforcement there are two regions distinguished for their analysis, each with its ow approach, the region cracked in bending and the region uncracked in bending. In case of discontinuity regions (near concentrated loads or geometric discontinuities) Eurocode 2 takes into the account the variable conditions with certain factor detailed next.

2.4.1.1 *Concrete resistance in regions cracked in bending*
These regions are dependent on the development of flexural cracks and their capacity to grow into flexural-shear cracks. Prestress force reduces the tensile stresses in the outer fibers, allowing

the beam to develop flexural cracks when it's subjected to higher external loads. EC2 calculation of the flexural-shear capacity of a prestressed beam without shear reinforcement is based the empirically derived expression [Eq. 2-10] that considers the prestress force as an axial compressive force that increases the shear capacity of the element as the crack width is reduced and the angle of inclination of the cracks is reduced [39]. The empirical factor $C_{Rd,c}$ used for characteristic shear strength calculation was calibrated through reliability analysis on 176 beam tests [40].

$$V_{Rd.c} = \left(C_{Rd.c} k (100 \rho_l \cdot f_{ck})^{\frac{1}{3}} + k_1 \sigma_{cp} \right) b_w d \ [MPa, mm]$$

[Eq. 2-10]

With: Recommended *values:* $C_{Rd.c} = \frac{0.18}{\gamma_c}$; $k_1 = 0.15$;

Partial factor for concrete: $\gamma_c = 1.5$ but for comparison between codes equal to 1

Size effect factor: $k = 1 + \sqrt{\frac{200}{d\,[mm]}} \leq 2$;

Reinforcement ratio for longitudinal reinforcement: $\rho_l = \frac{A_{sl}}{b_w d} \leq 0.02$;

Axial stress: $\sigma_{cp} = \frac{N_{Ed}}{A_c} [MPa] < 0.2 f_{cd}$; with $N_{Ed} > 0$ for compression

Characteristic compressive cylinder strength of concrete at 28 days: f_{ck} [MPa]

Area of concrete: $A_c \ [mm^2]$

Cross-sectional area of longitudinal reinforcement: $A_{sl} [mm^2]$

Cross-sectional area of concrete: $A_c [mm^2]$

Axial force: $N_{Ed} \ [N]$

Design value of concrete compressive strength: $f_{cd} = \alpha_{cc} f_{ck} / \gamma_c [MPa]$ with recommended $\alpha_{cc} = 1$

Web width: b_w [mm]

Effective depth of cross-section: $d = \frac{d_s^2 A_s + d_p^2 A_p}{d_s A_s + d_p A_p}$ [mm]

As the only conditional, the minimum value for the concrete shear resistance is stated in [Eq. 2-11]

$$V_{Rd.c} \geq (v_{min} + k_1 \sigma_{cp}) b_w d = \left(0.035 k^{\frac{3}{2}} f_{ck}^{\frac{1}{2}} + k_1 \sigma_{cp} \right) b_w d \ [MPa, mm]$$

[Eq. 2-11]

To calculate the mean shear strength of concrete in regions cracked in bending (V_{Rm}) according to EC2 applying [Eq. 2-10], it is required to use the mean compressive strength of concrete f_{cm} instead of the characteristic compressive strength of concrete f_{ck}, and the following recommended values $C_{Rm,c} = 0.15$ and $k_1 = 0.225$ as recommended by [41].

2.4.1.2 *Concrete resistance in regions uncracked in bending*

This region doesn't have flexural cracks in the ultimate limit state, the crack formation takes place within the web directly, where the principal tensile stresses exceed the concrete tensile strength. The principal tensile stresses caused by prestress (prestress is preload), and external loads will determine the shear capacity of the beam in case of shear-tension failure. Then using Mohr's circle (Figure 2-19) the principal tensile strength in the web is calculated as shown in [Eq. 2-12][18].
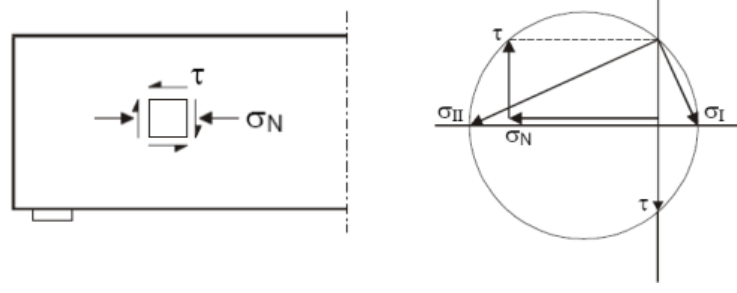
Figure 2-19 Mohr's circle for the calculation of the shear tension capacity

$$\sigma_I = -\frac{\sigma_N}{2} + \sqrt{\frac{\sigma_N^2}{4} + \tau^2} = f_{ctd} \ [MPa]$$

For constant cross-section over the length of the beam it is common to have the maximum principal stresses at the same height, but in case of variable cross-section the minimum value of shear resistance should be calculated at various axes in the cross-section.

From last equation, the shear stress will be $\tau = \sqrt{\sigma_I^2 + \sigma_I \sigma_N}$, and to consider the variation in prestress force within transfer length the factor α_l is added to multiply the prestress force applied.

In order to have a simplified version directly applicable to beams with rectangular cross-section, which are the most commonly used, the following expression [Eq. 2-13] is given

:

$$V_{Rd.c} = \frac{I \cdot b_w}{S} \sqrt{(f_{ctd})^2 + \alpha_l \sigma_{cp} f_{ctd}}$$

Having assumed: $\tau = \frac{V_{Rd,c} \cdot S}{b_w \cdot I_c} [MPa]$; $\sigma_N = \alpha_l \cdot \sigma_{cp} \ [MPa]$
With:
Moment of inertia: $I \ [mm^4]$
First moment of area above and about the centroidal axis: $S \ [mm^3]$
Design tensile strength of concrete: $f_{ctd} = \alpha_{ct} f_{ctk,0,05}/\gamma_c \ [MPa]$
Coefficient taking into account long term effects on the tensile strength (3.1.6(2)): $\alpha_{ct} = 1$
Axial stress: $\sigma_{cp} = \frac{N_{Ed}}{A_c} [MPa] < 0.2 f_{cd}$
Factor $\alpha_l = \frac{l_x}{l_{pt2}} \leq 1.0$ *for pretensioned tendons, 1 for other types of prestressing*
Distance of section considered from the starting point of the transmission length: l_x
Upper bound value of the transmission length of the prestressing element: $l_{pt2} = 1.2 \ l_{pt} \to EC2$ (8.18)

It is also noted that the regions uncracked in bending have a flexural tensile stress conditioned by $\sigma_t < \frac{f_{ctk,0.05}}{\gamma_c} = \frac{0.7 f_{ctm}}{\gamma_c}$.

2.4.2 Eurocode 2 proposal (draft 2020-11)

For this thesis the following draft version will be used: "Updated Draft by SC2/WG1/CDG prEN1992-D7 Working File (Rev. 7) 2020-11-16 after SC2 for CEN-enquiry" [38]. In its section 8.2 in this case, the general verification procedures for shear capacity are specified, where the particular case of members not requiring design shear reinforcement specified in section 8.2.2 is of interest for this document.

The base of the proposal is the Critical Shear Crack Theory explained before in section 2.3.1. The derivation of closed-form equation proposed for detailed verifications and the complete mechanical model will be explained in chapter 4. To then, the procedure will be exposed starting with the general verification from section 8.2.1 of the proposed design code. There, the first conditional is going to determine if a detailed verification is needed, and will be the case if the

shear stress derived from applied loads [Eq. 2-14] is less than the minimum shear stress resistance [Eq. 2-15] in the critical cross section $(\tau_{Ed} \leq \tau_{Rdc,min})$. The second condition determines whether the member requires shear reinforcement design, in case the shear stress resistance $(\tau_{Rd,c})$ of a member without shear reinforcement is not sufficient $(\tau_{Ed} \leq \tau_{Rd,c})$. And finally, if shear reinforcement has been designed, it is verified if the total shear stress resistance (τ_{Rd}) is enough to resist the applied loads $(\tau_{Ed} \leq \tau_{Rd})$.

$$\tau_{Ed} = \frac{V_{Ed}}{b_w \cdot z}; with \; z = 0.9d \qquad \text{[Eq. 2-14]}$$

$$\tau_{Rdc,min} = \frac{11}{\gamma_v} \cdot \sqrt{\frac{f_{ck}}{f_{yd}} \cdot \frac{d_{dg}}{d}} \qquad \text{[Eq. 2-15]}$$

Where f_{yd} is the design yield strength of non-prestressed steel reinforcement, but in case this is not used, the difference of the design and effective prestress is considered $(f_{pd} - \sigma_{p.\infty})$.

For the case study, the first two conditions are useful and the procedure for the detailed verification of the shear resistance of a member without shear reinforcement $(\tau_{Rd,c})$ will be explained below.

As a last remark, before starting with the detailed verification, the code indicates that it can be omitted for cross-sections that are at a distance less than *d* from the face of a support or from a significant concentrated load as shown in Figure 2-20. In case concentrated loads are applied closer that a distance *2d* from the face of a support, the cross section located at a distance *d* from the face of the support should be verified in detail.
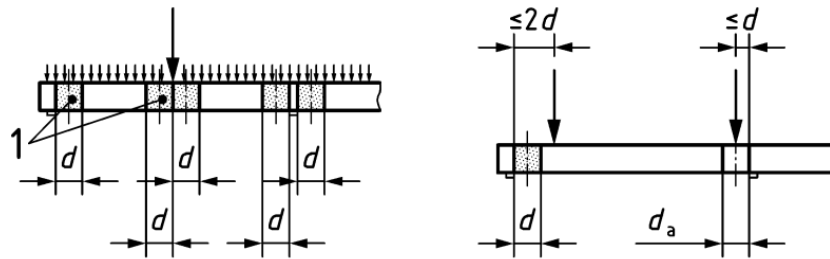

Figure 2-20 Regions where detailed shear strength verification may be omitted (left) predominant distributed load (right) predominant concentrated loads

The procedure of major interest in this document is presented in Figure 2-22, a flowchart with the steps to be followed to determine the shear strength of concrete and verify it. From it can be seen that the initial data required are the concrete characteristic compressive strength (f_{ck}), yield strength of reinforcement (f_y), shear partial factor (γ_V) and others parameters specified in Table 2-4

For the calculation of shear stress resistance there are two proposed procedures presented in equations [Eq. 2-16] and [Eq. 2-17]. Both differ in the way they take into account the influence of axial forces, the first through the term d_{nom} that divides the parameter of aggregate size, and the second similarly to current Eurocode 2, by subtracting the product of a factor k_1 by the axial stress in the cross-section σ_{cp}.

Something important to mention is that the procedure proposed only applies to slabs or beams with rectangular cross-sections in which there are predominant flexural-shear cracks. For the verification of prestressed beams of different shapes, there is another specific section where the calculation of shear stresses along the cross-section and at different critical locations is detailed.

$$\tau_{Rd,c} = \frac{0.66}{\gamma_V} \cdot \left(100\rho_l \cdot f_{ck} \cdot \frac{d_{dg}}{(d_{nom})}\right)^{\frac{1}{3}}$$

<div align="right">[Eq. 2-16]</div>

For the last equation ([Eq. 2-16]) the value of d_{nom} can vary according to the conditions shown in Figure 2-22. If the calculated value of a_{cs} is less than $4d$ then the value of d_{nom} is equal to a_v, else the value of d_{nom} is preserved equal to d. And in case of axial loads, the factor k_{vp} multiplies the obtained value of a_v, considering values of $k_{vp} \geq 0.1$.

$$\tau_{Rd,c} = \frac{0.66}{\gamma_V} \cdot \left(100\rho_l \cdot f_{ck} \cdot \frac{d_{dg}}{d_{nom}}\right)^{\frac{1}{3}} - k_1 \cdot \sigma_{cp}$$

<div align="right">[Eq. 2-17]</div>

In case of the alternative procedure proposed in [Eq. 2-17] the axial load is considered multiplied by a factor k_1, this procedure seems easier to follow, since there are much less factors to calculate.

Once the resistance has been obtained by either of the two methods, the following condition must be verified.

$$\tau_{Rd,c} \geq \tau_{Rdc,min}$$

<div align="right">[Eq. 2-18]</div>

- *With:*

  $\tau_{Rdc,min} = \frac{11}{\gamma_V} \cdot \sqrt{\frac{f_{ck}}{f_y} \cdot \frac{d_{dg}}{d}}$ *; in case of prestressed without ordinary steel reinforcement*

  $f_{yd} = f_{pd} - \sigma_p$
  Design tensile strength of prestress: f_{pd}
  Effective prestress (after losses): σ_p

Table 2-4 Parameter for detailed verification of shear resistance of members without shear reinforcement according to prEN1992 [38]

Parameters required	Clause (Section)
• Size parameter describing the failure zone roughness $\quad d_{dg} = 16\,mm + D_{lower} \leq 40\,mm; if\ f_{ck} \leq 60\,MPa$ $\quad d_{dg} = 16\,mm + D_{lower}\left(\frac{60}{f_{ck}}\right)^4 \leq 40\,mm; if\ f_{ck} > 60\,MPa$ Where D_{lower} is the smallest value of the upper sieve size D in an aggregate for the coarsest fraction of aggregates allowed by specification of concrete [EN206]	8.2.1 (4)
• Reinforcement ratio for bonded longitudinal reinforcement in the tensile zone due to bending referred to the nominal concrete area $\quad\quad \rho_l = \frac{A_{sl}}{b_w d}$	8.2.2 (2) Eq. (8.17)
• Effective shear span with respect to the control section $\quad\quad a_{cs} = \left|\frac{M_{Ed}}{V_{Ed}}\right| \geq d$ • Mechanical shear span $\quad\quad a_v = \sqrt{\frac{a_{cs}}{4} \cdot d}$	8.2.2 (3) Eq. (8.19) Eq. (8.18)

Alternative 1 from [Eq. 2-16]:

$$\tau_{Rd,c} = \frac{0.66}{\gamma_V} \cdot \left(100\rho_l \cdot f_{ck} \cdot \frac{d_{dg}}{k_{vp} \cdot d_{nom}} \right)^{\frac{1}{3}}$$

• Modification factor in case of axial forces $N_{Ed} \neq 0$	8.2.2 (4)
$$k_{vp} = 1 + \frac{N_{Ed}}{|V_{Ed}|} \frac{d}{3a_{cs}} \geq 0.1$$	Eq. (8.20)

Alternative 2 from [Eq. 2-17]:

$$\tau_{Rd,c} = \frac{0.66}{\gamma_V} \cdot \left(100\rho_l \cdot f_{ck} \cdot \frac{d_{dg}}{d_{nom}} \right)^{\frac{1}{3}} - k_1 \cdot \sigma_{cp}$$

• Axial stress in cross section	8.2.2 (5)
$$\sigma_{cp} = \frac{N_{Ed}}{A_c} < 0.2 f_{cd}$$	Eq. (8.21)
• Factor	
$$k_1 = \frac{1.4}{\gamma_V} \cdot \left(0.07 + \frac{e_p}{4d} \right) \leq 0.15 \cdot \frac{1.4}{\gamma_V}$$	Eq. (8.22)

2.4.2.1 Location of control sections

For consistency with the CSCT principles, the control section for checking the shear strength of one-way members is located at a distance d from a static discontinuity (intermediate support, end support, point of contraflexure or concentrated load) or a geometric discontinuity (change of cross-section geometry or reinforcement) as shown in Figure 2-21. In case of point loads applied at a distance less than $2d$ from the face of the support, the control section is located at a distance d from the face of the support.

a) distributed loads   b) concentrated loads
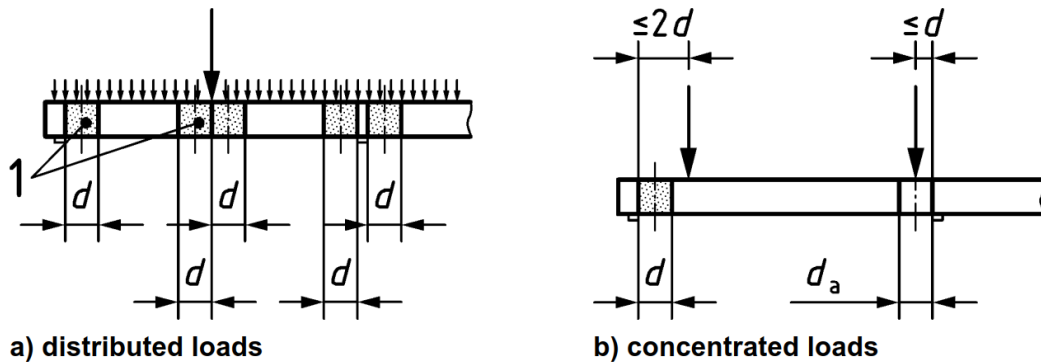
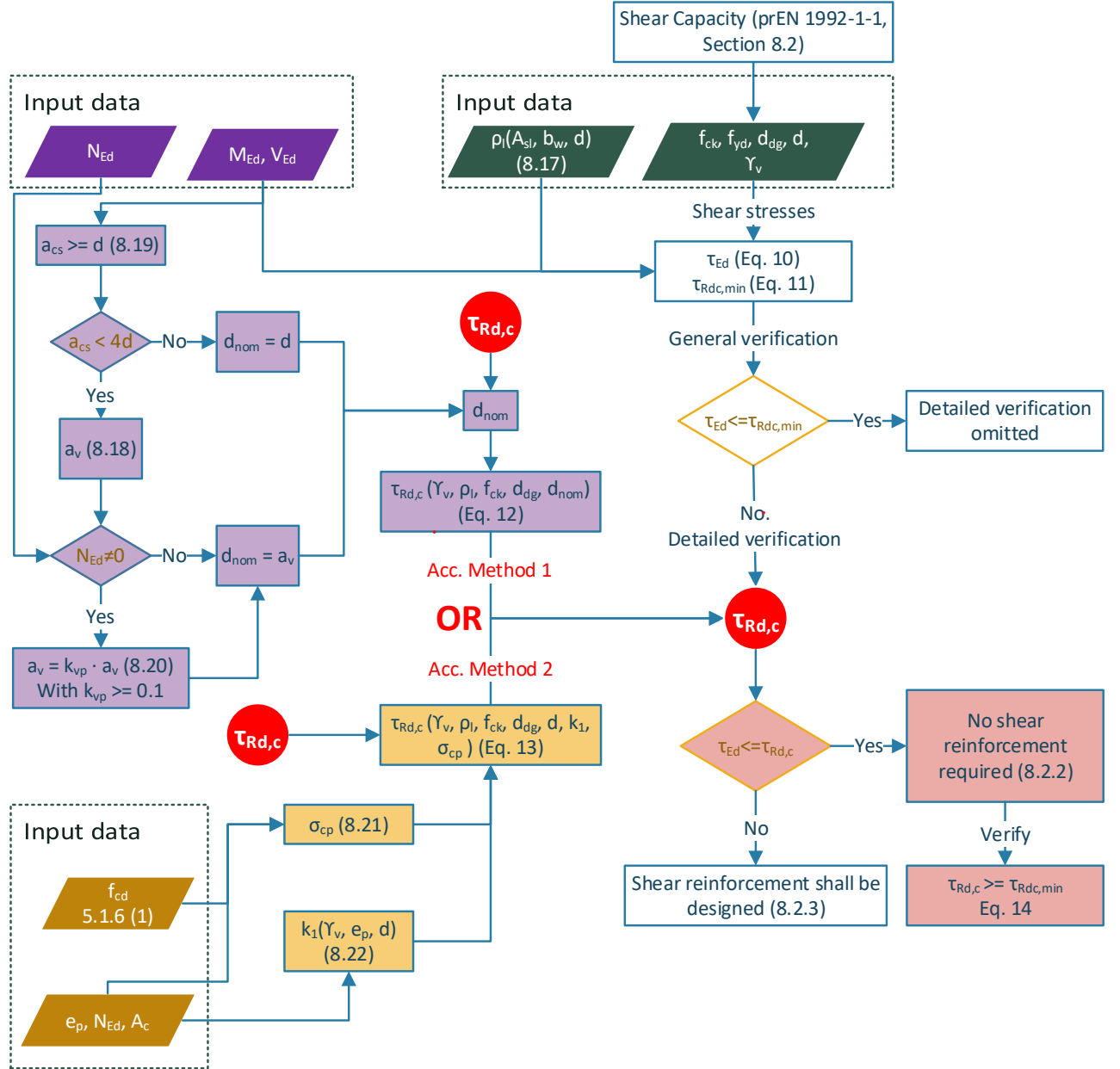*Figure 2-21 Locations for control sections according prEN1992*

Figure 2-22 Flowchart for the calculation of the shear strength of a member without shear reinforcement

2.4.2.2 Case of prestressed beam without shear reinforcement

To better illustrate the application of the proposed procedure, the formulas already presented above will be elaborated expanding the conditionals and the expressions given, like the mechanical shear span to consider (a_v) according to the effective shear span considered (a_{cs}).

In case of the application of alternative 1, from [Eq. 2-16], the final expression results as follow:

$$\tau_{Rd,c} = \begin{cases} \dfrac{0.66}{\gamma_V} \cdot \left(100\rho_l \cdot f_{ck} \cdot \dfrac{d_{dg}}{\sqrt{\left|\dfrac{M_{Ed}}{V_{Ed}}\right| \cdot \dfrac{d}{4}} \cdot k_{vp}} \right)^{\frac{1}{3}} when \left|\dfrac{M_{Ed}}{V_{Ed}}\right| \leq 4d \\ \\ \dfrac{0.66}{\gamma_V} \cdot \left(100\rho_l \cdot f_{ck} \cdot \dfrac{d_{dg}}{d \cdot k_{vp}} \right)^{\frac{1}{3}} when \left|\dfrac{M_{Ed}}{V_{Ed}}\right| > 4d \end{cases} ; with \ k_{vp} = 1 + \dfrac{N_{Ed}}{|M_{Ed}|}\dfrac{d}{3} \geq 0.1$$

In case of alternative 2 from [Eq. 2-17] the expression to apply is:

$$\tau_{Rd,c} = \begin{cases} \tau_{Rd,c} = \dfrac{0.66}{\gamma_V} \cdot \left(100\rho_l \cdot f_{ck} \cdot \dfrac{d_{dg}}{\sqrt{\left|\dfrac{M_{Ed}}{V_{Ed}}\right| \cdot \dfrac{d}{4}}}\right)^{\frac{1}{3}} - k_1 \cdot \sigma_{cp} \ when \ \left|\dfrac{M_{Ed}}{V_{Ed}}\right| \leq 4d \\[4ex] \tau_{Rd,c} = \dfrac{0.66}{\gamma_V} \cdot \left(100\rho_l \cdot f_{ck} \cdot \dfrac{d_{dg}}{d}\right)^{\frac{1}{3}} - k_1 \cdot \sigma_{cp} \ when \ \left|\dfrac{M_{Ed}}{V_{Ed}}\right| > 4d \end{cases}$$

Where $k_1 = \dfrac{1.4}{\gamma_V} \cdot \left(0.07 + \dfrac{e_p}{4d}\right) \leq 0.15 \cdot \dfrac{1.4}{\gamma_V}$ is the factor that relates the amount of shear resistance added by prestress $\sigma_{cp} = \dfrac{N_{Ed}}{A_c}$.

To obtain the design shear strength [Eq. 2-14] is applied, resulting $V_{Rd} = \tau_{Rd,c} \cdot b \cdot 0.9 \cdot d$. To calculate the mean shear strength (V_{Rm}) the mean compressive strength of concrete f_{cm} is used instead of the characteristic compressive strength of concrete f_{ck} and the partial factors used are equal to 1 ($\gamma_V = 1$).

2.4.3 American Concrete Institute (ACI318-19m)

Provisions for shear resistance of prestressed concrete members remain the same for the last versions of this standard code. In this latest version released in 2019, modifications were introduced to the expressions for non-prestressed beams with normal forces based on the joint work done by ACI-ASCE Committee 445, Shear and Torsion, and the German Committee for Structural Concrete (DAbStb). The proposal to update the expressions for prestressed beams is still under development for publication in future versions [42].

The approach to determine the shear resistance provided by the concrete, $\boldsymbol{V_c}$, is based on the work proposed by MacGregor and Hanson [43]. It is worth mentioning that the ACI318-19 code distinguishes axial forces from prestressing forces for analysis in two separate groups, and that the group considered in this document is the one composed of prestressed beams. The ACI318-19M defines a minimum area of stirrups to proceed to analyze a beam as a beam with or without shear reinforcement in case of non-prestressed beams, for prestressed beams there is no such distinction.

One of the main assumptions to consider that is detailed in [43], and remarked within the ACI318-19 code, is that the ultimate shear capacity of a beam without shear reinforcement can be taken equal to the shear that causes inclined cracking. When V_u is assumed to be equal to V_c, the failure of the beams is sudden when inclined cracking develops. After cracking, V_c is assumed to be equal to the sum of the shear-transfer actions like aggregate interlock, dowel action and the shear transmitted across the concrete compression zone. In case of a prestressed beam, the influence of the effective prestress is taken into account within the formulations too.

In addition, it is established that for prestressed members the distance from the extreme compression fiber to the centroid of prestressed and longitudinal reinforcement, **d**, may vary along the span, but this value should not be less than **0.8h** [43]**.**

2.4.3.1 *Shear resistance provided by concrete* ($\boldsymbol{V_c}$) *for prestressed members according to ACI318-19M*

Based on the work done by MacGregor [43] inclined cracking in reinforced or prestressed concrete beams is classified as either web-shear or flexural-shear cracking, of which the one with the lower strength value is the one that will govern the design.

The expressions provided apply to members having prestressed reinforcement only or a combination of prestressed and nonprestressed reinforcement, in regions where the effective prestress force is fully transferred to the concrete. The last condition is reflected in the following conditional [Eq. 2-19], and in case it is not fulfilled, the reduced effective prestress force shall be used for the detailed verification of web-shear and flexure-shear resistance.

$$A_{ps}f_{se} \; [N] \geq 0.4\big(A_{ps}f_{pu} + A_{s}f_{y}\big)[N]$$

[Eq. 2-19]

> *With*
> *Area of prestressed longitudinal tension reinforcement: $A_{ps}\,[mm^2]$*
> *Area of non-prestressed longitudinal tension reinf.: $A_{s}[mm^2]$*
> *Specified tensile strength of prestressing reinf.: $f_{pu}[MPa]$*
> *Effective stress in prestressed reinf. after prestress losses: $f_{se}[MPa]$*

The design code ACI318-19M defines two approaches for the verification of the concrete shear resistance, one simplified or approximate method and another detailed based in the calculation of the flexure-shear and web-shear strength. The following is a brief description of the procedure and the variables necessary for the calculation with both methods, for further information on the development of the design criteria used, reference is made to chapter 5 of [44].

- **Approximate method**

This method is favorable for its application to uniformly loaded members. The final value is the minimum value obtained from the following three equations, $V_c = \min(V_{c.a}, V_{c.b}, V_{c.c})$.

$$\frac{V_{c.a}}{b_w d} = \left(0.05\lambda\sqrt{f_c'} + 4.8\frac{V_u d_p}{M_u}\right)[MPa]$$

[Eq. 2-20]

$$\frac{V_{c.b}}{b_w d} = \left(0.05\lambda\sqrt{f_c'} + 4.8\right)[MPa]$$

[Eq. 2-21]

$$\frac{V_{c.c}}{b_w d} = \left(0.42\lambda\sqrt{f_c'}\right)[MPa]$$

[Eq. 2-22]

> With the condition that the final value needs to be greater than the lower limit defined below, and one must recognize that [Eq. 2-22] is the upper limit stated by ACI318-19 code.

$$V_{c.min} = 0.17\lambda\sqrt{f_c'}b_w d \; [N]$$

[Eq. 2-23]

> Where $d_p > 0.8h$ is the distance from the extreme compression fiber to the centroid of prestressed reinforcement, V_u and M_u the simultaneous factored shear and moment due to the total factored loads at the section considered. f_c' is the specified compressive strength of concrete.
> The design of prestressed beams without shear reinforcement with concrete compressive strength greater than 70 MPa. is not considered due to the lack of test data and practical experience. The modification factor accounting for the reduced mechanical properties of lightweight concrete relative to normalweight concrete of the same compressive strength is λ, as this document does not deal with lightweight concretes, this modification factor is always considered equal to 1.
> The derivation of the above expressions is detailed in appendix A.

- **Detailed method**
  > These shear design provisions were proposed by Macgregor [43], discussing additions and changes for the 1970 ACI Building code. A new design procedure for prestressed concrete beams lead to the following calculations.

The final concrete shear capacity will be the minimum between the flexural-shear and web-shear strength estimated.

$$V_c = \min(V_{ci}, V_{cw})$$

- o **Flexure-shear strength, V_{ci}**
  Assumed as the sum of the shear required to generate a flexural crack at the analyzed section [Eq. 2-25] plus the amount of shear required to change a flexural crack into a flexure-shear crack resulting in [Eq. 2-26]. Then, it is important to remark that the ACI318-19 code allows flexural-shear cracks only with the presence of flexural cracks. These flexural cracks are assumed to be caused by the cracking moment (M_{cre}) induced by an external load.

$$V = \frac{V_i M_{cre}}{M_{max}}$$

With:
Factored shear force at section due to external loads occurring simultaneously with M_{max}: V_i
Maximum factored moment at section due to external loads: M_{max}
Moment causing flexural cracking at section due to external loads:

$$M_{cre} = \left(\frac{I}{y_t}\right)\left(0.5\lambda\sqrt{f'_c} + f_{pe} - f_d\right)$$

Moment of inertia: I
Distance form centroidal axis of gross section to tension face: y_t
Compressive stress in concrete due to only prestress forces, after all prestress losses: f_{pe}
Stress due to unfactored dead load: f_d

$$V_{ci} = \begin{cases} 0.05\lambda\sqrt{f'_c}b_w d_p + V_d + \dfrac{V_i M_{cre}}{M_{max}} \ for \ composite \ members \\[2mm] 0.05\lambda\sqrt{f'_c}b_w d_p + \dfrac{V_u M_{ct}}{M_u} \ for \ noncomposite \ members \end{cases}$$

With:
Distance from extreme compression fiber to centroid of prestressed reinforcement: $d_p [mm]$
Web width: b_w
Moment causing flexural cracking at section due to total load:

$$M_{ct} = \left(\frac{I}{y_t}\right)\left(0.5\lambda\sqrt{f'_c} + f_{pe}\right)$$

The value obtained in [Eq. 2-26] need not be taken less than [Eq. 2-27]

$$V_{ci} \geq \begin{cases} 0.17\lambda\sqrt{f'_c}b_w d \ if \ A_{ps}f_{se} < 0.4\left(A_{ps}f_{pu} + A_s f_y\right) \\[2mm] 0.14\lambda\sqrt{f'_c}b_w d \ if \ A_{ps}f_{se} \geq 0.4\left(A_{ps}f_{pu} + A_s f_y\right) \end{cases}$$

- o **Web-shear strength, V_{cw}**
  Is based on the assumption that web-shear cracking takes place at a shear level causing a principal tensile stress of approximately $0.33\lambda\sqrt{f'_c}$ at the centroidal axis of the cross-section. The vertical component of the effective prestress, V_p, is taken into account and is calculated from the effective prestress force without load factors.

$$V_{cw} = \left(0.29\lambda\sqrt{f_c'} + 0.3f_{pc}\right) b_w d_p + V_p$$

<div align="right">*[Eq. 2-28]*</div>

With
Compressive stress in concrete, after all prestress losses, at centroid of cross section resisting external loads.: f_{pc}
Vertical component of effective prestress force: $V_p = A_p f_{se} sin\left(\theta_p\right)$
Angle on inclination prestressed tendon: θ

Also web-shear strength can be calculated as the resultant shear force, from dead load plus live load, required to have a principal tensile stress of $0.33\lambda\sqrt{f_c'}$ at the centroidal axis of the prestressed cross-section when it is within the web or at the flange-web intersection when the centroidal axis is in the flange [36].

2.4.4 American Association of State Highway and Transportation Officials (AASHTO)

As this code is based in the Simplified Modified Compression Field Theory (SMCFT) [45], in general terms, it looks at how strain in the beam is affected by flexure and shear stresses. The difference with respect to the ACI318-19 code is the truss analogy, with ACI318-19 the angle of inclination of the diagonal compressive stresses (θ) is assumed to be fixed at 45 degrees, while in AASHTO LRFD the angle θ is calculated based on the strain state in the member (affected by the "compression field").

The called "Sectional Design Model" specified in Article 5.7.3 is used for shear design, calculating the nominal shear resistance as detailed in [Eq. 2-29]. In case of a prestressed concrete beam without shear reinforcement, the term for shear contribution of shear reinforcement (V_s) can be neglected. In the first expression of [Eq. 2-29] the shear resistance is the sum of the shear strength of concrete (V_c), dependent on the concrete tensile stresses, and the vertical component of the prestressing force (V_p). The second formula prevents crushing of the concrete web, avoiding the crush of the concrete compressive struts before yielding.

$$V_n = \min \begin{cases} V_c + V_p \\ 0.25 f_c' b_v d_v + V_p \end{cases} [N]$$

<div align="right">*[Eq. 2-29]*</div>

With, Design compressive stress of concrete: f_c'
Effective web width (the minimum within the depth d_v): b_v
Effective shear depth: d_v

2.4.4.1 Shear stress on concrete

The effective shear depth and effective web width calculation are specified in article 5.7.2.8 according to the illustration shown in Figure 2-23.
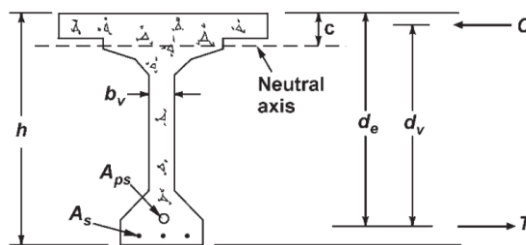

Figure 2-23 Illustration of parameters for shear stress according AASHTO LRFD

The effective web width b_v is measured parallel to the neutral axis, between tensile and compressive forces resultants due to flexure. For circular sections is equal to the diameter discounting the area taken up by the post-tensioning ducts. In Figure 2-23 the post-tensioning duct is in a position that doesn't affect the region where the width of the section is minimum, but in case the location of the tendon is raised such is located withing the narrow portion of the web, the value of b_v would be reduced.

For the effective shear depth value, the value is calculated according to [Eq. 2-30]. In addition, in the case of continuous elements, both the upper and lower reinforcement may be evaluated.

$$d_v = \frac{M_n}{A_s f_y + A_{ps} f_{ps}} \; [mm] \; but \; d_v > \max(0.9 d_e, 0.72h)$$

[Eq. 2-30]

Where:

f_{ps} = *effective stress in strands*

Effective depth between compressive face and tensile resultant: $d_e = \frac{A_{ps} f_{ps} d_p + A_s f_y d_s}{A_{ps} f_{ps} + A_s f_y}$

Nominal flexural resistance:

$$M_n = A_{ps} f_{ps} \left(d_p - \frac{a}{2} \right) + A_s f_s \left(d_s - \frac{a}{2} \right) - A'_s f'_s \left(d'_s - \frac{a}{2} \right) + \alpha_l f'_c (b - b_w) h_f \left(\frac{a}{2} - \frac{h_f}{2} \right)$$

Design compressive strength of concrete: f'_c

Width of the compression face of the member: b

Web width of diameter of circular section: b_w

Compression flange depth of an I or T member: h_f

Depth of equivalent stress block: $a = c \cdot \beta_l$

Distance from extreme compression fiber to centroid of prestressing tendons: d_p

Distance for extreme compression fiber to centroid of tensile reinf.: d_s

Distance for extreme compression fiber to centroid of compression reinf.: d'_s

Stress in prestressing steel at nominal flexural resistance: $f_{ps} = f_{pu} \left(1 - k \frac{c}{d_p} \right)$ *(Bonded tendons. In case of unbounded tendons review Article 5.6.3.1.2)*

Factor: $k = 2 \left(1.04 - \frac{f_{py}}{f_{pu}} \right)$

Distance from extreme compression fiber to neutral axis (with bonded tendons),

   rectangular section: $c = \frac{A_{ps} f_{pu} + A_s f_s - A'_s f'_s}{\alpha_l f'_c \beta_l b + \frac{k A_{ps} f_{pu}}{d_p}}$;

T-section: $c = \frac{A_{ps} f_{pu} + A_s f_s - A'_s f'_s - \alpha_l f'_c (b - b_w) h_f}{\alpha_l f'_c \beta_l b_w + \frac{k A_{ps} f_{pu}}{d_p}}$

Stress block factors: $\alpha_l = if \left(f'_c < 69 \; MPa, 0.85, 0.85 - 0.02 \cdot \frac{f'_c - 69}{7} \right)$

$$\beta_l = if \left(f'_c < 28 \; MPa, 0.85, 0.85 - 0.02 \cdot \frac{f'_c - 28}{7} \right)$$

Area of compression reinf.: A'_s

Area of nonprestressed tension reinf.: A_s

Area of prestressing steel on flexural tension side: A_{ps}

Stress in nonprestressed tension reinf.: f_s

Stress in nonprestressed compression reinf.: f'_s

Yield strength of prestressing steel: f_{py}

Specified tensile strength of prestressing steel: f_{pu}

Now proceeds the calculation of the concrete shear resistance (V_C), for which there are two procedures that can be used. The first is only applicable to non-prestressed beam, then is not useful for the case study of interest. The second method called "General procedure" (Article 5.7.3.4.2) is applicable for all cases, then will be useful for the case of prestressed beams without shear reinforcement that will be analyzed in this document.

For the "General procedure" there are two different approaches to determine the main parameters which are, the factor β and the angle for the compression chord θ. The first approach follows an analytical procedure considering the strain at the tension reinforcement (ε_s) (Figure 2-24 - left), and the second approach uses tables provided in Appendix B5 of the design code but considering the longitudinal strain at mid depth of the girder (ε_x) (Figure 2-24 - right). In any case, the same result should be obtained by using any approach.
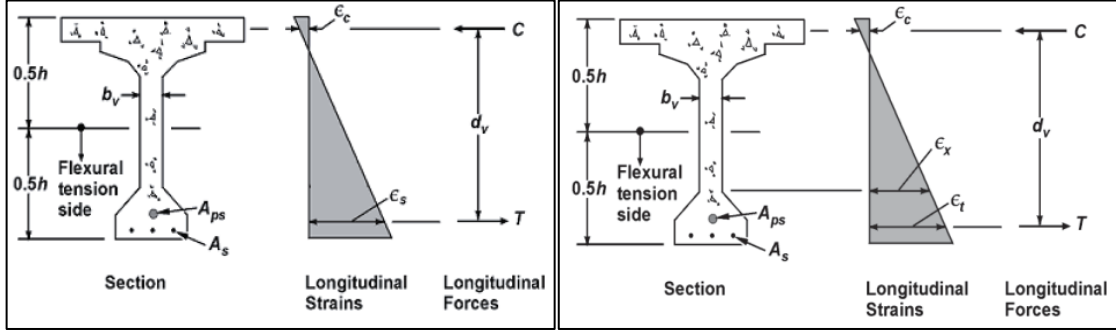
Figure 2-24 Illustration longitudinal strains. ε_s (left) ε_x (right), for sections containing less than the minimum amount of shear reinforcement

- **Method 1, Algebraic procedure**

  For members without the minimum amount of shear reinforcement stated in this design code the following expressions apply. Starting with the factor that is going to indicate the ability of the diagonally cracked concrete to transmit tension and shear β.

$$\beta = \frac{4.8}{1 + 750\varepsilon_s} \frac{1300}{1000 + s_{xe}}$$

[Eq. 2-31]

  With:
  Crack spacing parameter (influenced by aggregate size):
$$s_{xe} = 300 \leq s_x \frac{35}{a_g + 16 \, mm} \leq 2000$$
  Maximum aggregate size: a_g [mm]
  Crack spacing parameter: $s_x = d_v$ for members without shear reinf.

  The net longitudinal strain in the section at the centroidal axis of the reinforcement in tension is calculated with [Eq. 2-32](a) initially, but in case the value obtained is negative [Eq. 2-32](b) should be used.

$$\varepsilon_s = \frac{\left(\frac{|M_u|}{d_v} + 0.5N_u + |V_u - V_p| - A_{ps}f_{po}\right)}{E_s A_s + E_p A_{ps}} < 6.0 \cdot 10^{-3}$$

[Eq. 2-32]

(a)

$$\varepsilon_s = \frac{\left(\frac{|M_u|}{d_v} + 0.5N_u + |V_u - V_p| - A_{ps}f_{po}\right)}{E_c A_{ct} + E_s A_s + E_p A_{ps}} > -0.40 \cdot 10^{-3}$$

(b)

  With parameters:
  Modulus of elasticity of prestressing steel multiplied by the locked-in difference in strain between the prestressing steel and the surrounding concrete: $f_{po} = 0.7 f_{pu}$
  Factored moment at the section: $|M_u|$ but not less than $|V_u - V_p|d_v$
  Factored axial force: N_u; negative for compression
  Factored shear force: V_u
  Area of concrete on flexural tension side: A_{ct} for $0.5h$ (Figure 2-24)

  The diagonal compressive stresses that creates a longitudinal compressive force in the web of $(V_u - V_p)\cot(\theta)$ need to be balanced by tensile forces in the upper and lower part of the beam $0.5 \cdot (V_u - V_p)\cot(\theta)$ each. For simplicity in the expression, $0.5 \cdot \cot(\theta)$ is taken equal to 1, and the longitudinal demand due to shear in the longitudinal tension reinforcement is just $V_u - V_p$ for this reason, without considerable loss of accuracy.

- **Method 2, procedure with tables**
  This method may be easier in a manual calculation, since longitudinal strain values can be obtained from the s_{xe} calculated before. Or one can calculate the ratio between shear stress in the concrete $\left(v_u = (V_u - \phi V_p)\,/(d_v\,b_v)\right)$ and the concrete compressive strength (f_c') to obtain the same values of longitudinal strain. Linear interpolation between rows and columns of the table is allowed, and for detailed information refer to [37] Appendix B5.

Now, with the necessary parameters obtained (β, f_c', d_v, b_w) the shear resistance of concrete is calculated with the following expression:

$$V_c = 0.083\beta\sqrt{f_c'} \cdot b_w d_v;\,[MPa, mm]$$

[Eq. 2-33]

The vertical component of prestressing force is also required, this is calculated as follow:

$$V_p = A_p f_{ps}\sin(\theta_p)$$

[Eq. 2-34]

2.5 BACKGROUND OF THE RESEARCH

- Adding prestressing increments the required shear force to cause cracking due to the compression stresses introduced, then it provides an overall marginal improvement in shear strength. Prestressing generally reduces the angle of the flexural-shear cracks influencing the orientation of the principal stresses and reducing the actual collaboration of shear-transfer actions like aggregate interlock or dowel action.

- Design codes derived from physical-based models have greater clarity regarding the influence of the different parameters on the estimated shear resistance. This is not the case for empirical models, where there is some uncertainty regarding how to consider particular situations that are not consistent with the experiments with which the approach was calibrated.

- Also, note the similarity between the MCFT and the CSCT estimation of the shear stress on shear crack, [Eq. 2-9] and [Eq. 2-8] respectively. Shear stress on crack according both theories depends on the crack-width, aggregates size and concrete strength. Both theories have a strong influence from Kani [16] and the estimation of the influence of the aggregate size in shear resistance is based in his work. Both estimate the crack width taken the longitudinal strain as the main parameter, estimated at different heights of the cross-section depending the assumptions made for the approach.

- The prestressing force is considered as preload for Eurocodes and as a capacity for codes like ACI318-19 and AASHTO-LRFD. Thus, the prestressing force effect is considered as an external load acting on the member for the Eurocodes. While in the case of ACI318-19 and AASHTO-LRFD codes, the effect of the prestressing force is considered through the contribution of the vertical resultant of the prestressing force acting on the beam or like in AASHTO-LRFD through its effect on the nominal flexural moment and longitudinal strain.

- ACI318-19M detailed method assumes the concrete contribution to shear capacity V_c is directly related to the shear required to cause diagonal cracking though a semi-empirical approach. The EC2 doesn't consider the contribution of concrete in the stage of cracked concrete, and the effect of prestressing is incorporated with a linear empirical relation.

3 EXPERIMENTAL DATABASE CHARACTERISTICS

This chapter will present the shear test database for prestressed beams without shear reinforcement. This database was published as the *"2015 ACI-DAfStb database of shear tests on slender prestressed concrete beams without stirrups"* [3]. An overview of the available data will be presented, and the distribution of the most important parameters will be analyzed.

Then the parameters that have the most significant influence on shear strength ($a/d, f_{cm}, \rho_l, \sigma_{cp}$) will be analyzed in detail. Finally, the database will be divided into subsets based on different criteria established to reduce the bias of comparing test results with the estimations made by the chosen design codes reported in the next chapter.

3.1 GENERAL CHARACTERISTICS

To elaborate the shear database for the *"American Concrete Institute - Deutscher Ausschuss für Stahlbeton (ACI-DAfStb) group"*, information has been extracted from test reports or papers published in leading journals. One of the most significant contributors of the shear database for prestressed concrete members is the thesis published by Nakamura [46]. A total of 1696 tests published between 1954 and 2010 were collected. These tests were carried out in North America, Japan, and Europe to evaluate the local shear design provisions.

The 1,696 tests were reduced as different filters were applied to preserve tests with consistent information for analysis only. First, the relevant information was checked for each test, such as concrete compressive strength, prestressing steel yield strength, prestressing force in tendons, location of point loads, and shear failure force. Then, tests with shear slenderness values less than 2.4 ($a/d < 2.4$) were eliminated as these are related with the analysis of deep beams. Finally, to generate the final control database, 18 individual control criteria (called "koni") were defined to evaluate different parameters such as web width, beam height, inner lever arms, failure type described, longitudinal reinforcement characteristics and other conditionals described in detail in [47] and [2]. Most of the filters applied are mechanically justified like the minimum values for parameters like $a/d > 2.4$, $b_w >= 50\ mm$, $12\ MPa < f_{cm} < 100\ MPa$. Then come the so-called auxiliary filters, for the classification of the tests according to the use of shear or longitudinal reinforcement, method of prestressing used, and the control of anchorage or flexural failures (for detailed information about the control criteria applied, refer to Appendix B).

The final evaluation database obtained for prestressed concrete members without shear reinforcement generated combines data from prestressed and post-tensioned beams with and without non-prestressed longitudinal steel reinforcement. This database was stored in an excel file for manipulation and its name following the notation described in [47] is "vuct-PC-A2a+A3a_2015-05-19". Dr. Yuguang provided the information compiled in a excel file used for the development of this thesis. From now on, the abbreviation **"ACI-DAfStb-PC"** in this document refers to this database.

Starting to describe some of the features of the database used, Figure 3-1 below shows that prior to 1970, there were significant data collection campaigns for post-tensioned beams. The articles collected dated after 1970 focus mainly on prestressed beams, and the final amount obtained for both types of prestressing methods is even, with 114 post-tensioned and 100 prestressed beams.
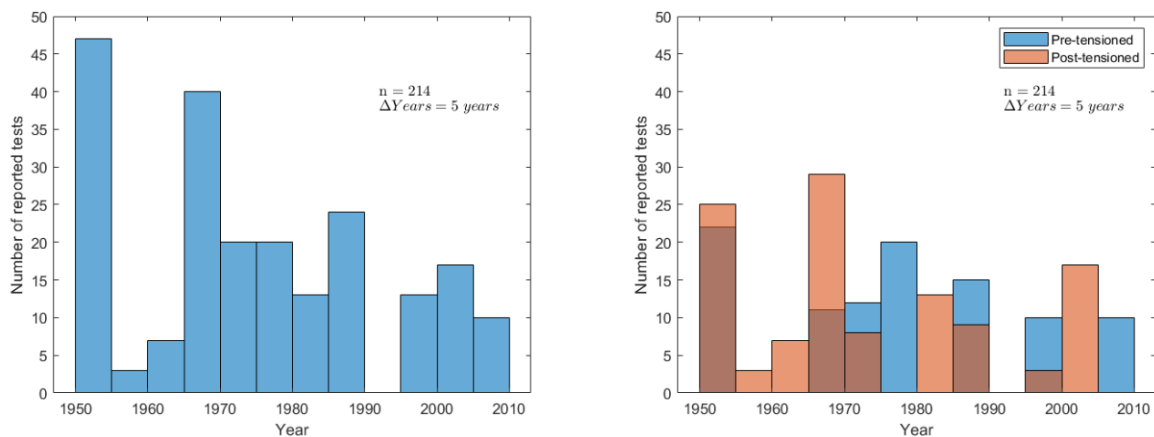
Figure 3-1 Number of tests for ACI-DAfStb-PC database

The information collected had to provide the minimum data to evaluate the shear capacity of the different beams. It is necessary to have at least the cross-section dimensions, the experimental setup, a description of the shear failure, and the material properties of concrete, non-prestressed and prestressed steel longitudinal reinforcement. The following is a brief description of the different parts of the data collected in the database used.

1. **General information**
   Capturing the label given by the author and the units used on the test paper (SI units or imperial units). Then, the beam is assigned with an internal number.
2. **Section properties,**
   Recording relevant beam dimensions, gross area, and location of the center of gravity.
3. **Load position and geometry**
   There are two significant variables. The effective span and the distance of the loading point from the support.
4. **Longitudinal reinforcement**
   a. **In tension**
      It is registered the longitudinal reinforcement area, longitudinal reinforcement ratio, type of anchorage, yield strength, and tensile strength. In cases where there are different diameters and yield strengths, the values used are equal to the calculated mean values.
   b. **In compression**
      The same information as 4a.
5. **Prestressing**
   a. **Prestressing steel**
      The file contains information about the types of strands or tendons and their dimensions. In addition, the database also includes the calculated center of gravity of the tendons, the effective depth, yield stress, and tensile strength.
   b. **Prestress**
      There is a summary of the prestressing force and the concrete stress at the centroid due to prestress
   c. **Axial force**
      In this case of analysis, for all beams, the axial force is equal to zero.
6. **Shear reinforcement**
   For beams without shear reinforcement, this part is not considered.
7. **Concrete**
   a. **Compressive strength**
      Depending on the dimensions of the test specimen, via conversion factors, the uniaxial concrete compressive strength (f_{1c}) is derived. From the uniaxial

compressive strength of concrete, the mean cylinder strength $(f_{cm,cyl})$ and the specified compressive strength (f_c') are calculated, based on relations explained in detail in section 3.2.1

    b. **Tensile strength**

The database reports that it uses the computed uniaxial tensile strength $(f_{1ct,test})$ as explained in [47]. However, considering that there are different design codes in this study case, the tensile strength is calculated as stated for each design code. Section 4.1.3 explains this case in detail.

8. **Mechanical ratios of longitudinal reinforcement**

The database provides helpful calculated relations for the analysis of the data captured in a later stage.

9. **Test**

The file presents at this part a summary of all the test results parameters like inner lever arm, flexural capacity, ultimate moment, and variables like the shear force acting considering the external point load and the self-weight of the beam.

10. **Control**

For the control and evaluation of the calculated results, all the beams pass through filters to check the integrity of the essential data and check different functional parameters to evaluate the possible factors influencing the failure of the beam (Flexural failure or Anchorage failure parameters detailed in section 3.5).

The following variables described in Table 3-1, captured from the nearly 100 variables, were used for the analysis of the different design codes proposed for this study.

Table 3-1 Notation used by ACI-DAfStb-PC database

Beam/flange width	b	mm	
Web width	b_w	mm	Equal to beam width in case of rectangular beams
Total beam height	h	mm	
Height of flange in compression	h_f	mm	
Height of flange in tension	h_{ft}	mm	
Gross area of concrete section	A_c	mm²	
Distance from centroidal axis of gross section, neglecting reinforcement, to tension face	y_t	mm	ACI-DAfStb-PC database uses z_{c2} related to the compression face then, $y_t = h - z_{c2}$
Moment of inertia	I_{cs}	mm⁴	
Area of concrete on the flexural tension side of the member	A_{ct}	mm²	Area below neutral axis (in tension) used for AASHTO-LRFD procedure
Effective span	L	mm	
Distance from extreme compression fiber to centroid of nonprestressed longitudinal reinforcement in tension	d_s	mm	
Area of nonprestressed longitudinal tension reinforcement	A_s	mm²	
Yield strength for nonprestressed reinforcement.	f_{sy}	MPa	Detailed in section 3.2.2
Modulus of elasticity of steel reinforcement	E_s	MPa	Equal to 200 [GPa] always
Distance from extreme compression fiber to centroid of nonprestressed longitudinal reinforcement in compression	d_{s2}	mm	
Area of nonprestressed longitudinal compression reinforcement	A_{s2}	mm²	
Distance from extreme compression fiber to centroid of prestressed reinforcement located at the bottom of the beam	d_{pbot}	mm	

Distance from extreme compression fiber to centroid of prestressed reinforcement located at the web of the beam	d_{pweb}	mm	
Distance from extreme compression fiber to centroid of prestressed reinforcement located at the top of the beam	d_{ptop}	mm	
Bond type	b_{type}	-	1 = strand 0 = wire
Nominal diameter of prestressed rebar	ϕ_{ps}	mm	From just 1 tendon
Area of prestressed reinforcement located at the bottom of the beam	A_{pbot}	mm²	
Area of prestressed reinforcement located at the web of the beam	A_{pweb}	mm²	
Area of prestressed reinforcement located at the top of the beam	A_{ptop}	mm²	
Modulus of elasticity of prestressing reinforcement	E_p	MPa	If not specified, it is assumed that $E_p = 200\ [GPa]$
Specified yield strength of prestressing reinforcement	f_{py}	MPa	
Specified tensile strength of prestressing reinforcement	f_{pu}	MPa	
Prestressing tendon angle	θ_p	rad	Equal to zero in all cases since straight tendons were used
Effective prestress after all losses	σ_{pp}	MPa	Estimated at the location of the critical shear crack x_r
Maximum aggregate size	a_g	mm	
Smallest value of the upper sieve size D in an aggregate for the coarsest fraction of aggregates (EN 206)	D_{lower}	mm	It is assumed equal to Æa /2
Modulus of elasticity of concrete	E_c	MPa	Calculated according to the design code specification as function of f_{cm} (for ACI318)
Reported shear force at failure considering external point load and self-weight	$V_{u.Rep}$	kN	
Estimated distance of failure crack from support axis	x_r	mm	Assumed equal to $0.65 \cdot a$ (refer to section 3.4)
Mean cylinder strength of concrete	$f_{cm.cyl}$	MPa	Refer to section 3.2.1
Characteristic cylinder strength	f_{ck}	MPa	Refer to section 4.1.2
Specified compressive strength of concrete	f_c'	MPa	Refer to section 4.1.2
Total shear load by external load and self-weight at critical location	$V_u(x_r, F)$	kN	Refer to section 4.1.1
Total bending moment by external load and self-weight at critical location	$M_u(x_r, F)$	kNm	Refer to section 4.1.1

Now, it is helpful to visualize the variables presented in the following illustrations. Of the parameters presented, the following Figure 3-2 illustrates the variables related to cross-section dimensions and the main variables related to prestressed and non-prestressed longitudinal steel reinforcement.

In addition, the following Figure 3-3 shows the experimental setup of all the tests recorded in the ACI-DAfStb-PC database. Two symmetric point loads applied on a simply supported beam. The effective span is considered to be the distance between central axes of the supporting plates. In cases where there is only one point load applied in the middle of the span, in order to maintain a uniform structural configuration, the load is divided into two point loads separated by a distance equal to half the length of the load plate $c = 2a_F$. The point load is divided in two equal loads separated by the calculated distance c as can be seen in Figure 3-4.
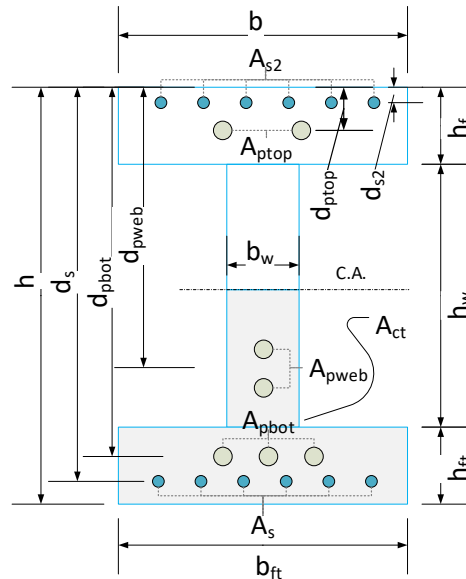
Figure 3-2 Notations used for cross-section dimensions and longitudinal reinforcement parameters
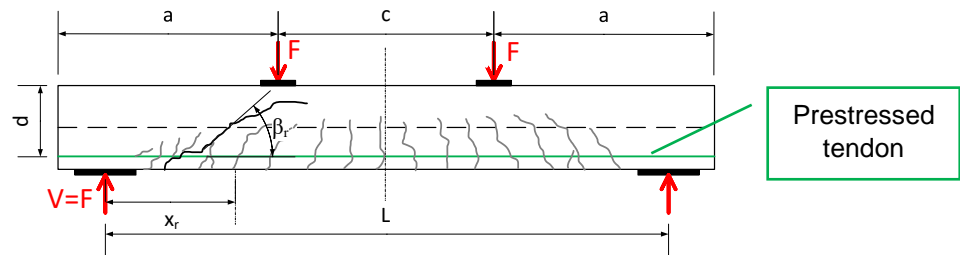
Figure 3-3 Notation used for load and beam

Figure 3-4 Definition in case of a single point load [47]

Different characteristics can be analyzed to continue describing the ACI-DAfStb-PC database and better understand the data used. Figure 3-5 (A) shows that almost half of the tests (48%) are rectangular beams, a small part (8%) are T-shape beams and the rest (44%) are I-shape beams. This is important because it should be noted that composite cross-sections can have a higher performance because they have a higher moment of inertia than rectangular beams, but at the cost of weaknesses in the webs, where shear-tension failure mode has to be verified checking the principal stresses along the height of the beam. This creates a break between rectangular and I/T-shape beams because the latter group requires the verification of one type of shear failure more than the rectangular beams.

Similarly, it is possible to argue about the influence of the non-prestressed longitudinal reinforcement on the shear capacity of prestressed beams. Figure 3-5 (B) indicates that most of the tests (68%) do not contain non-prestressed longitudinal steel reinforcement, which should be considered in the discussion of results. Since, as mentioned in the literature review, the longitudinal reinforcement is one of the main parameters for a shear-transfer action like the dowel action.

Finally, on can question the influence of the prestressing method used, where according to Figure 3-5 (C), one can see that the database has an even distribution. The main differences between both methods could be the differences considering prestressing losses and how the prestress force is transferred to the concrete.
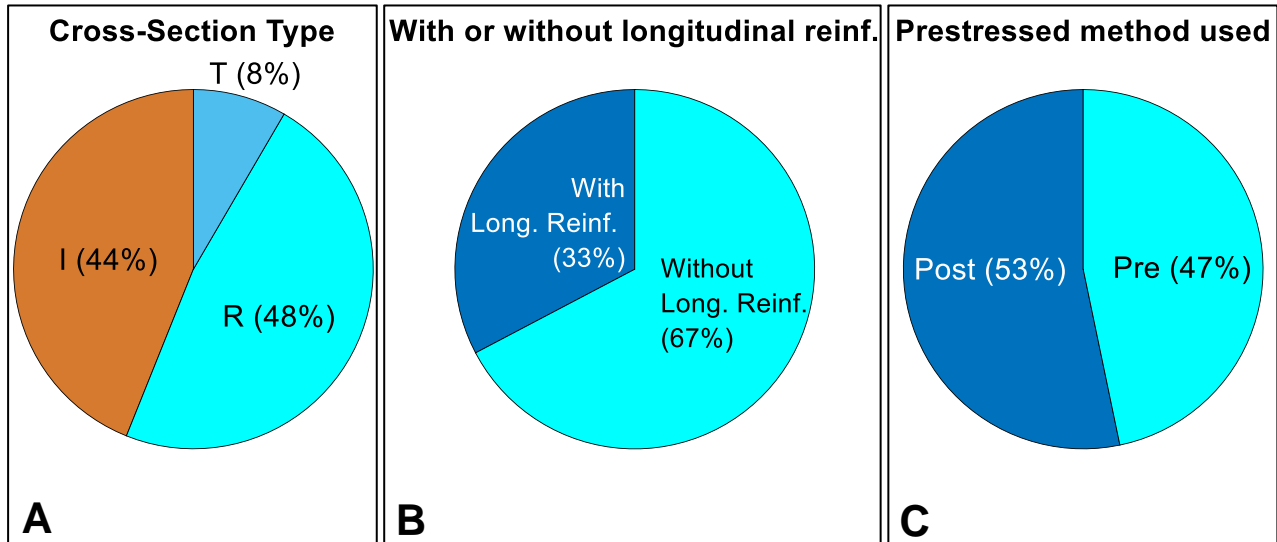
Figure 3-5 Main characteristic of the ACI-DAfStb-PC database.

Figure 3-6 shows that most of the beams have a height of less than 300 millimeters, although some experiments are in the range between 500 and 1100 millimeters in height. The largest group comprises beams between 200 and 300 millimeters high. It is not easy to perform many full-scale tests on tall beams, so it is understandable to see the trend favorable for small beams. This tendency does not seem to disturb the intended results in evaluating the effect of prestressing force, but the effect of beam size is currently being studied and considered in some design codes.

Figure 3-7 shows a feature that has been defined at the time of filtering the tests for ACI-DAfStb-PC database. The slenderness $a/d > 2.4$, in order to have a consistent database to evaluate, where beam shear-transfer actions mainly govern. It should be remembered that in the case of deep beams, the arching action governs, and the shear carried is equal to the plastic strength calculated [16], a case study that is different from the one intended.
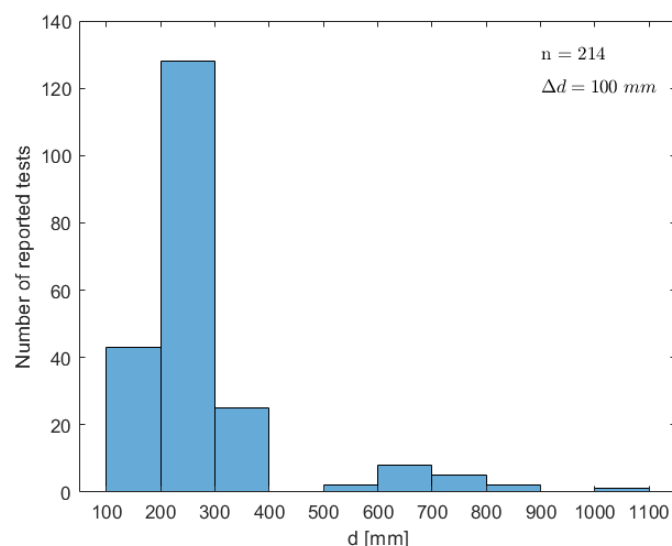
Figure 3-6 Effective depth distribution in ACI-DAfStb-PC database
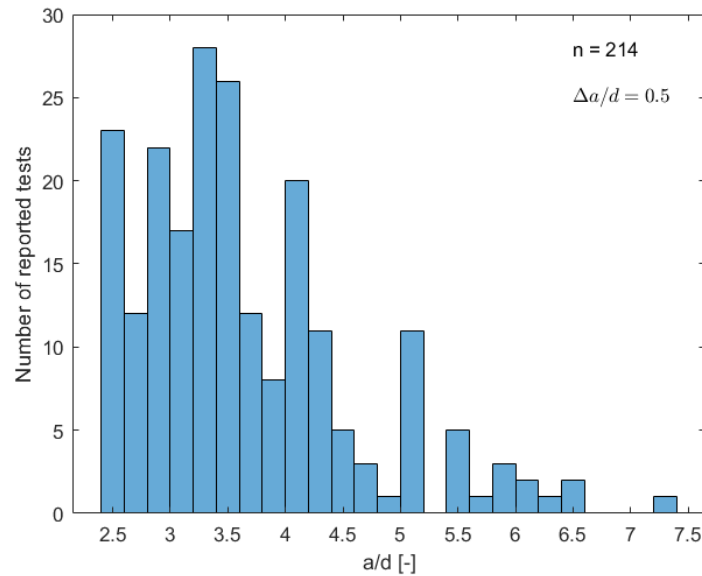
Figure 3-7 Slenderness distribuion in ACI-DAfStb-PC database

3.2 MATERIAL PROPERTIES

The materials and their properties are the most relevant factors influencing the results to be obtained; therefore, it is necessary to look at the database's characteristics for the concrete, steel, and prestressed steel used.

3.2.1 Concrete compressive strength

Of the data collected, this is perhaps the most influential one in which the standardization of methodologies applied to the different control specimens of varying dimensions needs a thorough evaluation. The conversion factors between the different dimensions of the specimens are listed in the reference document [47], where the author obtains the cylinder strength of the control specimens and realizes control of the conversions factors used, proposing a bi-linear approach for normal-strength concrete and high-strength concrete. From the database file, the required value is the average cylinder strength $(f_{cm,cyl})$ obtained from the reported specimens. In the cases where the cube resistance was reported instead, the mean cube strength is transformed into mean cylinder strength using the bi-linear approach proposed in the last reference.

Now, looking at the database, can be seen that the compressive strength of the concrete tends to be less than 50 MPa. The mode is in the range of 30 to 40 MPa. which is a typical concrete strength used in practical cases.
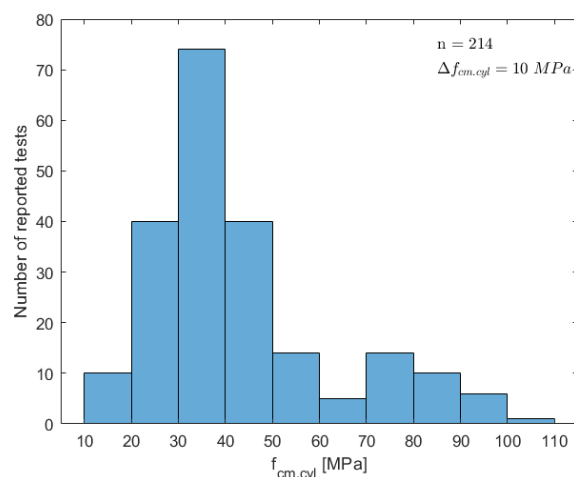
Figure 3-8 Mean cylinder compressive strength distribution in ACI-DAfStb-PC database

3.2.2 Longitudinal non-prestressed steel reinforcement

It is a parameter that influences the formation of flexural cracks in particularly, so it is necessary to visualize its relevance on the database under study. From the previous information, it is known that only 33% of the experiments contain longitudinal non-prestressed steel reinforcement. Of that percentage, 23% contain longitudinal reinforcement in compression as well.

Analyzing the characteristics of this group of experiments, Figure 3-9 shows that the most commonly observed values for yield strength are in the range of 400 to 450 MPa. Pointing to the commonly used steel rebar of 420 MPa, almost always used in everyday practice. Furthermore, there is a relevant group with high yield strength in the range greater than 550 MPa.

Similarly, the ratio of steel to gross area can also be analyzed by the called longitudinal reinforcement ratio of non-prestressed steel which is equal to:

$$\rho_s = \frac{A_s}{b \cdot d}$$

<div align="right">[Eq. 3-1]</div>

The histogram for this ratio in Figure 3-10, subdivided into class intervals of $\Delta \rho_l = 0.10$ %, shows that most tests have a small ratio, less than 0.5%. However, there is a considerable number of tests in the range of 1.5% to 2%, which is the upper limit for high reinforcement ratios according to some design codes. These high reinforcement ratios correspond to reinforcement with yield strength in a range between 350 and 500 MPa. as Figure 3-11 shows.
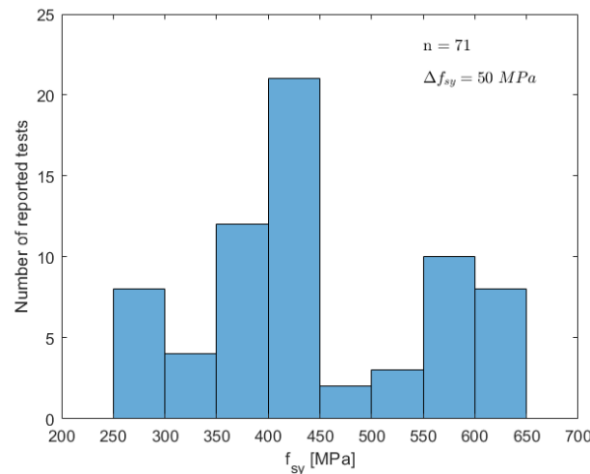
Figure 3-9 Yield strength distribution in ACI-DAfStb-PC database
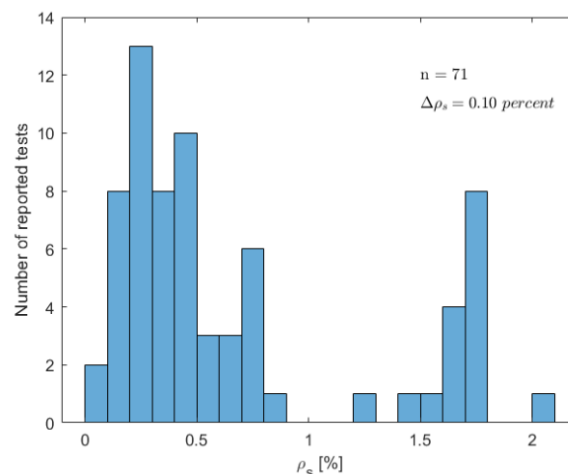
Figure 3-10 Non-prestressed longitudinal reinforcement steel ratio distribution in ACI-DAfStb-PC database
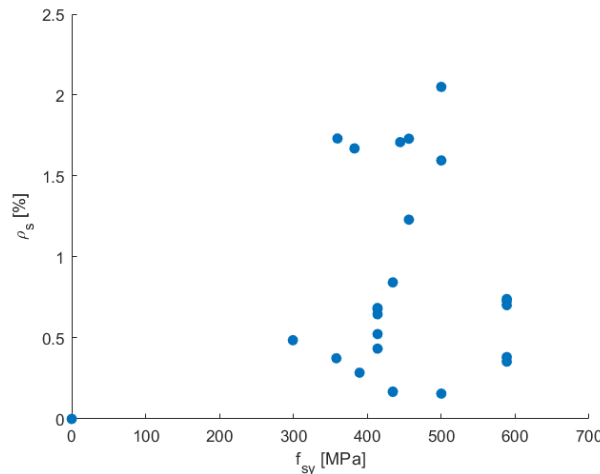
Figure 3-11 Scatterplot for non-prestressed longitudinal reinforcement steel ratio vs yield strength in ACI-DAfStb-PC database

3.2.3 Prestressing steel

This is the parameter to be studied in order to investigate its influence on flexural-shear failures. Therefore, the relevance of this parameter calls for an in-depth analysis of its characteristics within the database. It is known that out of the 214 experiments, 100 beams are pre-tensioned and 114 are post-tensioned, and analyzing these groups as a whole gives the following histograms.

Figure 3-12 shows that most of the tests are in the range of $1400 < f_{py} < 1800\ Mpa$, with the peak at the range of yield strength between 1400 and 1500 MPa. A small group is in the range of low yield strengths, less than 1000 MPa.

As this tensioned steel is added as longitudinal reinforcement, the longitudinal reinforcement steel ratio will also be modified. So, the total longitudinal reinforcement ratio is equal to:

$$\rho_l = \rho_s + \rho_p = \frac{A_s}{b_w \cdot d} + \frac{A_p}{b_w \cdot d} \qquad \text{[Eq. 3-2]}$$

Where A_p is the total area of longitudinal prestressed steel reinforcement, the histogram of this variable in Figure 3-13 indicates that most tests are configured for a small range of reinforcement ratios. The main group is in the range $(0\% < \rho_l < 1.25\%)$, which at first impression seems to indicate that the beams contain regular amounts of longitudinal reinforcement. However, this criterion can be refined with the called mechanical reinforcement ratio (ω_l) that is defined as follow.

$$\omega_l = \omega_s + \omega_p = \frac{A_s \cdot f_{sy}}{b_w \cdot d \cdot f_{cm}} + \frac{(A_{pbot} + A_{p.web}) \cdot f_{py}}{b_w \cdot d \cdot f_{cm}} \qquad \text{[Eq. 3-3]}$$

Where $(A_{pbot} + A_{p.web})$ is the area of longitudinal prestressed reinforcement in tension, as the database classifies the location of tendons. This parameter relates the ratio of the yield strength of steel and the mean compressive strength with the gross area. Figure 3-14 shows the histogram related, and the distribution indicates a peak at ratios of $0.1 < \omega_l < 0.2$, decreasing up to $\omega_l = 0.7$ approximately. Considering that $\omega_l > 0.20$ indicates highly reinforced beams as stated in [47], more than half of the tests are carried out for highly reinforced beams.
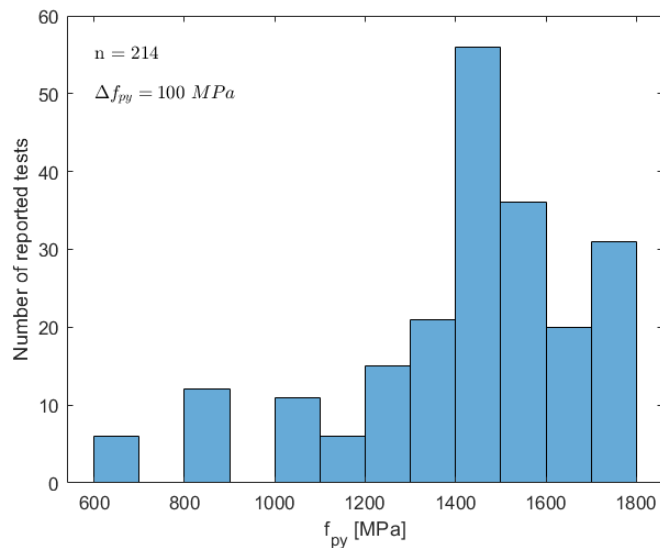
Figure 3-12 Prestressing steel yield strength for ACI-DAfStb-PC database
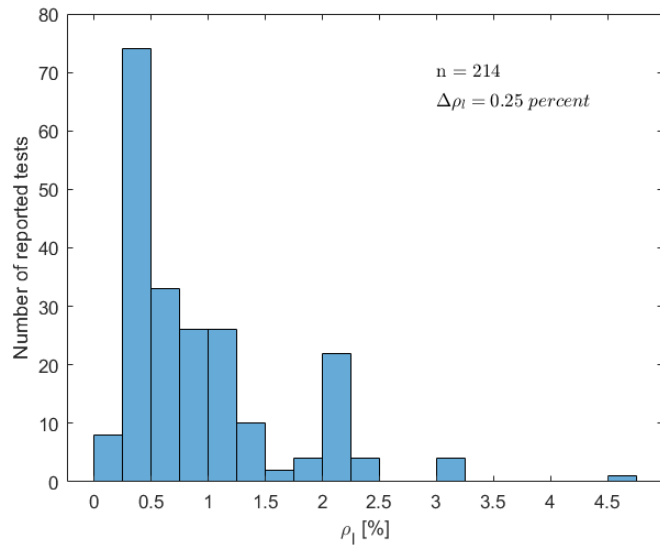
Figure 3-13 Total longitudinal reinforcement ratio for ACI-DAfStb-PC database
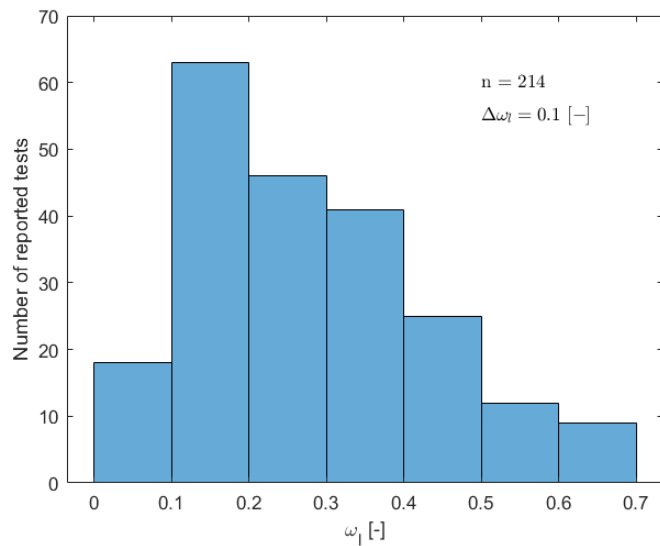
Figure 3-14 Mechanical reinforcement ratio for ACI-DAfStb-PC database

The magnitude of the prestressing force in the tests can be analyzed next. Figure 3-15 presents the histogram for the magnitude of the stress generated at the gross area due to the prestress force applied.

$$\sigma_{cp} = P/A_c$$

Where P is the total effective prestress force applied, and it is equal to the effective prestress (σ_{pp}) times the total area of prestressing steel (A_p). The gross area A_c is calculated easily for rectangular beams as $A_c = b \cdot h$, and for I/T shape beams the gross area is calculated according the given dimensions of the web and flanges. The magnitude of the prestress is distributed mainly in the range between 2 and 6 MPa. according to the histogram below.
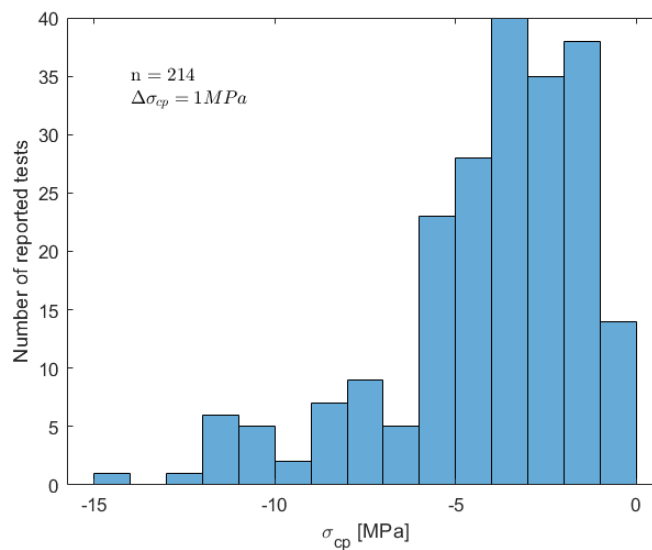
Figure 3-15 Axial concrete stress at center of gravity for ACI-DAfStb-PC database

The above figure may give more information if the prestress applied is related to the compressive strength of concrete. For this purpose, the factor called dimension-free axial force is defined as follow.

$$\nu_P = \sigma_{cp}/f_{cm}$$

Figure 3-16 presents the distribution of the dimension-free axial force. It can be interpreted as the percentage of prestressing applied in relation to the concrete strength. It is noted that this percentage is commonly in the range up to 15%.

The normal force applied is equal to the effective prestressed force, as all tendons are straight. To visualize the magnitude of this parameter, the scatterplot presented in Figure 3-17 relates it with the dimension-free axial force analyzed before. One group of experiments follows an almost linear trend between the two parameters shown in the scatterplot. An analysis of this group shows a ratio of equal to $1/850 = P/\nu_p$. The remaining 13% of the tests tend to have a much higher prestressing force applied for certain dimension-free axial force value. This denotes higher cross-sections or higher mean compressive strength of concrete for this group.
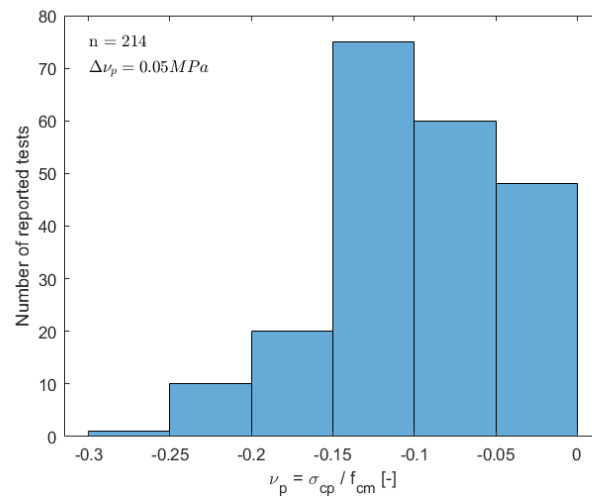
Figure 3-16 Dimension-free axial force for ACI-DAfStb-PC database. Considering prestress with negative sign.
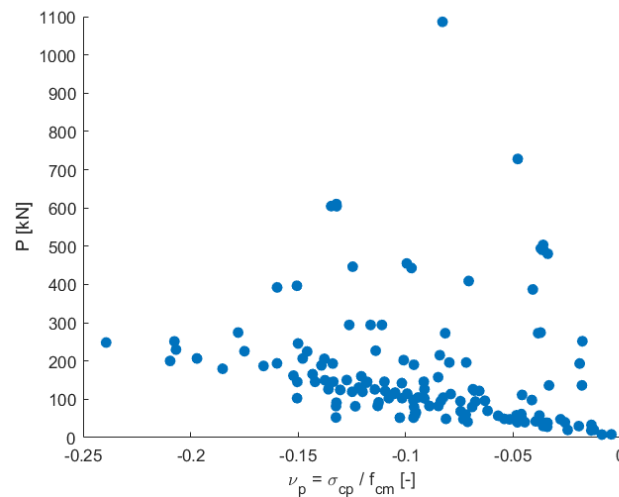
Figure 3-17 Scatterplot for dimension-free axial force vs prestressed force applied for ACI-DAfStb-PC

Another characteristic of the database seen in the Figure 3-18 is that the rectangular beams are mostly post-tensioned and less than 500 mm high and the prestressed rectangular beams are the tallest. The I-shape beams are also mostly less than 500 mm in height, and the T-shape beams, as most of the experiments, have a heigh of around 300 mm. Slenderness ratio values are also well distributed in the case of post-tensioned or pre-tensioned beams.
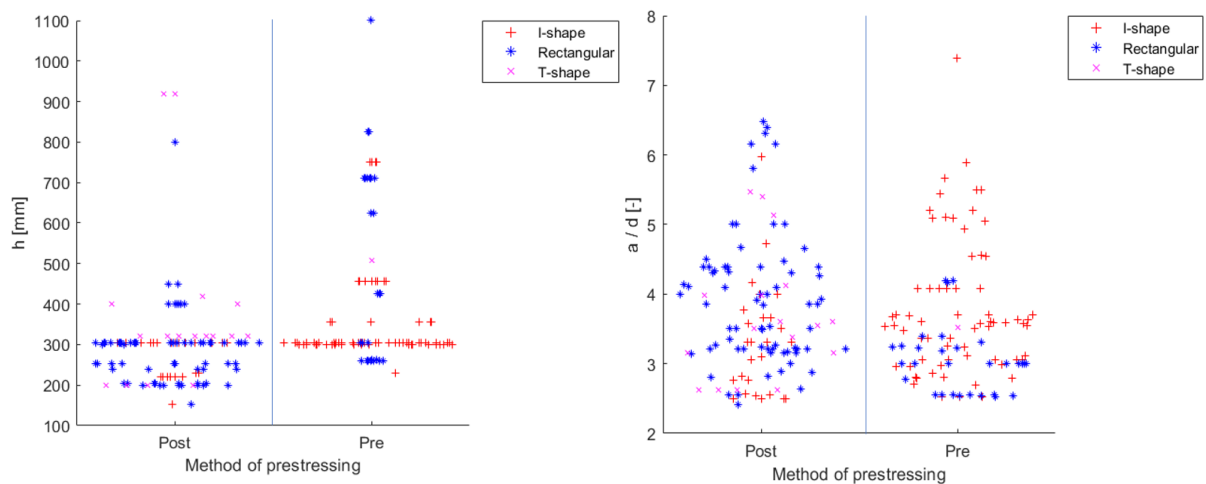
Figure 3-18 Distribution of Post- or Pre- tensioned beams according to the height or slenderness

3.3 SHEAR FAILURE MODES DESCRIBED

For the different tests collected from papers for the database some describe the shear failure modes according to the definitions given in Section 2.1.2 as follow.

- **ST**: Shear-tension failure observed.
- **SC**: Shear-compression failure observed.
- **FS**: Flexural-shear failure observed.

Some of them follow the classification stated by [8], then some beam's shear failure mode was denoted as web crushing failure (W-C), defined as the result of the loss of shear flow between flanges in tension and compression due to crack formation that transformed the beam into a tied arch. For I-beams, the thrust developed in the tied arch causes high compressive stresses in the web, causing a sudden and destructive failure.

- **W-C**: Web crushing failure observed.

Other papers report tests with mixed failure modes because they suspect a flexural failure before a shear failure, and in some cases, it was challenging to determine when a flexural-shear failure occurred instead of a shear-compression failure based only on observations.

- **SC-F**: Shear-compression and flexural failure observed.
- **FS-SC**: Flexural-shear or shear-compression failure (not distinguished).
- **FS-F**: Flexural-shear and flexural failure observed.

The last group of tests doesn't have a shear failure mode described by the author and were denoted as follow.

- **n**: Not described in paper/document.

Another helpful information given in the database is the description of the critical crack that led to the shear failure, according to the definitions provided in section 2.1.1. If the crack is not described, the test is marked as "without description" (n). Then the groups formed are as follow.

- **DC:** Flexural-shear crack.
- **WC:** Shear-tension crack.
- **n:** no specification given.

Figure 3-19 (A) below shows the percentages corresponding to each type of crack stated, and this is the starting point for selecting the tests related to flexural-shear failures, closely related to flexural-shear cracks. For Figure 3-19 (B), the failure modes derived from the flexural-shear crack (DC) are reported, where the flexural-shear failure is the most common case with 52% of the cases, followed by the shear-compression failure with 45%, the rest is for some individual cases for combined or not very clear failure modes. Finally, Figure 3-19 (C) shows that for the case of shear-tension cracks, the failure mode is not denoted always as shear-tension, some cases (36%) are described as Web-Crushing failure [8], without the presence of flexural cracks.

The classification proposed according to the type of shear crack and the shear failure mode is showed in Figure 3-19, using all the tests form ACI-DAfStb-PC database.

From the information given by Figure 3-19, it should be noted that the case of interest for the later results correspond to the group that develops the Flexural-Shear cracks, which is 52% of the reported experiments. From the group "n," there is no description, but it is possible to select from this group the rectangular beams, which will necessarily develop a flexural-shear failure.
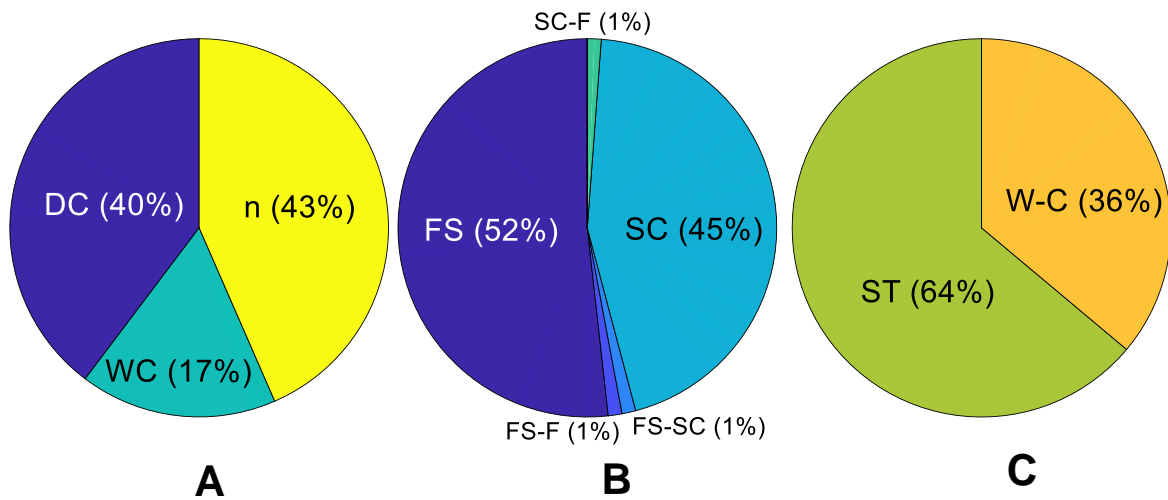
Figure 3-19 Description of the ACI-DAfStb-PC database according to the shear failure crack and shear failure mode.

3.4 LOCATION OF THE FAILURE CRACK x_r

To estimate the failure crack location (Critical Shear Crack (CSC) location), the background documents of ACI-DAfStb-PC database indicates that the location is equal to:

$$x_r = 0.65 \cdot a$$

[Eq. 3-6]

Where a is the distance of point load F_{ext} form support axis.

This relationship was determined based on an analysis of experiments that reported the location of the CSC in prestressed beams. The evaluation consisted of the results of 15 beams and the distance of the crack x_r was determined in accordance with [47] which is briefly explained below.

Determination of location of the failure crack for reinforced concrete members without shear reinforcement

The distance x_r is the distance of the CSC from the support axis. It is determined as the average of the distances $x_{r,o}$ and $x_{r,u}$ that are measures on the upper and lower surface of the beam as the following Figure 3-20 shows.
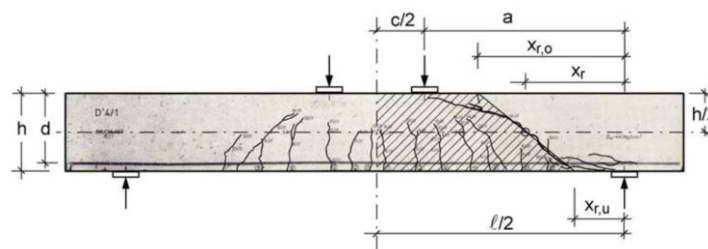
Figure 3-20 Measures for the location of the Critical Shear Crack (x_r) [47]

Most reports do not provide crack patterns and these were excluded from this calculation. The crack patterns provided for beams with a slenderness ($a/d > 2.4$) were examined plotting a scatterplot with dimension-free values for the axis, x_r/d versus a/d (Figure 3-21). Where x_r is equal to:

$$x_r = 0.5 \cdot \left(x_{r,o} + x_{r,u} \right)$$

[Eq. 3-7]

The region to look for the CSC is $(d < x_r < a - d)$, since the flexural-shear crack can only occur in this region as was reviewed in section 2.3.1. Beams exceeding the upper boundary are considered to perform a flexural failure since the failure cracks are close to midspan.

It is expected for prestressed members comparing with reinforced concrete members, that the location of the CSC is nearer the point load applied due to the influence of stresses in compression in the tensioned side of the beam. Analyzing the 13 tests that reported the location of the CSC, the lower boundary identified is $x_{r,min} = 0.25 \cdot a$ and the upper boundary reaches up to $x_{r,max} = a - d/2$. Between these two boundaries an intermediate relation that corresponds to the trend of the data $(x_r = 0.65 \cdot a)$ is the proposed relationship for beams without data of the location of the failure crack.
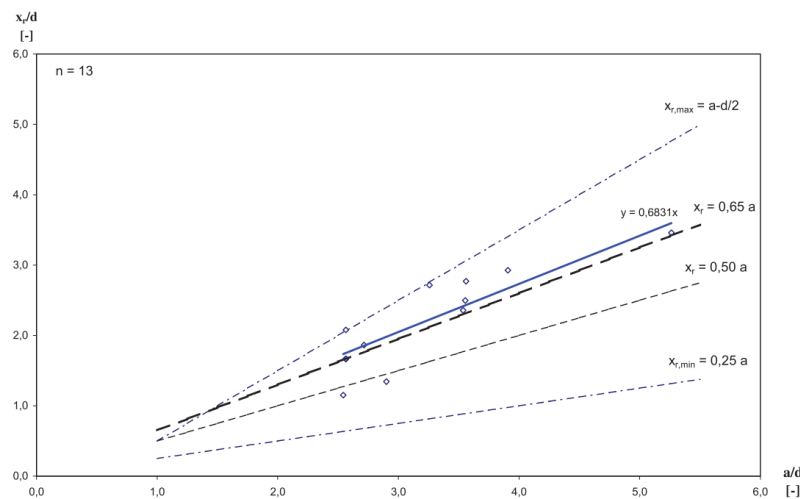
Figure 3-21 Proposed relationship for location of the CSC for prestressed concrete beams without shear reinforcement [47]

3.5 CONTROL CRITERIA FOR FLEXURAL AND ANCHORAGE FAILURE

These control criteria (called kon8 for assessing calculated flexural failures and kon11 for assessing anchorage failure) are developed based on the judgment of the database authors, as detailed in the following sections for each one. The result of these control criteria is specified in the database file, unlike the other control criteria used, because these are analytical results based on certain assumptions that can be very conservative, as in the case of anchorage failure control. The usefulness of these control criteria is left to the user's discretion and the results obtained in the analysis, but in principle, they did not condition the elimination of tests to keep a large number of them. As it is detailed in Table 3-2, these control criteria mark a total of 101 tests from the ACI-DAfStb-PC database, that has 214 tests, of which 44 correspond to the flexural failure assessment and 57 to the anchorage failure assessment.

3.5.1 Assessment of calculated flexural failures

It is necessary to have a parameter that indicates analytically whether a flexural failure occurred prior to a shear failure. Then, the relationship between the ultimate bending moment reached and the calculated value is functional and is defined as follows.

$$\beta_{flex} = \frac{\mu_u}{\mu_{flex}} \; [-]$$

[Eq. 3-8]

Where:

Non-dimensional moment at flexural failure: $\mu_u = \frac{M_u}{b \cdot d^2 \cdot f_{cm}} \; [-]$

Ultimate flexural moment: $M_u \; [N \cdot mm]$

Compression zone width: $b \; [mm]$

Effective depth: d $[mm]$

Mean concrete compressive strength: f_{cm} $[MPa]$

If the magnitude of this coefficient is greater than one $(\beta_{flex} > 1)$ means that the failure calculated was due to flexure. For a detailed explanation of this procedure refer to Appendix B.

3.5.2 Anchorage failure

The purpose of this conditional is to verify the anchorage capacity at the end support according to the criteria explained in detail in Appendix B. The provided anchorage length $l_{b,prov}$ is compared with the required anchorage length $(l_{b,req})$ through the relation:

$$\beta_{lb} = \frac{l_{b,req}}{l_{b,prov}} \ [-]$$

[Eq. 3-9]

If $\beta_{lb} > 1$, the intended anchorage length is not sufficient, an anchorage failure has likely occurred.

3.6 DEFINITION OF SUBSETS FOR ANALYSIS

It is crucial to have a database correctly correlated with the type of failure under study. In this case, the flexural-shear failure is the case of study, and the tests must be related.

The complete ACI-DAfStb-PC database contains 214 experiments, and not all of them failed due to the development of a flexural-shear crack, and different cross-section shapes were used. Then it is necessary to have different subsets to avoid biases in the results.

The first task to form the **first subset** was the exclusion of experiments that have not failed due to the development of a flexural-shear crack, the called "Critical Shear Crack" for some authors [9]. In this way, to form the first subset the following tests that meet any of the following conditions were excluded.

- Shear-Tension (ST) failure mode reported. (23 experiments)
    - Elzanaty 1985, CW: 1, 2, 3, 5, 6, 7, 8 and 9.
    - Funakoshi 1984: Specimen 3.
    - Mikata 2001: 014_T-0-20, 015_T-0-40, 017_HT-0-20 and 018_HT-0-40.
    - Funakoshi 1981: 006_10, 008_14 and 009_19.
    - Funakoshi 1982: 006_38, 007_39 and 008_40.
    - Choulli 2007: S1E, S1W, S2E and S2W.
- Web-Crushing (W-C) failure mode reported. (13 experiments)
    - Arthur 1965: 035_B9.
    - Evans 1963: 019_S19, 025_S25 and 027_S27.
    - Kar 1968: 021_I-15, 024_I-19, 025_I-20, 026_I-21, 029_D3, 030_D4, 031_D5, 034_D8 and 035_D9.
- Unknown failure mode (n) and composite shape of cross-section (I or T shape). (35 experiments)
    - Regan 1971, P: 10, 11, 12, 15, 16, 47 and 48.
    - Olesen 1967: B1434 and B1441.
    - Sozen 1959, B: 1120, 1129, 1140, 1210, 1226, 1229, 1234, 1235, 1250, 1261, 1316, 1326, 1341, 2126, 2209, 2223, 2230, 2241 and 2268.
    - Sato 1987: 001_3-4 and 004_3-7.
    - Takagi 2000: 001_IN-1 and 002_IN-2.
    - Ito 1997: 001_M-B 100.
    - Durrani 1987: 1.

This last group of beams was separated in a conservative manner since there is no certainty in the failure mode of an I/T beam without at least a report of the crack development and

observations made during the experiment. To verify some tests classification, other publications were useful, such as [5] and [12]. At the end, 71 tests were excluded from the original ACI-DAfStb-PC database to form subset 1.

To form the **second subset**, tests of beams with a I/T cross-section shape (41 tests) were excluded from subset 1. As intended for the new Eurocode (prEN1992) proposal, only rectangular beams remain, where the procedures outlined apply only for beams with flexural-shear cracks.

For the **third subset**, the verifications presented in Section 3.5 are considered, excluding experiments from subset 2 where the condition for flexural failure assessment or anchorage failure is not reached (36 tests). It is expected to increase the accuracy of the approaches, reducing possible biases related to anchor failures especially, although this verification is somewhat conservative, its usefulness will be evaluated assessing the shear design provisions in the next chapter 4.

Based on the above, the three subsets have different characteristics, of which the main ones are summarized in Table 3-2.

Table 3-2 Main characteristics of the subsets stated

Subsets for comparison	Cross-section shape			Total number of experiments	Verifications not fulfilled in:	
	Rectangular	I-shape	T-shape		Flexural Failure	Anchorage Failure
ACI-DAfStb-PC	102	94	18	214	44	57
Subset 1	102	41	0	143	31	39
Subset 2	102	0	0	102	20	16
Subset 3	66	0	0	66	0	0

Due to the selection of data to form the different subsets, slight changes in the distribution of certain variables are expected. In the case of the variables a/d, $f_{cm,cyl}$ and f_{py}, the mode remains in the same range for the histograms of all the subsets as Figure 3-22 -B, C, D show. In other cases, the histograms present changes between subsets. The variable d is one case, where for subset 3, the mode decreases to the range of 100 to 200 mm, as Figure 3-22-A shows. In the case of longitudinal reinforcement ratio (Figure 3-22-E), the mode in the range of 0.25 to 0.5, for ACI-DAfStb-PC and subset 1, increases to the range of 0.75 to 1 for subsets 2 and 3. This change the mechanical reinforcement ratio in the same way, which increased the mode range for subsets 2 and 3 as seen in Figure 3-22-F.
Certain variations exist between subsets for the histograms for prestressing stress at the concrete face. ACI-DAfStb-PC mode is located between 3 to 4 MPa, but for subsets 1 to 3 range from 1 to 2 MPa, as Figure 3-22-G shows. Almost the same behavior for the distribution of the dimension-free axial force histograms (Figure 3-22-H), where the peak is shifted to lower values, the peak or mode located in range -0.15 to -0.15 MPa. for ACI-DAfStb-PC is gradually decreasing to the range of -0.05 to 0 MPa. for subsets 2 and 3, denoting again the reduction of tests with high prestressing forces applied. The variation of prestressing losses between subsets is 5% to 10%. Subset 1 has an average of 64.7%, subset 2 68.9% and subset 3 73%. This amount of losses is unusual in today's common practice.
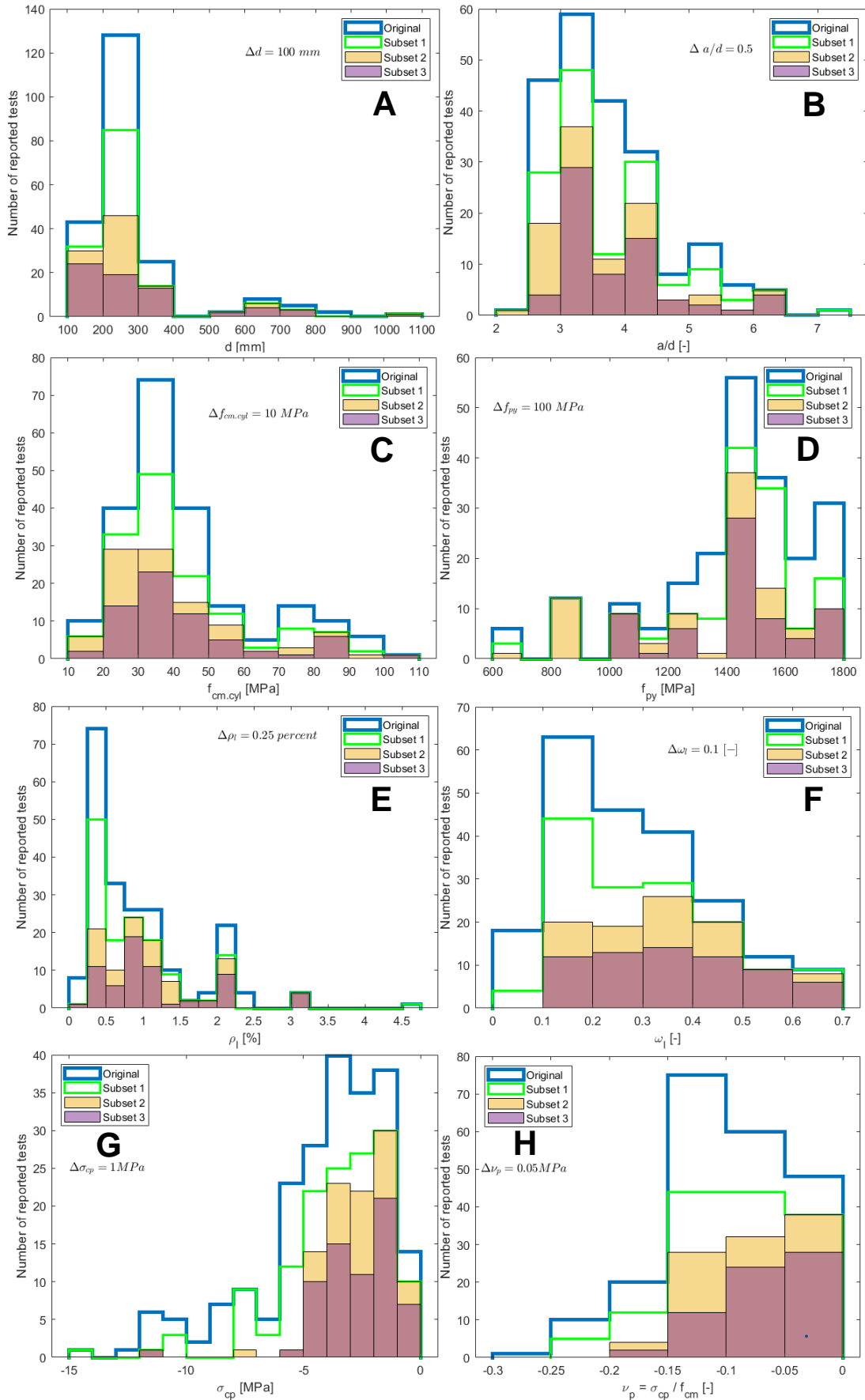
Figure 3-22 Histograms of the ACI-DAfStb-PC database for the different subsets for the variables: (A) effective height (B) shear span-to-effective depth ratio (C) mean compressive strength of concrete (D) Yield strength of prestressed steel (E) longitudinal reinforcement ratio (F) mechanical reinforcement ratio (G) axial concrete stress (H) dimension-free axial force

Finally, it is essential to see the information provided in Table 3-3. How the proportion between beams with longitudinal reinforcement and without varies between subsets +/- 7%, and the proportion between post-tensioned and pre-tensioned beams varies +/- 24% in favor of post-tensioned beam tests.

But the most relevant information can be said to be that concerning the variation in the classification of the failure modes and types of crack observed. Based on this classification, a criterion of the validity of the results obtained will be given.

Firstly, the ACI-DAfStb-PC or initial set of tests will not be included in the evaluation of shear design provisions as the study case is closely related to the flexural-shear failures. Then is convenient to exclude the selected experiments detailed before that represents 17% of the total 214 tests given at the beginning. For subset 1, 52% of tests were identified with a flexural-shear failure, 45% with a shear-compression failure and 3% other type of failure. Subset 1 compared to the other subsets, is the only one that includes tests with I-shape beams.

For subset 2, as mentioned before, only tests with beams with rectangular cross-section are included, modifying the proportions to 30% of beams reported with flexural-shear failure, 68% with shear-compression failure and 2% for other type. This subset of tests can be said that are the most related with the case study chosen, because I-shape beams require verification of web-shear (shear-tension) failure mode in addition to the failure modes related with the development of the critical shear crack, as is going to be shown later in the evaluation of the shear design provisions. Then this subset will be the most important to discuss the results and analyze the different approaches proposed later.

Subset 3 excludes the tests that don't comply with the control criteria stated within ACI-DAfStb document (Section 3.5) to assess flexural and anchorage failures. It seems that this subset ends up not being very useful, since a large number of tests are discarded because the anchorage control criteria stated ends up being very conservative as anticipated. Only 66 out of 102 potential tests end up being considered in this subset as shown in Table 3-3.

Table 3-3 Summary of relevant variations between subsets

	Number of tests	non-prestressed longitudinal reinforcement		Prestressing method		Shear crack			Failure modes for flexural-shear cracks (DC)		
		With	Without	Post	Pre	DC	n	WC	FS	SC	Other
ACI-DAfStb-PC	214	33%	67%	53%	47%	40%	43%	17%	52%	45%	3%
Subset 1	143	27%	73%	55%	45%	59%	41%	0%	52%	45%	3%
Subset 2	102	31%	69%	70%	30%	43%	57%	0%	30%	68%	2%
Subset 3	66	24%	76%	79%	21%	33%	66%	0%	0%	100%	0%

- **DC**: *Flexural-shear crack*
- **n**: *Not described in paper/document.*
- **WC**: *Shear-tension crack.*
- **FS**: *Flexural-shear failure observed.*
- **SC**: *Shear-compression failure observed.*
- **Other: FS-SC**: *Flexural-shear or shear-compression failure (not distinguished).* **FS-F**: *Flexural-shear and flexural failure observed.*

3.7 COMMENTS AND DISCUSSION

- In the different experiments that have been carried out over time, it is difficult to correctly identify the type of shear failure without the proper measuring instruments. Different estimations were made based on the shape of the cracks and their development throughout the experiment, but it was not possible to recognize the failure in several cases. As shear failure has brittle behavior, it is necessary to observe extremely short periods, which is now possible by employing modern measurement techniques such as DIC.

- The case study chosen of flexural-shear failure, must be represented in the experiments to avoid biased results. For this reason, different published works were used in which the different types of failure were recognized to corroborate the data handled and expand the information regarding the ACI-DAfSt-PC database. This is very important to have a correct correlation between the assumed failure mechanism and the one presented in the experiments.

- The document that explains most of the data collection process is [47], and the main assumption that affect the results obtained is the assumption regarding the location of the critical crack (or critical shear crack called according CSCT). The assumed location of $x_r = 0.65a$ for the experiments that did not have this information (more than 92%) is the only way to assume an intermediate value logically and not discard a considerable number of experiments for analysis. One of the extreme values $(d \ or \ a - d)$ could have been assumed as well, so an intermediate study was made in the next section for the evaluation of shear design provisions.

- From the different subsets defined, subset 3 is the one that could group the most conservative filters, considering that the method used to determine the anchorage capacity assumes some values that are on the safe side. Subset 2 is the one that most closely matches the assumptions made for the new Eurocode proposal alternatives, and subset 1 would fit well with the AASHTO-LRFD code, mainly because its detailed method considers the shape of the cross-section to determine the nominal flexural moment.

4 EVALUATION OF SHEAR DESIGN PROVISIONS

This chapter aims to obtain the mean shear capacity estimated by each proposed code (ACI318-19M, AASHTO-LRFD, EC2, and prEN1992), and with the obtained results compare codes in terms of accuracy or precision, and evaluate their reliability for the shear evaluation of prestressed beams without shear reinforcement.

The variables presented in Table 3-1 are used at least in one of the codes studied, but within each one, they may have a different notation or be agglutinated in another variable. Then the procedure to calculate the mean shear capacity and correlation of variables given in the database with the variables used within each design code will be explained in section 4.2 for ACI318-19M, section 4.3 for AASHTO-LRFD, section 4.4 for EC2, and section 4.5 for the EC2 proposal.

It is necessary to define some terms so that they can be used to calculate the mean shear capacity (V_{cm}). That means that the approaches given by the design codes are going to be changed to have at the end values that can be compared with experimental results. Some of these terms are explained in section 4.1 below.

4.1 APPLICABLE GENERAL CRITERIA

4.1.1 Forces acting on the critical section

The shear force reported in the ACI-DAfStb-PC database, considering the self-weight $(V_{u,Rep})$, is the experimental result that will be compared with the shear capacity obtained by the design codes. This shear force is the one obtained at the location of the critical shear crack (CSC) which is equal to $x_r = 0.65 \cdot a$ (refer to section 3.4).

Then, it is necessary to calculate the cross-sectional forces at x_r by applying an external load or prestress force and by consideration of self-weight. This can be done as follow considering that in all cases the structural configuration is a simple supported beam with to point loads located each at a distance a from the support axis (Figure 3-3).

It is convenient to capture the cross-sectional forces as function of the distance from the support axis in order to verify at different critical location if it's necessary for further analysis later.

- **Cross-sectional forces due to external load**
  Shear:

$$V_{ext}(x, F) = F - F \cdot (x \geq a) - F \cdot (x \geq L - a) + F \cdot (x = L) \, [N] \qquad \text{[Eq. 4-1]}$$

  Moment:

$$M_{ext}(x, F) = F \cdot x - F \cdot (x - a) \cdot (x \geq a) - F \cdot (x - L + a) \cdot (x \geq L - a) \, [N \cdot mm] \qquad \text{[Eq. 4-2]}$$

  Where, the external point load applied is $F \, [N]$, its distance from support axis is $a \, [mm]$, the distance of cross-section analyzed from support axis is $x \, [mm]$, and the effective span is $L \, [mm]$.

- **Cross-sectional forces due to self-weight**

  Shear:

  $$V_{sw}(x) = q \cdot \frac{L}{2} - q \cdot x \ [N]$$

  Moment:

  $$M_{sw}(x) = q \cdot \frac{x^2}{2} \ [N \cdot mm]$$

  Considering concrete density $q = 24 \ [kN/m^3] = 24 \cdot 10^{-6} \ [N/mm^3]$.

- **Cross-sectional forces due to prestress**
  As the database used distinguish three groups for the location of the prestressed tendons (top, web, bottom), this consideration is taken into account for the calculations too. The effective prestress force (σ_{pp}) applied to the different tendons area $(A_{p(top,web,bot)})$ exerts a bending moment dependent of the eccentricity of the tendons as follow.
  Shear:

  $$V_p = 0 \ [kN]$$

  Since the angle of inclination of the tendons is 0 degrees $(\theta = 0°)$, there is no vertical force due to the prestressing force.
  Moment:

  $$M_p = \sigma_{pp} \cdot A_{pbot} \cdot e_{pbot} + \sigma_{pp} \cdot A_{pweb} \cdot e_{pweb} + \sigma_{pp} \cdot A_{ptop} \cdot e_{ptop} \ [N \cdot mm]$$

  Considering the eccentricity for the different locations of the tendons:
  $$e_{pbot} = y_t - (h - d_{pbot}) \ [mm]$$
  $$e_{pweb} = y_t - (h - d_{pweb}) \ [mm]$$
  $$e_{ptop} = y_t - (h - d_{ptop}) \ [mm]$$
  Where, $d_{p(top,web,bot)}$ is the effective depth for the tendon locations considered.
  An important fact to note is that the effective prestress given in the database is assumed constant over the entire beam length, which is unrealistic because prestress losses are not constant along the span of the beam. However, it is practical as it avoids incorporating more factors that may bias the results related to shear capacity, as each design code has its approach to deal with prestress losses.

- **Ultimate cross-sectional forces acting:**
  Considering external load and self-weight.
  Shear:

  $$V_u(F) = V_{ext}(x_r, F) + V_{sw}(x_r) \ [N]$$

  Moment:

  $$M_u(F) = M_{ext}(x_r, F) + M_{sw}(x_r) \ [N \cdot mm]$$

- **Mean cross-sectional forces acting:**
  Considering external load, self-weight and prestress.
  Shear:

  $$V_{Em}(F) = V_{ext}(x_r, F) + V_{sw}(x_r) + V_p \ [N]$$

  Moment:

  $$M_{Em}(F) = M_{ext}(x_r, F) + M_{sw}(x_r) + M_p \ [N \cdot mm]$$

4.1.2 Concrete compressive strength

In the case of standards like ACI318-19M and AASHTO-LRFD, the specified compressive strength of concrete (f_c') is the necessary value for calculating the design shear resistance. The difference with the characteristic cylinder strength (f_{ck}), used in European standards, is that f_c' only represents a 9%- fractile, whereas f_{ck} represents a 5%- fractile value. So, in case one wants to generate comparable **design shear resistance** values, the relationship between f_c' and f_{ck} given by [48] and detailed in the relations below can be applied.

$$f_{ck} = f_{cm} - 8 \ [MPa]$$

$$f_c' = f_{ck} + 1.60 \ [MPa]$$

[Eq. 4-11]

To generate the intended **mean shear resistance** predicted by each design code to compare them with the shear resistance reported in experiments, it is necessary to use the mean concrete strength rather than the design value. Then, for the approaches according to Eurocode 2 or the new Eurocode proposal (prEN1992 draft 7), the value of the characteristic cylinder strength (f_{ck}) required in both codes will equal the reported mean compressive strength of concrete $(f_{ck} = f_{cm})$. For the approaches according to ACI318-19M and AASHTO-LRFD the specified compressive strength of concrete will be replaced too by the reported mean compressive strength of concrete $(f_c' = f_{cm})$.

4.1.3 Concrete tensile strength

It is reported that in many cases, no control specimens were cast to determine the concrete tensile strength. Then, for the database, the tensile strength of concrete was determined by empirical relationships using the compressive strength of concrete. Different equations are discussed in the background document [47], but for low strength concrete up to $f_{ck} = 50 \ MPa$ the average concrete tensile strength is calculated following the CEB-FIP MC 90 proposal, and for high-strength concrete $f_{ck} > 50 \ MPa$, the German standard DIN 1045-1 (2201) approach was used.

$$f_{ctm} = \begin{cases} 0.302 \cdot f_{cm}^{2/3} \ [MPa] \ for \ f_{cm} \leq 50 MPa \\ 2.12 \cdot \ln\left(1 + \left(\frac{f_{cm}}{10}\right)\right) \ [MPa] \ \ for \ f_{cm} > 50 MPa \end{cases}$$

[Eq. 4-12]

Where:
Mean compressive strength of concrete is: f_{cm}

The mean tensile strength of concrete will be useful for the calculation of the transmission length (l_{tr}) according to the approaches stated for the Eurocode in section 4.1.5. This term will have no relevance in the calculation of the shear capacity in case the minimum transfer length is met.

4.1.4 Yield strength of non-prestressed steel

It is assumed that the yield strength reported for the group of experiments containing longitudinal steel reinforcement is the value that corresponds to the mean yield strength (f_{ym}). Details about this parameter is provided in section 3.2.2.

4.1.5 Transfer of Prestress

The transfer of the effective prestressing stress from the tendon to the concrete varies according to the prestressing method employed. For pre-tensioned members, the force is transmitted through the bond; then, it requires a certain length to transmit the entire prestressing force from tendons. For post-tensioned beams, the tendons are connected to a steel anchorage embedded in the concrete, tendons are stressed against the concrete member itself, and the force is transferred directly between the prestressing strands and anchor [49].

Post-tensioning anchorage

The configuration of the anchorages that directly transmit the prestressing force causes a stress concentration in the anchorage zone; this causes transverse splitting stresses as the concentrated force gradually spreads in the structure. It is required a called disturbance length of de St.-Venant to have a uniform load distribution over the cross-section. The disturbance length is independent of the force magnitude and only depends on the member's geometry and the position of the prestressing anchors. According to de St.-Venant, the disturbance length is equal to the largest dimension of the cross-section, most of the cases the height of the beam [49]. Usually, the disturbance length should be treated in detail in case of analyzing the area near the supports in deep beams specially, but for the present case study that has slender beams, this case will not be a problem.

Introducing prestressing by bonding

To introduce the total effective prestressing force by bond it is required a transmission length (l_{pt}), and this is the case of pre-tensioned prestressing steel. The stress distribution is affected by the transfer of the prestress by bond along the transmission length, as mentioned before. Then, depending on the distance of the considered cross-section from the starting point of the transmission length, the effective prestress transmitted varies linearly from zero to its full value.

Consideration for calculation of shear strength according different design codes

It is necessary to verify the different cases that are treated in the database. At the same time, the different design codes have their approach to calculate the transmission length. Then, considering that the critical section location assumed equals $x_r = 0.65 \cdot a \, [mm]$, it will be verified if this distance is less than the required transmission length (l_{pt}) according to the different codes. In case $(x_r < l_{pt})$, the effective prestressing force applied (σ_{pp}) will be reduced according to each design code procedure, which in most cases is a linear relationship of distances.

To verify if it is necessary to consider a reduction of the effective prestressing force acting at the critical location in the procedures, the required transmission length is calculated according to each design code, then the calculated values are compared with the critical location x_r.

It is necessary to know the bond type to assume the factor related to the type of tendon that appears in the codes. This variable is given in the ACI-DAfStb-PC database with the notation b_{type} that is equal to 1 to consider strands and equal to 0 to consider wires in the procedure.

- **Eurocode 2 (EN1992-1-1:2004)**
  Section 8.10.2.2 from [35] details the procedure to estimate the transfer length, where different factors are assumed as follow:
    ○ Typo of tendon factor: $\eta_{p1} = 2.7 \, (wires) \; or \; 3.2 \, (strands)$
    ○ Bond conditions factor: Assumed for good conditions. $\eta_1 = 1$.
    ○ Assumed gradual release: $\alpha_1 = 1.0$
    ○ For mostly used 3 and 7-wire strands: $\alpha_2 = 0.19$
    ○ Tendon stress just after release: $\sigma_{pm0} = 0.85 \cdot f_{pu} \, [MPa]$, assumed.

  The transmission length considering a verification for ultimate limit states is equal to:

$$l_{pt2} = 1.2 \cdot \alpha_1 \cdot \alpha_2 \cdot \frac{\sigma_{pm0}}{\eta_{p1} \cdot \eta_1 \cdot f_{ctm}} \cdot \phi_p \, [mm] \qquad \text{[Eq. 4-13]}$$

  Where the mean tensile strength of concrete $(f_{ctm} \, [MPa])$ calculated according to EN1992-1-1 [35], and the diameter of the prestressing steel is $(\phi_p \, [mm])$.

- **prEN1992, draft 7**
  Section 13.5.3 of this document [38] details the procedure. The assumed factors to estimate the transfer length are as follow:
    - Assuming gradual release: $\alpha_1 = 1.0$
    - Typo of tendon factor: $\alpha_2 = 0.4 \ (wires) \ or \ 0.26 \ (strands)$
    - Bond conditions factor: Assumed for good conditions. $\eta_1 = 1$.
    - Tendon stress just after release: $\sigma_{pm0} = 0.85 \cdot f_{pu} \ [MPa]$, assumed.
    - Design factor for concrete: $\gamma_c = 1$

  The transmission length considering a verification for ultimate limit state is equal to:

  $$l_{pt2} = 1.2 \cdot \frac{\gamma_c}{1.5} \cdot \frac{\alpha_1 \cdot \alpha_2 \cdot \sigma_{pm0}}{\eta_1 \cdot \sqrt{f_{ck}}} \cdot \phi_p \ [mm]$$

  [Eq. 4-14]

  Where the mean compressive strength was used instead of the characteristic value, and the diameter of the prestressing steel is considered in millimeters.

- **ACI318-19M**
  The transmission length only depends on the diameter of the prestressing steel (ϕ_p) and the type of tendon used according to:

  $$l_{tr} = \begin{cases} 50 \cdot \phi_p \ [mm] \ for \ strand \\ 100 \cdot \phi_p \ [mm] \ \ for \ wire \end{cases}$$

  [Eq. 4-15]

- **AASHTO-LRFD**
  The procedure in this case study is much simpler and only requires part of the procedure, as there are only straight tendons in the database the vertical component of prestress (V_p) is equal to zero. Then, it's only necessary to work with the factor f_{po} that is defined as the modulus of elasticity of prestressing tendons multiplied by the locked-in difference in strain between the prestressing tendons and surrounding concrete.
  This factor f_{po} is stated that should increase linearly within the transfer length from zero at the location where bond starts to its full value at the end of the transfer length (l_t) defined as follow:

  $$l_{tr} = 60 \cdot \phi_p \ [mm]$$

  [Eq. 4-16]

  With the diameter of the prestressing steel (ϕ_p) in millimeters.

The procedures for each code were applied with all the tests in the ACI-DAfStb-PC database. With the transmission lengths calculated, the relation with the critical location is calculated as l_{tr}/x_r. If this relation results greater than 1 means that the transmission length is greater than the critical location, then the effective prestressing force needs to be reduced.

Figure 4-1 shows the case of Eurocodes, where the percentage of tests with $x_r < l_{tr}$ is 13% for prEN1992 and 1% for the current Eurocode. Figure 4-2 shows that for ACI318 and AASHTO-LRFD codes, 27% and 15% respectively, of tests have the critical location within the transmission length. This makes it necessary to consider within the calculation procedures the transmission length for the calculation of the shear resistance, having as input data the effective prestressing stress as a function of the condition of the transmission length as stated below.

$$\sigma_{pp} = \sigma_{pp} \cdot \frac{x_r}{l_{tr}} \ [MPa]$$

[Eq. 4-17]
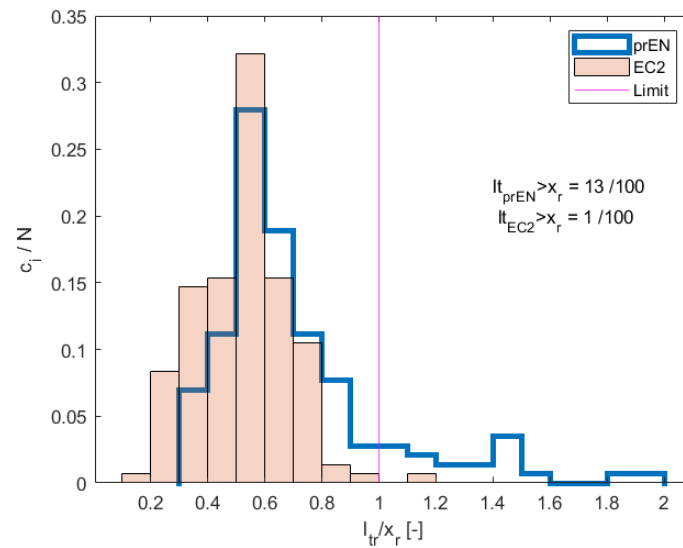
Figure 4-1 Histogram for transmission length in relation to critical location. For prEN1992 and EN1992-1-1
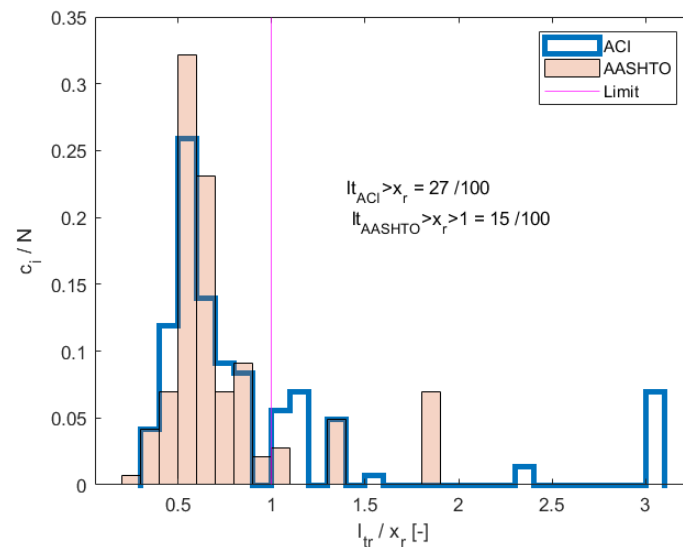
Figure 4-2 Histogram for transmission length in relation to critical location. For ACI318-19M and AASTHO-LRFD

The estimated values for the minimum transmission length are known to be conservative for any of the approaches studied. The results obtained in Figure 4-1 and Figure 4-2 indicated low percentages of tests with shorter transmission lengths than the required transmission length. To avoid further bias of the results due to different assumptions on the transmission length and to preserve a significant number of valid tests, it will be assumed that the required transmission length is met in all cases. This ends up ruling out the usefulness of subset 3 for comparative conclusions between approaches and makes subset 2 the most relevant for the conclusions.

4.1.6   Condition for Iterative process to calculate shear capacity

The iterative process for the calculation of the shear capacity in different design codes is necessary due to the dependence of certain factors (detailed in the last part of this section) on the applied external force F_{ext}. Keeping in mind that the overall ability of a structural member to withstand an imposed demand is called capacity, the external load related with the shear strength calculated (F_{cal}) must be equal to the external load assumed (F_{ext}). Considering the uniform structural configuration for all tests (simple supported beams with equidistant point loads), one can state the following equality:

$$F_{cal} = F_{ext} \ [N]$$

<div align="right">[Eq. 4-18]</div>

Considering that the equivalent external load at a critical location $x_r < a$ can be calculated after the estimation of the shear strength of concrete as follow:

$$F_{cal} = V_c - V_{sw}(x_r) \ [N]$$

<div align="right">[Eq. 4-19]</div>

The mentioned iterative procedure is applied for the following design codes due to:

- **ACI318-19M, approximate method.**
  Because one of the terms (V_u/M_u), the ultimate shear force divide by the ultimate bending moment, depends on the applied external force applied (refer [Eq. 2-20], [Eq. 4-7] and [Eq. 4-8]).

- **ACI318-19M, detailed method.**
  The calculation of flexure-shear strength is dependent on the external load applied, the last term $((V_i \cdot M_{cre})/M_{max})$ includes the shear (V_i) and bending moment (M_{max}) due to external loads (refer [Eq. 2-26], [Eq. 4-22], and [Eq. 4-23]).

- **AASHTO-LRFD**
  The net longitudinal tensile strain (ε_s) depends on the factored shear and bending moment (M_u, V_u) at the section being analyzed (refer [Eq. 2-32], [Eq. 4-7], and [Eq. 4-8]).

- **prEN1992**
  The effective shear span a_{cs} with respect to the control section depends on the relation (M_{Em}/V_{Em}), that varies according the external load applied. This factor is taken into account in the main formulation through the term d_{nom} (refer [Eq. 2-16], [Eq. 4-9]and [Eq. 4-10]).

The only case that doesn't requires an iterative procedure is the procedure stated for the current Eurocode (EN1992-1-1:2004). The iterative procedure explained to calculate the shear capacity can be summarized as shown in Figure 4-3 too.
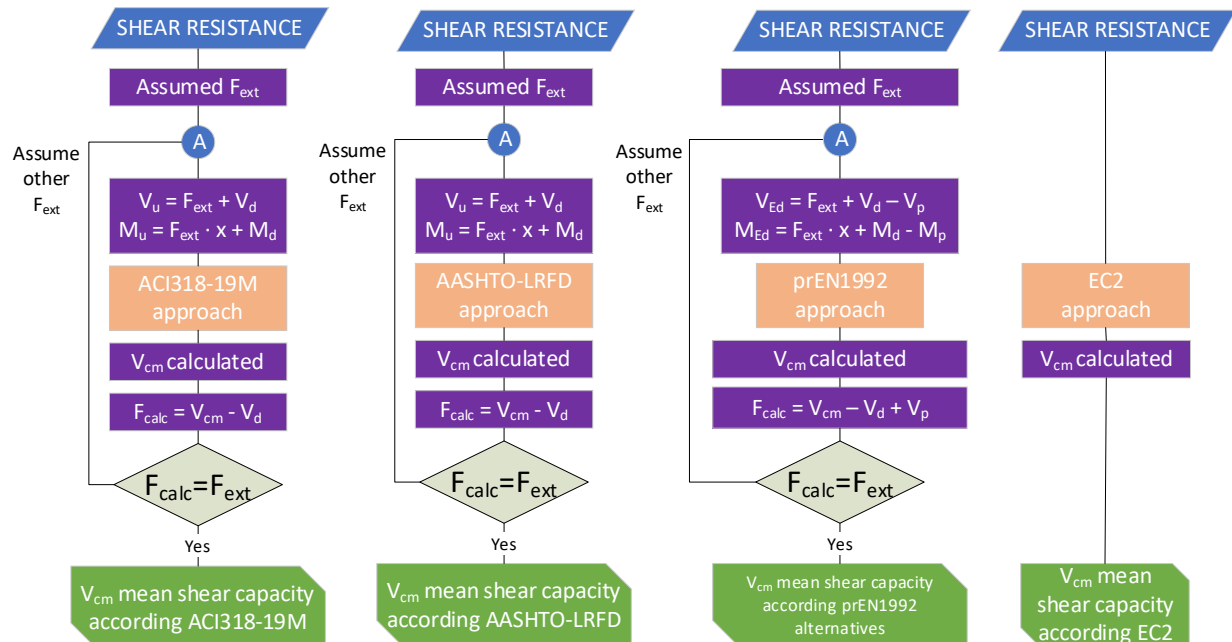
Figure 4-3 Iterative procedure for the calculation of the shear capacity according to the design codes studied.

4.2 SHEAR CAPACITY ACCORDING ACI318-19M

Unlike the Eurocode, the ACI318-19 code considers the prestressing force as a capacity and not as a preload. Thus, this design code distinguishes the prestressing force from the external axial forces (N_u), each case has its own procedure.

Considering the uniform test set-up detailed in the last chapter, no axial loads applied, and straight tendons, the acting forces at the critical cross-section will be defined as follows.

The shear and bending moment due to the unfactored dead load are going to be equal to:

Shear:

$$V_d = V_{sw}(x_r) = q_{sw} \cdot \left(\frac{L}{2} - x_r\right) [N]$$

[Eq. 4-20]

Moment:

$$M_d = M_{sw}(x_r) = q_{sw} \cdot \frac{L}{2} x_r - q_{sw} \cdot \frac{x_r^2}{2} [N \cdot mm]$$

[Eq. 4-21]

And the cross-sectional forces acting due to externally applied factored loads are equal to:

Shear:

$$V_i = V_{ext}(x_r, F) = F_{ext} [N]; \ while \ x_r < a$$

[Eq. 4-22]

Moment:

$$M_{max} = M_{ext}(x_r, F) = F_{ext} \cdot x_r [N \cdot mm]; \ while \ x_r < a$$

[Eq. 4-23]

It is necessary to correlate the information provided in the database with the required variables in this code. Some variables will be used with same notation as Table 3-1, like $h, h_f, h_{ft}, A_c, y_t, I_{cs}, L, x_r$ and others are going to be combined or redefined. This last group will be detailed below.

The effective depth of the prestressed tendons needs to be defined into a unique value, so it is necessary to calculate this value considering the tendons that are tensioned, resulting in the following expression:

$$d_p = \frac{d_{pbot}^2 \cdot A_{pbot} + d_{pweb}^2 \cdot A_{pweb}}{d_{pbot} \cdot A_{pbot} + d_{pweb} \cdot A_{pweb}} [mm]$$

[Eq. 4-24]

And the area of prestressing steel is considered as:

$$A_{ps} = A_{pbot} + A_{pweb} + A_{ptop} [mm^2]$$

[Eq. 4-25]

The aggregate factor is equal to one $(\lambda = 1)$ as all the experiments use normal aggregates, and the specified concrete strength (f_c') is replaced by the mean compressive strength of concrete (f_{cm}), following the explanation given in section 4.1.2 to obtain mean values comparable between design codes.

With this information it is possible to start with the calculation detailed below for the approximate and detailed method stated by ACI318-19M.

The procedure of design starts with the conditional that states that this method is valid if the effective prestressing force is greater than the lower bound, as stated below in [Eq. 2-19] $\left(A_{ps}f_{se} [N] \geq 0.4\left(A_{ps}f_{pu} + A_s f_y\right) [N]\right)$.

Where f_{se} is the effective stress in prestressed strand after all losses, defined in ACI-DAfStb-PC database as σ_{pp}. The specified tensile strength of prestressing steel f_{pu} is provided in the database as f_p, and as all the cases are beams without shear reinforcement the second term is

going to be equal to zero $(A_s f_y = 0\ [kN])$. Complying with this conditional the following simplified and detailed procedures are applicable.

4.2.1 ACI318-19M, Approximate method to estimate the shear capacity of concrete
Is one of the most straightforward methods where it is only necessary to calculate 4 values. The minimum concrete shear resistance $(V_{c.min})$ defined in [Eq. 2-23], and the concrete shear resistance (V_c) according to the three approaches defined in ([Eq. 2-20], [Eq. 2-21], and [Eq. 2-22]), where only the minimum value is captured. Then, the maximum value between $V_{c.min}$ and V_c will be considered the calculated shear strength of concrete.

In case the effective prestressing force results less than the lower bound ([Eq. 2-19]) the calculated shear strength by the approximate method is limited by the web-shear strength V_{cw} ([Eq. 2-28]) calculated using the reduced effective prestress force.

As the mean compressive strength of concrete is being used, the final calculated strength is a mean value denoted as $V_{c,m}$.

4.2.2 ACI318-19M, Detailed method to estimate the shear capacity of concrete
In this case the shear strength is equal to the minimum value of the flexural-shear strength (V_{ci}) and the web-shear strength (V_{cw}) calculated.

- **Flexural-shear strength (V_{ci})**
  It is calculated according to [Eq. 2-27], considering the following equalities for the use of the data from ACI-DAfStb-PC.
  The stress at the tensioned extreme fiber is calculated considering the three groups of prestress tendons that the ACI-DAfStb-PC defines (top, web, bottom) as follow.

  $$f_{pe} = \frac{A_{ps} \cdot f_{se}}{A_c} + \frac{\sigma_{p,(i)} \cdot e_{p.(i)} \cdot y_t}{I_{cs}}\ [MPa] \qquad \text{[Eq. 4-26]}$$

  Where A_c is equal to the gross area of the cross-section, I_{cs} the moment of inertia, y_t the distance of centroidal axis from bottom fiber, $e_{p,(i)}$ the eccentricity of tendons, and $\sigma_{p,(i)} = f_{se}(A_{p,(i)}/A_{ps})$ the effective stress at tendon for locations $i = top, web\ or\ bottom$.
  Then, the mean cracking moment due to external loads can be calculated as stated below

  $$M_{cre.m} = \frac{I_{cs}}{y_t} \cdot \left(0.5\lambda \cdot \sqrt{f_{cm}} + f_{pe} - \frac{M_d \cdot y_t}{I_{cs}} \right)\ [N \cdot mm] \qquad \text{[Eq. 4-27]}$$

  Obtained all the required values to calculate the flexural-shear strength, one has to compare the calculated V_{ci} with the lower bound stated in [Eq. 2-27].

- **Web-shear strength (V_{cw})**
  It is necessary to calculate the compressive stress in the concrete after all prestress losses, at the centroid of cross-section resisting externally applied loads ([Eq. 4-28]). In case the centroidal axis is located within one of the flanges $(y_t < h_{ft}\ or\ y_t > h - h_f)$ it is necessary to calculate the compressive stress at the junction of the web and flange.

  $$f_{pc} = \frac{A_{ps} \cdot f_{se}}{A_c}\ [MPa] \qquad \text{[Eq. 4-28]}$$

  All the experiments, in this database are straight, then the angle of inclination of the tendons is always zero $(\theta_p = 0\ [deg])$, then the vertical component of effective prestress force (V_p) will be zero too.

  With this information, [Eq. 2-28] can be applied to calculate V_{cw}.

Same as the approximate method, as the mean compressive strength of concrete is being used in the procedure, the calculated values represent the mean flexural-shear strength $V_{ci,m}$ and the mean web-shear strength $V_{cw,m}$. Both mean values are compared, keeping the lowest as the mean concrete shear strength $V_{c,m}$ calculated by the detailed method from ACI318-19M.

4.3 SHEAR CAPACITY ACCORDING AASHTO-LRFD

In this case, the procedure to follow is one of the most laborious and time-consuming since it also requires the most variables. Like ACI318, prestressing is considered a capacity, so the ultimate cross-sectional forces acting on the beam (V_u, M_u) are considered for the calculations.

The first step of this procedure is the calculation of the nominal flexural resistance (M_n). The main value required for this is the stress in prestressing steel at nominal flexural resistance. In order to refine the results, the stress in the prestressing steel is computed by a detailed analysis using the **strain compatibility** approach, where the following values where used.

- Concrete ultimate strain: $\varepsilon_{cu} = 3/1000 \; [-]$
- Ultimate strain of prestressing steel: $\varepsilon_{pu} = 35/1000 \; [-]$
- Yield strain of prestressing steel: $\varepsilon_{py} = f_{py}/E_p \; [-]$
- Ultimate strain of non-prestressed steel reinforcement: $\varepsilon_{su} = 45/1000 \; [-]$
- Yield strain of non-prestressed steel reinforcement: $\varepsilon_{sy} = f_{ym}/E_s \; [-]$

To start the calculation procedure is possible to begin dividing in a useful way the strain in the prestressing steel (ε_{ps}) into three separate states. The first is the effective strain in the tendon after losses (ε_{pe}), the second is the necessary strain to decompress the section to a condition of zero strain (ε_d), and lastly the strain resulted from strain compatibility, the strain due to nominal flexural strength $(\Delta\varepsilon)$. These can be calculated with the following relations.

$$\varepsilon_d = \frac{P_e}{A_c \cdot E_c} + \frac{M_p \cdot e_p}{I_{cs} \cdot E_c} \; [-]$$

[Eq. 4-29]

Considering the total effective prestress load equal to: $P_e = f_{pe} \cdot A_{ps} \; [N]$, where the effective stress after all losses is $f_{pe} = \sigma_{pp} \; [MPa]$.

$$\varepsilon_{pe} = f_{pe}/E_p \; [-]$$

[Eq. 4-30]

$$\Delta\varepsilon = \frac{d_p - c}{c} \cdot \varepsilon_{cu} [-]$$

[Eq. 4-31]

Where $c \; [mm]$ is the height of the compression zone, as can be seen in Figure 4-4 along with the illustration of all other variables of interest.

$$\varepsilon_{ps} = \varepsilon_d + \varepsilon_{pe} + \Delta\varepsilon \; [-]$$

[Eq. 4-32]

The total stain in prestressing steel can be estimated with approximate methods given in the same design code, but care must be taken to verify the prestressing stresses acting, since certain limits are given to the applicability of these simplified methods.
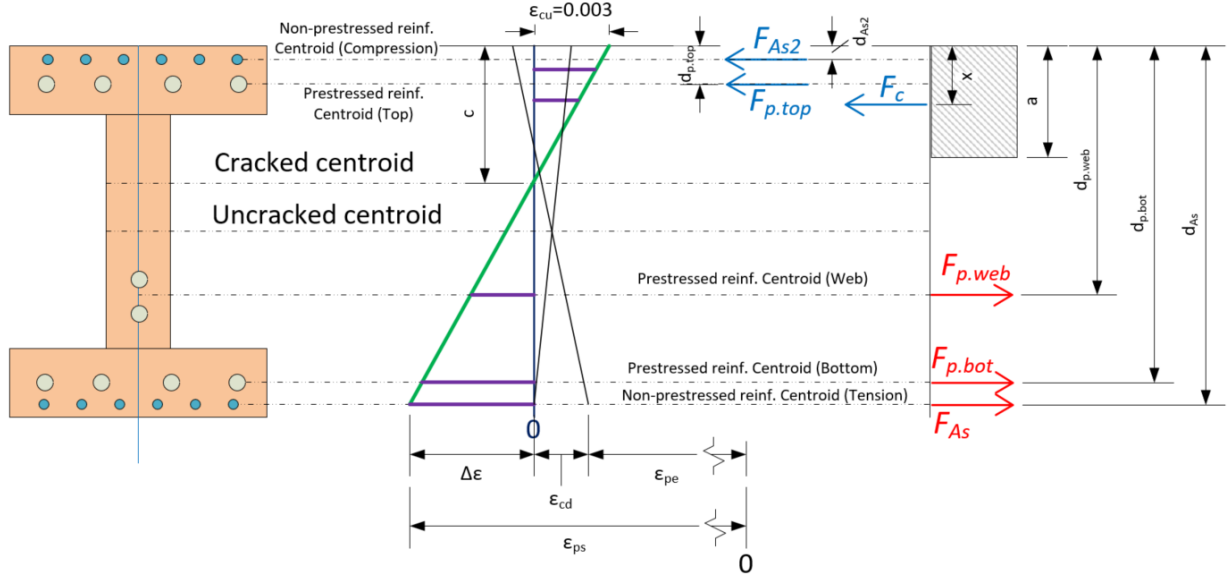
Figure 4-4 Strain and equivalent stress as section is loaded to nominal strength

With what has been established so far, it is possible to calculate the nominal flexural strength. Guided with the last Figure 4-4 to visualize a general case from the database, it is required to find the equilibrium on the cross-section looking for the equality between tensile and compressive forces. To achieve this the following condition must be met.

$$F_c + F_{As2} + F_{p.top} = F_{p.web} + F_{p.bot} + F_{As} \ [N]$$

[Eq. 4-33]

This is a general case, so in some tests, some terms may be excluded from the last equation, which can be started to be unpacked as follows.

The concrete compressive force resultant (F_c) is the first term. As show in Figure 4-4 an equivalent rectangular stress block is used by AASTHO-LRFD for the concrete compression stress-strain behavior to make it easier to calculate the nominal moment. This rectangular stress block is altered by the factors α_1 and β_1 to provide the same total compression force and force centroid as the integration of the nonlinear stress-strain curve over the same area [49]. In the case of rectangular beams or if the compressive zone is located within the flange in compression, the compression force by concrete is equal to:

$$F_c = \alpha_1 \cdot f_{cm} \cdot \beta_1 \cdot c \cdot b \ [N]$$

[Eq. 4-34]

In case the compressive zone cannot be assumed rectangular and instead is considered as a T-shape the following relation applies.

$$F_c = \alpha_1 \cdot f_{cm} \cdot \left(b_w \cdot \beta_1 \cdot c + \left(b \cdot h_f - b_w \cdot h_f \right) \right) \ [N]$$

[Eq. 4-35]

The defined stress block factors ($\alpha_1 \ [-], \beta_1 \ [-]$) detailed in [Eq. 2-30], depend on the magnitude of the compressive strength of concrete (f_{cm}).

Now, it is necessary to calculate the resultant forces by the non-prestressed longitudinal steel reinforcement with the following relations.

$$F_s = A_s \cdot f_{sy} \ [N]$$

[Eq. 4-36]

Where A_s is the area of non-prestressed steel and f_{sy} is the effective stress acting in the steel rebar, which depends on the calculated longitudinal strain obtained with the following relation.

$$\varepsilon_s = \frac{d_s - c}{c} \cdot \varepsilon_{cu} \ [-] \qquad\qquad \textit{[Eq. 4-37]}$$

Where d_s is the effective depth of the non-prestressing longitudinal steel reinforcement.

Assuming the stress-strain relationship showed in Figure 4-5-A, then the stress at the steel rebar can be calculated with the conditional set below.

$$if\left(\varepsilon_s < \varepsilon_{sy}\right) then : f_{sy} = E_s \cdot \varepsilon_s \ [MPa]$$

$$else: f_{sy} = f_{ym} \ [MPa]$$

[Eq. 4-38]

For the non-prestressed rebars, there are two possible locations, the tension side or the compression side. For both, the same procedure applies to calculate the resultant force. The only thing that changes is the variables corresponding to the reinforcement in tension (A_s, d_s) for those corresponding to the reinforcement in compression (A_{s2}, d_{s2}).

The resultant forces by prestressed steel are obtained with [Eq. 4-39] detailed below, where A_p refers to the prestressed steel area of the region analyzed (top, web, bottom). The effective stress f_{ps} in this case depends on the total strain in the prestressing steel (ε_{ps}) calculated with [Eq. 4-29], [Eq. 4-30], [Eq. 4-31], and [Eq. 4-32]. According to the obtained value for the total strain the effective stress is calculated following the stress-strain relationship showed in Figure 4-5-B, that derives in the conditional given in [Eq. 4-40].

$$F_p = A_p \cdot f_{ps} \ [N] \qquad\qquad \textit{[Eq. 4-39]}$$

$$if\left(\varepsilon_{ps} < \varepsilon_{py}\right) then: f_{ps} = E_p \cdot \varepsilon_{ps} \ [MPa]; \qquad \textit{[Eq. 4-40]}$$

$$else: f_{ps} = \frac{f_{pu} - f_{py}}{\varepsilon_{pu} - \varepsilon_{py}} \cdot \left(\varepsilon_{ps} - \varepsilon_{py}\right) + f_{py} \ [MPa]$$
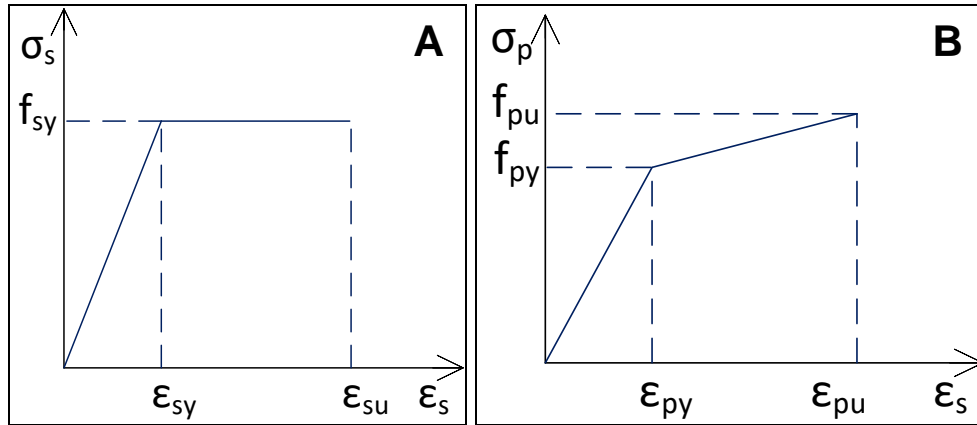
Figure 4-5 Stress-strain diagram for (A) non-prestressed and (B) prestressed longitudinal steel reinforcement

The calculated resultant forces in all cases are dependent on the assumed concrete compressive height (c). By means of the assumed compressive zone height, the iterative process will be carried out until the tensile forces are equal to the compression forces. This iterative process can then be summarized in the following general steps.

- o Assume a value c.
- o Calculate the resultant forces $\left(F_c, F_s, F_p\right)$
- o Verify condition of equilibrium of forces within the cross-section [Eq. 4-33], otherwise, start again assuming another value for c.

Then, with the average prestress in prestressed tendons f_{ps} obtained one can proceed to calculate the mean nominal flexural resistance $(M_{n,m})$ detailed in [Eq. 2-30], using the mean compressive strength of concrete in the calculation.

After that the procedure detailed in section 2.4.4 can be followed considering the area of prestressed tendons A_{ps} equal to the sum of the tendons located at the web or bottom part of the beams. Same case for the average stress in prestressed tendons (f_{ps}) only considers the tendons acting in tension. To calculate the distance from extreme compression fiber to the centroid of prestressing reinforcement (d_p), [Eq. 4-24] applies, considering the variety of cases within the database.

This design code considers the axial force (N_u) in its procedure, which is zero in all cases, and so is the vertical prestressing force since in all cases the tendons are straight as it is well known. At a certain point to calculate the crack spacing parameter (s_{xe}), the value of maximum aggregate size is required, and this data is contained in the ACI-DAfStb-PC database with the notation Æa [mm].

One thing that shout be detailed is about f_{po} that can be interpreted as the effective prestress, the stress of decompression at the level of the prestressing steel [Eq. 4-41], or the prestress just before transfer $(0.7f_{pu} \ to \ 0.75f_{pu})$. AASTHO-LRFD indicates that for "usual" levels of prestressing a value of $0.7f_{pu}$ is appropriate for both pretensioned and post-tensioned members. Likewise, it is stated that f_{po} for pretensioned members can be taken as the jacking stress, and for post-tensioned members f_{po} can be the average stress in tendons [50].

It can be understood that taking the effective stress is somewhat conservative, since it leads to an increase of the longitudinal strain, thus a decrease in β that reduces the final value of the concrete shear resistance V_c. Wishing to comply with the criterion stablished by AASTHO, it was deemed convenient to assume this parameter according to [Eq. 4-41] reported by Dolan [49].

$$f_{po} = f_{pe} + f_{pc} \cdot \frac{E_p}{E_c} = \frac{P_{p.inf}}{A_p} + \frac{P_{p.inf}}{A_c} \cdot \frac{E_p}{E_c} \ [MPa] \qquad \text{\textit{[Eq. 4-41]}}$$

As in the previous design code, having used mean values for concrete compressive strength and yield strength of steel reinforcement, one obtains as final result the mean shear strength according to [Eq. 2-29]. Since the database contains only beams with straight tendons, the vertical component of the prestressing force equals 0, and the final expression will be as follows.

$$V_{n,m} = min \begin{cases} V_{c,m} \\ 0.25(f_{cm} + 1.6)b_v d_{v,m} \end{cases} \ [N] \qquad \text{\textit{[Eq. 4-42]}}$$

4.4 SHEAR CAPACITY ACCORDING EUROCODE 2 (EN1992-1-1:2004)

It is the most straightforward procedure among all, and it requires a small number of parameters. As mentioned before, it does not require an iterative procedure to calculate the shear capacity since this approach does not depend on the applied external force. This model does not distinguish between axial forces and prestressing forces. In the European codes, prestressing will always be considered as preload, then the mean cross-sectional forces are used in the calculations (V_{Em}, M_{Em}).

So, again, to correlate the database with the parameters required for this design code, the following relations were used. To quantify the reinforcement ratio of longitudinal reinforcement with the information available in the database, considering the generic case and only the reinforcement in tension, the ratio is given by:

$$\rho_l = \frac{A_{pbot} + A_{pweb} + A_s}{b_w \cdot d} \quad [-] \qquad \text{[Eq. 4-43]}$$

Also, this code requires the distance between the compression face and the tensile resultant of the prestressed and non-prestressed longitudinal reinforcement. For this purpose, the following equation is used considering a generic case.

$$d = \frac{d_s^2 \cdot A_s + d_{pbot}^2 \cdot A_{pbot} + d_{pweb}^2 \cdot A_{pweb}}{d_s \cdot A_s + d_{pbot} \cdot A_{pbot} + d_{pweb} \cdot A_{pweb}} \quad [mm] \qquad \text{[Eq. 4-44]}$$

In order to obtain comparable values, i.e., to calculate the mean shear strength (V_{Rm}), some factors differ from their value stated in the standard. $C_{Rd,c}$ and k_1 values stated (Section 2.4.1.1) include some resistance factors that correspond for the design of new structures. For the assessment and comparison of mean values these factors are taken as $C_{Rm,c} = 0.15$ and $k_1 = 0.225$ according to [41].The characteristic concrete compressive strength as stated in section 4.1.2 is replaced by the mean compressive strength $(f_{ck} = f_{cm})$ too.

The last necessary value to obtain is the compressive stress in concrete from prestressing $(\sigma_{cp} = P_{p.\infty}/A_c)$. Where the effective prestress load $P_{p.\infty}$ is calculated multiplying the effective stress on tendons σ_{pp} with the total area of prestress tendons A_{ps}, both values given in the database. Then all parameter required to calculate the mean shear capacity are given ([Eq. 2-10]).

4.5 SHEAR CAPACITY ACCORDING PREN1992, DRAFT 7

As in EC2, the mean cross-sectional forces (V_{Em}, M_{Em}) will be used for the calculations in this design code. Also, to calculate mean shear strength values (V_{Em}), the partial factors are considered equal to 1 $(\gamma_V = 1)$, and the mean values of compressive strength of concrete $(f_{ck} = f_{cm})$ and yield strength of steel reinforcement $(f_y = f_{ym})$ are used.

The aggregate size parameter required for this procedure is the smallest value of the upper sieve size for the coarsest fraction of aggregates. As it is not given in the used database, this parameter is assumed equal to half the maximum aggregate size that is reported in the database $(D_{lower} = a_g/2)$.

The prEN1992 draft 7 code indicates two formulations to estimate the shear strength of prestressed member without shear reinforcement that are going to be distinguished for the whole document as follow.

- **prEN1:** The main formulation is given by [Eq. 2-16] that considers the prestressing effect by means of the k_{vp} factor. The resultant equation to evaluate the shear resistance applying all the conditions stated in section 2.4.2 and assuming that $k_{vp} > 0.1$ is as follow.

$$\tau_{Rm,c} = 0.66 \cdot \left(100\rho_l \cdot f_{cm} \cdot \frac{d_{dg}}{a_v \cdot \left(1 + \frac{N_{Em}}{|V_{Em}|} \cdot \frac{d}{3}\right)} \right)^{\frac{1}{3}} \quad [MPa] \qquad \text{[Eq. 4-45]}$$

Where the conditional for the effective shear span can be expressed as:

$$a_v = \begin{cases} d & if\ a_{cs} \geq 4 \cdot d \\ \sqrt{a_{cs} \cdot \dfrac{d}{4}} & if\ a_{cs} < 4 \cdot d \end{cases} \quad [mm],\ with\ a_{cs} = \left| \frac{M_{Em}}{V_{Em}} \right| \quad [mm] \qquad \text{[Eq. 4-46]}$$

Recognizing that the role of the k_{vp} factor was to modify the longitudinal strain term ending with an additional second term that is function of the normal load applied N_{Em} which is equal to the effective prestress force applied $\left(P_{p,\infty} = \sigma_{cp} \cdot A_c\right)$.

- **prEN2:** The main equation [Eq. 2-17] considers the prestressing effect by adding a second factor $\left(k_1 \sigma_{cp}\right)$ where k_1 has an upper limit of $(0.15 \cdot 1.4/\gamma_V)$, and σ_{cp} has an upper limit of $0.2 \cdot f_{cd}$ being f_{cd} the design concrete compressive strength according 5.1.6-1 from the draft document [38]. However, the latter limit is not considered to calculate the mean shear strength that will be compared with experiments.

  The resulting expression considering the additional factors results as follow explicitly.

$$\tau_{Rm,c} = 0.66 \cdot \left(100\rho_l \cdot f_{cm} \cdot \frac{d_{dg}}{a_v}\right)^{\frac{1}{3}} - 1.4 \cdot \left(0.07 + \frac{e_p}{4d}\right) \cdot \frac{N_{Em}}{A_c} \; [MPa] \qquad \text{[Eq. 4-47]}$$

Where the same conditional [Eq. 4-46] applies for the effective shear span, and N_{Em} is equal to the effective prestress force too. The tendons eccentricity in the critical cross-section being analyzed is calculated according the effective depth of the prestressed steel in tension as follow.

$$e_p = \frac{e_{p.bot} \cdot A_{p.bot} + e_{p.web} \cdot A_{p.web}}{A_{p.bot} + A_{p.web}} \; [mm] \qquad \text{[Eq. 4-48]}$$

The final value obtained by each approach is compared at the end with the lower bound indicated in [Eq. 2-15]. For more details about both approaches refer to section 5.2.1, in this part of the document it is only intended to apply the codes and highlight where prestressing forces are included

Unlike the current EC2, in this case an iterative process is required for both formulas as stipulated in section 4.1.6, because the effective shear span (a_{cs}) depends on the applied external F_{ext}.

4.6 COMPARISON WITH EXPERIMENTAL RESULTS FROM ACI-DAFSTB-PC DATABASE

The following two sub-sections will present the results of two critical filters applied to form the subset 1 and 2 of tests. First, the selection of the experiments according to the type of failure reported in the database. Then, the influence of the cross-section shape will be analyzed to quantify variations in results according to different assumptions made for the evaluation of the shear capacity according to prEN1992 approaches particularly. These two sections will give a criterion to evaluate the final results obtained with the subsets established.

4.6.1 Shear failure mode influence

This will be evaluated by comparing the original database (ACI-DAfStb-PC) with the subset 1. As detailed in section 3.6, the subset 1 tries to work with rectangular and I/T shape beams that develop a flexural-shear failure only, excluding the identified experiments with another type of failure reported.

Table 4-1 shows the differences in the statistical indicators between the original database and the first subset, just to have an overview of the consequences of this selection process. It is essential to note that this process was initiated to correctly correlate the type of shear failure analyzed by the studied approaches with the observed shear failure types. This relationship must occur since the shear failure mechanism would not be the same as the one assumed by some approaches.

It can be observed in Table 4-1 that the selection of the experimental results related to the type of shear failure being analyzed affects EC2 and ACI318-19M approximate method considerably,

both empirical methods but EC2 distinguish zones cracked in bending, being exclusively related with flexural-shear failure strength calculation. The accuracy is improved for both approaches and the precision experiences a small favorable change.

ACI318-19M detailed method considers the verification of shear-tension and flexural-shear failures; AASHTO-LRFD is a generic approach covering various types of shear failures, both approaches do not suffer relevant changes in terms of precision. In terms of accuracy, AASHTO-LRFD tends to improve with a mean value closer to 1, but the opposite occurs with ACI318-19M detailed method, suggesting that the web-shear evaluation is accurate and favors the evaluation of groups of tests not classified by the type of shear failure.

prEN-1 does not suffer major changes and prEN-2 improves its accuracy reducing its mean value from 1.54 to 1.45. Both methods by the assumptions that underlie them are related to flexural-shear failures.

Table 4-1 Statistical characteristics of ACI-DAfStb-PC database and subset 1. Assumed $x_r = 0.65\alpha$

	Mean of $\alpha = V_{test}/V_{cal}$		Standard Deviation of $\alpha = V_{test}/V_{cal}$		Coefficient of variation of $\alpha = V_{test}/V_{cal}$	
	ACI-DAfStb-PC	Subset 1	ACI-DAfStb-PC	Subset 1	ACI-DAfStb-PC	Subset 1
ACI-s	1.37	1.20	0.63	0.54	0.46	0.45
ACI-d	1.41	1.44	0.55	0.58	0.39	0.40
AASHTO	1.73	1.68	0.42	0.41	0.24	0.24
EC2	1.62	1.51	0.49	0.44	0.30	0.29
prEN-1	1.38	1.37	0.34	0.35	0.25	0.25
prEN-2	1.56	1.47	0.45	0.43	0.29	0.30

4.6.2 Cross-section shape influence

For this evaluation, the differences between the subset 1 and subset 2 shown in Table 4-2 are helpful. Nevertheless, to visualize the effect of the cross-section shape better, the histograms in Figure 4-6 have been generated, where the experiments grouped at subset 1 are separated into two groups, rectangular beams, and T- or I- shape beams. The histograms were generated for both groups to visualize that in approaches assuming a rectangular cross-section, the mean resistance of the I or T beams tends to be higher than the mean resistance of rectangular beams. It is visually observed that the crest of the histogram for I or T beams tends to higher ranges than the histogram for rectangular beams for design codes like EC2 or prEN1992.

With the results presented, it can be said that subset 2 is suitable for comparing results of code designs that consider the type of failure and the type of cross-section being used (Flexural-shear failure in rectangular beams – proposal for new Eurocode).

Figure 4-6 shows that the empirical methods (ACI318-19 approximate method and EC2) do not obtain precise results for rectangular beams group (COV values of 0.34 and 0.31 respectively), which is improved for the I/T beams group with COV=0.31 for ACI318-19 approx. method and COV=0.22 for EC2. It has to be remarked that both methods obtain higher mean values for I/T beams, case of ACI318-19 approx. method with a mean value of 0.96 for rectangular beams and 1.75 for I/T beams, EC2 does not have such a difference between the two groups with a mean value for rectangular beams of 1.44 and 1.69 for I/T beams.
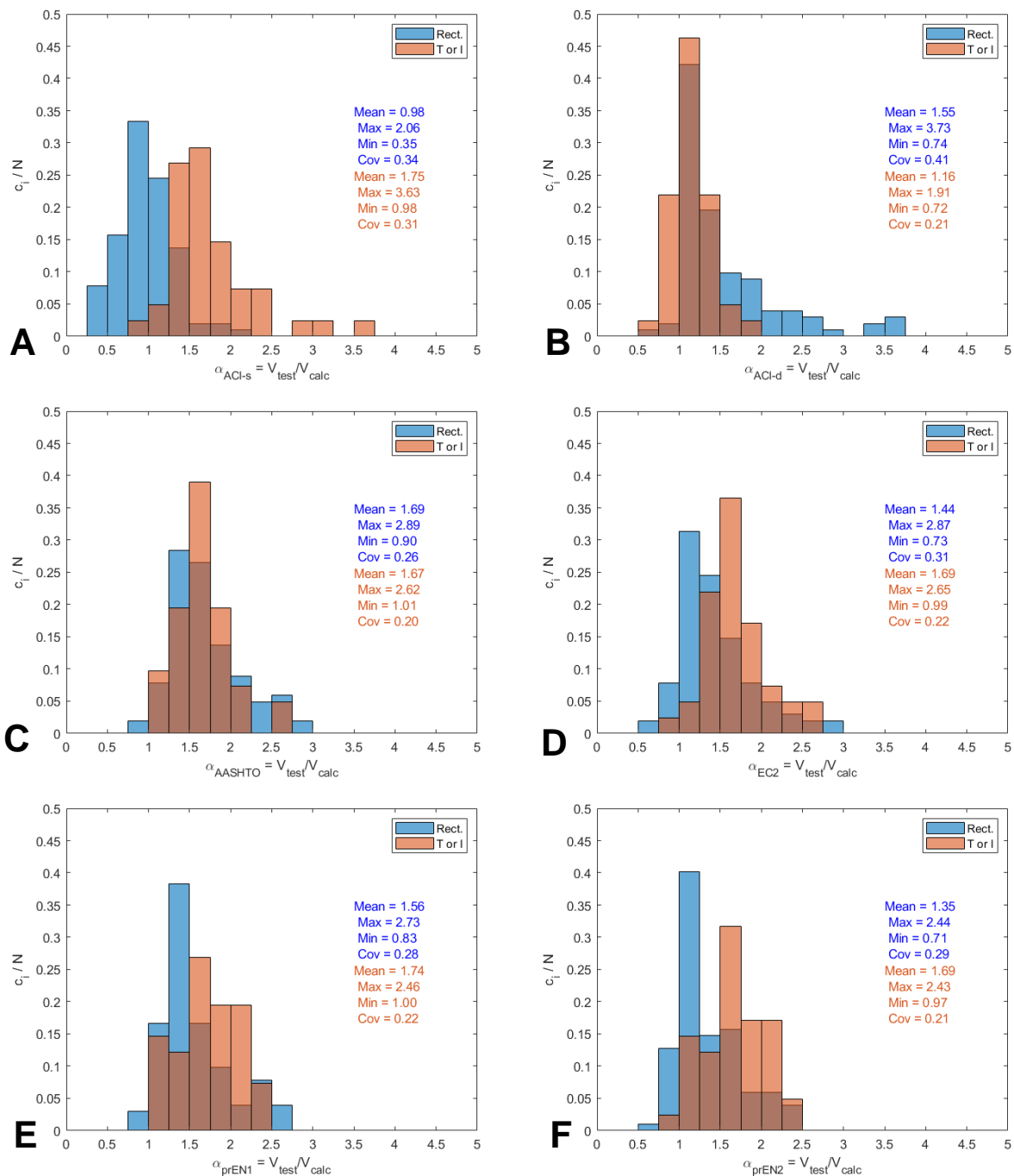
*c_i/N: *refers to the number of tests within the bin* (c_i) *over the total number of elements* (N)

Figure 4-6 Histograms comparing results obtained using subset 1 and x_r=0.65a, for beams with rectangular cross-section and beams with I- or T-shape cross-section. (A) ACI318-19M approximate approach (B) ACI318-19M detailed approach (C) AASHTO-LRFD (D) Eurocode 2 (E) prEN1 (F) prEN2

Case of ACI318-19 detailed method, tends to obtain higher accuracy and precision for the analysis of I/T beams flexural-shear failure. The mean value equal to 1.16 for the I/T beam group is much better than the 1.55 obtained for the rectangular beam group, and the latter group has a COV=0.41 which is much higher than the COV=0.21 obtained for the I/T beams group. This approach is based on estimating the critical crack formation, so it can be assumed that the estimated empirical value of $\left(0.05\lambda\sqrt{f_c'}\right)$ required to transform a flexural crack into a flexural-shear crack is better calibrated for I/T beams in terms of accuracy and precision.

AASHTO-LRFD has similar accuracy for both groups of beams (rectangular: mean=1.69, I/T shape: mean=1.67), with a tendency of more precise results for I/T beams (COV=0.20) compared

with rectangular beams (COV=0.26). These results were expected since the detailed approach used to calculate the shear capacity applies the strain compatibility method to calculate the nominal flexural strength of the beam considering the shape of the cross-section in the procedure.

The approaches proposed for the new Eurocode (prEN1 and prEN2) are based on the assumption that the cross-section is rectangular to assume a constant location of the resultant compressive force on the cross-section. This resulted in a higher mean value for the I/T beams group (prEN1 mean=1.74; prEN2 mean=1.69) than for the rectangular beams group (prEN1 mean=1.56; prEN2 mean=1.35).

One has to consider the dependency of the accuracy and precision of the approaches on the critical location (x_r) assumed to analyze the flexural-shear strength. As long as this assumption is mainly related to those established by the approach, more objective and valid comparisons will be obtained. Chapter 5 will inquire into the analysis of the new proposals for prEN1992, and assuming $x_r = (a - d)$ as suggested in these proposals, the influence of the cross-section shape will be analyzed again as is of interest for these approaches.

4.6.3 Accuracy, precision and conservativeness of shear design procedures proposed by design codes

Subset 3 excludes tests that do not comply with the verifications given in section 3.5. It is useful to evaluate the performance of the tests when trying to filter out tests possibly disturbed by anchorage failures or the flexural capacity of the beam. As shown in Table 4-2, the coefficient of variation is reduced/maintained for all design codes comparing only tests from subset 3, and the mean values are shifted to the left, closer to 1, for all design codes except for ACI318-19. Subset 3 can generate different results if one takes a different approach for the verifications stated in section 3.5. So as the ideal group of tests without any biases due to the inclusion of evaluation factors that may vary, subset 2 can be said to be the most useful.

Table 4-2 Statistical information from comparing the design codes results with tests for the defined subsets when critical location is x_r = 0.65a

	Mean of $\alpha = V_{test}/V_{cal}$ [-]			Coefficient of variation of $\alpha = V_{test}/V_{cal}$ [-]			5th Percentile lower bound of $\alpha = V_{test}/V_{cal}$ [-]		
	Subset 1	Subset 2	Subset 3	Subset 1	Subset 2	Subset 3	Subset 1	Subset 2	Subset 3
ACI-s	1.20	**0.98**	0.93	0.45	**0.34**	0.32	0.48	**0.47**	0.45
ACI-d	1.44	**1.55**	1.58	0.40	**0.41**	0.35	0.90	**1.03**	1.03
AASHTO	1.68	**1.69**	1.67	0.24	**0.26**	0.25	1.12	**1.11**	1.12
EC2	1.51	**1.44**	1.41	0.29	**0.31**	0.28	0.89	**0.82**	0.78
prEN1	1.37	**1.36**	1.36	0.25	**0.26**	0.26	0.93	**1.00**	0.97
prEN2	1.47	**1.37**	1.36	0.30	**0.31**	0.29	0.92	**0.84**	0.79

Based on the information presented in Table 4-2, the mean value, coefficient of variation, and 5th percentile lower bound of the different design codes have been evaluated, and it can be seen that ACI318-19 approximate method is the one that obtains mean values closer to 1, although, for last two subsets, these values are not higher than one. AASHTO-LRFD has the mean value furthest from unity with values between 1.67 and 1.69, and the other design codes have mean values in the range between 1.36 and 1.58, being prEN1 the one with values closer to 1. In other words, in terms of accuracy one has to highlight ACI318-19 approximate method and prEN1 approach.

Coefficients of variation for subset 1 are even for AASHTO-LRFD, EC2, prEN1, and prEN2, varying from 0.24 to 0.31. For ACI318-19, the highest values appear for subset 1, with 0.45 for the approximate method and for the detailed method the worst COV=0.41 is for subset 2. AASHTO-LRFD always has the lowest coefficients of variation for all subsets, although prEN1 for

subset 2 has the lowest value (COV=0.26), as well. ACI318-19 is the opposite, with the highest coefficients of variation (between 0.32-0.45) for all subsets. The ACI318-19 detailed method is the worst performing in terms of precision for subsets 2 and 3.

The 5th percentile value helps evaluate the approaches in terms of safety, with values between 0.8 and 1 indicating good levels of safety. EC2, prEN1, and prEN2 obtain values that indicate good safety levels, AASHTO, and the detailed method ACI318-19 also obtain values that indicate good safety levels but tend to be conservative since values higher than values 1 are observed. ACI318-19 obtains undesirable safety levels according to this analysis with values lower than 0.5.

An interesting thing to note is the change in the histograms generated for the different subsets to visualize the statistical indicators presented before. Figure 4-7 shows, for all the design codes studied, the evolution of the histogram from subset 1 to subset 3. What can be observed is the variation of the mode (the range containing the highest number of results) and the evolution of the distribution of the comparative results considering the different group of tests (subsets) defined.
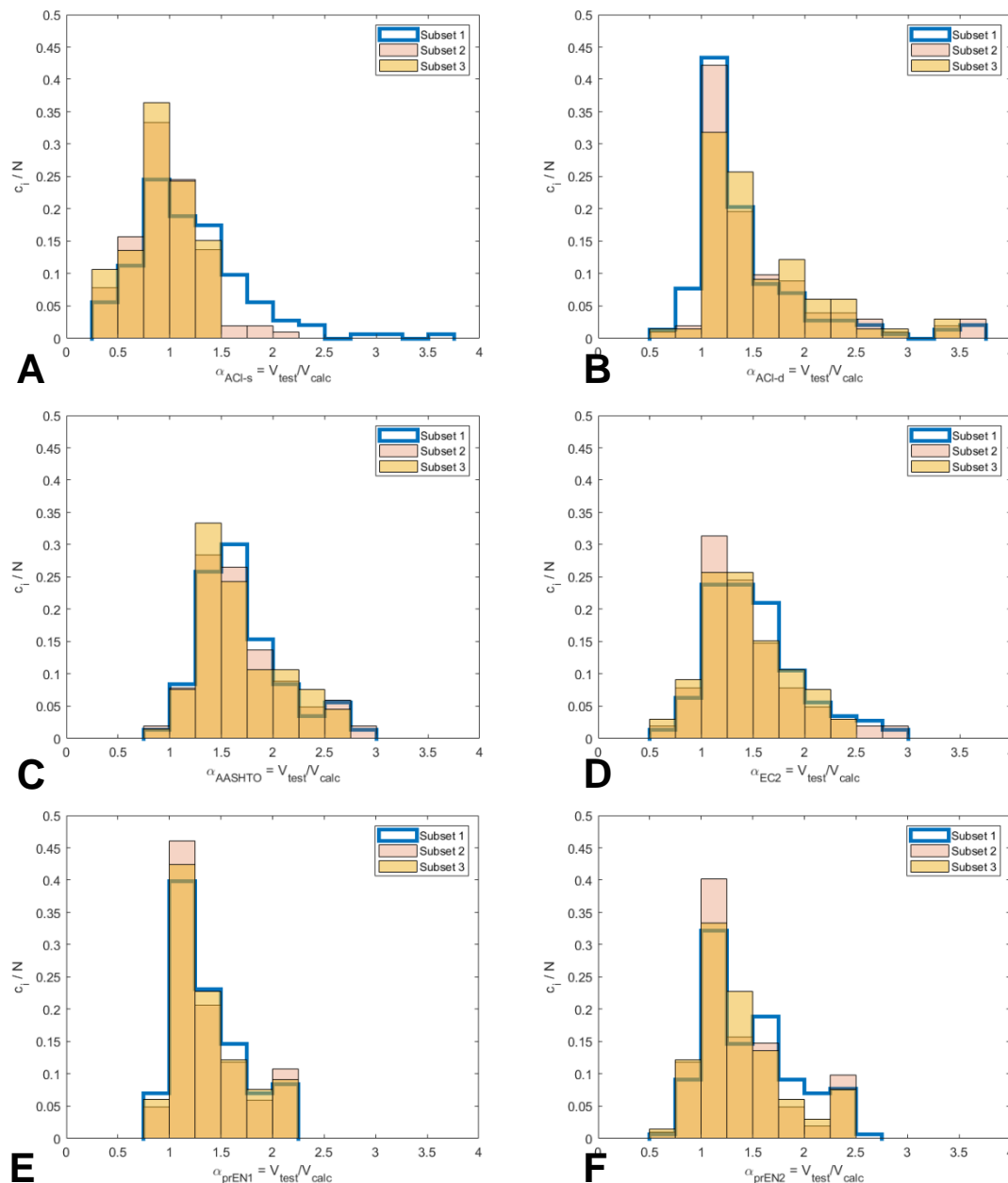
*c_i/N: *refers to the number of tests within the bin* (c_i) *over the total number of elements* (N)

Figure 4-7 Histograms from comparison of design codes with experimental data for all the defined subsets. (A) ACI318-19M approximate approach (B) ACI318-19M detailed approach (C) AASHTO-LRFD (D) Eurocode 2 (E) prEN1 (F) prEN2

At this point, it is convenient to analyze a fundamental assumption made at the beginning, the critical location where the estimated shear resistance is analyzed with the different design codes (section 3.4). Recapitulating the initial hypothesis about the critical location based on experimental observations, equal to $x_r = 0.65a$, it is questionable when comparing certain design code approaches with tests, since some of them suggest the critical location at a distance $x_r = d$ or $x_r = (a - d)$. This leads us to compare at least the subset 2 of tests results with the mean shear capacity estimated by different design codes at different suggested critical locations.

For this purpose, the statistical information from comparing the design codes results with tests for the defined subsets was generated (Table 4-3 and

Table 4-4) assuming the critical locations as proposed before at a distance d from the support or point load.

Table 4-3 Statistical information from comparing the design codes results with tests for the defined subsets when critical location is $x_r = a-d$

	Mean of $\alpha = V_{test}/V_{cal}$ [-]			Coefficient of variation of $\alpha = V_{test}/V_{cal}$ [-]			5th Percentile lower bound of $\alpha = V_{test}/V_{cal}$ [-]		
	Subset 1	Subset 2	Subset 3	Subset 1	Subset 2	Subset 3	Subset 1	Subset 2	Subset 3
ACI-s	1.28	**1.04**	1.00	0.45	**0.32**	0.29	0.52	**0.50**	0.49
ACI-d	1.51	**1.62**	1.66	0.38	**0.39**	0.33	0.98	**1.02**	1.10
AASHTO	1.76	**1.78**	1.76	0.22	**0.23**	0.23	1.26	**1.30**	1.23
EC2	1.51	**1.44**	1.41	0.29	**0.31**	0.28	0.89	**0.82**	0.78
prEN1	1.44	**1.41**	1.42	0.23	**0.24**	0.24	1.05	**1.04**	1.03
prEN2	1.49	**1.39**	1.38	0.29	**0.30**	0.29	0.95	**0.86**	0.81

Table 4-4 Statistical information from comparing the design codes results with tests for the defined subsets when critical location is $x_r = d$

	Mean of $\alpha = V_{test}/V_{cal}$ [-]			Coefficient of variation of $\alpha = V_{test}/V_{cal}$ [-]			5th Percentile lower bound of $\alpha = V_{test}/V_{cal}$ [-]		
	Subset 1	Subset 2	Subset 3	Subset 1	Subset 2	Subset 3	Subset 1	Subset 2	Subset 3
ACI-s	1.09	**0.93**	0.87	0.39	**0.36**	0.35	0.48	**0.46**	0.45
ACI-d *	0.95	**0.90**	0.88	0.39	**0.45**	0.41	0.44	**0.41**	0.40
AASHTO	1.57	**1.50**	1.48	0.34	**0.34**	0.33	0.82	**0.69**	0.68
EC2	Critical location within region uncracked in bending, then used approach doesn't apply								
prEN1	1.14	**1.11**	1.09	0.28	**0.30**	0.29	0.69	**0.64**	0.59
prEN2	1.41	**1.29**	1.27	0.31	**0.32**	0.31	0.83	**0.74**	0.70

*Web-shear failure resistance as final result for some test (Web-shear resistance dominant case/ # tests = subset 1: 103/143, subset 2: 64/102, subset 3: 37/66)

To visualize the changes in the generated values presented in Table 4-2, Table 4-3 and

Table 4-4, the following Figure 4-8, Figure 4-9 and Figure 4-10 plot the mean values, coefficients of variation (COV) and the 5th percentile lower bound values for the different assumed critical locations using the results obtained for **subset 2** as this is the most representative for flexural-shear failure of rectangular beams.
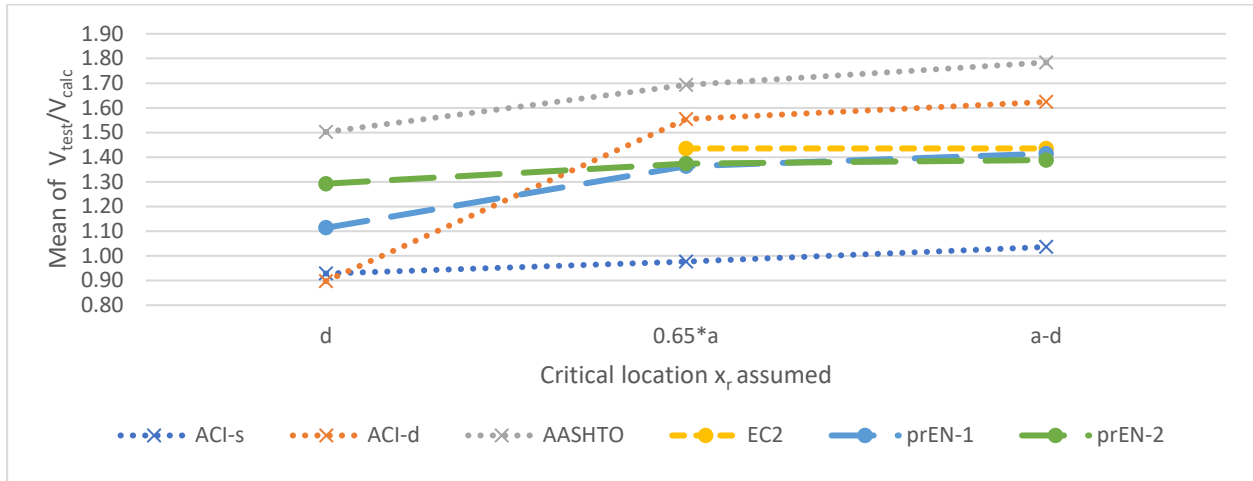
Figure 4-8 Subset 2 mean values for comparison of V_{test}/V_{calc} as function of the critical location for different design codes.
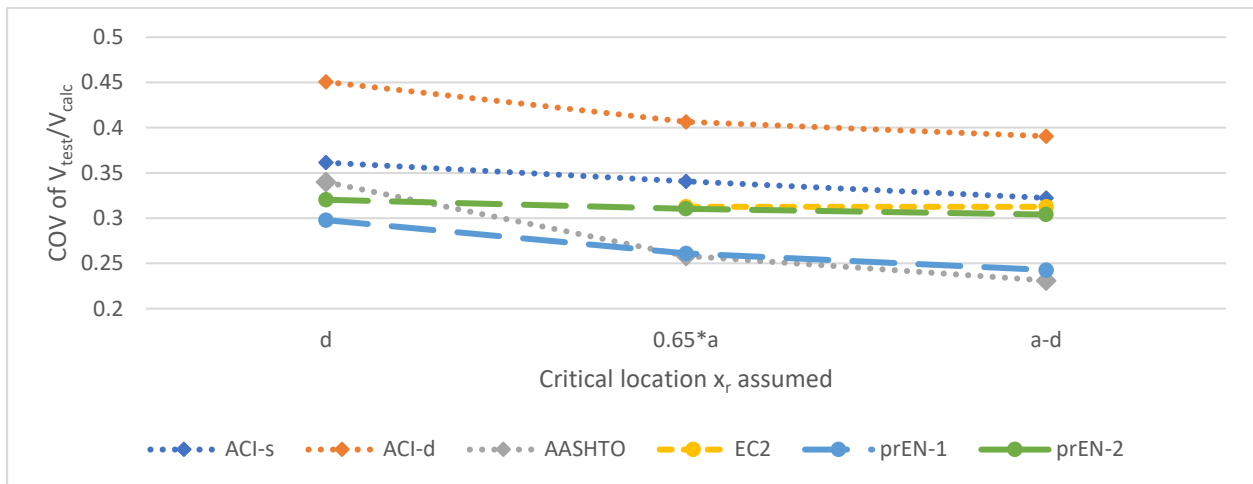
Figure 4-9 Subset 2 coefficients of variation for comparison of V_{test}/V_{calc} as function of the critical location for different design codes.
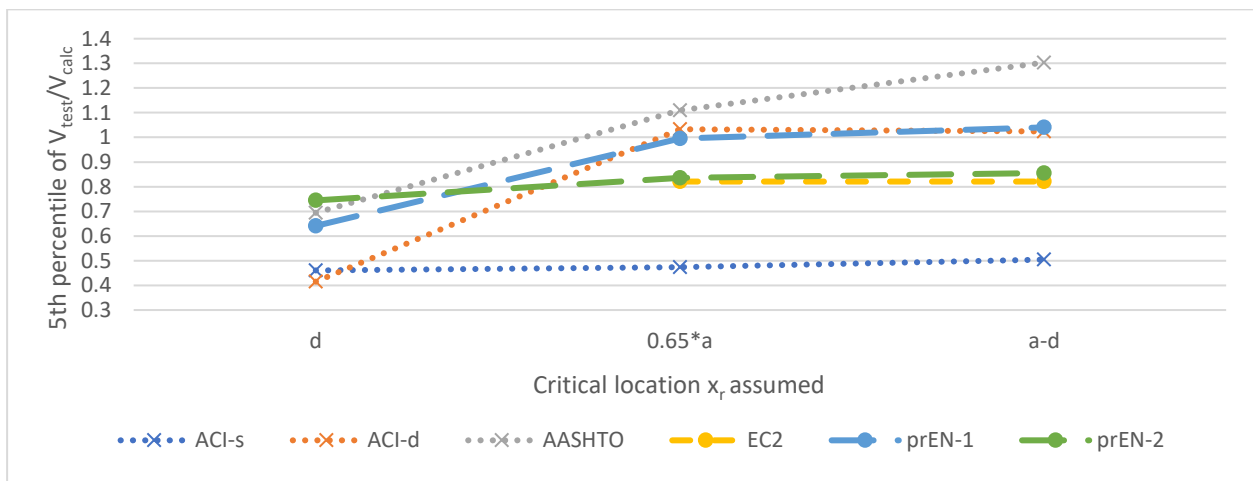
Figure 4-10 Subset 2, 5th percentile lower bound of V_{test}/V_{calc} as function of the critical location for different design codes.

Let us start talking about the mechanics of the problem to try to explain the variation of the results with the different approaches at different critical locations assumed.

First, analyzing the problem as uncracked concrete, the different critical locations have different flexural and shear stresses, depending on the magnitude of the shear forces and bending moments, important for the analysis of first stage in the typical reaction of slender members without shear reinforcement to shear.

In this first stage, the formation of flexural cracks is decisive for the development of the critical shear crack in a later stage. The region most likely to generate a flexural crack is the one with the highest tensile stresses exceeding the tensile strength of concrete. In this case of analysis with equidistant point loads and assuming constant normal stress from prestressing, it can be seen from Figure 4-11 that the region closer to the point load develops higher tensile stresses due to the higher bending moment. The shear stress magnitude, assumed parabolically distributed in cross-section, is considered constant until the point load since the analysis is on rectangular beams only. At this stage, the shear-transfer actions of aggregate interlock, residual tensile stress, or dowel action are not present. The prestressing influences the longitudinal stresses collaborating in reducing flexural stresses in tension. In the same way, the vertical component of the prestressing force already acts for harped tendons, reducing the acting shear force. In ACI-DAfStb-PC database there are only straight tendons, then this last vertical component is neglected.
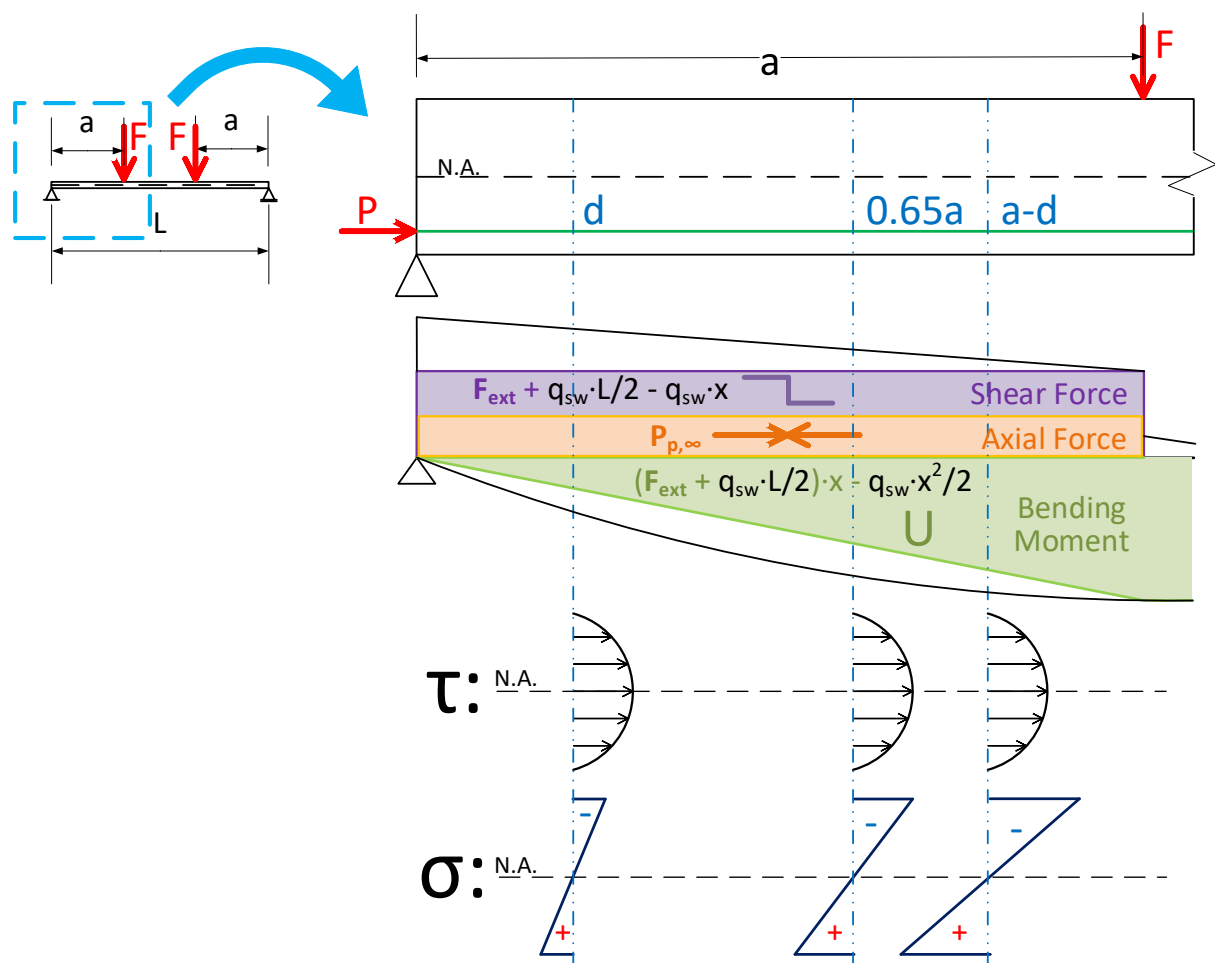
Figure 4-11 Flexural and shear stresses along the beam length for typical structural configuration of tests from ACI-DAfStb database used.

In the second stage, already with cracked concrete but with cracks not yet crossing the neutral axis, the shear stress is distributed parabolically in the uncracked concrete with the maximum value at the neutral axis. At the crack, the shear stresses decrease as the crack width increases. Residual tensile stresses, aggregate interlock, and dowel action already act at this stage. The vertical component of the additional tensile force in inclined tendons due to applied loads that depend on the crack width emerges too.

By the third stage, the critical shear crack develops deep in the compression zone, and probably the shear stress is parabolically distributed in the uncracked concrete. By this stage, all shear-transfer actions are activated.

To illustrate the 3 stages described before, the following Figure 4-12 generated by [51] is useful although the case was for reinforced concrete member without shear reinforcement. Including prestressing the required force for the same displacement increases, and point B and C tends to be closer and often overlap due to the higher compressive stresses acting on cross-section.
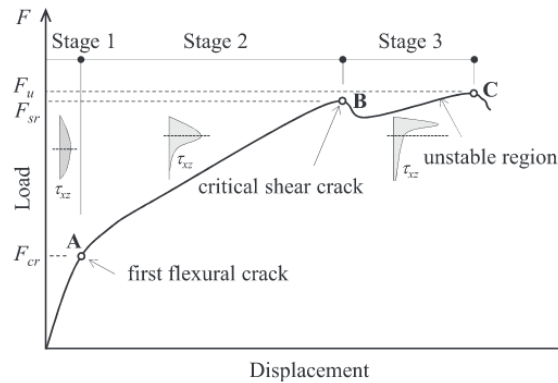
Figure 4-12 Typical load-deformation curve of a beam with shear failure [51]

Collapse tends to occur at point B, and the shear capacity, defined as the shear force corresponding to the formation of the critical shear crack (point B, end of stage 2), is considered the shear strength of concrete (V_c), and its estimation is given by empirical (ACI318-19M, EC2), MCFT-based (AASHTO-LRFD), and CSCT-based (prEN1992) models. The latter two assuming the dependence of the concrete shear strength on the crack width and its roughness with very similar proposed equations ([Eq. 2-6] and [Eq. 2-9]).

Based on the aforementioned, it can be expected that the different models tend to estimate the flexural-shear capacity with higher precision at the critical location assumed closer to the point load, something that can be seen in Figure 4-9 where the coefficients of variation are the lowest for $x_r = a - d$.

Now, having demonstrated the most suitable critical location to evaluate the results obtained $(x_r = (a - d))$, the following considerations detailed in Table 4-5 are used for the relative assessment of the design codes, to have a uniform criteria.

Table 4-5 Relative assessment for statistical indicators (captured from [52]*)*

5TH PERCENTILE LOWER BOUND

> 1	Conservative
0.8 – 1	Good levels of safety
0.7 – 0.8	Moderate levels of safety
< 0.7	Less than desirable level of safety

COV

< 0.15	Excellent
0.15 – 0.20	Very good
0.20 – 0.25	Good
0.25 – 0.30	Reasonable
0.30 – 0.35	Poor
> 0.35	Bad

So, for evaluating the flexural-shear strength of prestressed concrete members without shear reinforcement, the following observations can be made from examining the data in Table 4-3.

- The COV obtained for the ACI318-19M approximate method usually denotes a poor precision of the results, with a less than desirable level of safety.

- Case of the ACI318-19M detailed method, a good level of safety and poor precision is obtained for beams with various cross-section shapes and a conservative level of safety with poor precision for rectangular beams.
- AASHTO-LRFD has good precision to evaluate beams with different cross-sections shapes, but it has the most conservative levels of safety.
- EC2 has reasonable precision and a good level of safety for beams with different cross-section shapes and poor precision with good or moderate levels of safety for rectangular beams.
- prEN1 for the analysis of beams with different cross-section shapes has good precision and a conservative level of safety. Rectangular beams only have reasonable precision and a conservative level of safety.
- prEN2 in all cases, has a reasonable precision and a good level of safety.

4.6.4 Assessment of design codes considering the main parameters involved

In this subsection, the results obtained and the differences between the various approaches in the shear strength estimation will be evaluated in detail. Subset 1 of the ACI-DAfStb-PC database containing 143 tests strictly related to a flexural-shear failure of beams with rectangular, I-shape, or T-shape cross-section will be used.

It is interesting to look at one of the most used parameters to start this analysis. Figure 4-13 shows the shear strength ratio (V_{test}/V_{calc}) versus mean concrete compressive strength (f_{cm}). The influence of the compressive strength of concrete is included in all the approaches presented. For ACI318-19M and AASHTO-LRFD, the shear strength is proportional to $\sqrt{f_c'}$, and for EC2 or prEN1992, it is proportional to $(f_{ck})^{1/3}$. For all approaches it can be seen in the scatterplots that there is a tendency for the shear strength to increase as the compressive strength of the concrete increases.
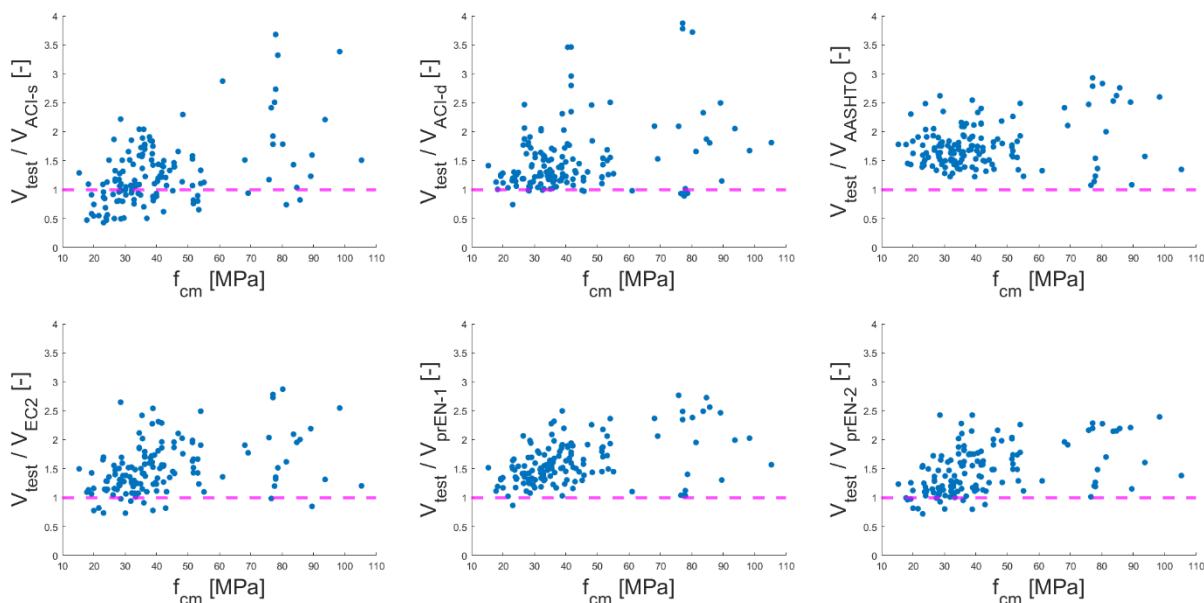
Figure 4-13 Shear strength ratio (V_{test}/V_{calc}) versus mean concrete compressive strength (f_{cm}) for subset 1 from ACI-DAfStb-PC database

Figure 4-14 shows the shear strength ratio (V_{test}/V_{calc}) versus the effective depth (d). The influence of the size effect has been recognized as a relevant parameter for shear behavior, and it is taken into account in EC2, prEN1992, and AASHTO-LRFD approaches. However, ACI318-19M does not consider the size effect in the approach applied for prestressed members. EC2 considers a size effect factor $k = 1 + \sqrt{200/d} \leq 2$ in its main equation. AASHTO-LRFD approach considers the member depth indirectly through a crack spacing parameter that affects the crack width, thus the estimated shear strength. prEN1992 maintains in its approach the effective depth

parameter in the main equation, and one has to recognize that according to the background of the CSCT, this parameter directly affects the longitudinal strain and consequently the crack width. According to the scatterplots presented in Figure 4-14, there is not a descending or ascending trend with member depth for all approaches.
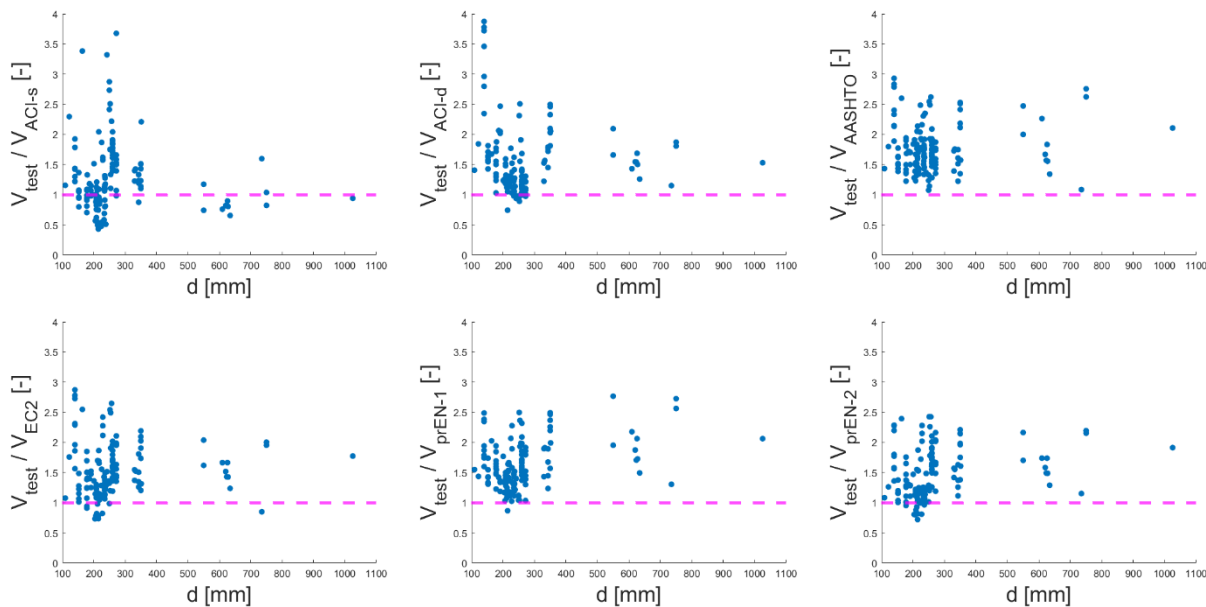
Figure 4-14 Shear strength ratio (V_{test}/V_{calc}) versus effective depth (d) for subset 1 from ACI-DAfStb-PC database

Figure 4-15 shows the shear strength ratio (V_{test}/V_{calc}) versus the longitudinal reinforcement ratio (ρ_l). This parameter is important for the amount of longitudinal strain that directly affects the crack width, aggregate interlock, dowel action, and finally the shear strength. ACI318-19 doesn't take into account the influence of longitudinal reinforcement, although for prestressed concrete members the prestressing steel ratio is directly related to the axial stress level, then ACI318-19M detailed method approach may capture part of the influence of the longitudinal reinforcement ratio. AASHTO-LRFD seems to include the effect of longitudinal reinforcement ratio as it is reflected in the longitudinal strain, thus it affects the crack width and shear strength too. prEN1992 and EC2 take into account the longitudinal reinforcement ratio into the main equation, EC2 included it since it was known the influence of this parameter on the shear strength of concrete, this formula is empirical but for prEN1992 the effect of longitudinal reinforcement ratio is included in a logical way based on the CSCT, deriving this factor from the longitudinal strain, so it is implicitly related to this and to the crack width consequently.

Figure 4-16 shows the shear strength ratio (V_{test}/V_{calc}) versus the shear span-to-effective depth ratio (a/d). This parameter is a relative value of the shear and bending moment applied (M/Vd). ACI318-19 approximate method considers it into its approach by using M/Vd ratio, and ACI318-19 detailed method also uses the same ratio to calculate the shear force required to generate a flexural crack ($V_i M_{cre}/M_{max}$). For AASHTO-LRFD this sectional forces are considered directly on the longitudinal strain calculation. EC2 considers the shear capacity independent of a/d, but prEN1992 recognized its strong influence and included it although this now makes it necessary to employ an iterative process for the calculation of the shear capacity. For prEN1992 the sectional forces considered, that derive into the shear span-to-effective depth ratio, were derived from the approximation of the longitudinal strain and are therefore implicitly related to it. The scatterplots in Figure 4-16 clearly shows that there is no defined trend for ACI318-19, and for the others there is a tendency to decrease the shear strength for high ratios, since in slender beams cracking is more prominent and the stiffness of the beam is reduced.
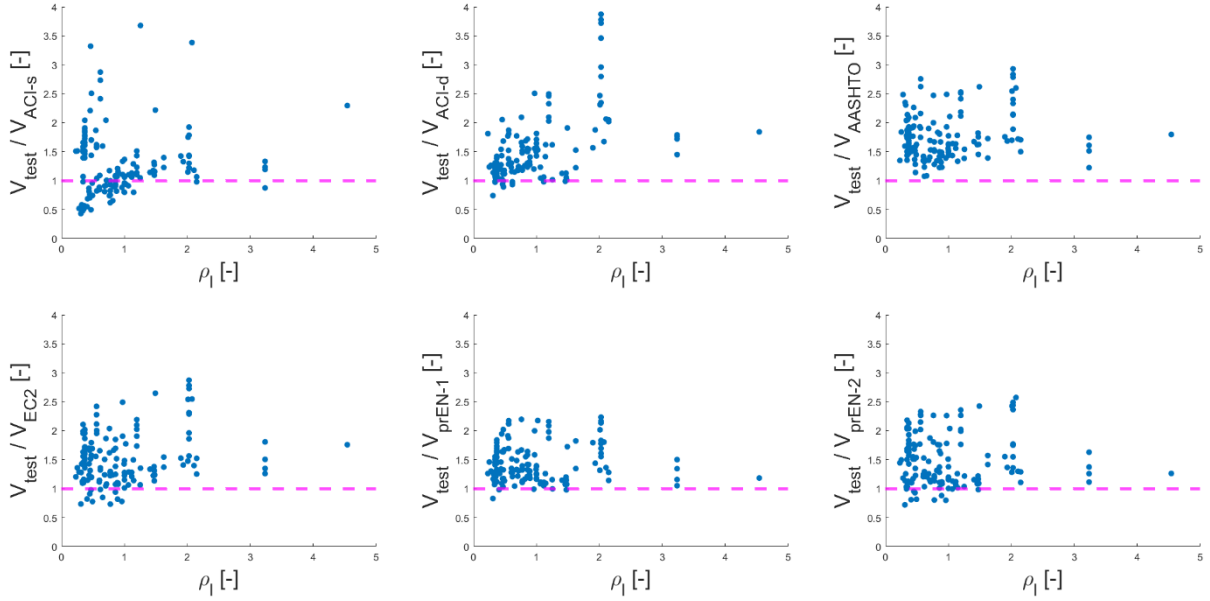
Figure 4-15 Shear strength ratio (V_{test}/V_{calc}) versus longitudinal reinforcement ratio (ρ_l) for subset 1 from ACI-DAfStb-PC database
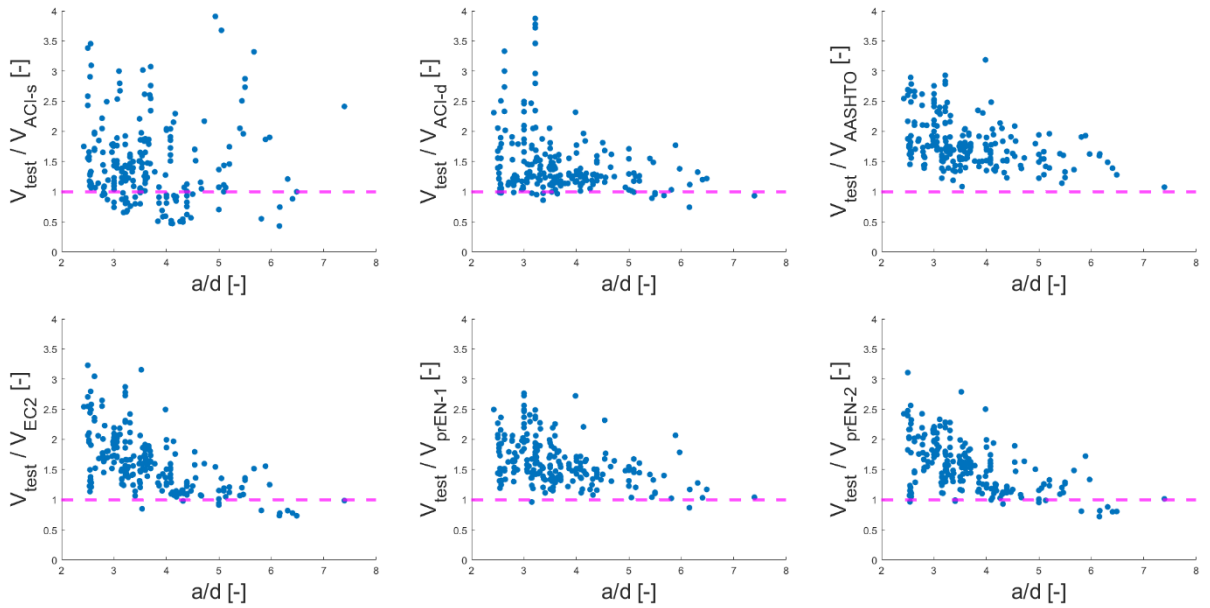
Figure 4-16 Shear strength ratio (V_{test}/V_{calc}) versus shear span-to-effective depth ratio (a/d) for subset 1 from ACI-DAfStb-PC database

Figure 4-17 shows the shear strength ratio (V_{test}/V_{calc}) versus the dimension-free axial force (σ_{cp}/f_{cm}). ACI318-19 approximate method doesn't consider the collaboration of the prestressing force into the concrete resistance, what the respective scatterplot reflects is the influence of the mean compressive strength of concrete. ACI318-19 detailed method takes into account the prestressing influence into the flexural crack formation in the calculation of the cracking moment, then the vertical component for harped tendons is also included. AASHTO-LRFD takes into account the effect of the vertical component of prestressing force and considers it in the calculation of the nominal flexural moment that is used for the calculation of the longitudinal strain, influencing the crack width and shear strength. EC2 with its empirical formulation includes the axial stress on cross-section multiplied by an empirical factor $k_1 = 0.15$. The new Eurocode proposals include the effect of prestressing by two different ways, prEN1 including the effect of normal load into the longitudinal strain modifying the effective shear span (a_v) multiplying it with a factor ($k_{vp} = 1 + N_{Ed}d/V_{Ed}3a_{cs}$). prEN2 uses a linearized approach similar to EC2, adding the effect of normal stresses multiplying it by a factor $k_1 = 1.4/\gamma_v\left(0.07 + e_p/4d\right)$ that assumed a fixed $a/d = 4$ and takes into account the eccentricity of the tendon. The major differences between the

two methods are the last two assumptions mentioned for prEN2. prEN1 instead does not assume a fixed a/d and the axial stresses are assumed to be applied on the neutral axis.
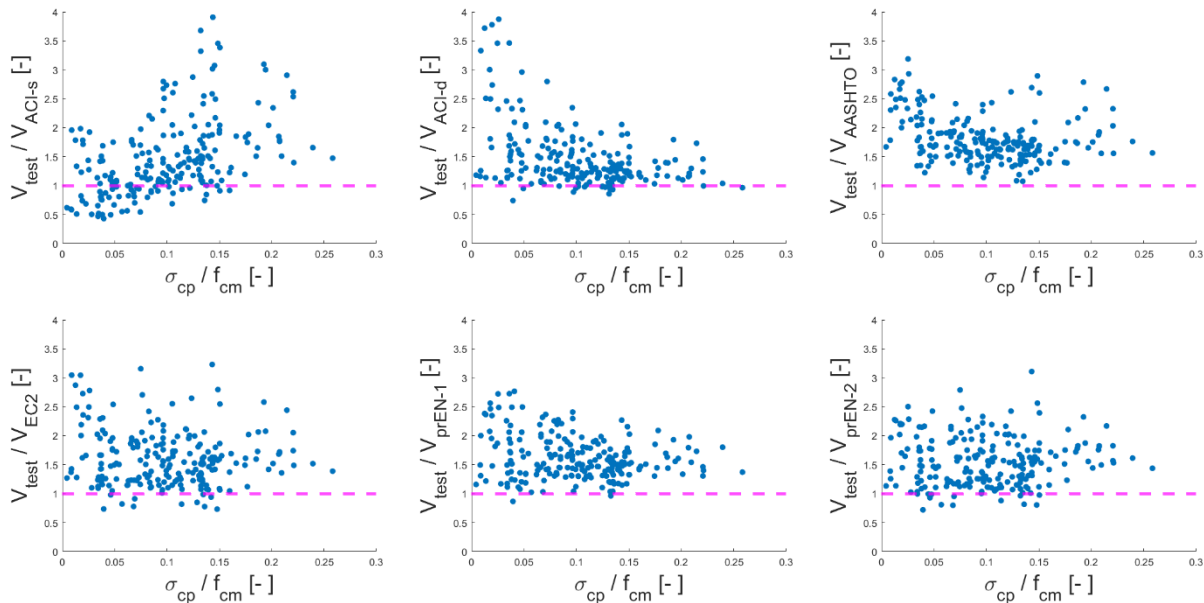
Figure 4-17 Shear strength ratio (V_{test}/V_{calc}) versus dimension free axial force (σ_{cp}/f_{cm}) for subset 1 from ACI-DAfStb-PC database

4.7 DISCUSSION AND CONCLUSIONS

4.7.1 Discussion about design codes

- Of all the parameters studied, the one that clearly influences the shear strength estimation is the shear span-to-effective depth ratio. Since the location of the critical crack is highly dependent on this parameter and provides an idea of the type of failure to be analyzed in different ranges of values, as recalled in the Kani's Valley concept for example. There is a correlation between a/d and the estimated shear strength for all the approaches studied except EC2, which maintains a constant value for the span length no matter the changes on the relation a/d. EC2 formulation is the only one studied in this document that doesn't required an iterative procedure to calculate the shear capacity as this approach doesn't depend on the external load applied too.

  For the ACI318-19 and AASHTO-LRFD design codes, the nominal shear strength (V_n) is the result of the sum of the contribution of the concrete shear resistance (V_c) and the vertical component of the prestressing force (V_p), while for the Eurocodes, the design shear force (V_{Ed}) considers the influence of prestressing force as prestress is preload for design codes applied in Europe. This last notion must be maintained for any alternative for the new Eurocode, and only alternative 1 (prEN1) complies to this concept up to this point due to the following observations.

  o prEN1 assumes prestressing effect included through the effective shear span (a_{cs}), which considers the ratio between the acting bending moment and acting shear force $(|M_{Ed}/V_{Ed}|)$. The k_{vp} factor, used by this alternative to include the effect of normal load on the longitudinal strain, alters a_{cs} such that it is also a function of a normal load (N_{Ed}) applied at the neutral axis.

  o The second term $(k_1\sigma_{cp})$ used by prEN2 to add the effect of axial stresses on shear resistance, questionably considers the eccentricity of the tendons despite the fact that, in the first term of the equation , the effective shear span (a_{cs}) already

considers eccentric axial loads effect to calculate the mean shear stress (τ_0). This leads to consider that this alternative is considering double the effect of eccentric axial loads.

- ACI318-19M detailed method defines the shear resistance as the minimum between the web-shear and flexural-shear strength calculated, this last one due to its dependence on the shear required to form a flexural crack ($V_i M_{cre}/M_{max}$) in regions with low bending moments and high shear forces tends to infinite. The current Eurocode (EC2) defines regions cracked and uncracked in bending for the verification of flexural-shear resistance in cracked regions. The new proposal for the Eurocode (prEN1992), only considers the case of flexural-shear failures in its approach (except for prefabricated elements) due to the limitation of its application for rectangular beams or one-way slabs. AASHTO-LRFD doesn't distinguish any region, the approach applies for cracked and uncracked regions in bending, the estimated shear strength is very dependent on the longitudinal strain. These differences in the consideration of the type of failure and its location can be reflected in the varied results obtained when analyzing the shear strength at different critical locations (Figure 4-8, Figure 4-9 and Figure 4-10). To correctly estimate the shear strength, one should be aware of the recommended critical locations and the assumptions made to distinguish the type of failure related with the problem and the design code used.

- AASHTO-LRFD and prEN1992, derived from similar theories (MCFT and CSCT, respectively), consider the aggregate size to calculate the shear resistance directly influencing the final calculated value. Roughness between faces of the critical shear crack collaborates to the shear resistance through aggregate interlock shear-transfer action, although it depends on the shear crack angle, which is reduced by the prestress load applied, decreasing its relevance to the minimum.

- According to the results obtained, prEN1 has a smaller COV than prEN2 and is more precise. However, its usability should be enhanced because determining shear capacity for design optimization requires an iterative procedure. Since the process is computationally expensive because it is a nonlinear equation, a properly linearized expression would be desirable to increase its usability.

4.7.2 Discussion on comparison results
- From the statistical results presented in Table 4-2, Table 4-3, and
- Table 4-4 it is proven that the critical location is important to evaluate the precision and accuracy of the presented approaches. Because the flexural-shear failure mode is dependent of the formation of the flexural cracks that may vary according to the distribution of the principal stresses along the beam's length and cross-section height. Then, most design codes consider the most probable location of the critical shear crack near geometrical discontinuities, contraflexure points, point loads and supports or the location with the highest bending moment and shear force. According that, for the case study of this document the appropriate critical location is $x_r = (a - d)$, something that is also demonstrated by the evolution of the coefficient of variation values for the different design codes shown in Figure 4-9, where it is observed that the values reach their best performance in terms of precision at the critical point closer to the point load.

- Taking into account the explanation in the preceding paragraph, one can conclude that AASHTO-LRFD is the most precise approach with COV=0.22 for rectangular and I/T shape beams with flexural-shear failure and COV=0.23 for rectangular beams only. Although the obtained 5th percentile lower bound values (1.23 to 1.30) indicate conservative estimation of shear strength. On the other hand, ACI318-19M is the less

precise to evaluate flexural-shear cracks obtaining COV=0.29-0.45 for the approximate method and COV=0.33-0.39 for the detailed method assuming a critical location $x_r = (a - d)$. ACI318-19 approximate method obtains results with a safety level less than desirable but the detailed method is the opposite with conservative level of safety according to the 5th percentile lower bound values obtained (0.49-0.52 for approximate method and 0.98-1.02 for detailed method).

- One can observe the great change that occurs in the mean values obtained for the ACI318-19 detailed method in the critical location assumed $x_r = d$, where there is a radical change in the trend and one of the best performances in terms of accuracy is obtained (mean values= 0.88-0.95). This is since this method in its procedure also verifies the web-shear strength (V_{cw}), so it can be said that the estimation of this type of failure is more accurate although it maintains the same level of precision considered low (COV= 0.39-0.41) because it still considers almost half of the tests with flexural-shear failure. It must also be recognized that EC2 recognizes this critical location $x_r = d$ as a location without flexural cracks. However, EC2 does not compare flexural-shear and web-shear strength values as the ACI318-19 detailed method does, then this location does not obtain any result as the focus is on flexural-shear strength.

- Table 4-2, Table 4-3, and
- Table 4-4 show that for the estimated shear resistance for the different subsets established, the alternative prEN1 maintains estimations with good level of precision (COV from 0.23 to 0.29) for different critical locations assumed. This indicates a consistent analysis of the problem through this approach, although the assumptions are not related with I/T shape beams included within subset 1.

- For all critical locations, and for all design codes except AASHTO-LRFD and ACI318-19 detailed method, there is an improvement in the accuracy of the results obtained with subset 1 using subset 2. That may be related with the inclusion of other failure modes within subset 1, there is greater certainty of flexural-shear failure when dealing with rectangular beams only, since they do not suffer a web-shear (shear-tension) failure. AASHTO-LRFD doesn't distinguish failure modes in its procedure, as it is dependent on the longitudinal strain, which is dependent on the external loads acting on the beam. AASHTO-LRFD recognized the influence of the cross-section shape too, as the detailed method (strain compatibility) has been applied to calculate the nominal flexural moment. prEN1 and prEN2 assume in their theoretical derivation a rectangular cross-section, then as expected, the accuracy improved for subset 2 for both approaches. ACI318-19 detailed method as stated in the previous paragraph improves its accuracy evaluating beams that fail by web-shear failure, hence it obtains a better mean value for subset 1.

- Subset 2 is the most useful group of experiments to compare the estimated flexural-shear strength by the design codes used with test results. Then, subset 2 statistical results demonstrate that AASHTO-LRFD and prEN1 have the best COV values for different critical locations assumed comparing the shear strength reported with the estimated shear strength by the design code. prEN1 and ACI318-19 approximate method obtain the best mean values in the range of 0.93 to 1.28 for ACI318-19, and 1.09 to 1.44 for prEN1, then in terms of accuracy they have the best performance. AASHTO-LRFD on the other hand obtains the highest mean values in the different subsets and critical locations, with mean values between 1.48 and 1.78, being the less accurate method, something that is also observed with the value obtained for the 5th percentile lower bound value that varies between 1.23 and 1.30 for the critical location $x_r = a - d$.

- ACI318-19M does not consider a size factor but the necessity to include it has been identified to reduce the shear strength as the effective depth increases, the influence of the longitudinal reinforcement ratio is not included too, then the approaches are too dependent on the concrete compressive strength (section 4.6.4). The collaboration of prestressing into the shear resistance is not considered in the approximate method giving unsafe estimations according to the 5th percentile lower bound values (Table 4-3). The detailed method for flexural-shear strength introduces the effect of prestressing in the cracking moment (M_{cre}) and adds the collaboration of the resultant vertical component (V_p). Both include the shear span-to-effective depth ratio trough the relation M/Vd, although according to the parameter analysis unintentionally for the approximate method.

- AASHTO-LRFD is the result of the SMCFT that simplifies the relation for β that takes into account the influence of all actions on a section, including prestressing, axial loads, and flexure. The size effect of the relationship for members without shear reinforcement is based on the crack spacing parameter (s_{xe}), which depends on the effective shear depth (d_v) with the lower and upper boundary of 300 and 2000 millimeters, respectively. From the design codes studied this approach in one that considers all the identified main parameters that influence the shear strength of concrete.

- EC2 is an approach that according to the parameter analysis considers almost all the parameters except the shear span-to-effective depth ratio into its empirical formulation, this is corrected with the alternatives for the new Eurocode proposal (prEN1992), improving the accuracy, precision and safety of the flexural-shear strength estimation. The empirical formulation of EC2 is replaced by approaches based on a physical model like the CSCT.

5 IMPROVEMENTS TO PREN1992 DRAFT 7

The proposals to estimate the shear strength of prestressed concrete members without shear reinforcement are based in the initial formulation for prEN1992 for reinforced concrete members without normal loads, i.e. the approach presented in section 2.4.2 without considering the k_{vp} factor for the first approach (prEN1-[Eq. 2-16]) or without the addition of $k_1 \sigma_{cp}$ for the second approach (prEN2-[Eq. 2-17]). In order to have a terminology that can be applied to a physical model, in this section the prestressed load will be referred to as normal load.

It's necessary to initiate the discussion with detailed observations on the procedure proposed for reinforced concrete members without shear reinforcement and without normal loads. Then the different proposals to include the effect of normal loads into the current procedure will be analyzed.

5.1 DERIVATION OF THE ENGINEERING MODEL PROPOSED FOR PREN1992 DRAFT 7

The failure criterion given by the analytical formulation in [Eq. 2-8] which is brought up again after this paragraph, correlates the product of the longitudinal strain (ε) and effective depth of the member (d) with the width of the critical shear crack (CSC), to follow the principles of the CSCT mentioned in section 2.3.1.

$$\frac{V_c}{bd\sqrt{f_c}} = \frac{1}{3 \cdot \left(1 + 120 \frac{\varepsilon d}{16 + d_g}\right)} \quad [MPa, mm]$$

It should be noted that ε refers to the longitudinal strain at a distance $0.6d$ from the compression face, obtained adopting a linear-elastic behavior of the materials and assuming no contribution of the concrete in tension.

As the CSCT considers that failure occurs when the shear force acting on the beam is equal to the capacity to transfer shear forces across the CSC, then the intersection of the load-deformation relationship and the failure criterion is the shear strength as shown in the following Figure 5-1.
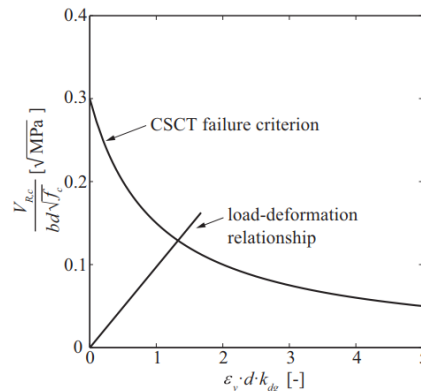
Figure 5-1 Design applying CSCT failure criterion and load-deformation relationship [12]

In order to simplify the procedure described to estimate the shear strength, the equation for failure criterion (hyperbolic curve) will be combined with the load-crack opening relationship.

Nevertheless, before combining both expressions, the longitudinal strain is defined in a smarter way.

- Assuming the depth of the compression zone **c equal to 0.35d**, the strain can be estimated as function of the strain at the longitudinal reinforcement with the following expression. To visualize this step refer to Figure 5-2.

$$\varepsilon = \varepsilon_v \cdot \frac{0.6d - c}{d - c} \cong 0.4\varepsilon_v \ [-]$$

[Eq. 5-1]
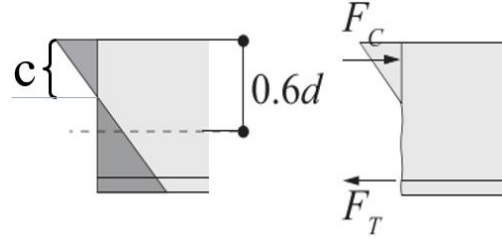
Figure 5-2 Reference fibre assumed for CSCT [12]

- Then, the initial failure criterion can be modified to be function of the longitudinal reinforcement strain as shown in the following expression

$$\frac{V_c}{bd\sqrt{f_c}} = \frac{0.3}{1 + 48\frac{\varepsilon_v d}{d_{dg}}} \ [MPa, mm]$$

[Eq. 5-2]

- One should note that, for simple supported beams with point loads, the longitudinal strain can be defined as function of the shear span ($a_{cs} = |M_E/V_E|$), to consider the effect of the structural configuration of the member on the proposed formulation.

$$\varepsilon_v = \frac{\sigma_s}{E_s} = \frac{M_E}{A_s \cdot E_s \cdot z} = \frac{V_E \cdot a_{cs}}{A_s \cdot E_s \cdot z} \ [-]$$

[Eq. 5-3]

Where the stress at the longitudinal reinforcement $\sigma_s = \frac{M_E}{A_s \cdot z}$, taking M_E as the bending moment at the control section which is equal to shear load times the shear span ($V_E \cdot a_{cs}$). A_s: Area of longitudinal reinforcement
z: Inner lever arms
E_s: Young Modulus of steel reinforcement.

The shear span a_{cs} later will be the main parameter to include the effect of normal loads into the longitudinal strain, something that will be explained in detail in the later section 5.2

5.1.1 Closed-form design equation

To further improve ease of use, the later expression derived [Eq. 5-2] will be approximated by a power-law expression [Eq. 5-4] proposed by [53]. The procedure to derive this expression is explained in detail in [12] and [54], where the researchers demonstrate that by means of parametric analysis, shear failures occur in a narrow band, as can be seen in (Figure 5-3). The value of k is set as constant and equal to 0.021, a parameter that depends on the main mechanical and geometrical parameters (slenderness ratio a/d, compressive strength f_c, reinforcement ratio ρ, effective depth d and shear slenderness ratio $\lambda = M/V \cdot d$).

$$\frac{V_c}{bd\sqrt{f_c}} = k \cdot \left(\frac{d_{dg}}{\varepsilon_v d}\right)^{\frac{1}{2}} \le V_{c,0} \ [N]; with \ k = 0.021$$

[Eq. 5-4]

The maximum shear strength ($V_{Rc,0}$ [N]) correspond to the shear strength for zero strain according to [Eq. 5-2], which is equal to 1/3 as [Eq. 2-8] marks.

To stablish parameter *"k"*, according to the literature review, was set for a critical shear crack located at mid-span ($x_r = 0.5a \, [mm]$) and consequently the tip of the CSC will be located at $x_F = 0.5a + 0.5d$. It is also reported that the values of concrete compressive strength vary between 20-100 MPa, longitudinal reinforcement ratios range between 0.5% and 3%, maximum aggregate size range from 8 to 32 millimeters, effective depth ranges from 200 to 2000 millimeters and slenderness ratio ranges from 2.5 to 8 [12].
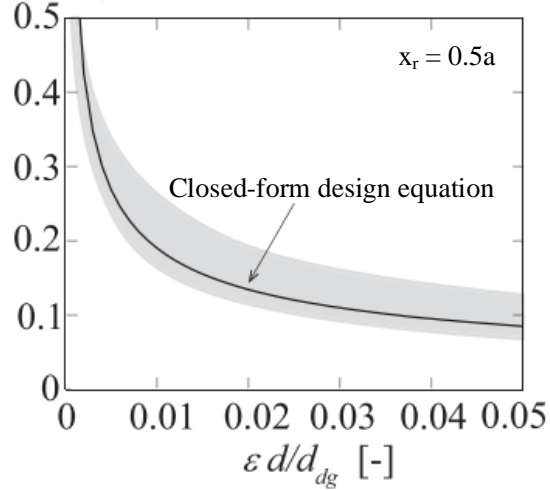
Figure 5-3 Failure envelopes for simple supported beam with point loads [12]

Now, combining the called power-law failure criterion with the load-deformation relationship, an expression for a direct calculation of the shear strength can be derived assuming that the acting shear force is equal to the shear capacity when failure takes place ($V_E = V_c$).

$$\frac{V_c}{bd\sqrt{f_c}} = k \cdot \left(\frac{d_{dg}}{d} \cdot \frac{d \cdot b \cdot \rho \cdot E_s \cdot z}{V_c \cdot a_{cs}} \right)^{\frac{1}{2}} [-]$$

[Eq. 5-5]

Then, the expression for the shear strength of concrete results:

$$V_c = k^{2/3} \cdot b \cdot d \cdot \left(\frac{d_{dg} \cdot f_c}{d} \cdot \frac{\rho \cdot E_s \cdot z}{a_{cs}} \right)^{\frac{1}{3}} [N]$$

[Eq. 5-6]

From that point some terms are grouped as shown below in a term that is called κ.

$$V_c = \kappa \cdot b \cdot d \cdot \left(100\rho \cdot f_c \cdot \frac{d_{dg}}{a_{cs}} \right)^{1/3} [N]; \quad with \; \kappa = \left(\frac{E_s}{100} \cdot z \right)^{\frac{1}{3}} \cdot k^{2/3}$$

[Eq. 5-7]

Assuming $z = 0.9d \, [mm]$ and $E_s = 200000 \, [MPa]$ the term $\kappa = (0.9 \cdot 2000)^{1/3} \cdot 0.021^{2/3} \approx 1$.

But it must be remembered that the assumed value of k depends on the assumed critical crack location ($x_r = 0.5a$), and that this value also depends on the values of $f_c, d_{dg}, \rho, d, a/d$. This is tested for the final equation to be defined, then different load cases are analyzed, concluding that the critical location needs to be defined at a distance d from geometric discontinuities, point loads, and supports. Therefore, as the critical location doesn't coincide with the assumed initially, a reliability analysis was made as summarized below to define an equation accordingly.

[Eq. 5-7] shows the dependence of the shear strength on the shear span (a_{cs}), aggregate size (d_{dg}), concrete strength (f_c), flexural reinforcement ratio (ρ) and the coefficient κ. This last coefficient can be directly obtained from the mechanical model of the critical shear crack,

calculating the contribution of the various shear transfer actions, integrating the stresses thought the crack surface and in the compression zone (details related to the constitutive laws adopted for the shear transfer actions and the assumed shape and kinematics can be found in [12]). Evaluating the obtained values for the coefficient κ comparing with experimental results, has been stated a constant value of $\kappa = 0.66$ for the final expression stated for the new Eurocode proposal, which is similar to the current Eurocode (EN1992-1-1:2004) expression that takes into account the influence of ρ_l and f_{ck}, but the proposed model based on CSCT describes the influence of size, slenderness and aggregate type in a consistent manner.

$$V_c = 0.66 \cdot \left(100 \rho_l \cdot f_{ck} \cdot \frac{d_{dg}}{a_{cs}} \right)^{1/3} b \cdot d \ [N]$$

[Eq. 5-8]

Different limits have been added to this formula, starting with the shear span a_{cs}, which will be replaced by the effective shear span a_v, governed by the condition shown in [Eq. 5-9].

$$a_v = \begin{cases} d \quad [mm] \quad when \ a_{cs} \geq 4 \cdot d \ [mm] \\ \sqrt{a_{cs} \cdot \dfrac{d}{4}} \ [mm] \quad when \ a_{cs} < 4 \cdot d \ [mm] \end{cases}$$

[Eq. 5-9]

It can be noticed that the last expression reduces the distance that represents the critical location practically in case the shear span-to-effective depth ratio is not greater than 4. The following Figure 5-4 illustrates this last statement.
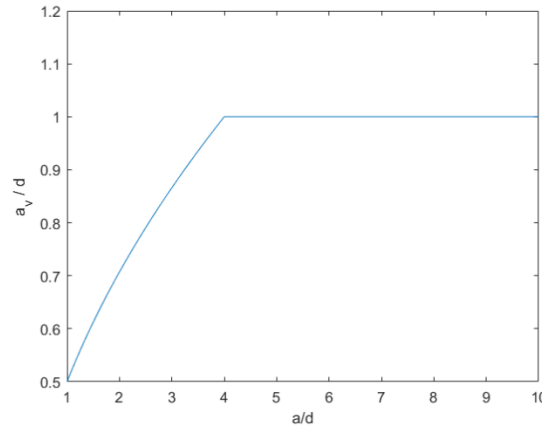
Figure 5-4 Evolution of the effective shear span in relation to the shear span-to-effective depth ratio

For the design shear resistance was included the partial factor for shear and punching resistance without shear reinforcement stated in prEN1992 as $\gamma_V = 1.4$, obtaining the following expression:

$$\tau_{Rd,c} = \frac{V_{Rd,c}}{b \cdot d} = \frac{0.66}{\gamma_V} \cdot \left(100 \rho_l \cdot f_{ck} \cdot \frac{d_{dg}}{a_v} \right)^{1/3} [MPa]$$

[Eq. 5-10]

This last expression has been analyzed in several publications and validated for use in reinforced concrete members without axial/prestress forces. Now, to include the effects of normal loads, the purpose of this document, several proposals will be analyzed and evaluated in terms of accuracy, precision, ease of use, and consistent derivation based on theory and assumptions made.

5.2 PROPOSALS FOR MEMBERS WITHOUT SHEAR REINFORCEMENT INCLUDING THE EFFECT OF NORMAL LOADS

For the sake of simplicity, the derivation of all the alternatives will have as start point [Eq. 5-8], the expression obtained before applying the reliability analysis and incorporate the limit of the

effective shear span a_v. Once the final expressions are obtained the limit and safety factors can be applied again to obtain the design equation as in [Eq. 5-10].

5.2.1 Alternative 1 (prEN1), presented in prEN1992 draft 7 document

In this case the original formulation [Eq. 5-8] wants to be applied to members with normal loads adding a coefficient (k_{vp}) to consider normal load influence into longitudinal strain. This coefficient is defined as follow

$$k_{vp} = 1 + \frac{N_E}{|V_E|} \cdot \frac{d}{3 \cdot a_{cs}} \ [-]$$

[Eq. 5-11]

An to explain it, it is necessary to stablish some assumptions like:
- ○ The location of the resultant compression force within the cross-section is assumed to be located at a distance equal to $d/6$ from the compression face (Figure 5-5).
- ○ Prestress is preload, then the eccentricity of the tendons is taken into account into the calculation of the resultant moment. Then, for the moment equilibrium of a cross-section it is necessary to include only the axial force applied at the centroid.
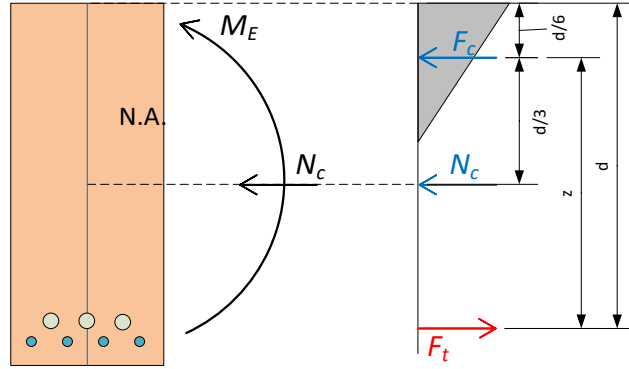
Figure 5-5 Moment of equilibrium of a cross-section under normal force.

By equilibrium of the cross-section forces, and applying the same assumptions mentioned before, the strain at the longitudinal reinforcement is equal to:

$$\varepsilon_v \cong \frac{M_E + N_E \cdot d/3}{z \cdot A_l \cdot E_s} \ [-]$$

[Eq. 5-12]

Then, the shear span can be defined as:

$$a_{cs,N} = \left|\frac{M_E}{V_E}\right| + \frac{N_E}{|V_E|} \cdot \frac{d}{3} \ [mm]$$

[Eq. 5-13]

Where can be observed, it coincides with the factorized term k_{vp}, remembering that the shear span is defined initially as $a_{cs} = |M_E/V_E|$. Then the shear span including normal loads is expressed as:

$$a_{cs,N} = a_{cs} \cdot \left(1 + \frac{N_E}{|V_E|} \cdot \frac{d}{3 \cdot a_{cs}}\right) = a_{cs} \cdot k_{vp} \ [mm]$$

[Eq. 5-14]

Obtaining as final expression the base equation ([Eq. 5-8]), with a modified shear span $a_{cs,N}$

$$V_c = 0.66 \cdot \left(100\rho \cdot f_{ck} \cdot \frac{d_{dg}}{a_{cs,N}}\right)^{1/3} \cdot b \cdot d = 0.66 \cdot \left(100\rho \cdot f_{ck} \cdot \frac{d_{dg}}{a_{cs} \cdot k_{vp}}\right)^{1/3} \cdot b \cdot d \ [N];$$

For this alternative k_{vp} depends on the design shear force from the explicit term V_E included in the calculation of the shear span a_{cs}. This makes this procedure useful for

verifications, but it is necessary to perform an iterative process to calculate the shear capacity as stated in section 4.1.6.

5.2.2 Alternative 2 (prEN2), presented in prEN1992 draft 7 document

This alternative adds shear resistance with a separated term that represents the shear resistance added due to normal loads applied at the centroid of the cross-section, [Eq. 2-17] mentioned before is applied and shown again below to go through the derivation process of this alternative.

$$\tau_c = 0.66 \cdot \left(100\rho_l \cdot f_{ck} \cdot \frac{d_{dg}}{d_{nom}} \right)^{\frac{1}{3}} - k_1 \cdot \sigma_{cp} \ [MPa];$$

$$with \ \ k_1 = \frac{1.4}{\gamma_V} \cdot \left(0.07 + \frac{e_p}{4 \cdot d} \right) \leq 0.15 \cdot \frac{1.4}{\gamma_V}$$

$$\sigma_{cp} = \frac{N_E}{A_c} \ [MPa] < 0.2 f_{cd}$$

The derivation of this expression is based on the approximation of the moment acting on the cross section due to prestress as:

$$M_p = \frac{N_p \cdot I_y}{A_c \cdot h/2} + N_p \cdot e_p \ [N \cdot mm] \qquad \text{[Eq. 5-15]}$$

Assuming the approximation of the bending moment by $M_p = V_p \cdot a$, and considering only rectangular cross-sections into the analysis, the shear strength added by the normal load is equal to:

$$V_p = \frac{N_p \cdot I_y}{A_c \cdot h/2 \cdot a} + N_p \cdot \frac{e_p}{a} \xrightarrow{rectangular \ c-s} N_p \cdot \left(\frac{h}{6 \cdot d} + \frac{e_p}{d} \right) \cdot \frac{d}{a} \ [N] \qquad \text{[Eq. 5-16]}$$

Assuming the relation $d = 0.85h$ and with a fixed $a/d = 4$, the contribution of the normal load is equal to:

$$V_p = N_p \cdot \left(0.2 + \frac{e_p}{d} \right) \cdot \frac{1}{4} = N_p \cdot \left(0.05 + \frac{e_p}{4d} \right) \ [N] \qquad \text{[Eq. 5-17]}$$

But the first term considers the normal load applied at the centroid, and to consider it correctly, it has to be applied at the decompression point, when prestressed moment is equal to the acting bending load. Taking this point at a distance $(a - d)$ from the point load, the first value within the parenthesis has to be multiplied by $\frac{d}{a-d} / \frac{d}{a} = \frac{4}{3}$. And finally, dividing by the concrete area to convert it to shear stress, the following expression is obtained.

$$\tau_p = \frac{V_p}{A_c} = \frac{N_p}{A_c} \cdot \left(0.07 + \frac{e_p}{4d} \right) = \sigma_{cp} \cdot k_1 \ [MPa] \qquad \text{[Eq. 5-18]}$$

5.2.3 Alternative 3 (prEN3)

Approach based on a linearization of the failure criterion stated with the closed-form design equation [Eq. 5-4]. For this alternative the design value of shear stress resistance in presence of normal loads (compression or tension) may be calculated as follows:

$$\tau_{Rc} = \tau_0 - k_1 \cdot \sigma_d \leq 0.33 \frac{\sqrt{f_{ck}}}{\gamma_V} \ [MPa] \qquad \text{[Eq. 5-19]}$$

$$k_1 = 0.67 \cdot \frac{e_p + \frac{d}{3}}{a_{cs}} \leq 0.15 \qquad \textit{[Eq. 5-20]}$$

Where:
τ_0: *shear stress resistance according [Eq. 5-8] without considering axial forces.*

$$\tau_0 = 0.66 \cdot \left(100 \rho_l \cdot f_{ck} \cdot \frac{d_{dg}}{a_{cs}} \right)^{\frac{1}{3}}$$

σ_d: *average normal stresses*
e_p: *eccentricity of the prestressing force, positive towards the tensile side*
a_{cs}: *effective shear span* (M_E / V_E) *without considering axial forces*

Considering the same lower bound as stated for the last two alternatives by [Eq. 2-15]

- **Theoretical derivation**

  The linear approximation of the failure criterion is defined by three points represented in Figure 5-6:

  - **Point A:** the shear stress resistance without axial force (τ_0) according [Eq. 5-4].
  - **Point B:** maximum shear stress resistance (τ_{max}), that correspond to a longitudinal reinforcement strain equal to zero ($\varepsilon_v = 0$), stated equal to 1/3.
  - **Point C:** minimum shear resistance (τ_{min}), that correspond to the yielding longitudinal reinforcement strain $(\varepsilon_v = \varepsilon_{yd})$, calculated again according [Eq. 5-4].
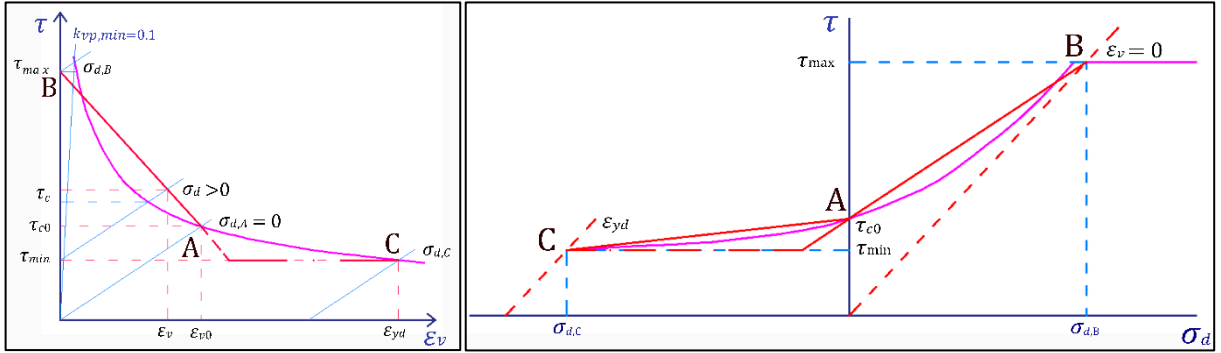
Figure 5-6 Linear approximation of the failure criterion for Alternative 3

Taking point "A" as the reference and considering that one can have either compressive or tensile stresses, the stress-strain relationship can also be extended to the left or right of the reference. Then in the presence of normal forces in compression, the failure criterion is as follow:

$$\tau_{Rc} = \tau_0 + \frac{\tau_{max} - \tau_0}{\varepsilon_{v0}} \cdot (\varepsilon_{v0} - \varepsilon_v) \leq \tau_{max} \qquad \textit{[Eq. 5-21]}$$

And in case of normal forces acting in tension

$$\tau_{Rc} = \tau_0 + \frac{\tau_{max} - \tau_0}{\varepsilon_{yd} - \varepsilon_{v0}} \cdot (\varepsilon_v - \varepsilon_{v0}) \geq \tau_{min} \qquad \textit{[Eq. 5-22]}$$

However, it is not convenient to start the derivation of a simplified approach with two expressions, then to simplify the procedure, the expression derived for compressive forces is extended for the range of tensile forces.

Now, it is necessary to define the strain of the longitudinal reinforcement (ε_v) as a function of the shear stress value (τ_E). Similar to [Eq. 5-12] above, an expression grouping the following parameters is proposed.

$$\varepsilon_v = \frac{V_E \cdot a_{cs} - P_d \cdot \left(e_p + \frac{d}{3}\right)}{z \cdot \rho_l \cdot E_s \cdot b_w \cdot d} = \frac{\tau_E \cdot a_{cs} + 1.25 \cdot \sigma_d \cdot \left(e_p + \frac{d}{3}\right)}{\rho_l \cdot E_s \cdot d} \qquad \text{[Eq. 5-23]}$$

Where the compressive stress in the concrete due to the normal loads (P_d) is equal to:

$$\sigma_d = -\frac{P_d}{b_w \cdot h} \; (< 0 \; compression) \qquad \text{[Eq. 5-24]}$$

And the eccentricity is considered positive towards the tensile side.

With this definition of strain used before, one has that for point A $(\sigma_d = 0)$ the strain is equal to:

$$\varepsilon_{v0} = \frac{\tau_0 \cdot a_{cs}}{\rho_l \cdot E_s \cdot d} \qquad \text{[Eq. 5-25]}$$

Thus, with the current definitions stated, an expression can be obtained by substituting [Eq. 5-25] and [Eq. 5-23] in [Eq. 5-21]. Assuming that the shear stress resistance is equal to the design shear stress $(\tau_{Rd,c} = \tau_{Ed})$ at the intersection point the following relation is obtained.

$$\tau_{Rc} = \tau_0 - 1.25 \cdot \left(1 - \frac{\tau_0}{\tau_{max}}\right) \cdot \frac{e_p + \frac{d}{3}}{a_{cs}} \cdot \sigma_d \qquad \text{[Eq. 5-26]}$$

Expression that can be simplified grouping some terms as below.

$$\tau_{Rc} = \tau_0 - k_1 \sigma_d \le \tau_{max} \qquad \text{[Eq. 5-27]}$$

With:

$$k_1 = 1.25 \cdot \left(1 - \frac{\tau_0}{\tau_{max}}\right) \cdot \frac{e_p + \frac{d}{3}}{a_{cs}} \qquad \text{[Eq. 5-28]}$$

The term within the parenthesis in [Eq. 5-28] can be simplified for ease of use. It is known that both terms are equal to the following expressions

$$For \; \sigma_d = 0 \rightarrow \tau_0 = 0.66 \cdot \left(100 \cdot \rho_l \cdot f_{ck} \cdot \frac{d_{dg}}{a_{cs}}\right)^{\frac{1}{3}} \qquad \text{[Eq. 5-29]}$$

$$For \; \varepsilon_v = 0 \rightarrow \tau_{max} = 0.66 \cdot \left(100 \cdot \rho_l \cdot f_{ck} \cdot \frac{d_{dg}}{k_{vp,min} \cdot a_{cs}}\right)^{\frac{1}{3}} ; \qquad \text{[Eq. 5-30]}$$

Therefore, the relation between both terms results in the expression below.

$$\frac{\tau_0}{\tau_{max}} = k_{vp,\min}^{1/3} \qquad \text{[Eq. 5-31]}$$

The expression stated in [Eq. 5-20] is obtained below substituting [Eq. 5-31] into [Eq. 5-28] considering $k_{vp,min} = 0.1$, as follow.

$$k_1 = 1.25 \cdot \left(1 - 0.1^{\frac{1}{3}}\right) \cdot \frac{e_p + \frac{d}{3}}{a_{cs}} = 0.67 \cdot \frac{e_p + \frac{d}{3}}{a_{cs}} \; [-] \qquad \text{[Eq. 5-32]}$$

Finally substituting the last result ([Eq. 5-32]) into [Eq. 5-27] one obtains the initial equation mentioned ([Eq. 5-19]). Including the partial factor for shear design into the expression the design shear strength is obtained with the following equation:

$$\tau_{Rd,c} = \frac{0.66}{\gamma_V} \cdot \left(100\rho_l \cdot f_{ck} \cdot \frac{d_{dg}}{a_v}\right)^{\frac{1}{3}} - 0.67 \cdot \frac{e_p + \frac{d}{3}}{a_v} \cdot \sigma_{cp} \ [MPa]$$

<div align="right">[Eq. 5-33]</div>

This alternative will be added to the comparison with experimental test results, then to obtain comparable mean values, as stated in last chapter, the average compressive strength of the concrete was used instead of the characteristic compressive strength of the concrete ($f_{ck} = f_{cm}$), and a partial shear factor equal to one ($\gamma_V = 1$) was stated.

$$\tau_{Rm,c} = 0.66 \cdot \left(100\rho_l \cdot f_{cm} \cdot \frac{d_{dg}}{a_v}\right)^{\frac{1}{3}} - 0.67 \cdot \frac{e_p + \frac{d}{3}}{a_v} \cdot \sigma_{cp} \ [MPa]$$

<div align="right">[Eq. 5-34]</div>

$$with: a_v = \begin{cases} d & if \ a_{cs} \geq 4 \cdot d \\ \sqrt{a_{cs} \cdot \dfrac{d}{4}} & if \ a_{cs} < 4 \cdot d \end{cases}, with \ a_{cs} = \left|\frac{M_{Em}}{V_{Em}}\right| \ [mm]$$

5.2.4 Alternative 4 (prEN4)

This alternative applies the same principles stated for prEN1992. The proposal is based on the linearization of the failure criterion stated initially (hyperbolic curve - [Eq. 5-4]). In this proposal, the effect of normal loads is decoupled. This allows a more straightforward estimation of the shear strength of concrete in the first instance. Later, adding the effect of normal loads, it is possible to affect the initial shear strength with the applied normal load. The way normal loads are considered is almost the same as the current EC2, although in this case, the factor k_1 is replaced by another factor that depends on the relation d/a_{cs} as stated below.

$$\tau_{Rc} = \tau_0 - 0.17 \cdot \frac{d}{a_{cs}} \sigma_{cp} \ [MPa]$$

<div align="right">[Eq. 5-35]</div>

Where, as was stablished before, the shear capacity of concrete without normal load τ_0 is:

$$\tau_0 = 0.66 \cdot \left(100\rho_l f_{ck} \frac{d_{dg}}{a_{cs}}\right)^{1/3} \ [MPa]$$

And the normal stress in concrete is calculated as follows, considering negative values for the normal loads applied in compression and positive values when they are applied in tension.

$$\sigma_{cp} = \frac{N_{Em}}{A_c} \ [MPa]$$

<div align="right">[Eq. 5-36]</div>

- **Theoretical derivation**

To explain its derivation, it is necessary to have a look at the derivation of the longitudinal strain again. Figure 5-5 will be helpful to visualize the problem. Then by equilibrium, the tension force can be derived, resulting in the expression below.

$$F_t = \frac{M_{Em}}{z} + \frac{N_{Em}}{z} \cdot \frac{d}{3} = \frac{M_{Em}}{z} \cdot \left(1 + \frac{N_{Em}}{M_{Em}} \cdot \frac{d}{3}\right) = k_{vp} \cdot \frac{M_{Em}}{z} \ [N]$$

<div align="right">[Eq. 5-37]</div>

And now the last defined term used to calculate the longitudinal strain results in

$$\varepsilon_v = \frac{\sigma_t}{E_s} = \frac{F_t}{A_s E_s} = k_{vp} \cdot \frac{M_{Em}}{A_s E_s z} = k_{vp} \cdot \varepsilon_{v0} \ [-]$$

<div align="right">*[Eq. 5-38]*</div>

Where ε_{v0} is the longitudinal strain for a case without normal loads or $k_{vp} = 1$.

What has been defined above will now be useful to define the end points to apply the linearization. It is necessary to define the upper and lower bound of the formulation as can be seen in Figure 5-7.

The upper bound corresponds to the case of shear resistance when k_{vp} has its maximum value, which is 0.1 as stated before. This will result in the following relation:

$$\tau_{max} = 0.66 \cdot \left(100 \rho_l f_{ck} \frac{d_{dg}}{\mathbf{0.1} \cdot a_{cs}} \right)^{1/3} [MPa]$$

<div align="right">*[Eq. 5-39]*</div>

And the lower bound corresponds to a case of shear resistance without normal load, that it is already known as τ_0.
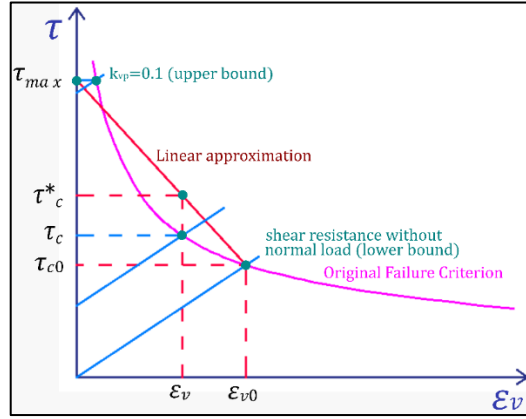
<div align="center">*Figure 5-7 Linear approximation of the failure criterion for Alternative 4*</div>

Having both extremes located, the corresponding shear strength (τ_c) according to the calculated strain (ε_v) can be calculated using the linear relationship between extremes values.

$$\frac{\tau_c - \tau_0}{\varepsilon_{v0} - \varepsilon_v} = \frac{\tau_{max} - \tau_0}{\varepsilon_{v0}}$$

<div align="right">*[Eq. 5-40]*</div>

Including the expression found in [Eq. 5-38] into the last expression the equation below is results.

$$\tau_c = \tau_0 - \frac{N_E}{M_E} \cdot \frac{d}{3} \cdot (\tau_{max} - \tau_0) \ [MPa]$$

<div align="right">*[Eq. 5-41]*</div>

Which is the desired condition, but one would like to simplify it even more by looking at the relationship between the extremes $\tau_{max} = 10^{1/3} \tau_0$. Then substituting into last equation, the result is:

$$\tau_c = \tau_0 - \frac{N_E}{M_E} \cdot \frac{d}{3} \cdot \left(10^{\frac{1}{3}} - 1 \right) \tau_0 = \tau_0 \cdot \left(1 - \frac{N_E \cdot d}{M_E} \cdot \frac{1.15}{3} \right)$$
$$= \tau_0 \cdot \left(1 - 0.38 \cdot \frac{N_E \cdot d}{M_E} \right) [MPa]$$

<div align="right">*[Eq. 5-42]*</div>

Again, one can reformulate the last expression considering the definition of axial stress $\sigma_{cp} = N_E/A_c$, a term used in the current Eurocode

$$\tau_c = \tau_0 \cdot \left(1 - 0.38 \cdot \frac{A_c \cdot d}{M_E} \sigma_{cp}\right) \; [MPa] \qquad \text{[Eq. 5-43]}$$

Into the last expression, it should be noted that according to the definition of average shear stress in Eurocode $V_0 = \tau_0 \cdot b_w \cdot z = \tau_0 \cdot b_w \cdot 0.9d$, then last expression can be stated as:

$$\tau_c = \tau_0 - 0.38 \cdot \frac{\tau_0 \cdot A_c \cdot d}{M_E} \sigma_{cp} = \tau_0 - 0.38 \cdot \frac{V_0}{M_E} \frac{A_c \cdot d}{b_w \cdot 0.9d} \sigma_{cp} \; [MPa] \qquad \text{[Eq. 5-44]}$$

At this point one should stop to analyze what τ_0 involves. Knowing that the formulation includes the effect of prestressing in the acting bending moment and shear force (M_E, V_E), the obtained value is the shear resistance of the member without the effect of axial forces. Then, to accurately calculate the value of V_0 one should remove the effect of the normal force.

In order not to worsen the ease of use of this approach, it can be considered the use of the maximum value for shear resistance in the second term, being on the safe side. Then, applying again the known relationship between τ_0 and τ_{max}, the following relation results.

$$\tau_c = \tau_0 - 0.38 \cdot \frac{\tau_0 \cdot A_c \cdot d}{M_E} \sigma_{cp} = \tau_0 - 0.38 \cdot \frac{10^{-\frac{1}{3}} \cdot \tau_{max} \cdot A_c \cdot d}{M_E} \sigma_{cp}$$
$$= \tau_0 - 0.2 \cdot \frac{V_{max}}{M_E} \frac{A_c}{b_w} \sigma_{cp} \; [MPa] \qquad \text{[Eq. 5-45]}$$

Finally, knowing that the actual shear force $(V_E = V_c)$ will be equal or lower than V_{max} in all cases, and that the main application of this approach is concrete solid slabs or rectangular beams, one ca simplify further the expression as one knows that $A_c = b_w \cdot h$ and assuming $d = 0.85 \cdot h$, then the formula results in:

$$\tau_c = \tau_0 - 0.2 \cdot \frac{V_E}{M_E} \frac{A_c}{b_w} \sigma_{cp} = \tau_0 - 0.17 \cdot \frac{V_E \cdot d}{M_E} \sigma_{cp} = \tau_0 - 0.17 \cdot \frac{d}{a_{cs}} \sigma_{cp} \; [MPa] \qquad \text{[Eq. 5-46]}$$

Further improvements can be proposed to the last expression, but the analysis will end at this point. This expression after the inclusion of the partial factor for shear design ends up being equal to:

$$\tau_{Rd,c} = \frac{0.66}{\gamma_V} \cdot \left(100\rho_l \cdot f_{ck} \cdot \frac{d_{dg}}{a_v}\right)^{\frac{1}{3}} - 0.17 \cdot \frac{d}{a_{cs}} \sigma_{cp} \; [MPa] \qquad \text{[Eq. 5-47]}$$

The upper limit stablished for the proposed expression is equal to:

$$\tau_{max} = \left(\frac{1}{0.1}\right)^{1/3} \tau_0 = 2.15\tau_0 \qquad \text{[Eq. 5-48]}$$

Also due to the dependence of the calculated shear resistance on the applied external force for $a_{cs} > 4d$ an iterative process must be performed in case the capacity is required. And in case the mean shear capacity is required the mean compressive strength of concrete is used instead of the characteristic strength of concrete and the partial shear factor is equal to 1.

$$\tau_{Rd,c} = 0.66 \cdot \left(100\rho_l \cdot f_{cm} \cdot \frac{d_{dg}}{a_v} \right)^{\frac{1}{3}} - 0.17 \cdot \frac{d}{a_{cs}} \sigma_{cp} \ [MPa]$$

$$with: a_v = \begin{cases} d & if \ a_{cs} \geq 4 \cdot d \\ \sqrt{a_{cs} \cdot \dfrac{d}{4}} & if \ a_{cs} < 4 \cdot d \end{cases}, with \ a_{cs} = \left| \frac{M_{Em}}{V_{Em}} \right| \ [mm]$$

5.2.5 Discussion on the difference between the proposed simplifications

Evaluating the proposal for the new Eurocode, alternatives prEN1 to prEN4 can be divided into three groups. Alternative prEN1 in the first group, its derivation is closely related to the original approach derived from the CSCT. Later the second group with Alternative prEN4 that linearizes the original failure criterion and ends with a consistent formula that deviates slightly from the original approach when assuming $(V_0 = V_{max})$ for simplicity in one of the intermediate steps of its derivation (section 5.2.4). The last group of alternatives prEN2 and prEN3 with similar equations, but the problem is that the derivation of their factors that consider the prestressing effect contain some debatable assumptions. e.g., alternative prEN2 assumed a fixed a/d=4, and both consider the eccentricity in the factor that multiplies the axial stress on concrete. Then let's discuss the last two alternatives (Alternative prEN3 and prEN4) presented below in a simplified manner, considering τ_0 as the shear resistance without normal loads.

$$\tau_3 = \tau_0 - \left(0.22 \frac{d}{a_{cs}} + 0.67 \frac{e_p}{a_{cs}} \right) \sigma_{cp}$$

$$\tau_4 = \tau_0 - 0.17 \frac{d}{a_{cs}} \ \sigma_{cp}$$

If we remember that τ_0 already considers the prestressing effect through the effective shear span that is calculated with the acting bending moment and acting shear force $(a_{cs} = |M_E/V_E|)$, it is questionable the use of the eccentricity (e_p) that comes to incorporate the prestressing effect again when it only remains to add the axial strains caused by the prestressing applied on the centroidal axis. Also, if the last term that considers the eccentricity in alternative prEN3 is excluded, an expression very similar to alternative prEN4 appears.

5.3 EVALUATION OF THE ALTERNATIVE APPROACHES (PREN3 AND PREN4)

Considering that the assumed critical location is $x_r = a - d$ as suggested in the proposal for the new Eurocode, the performance of the proposed models is evaluated and compared according to the results presented in Table 5-1.

Looking at the COV and mean values of the shear strength ratio (V_{test}/V_{calc}), prEN4 is more precise and accurate than prEN3, because prEN4 has mean values in the range 1.30-1.39 and prEN3 in the range 1.50-1.64, and prEN4 has COV=0.25-0.26 and prEN3 has COV=0.29-0.30. prEN4 is a good alternative but does not surpass the accuracy of the prEN1 approach which has COV=0.23-0.24, the lowest values among the alternatives proposed for the new Eurocode, and the second approach after AASHTO-LRFD which has COV=0.23-0.24.

Table 5-1 Statistical information from comparing the design codes results with tests for the defined subsets when critical location is x_f = a-d including new proposals (prEN3 and prEN4)

	Mean of $\alpha = V_{test}/V_{cal}$ [-]			Coefficient of variation of $\alpha = V_{test}/V_{cal}$ [-]			5th Percentile lower bound of $\alpha = V_{test}/V_{cal}$ [-]		
	Subset 1	Subset 2	Subset 3	Subset 1	Subset 2	Subset 3	Subset 1	Subset 2	Subset 3
ACI-s	1.28	1.04	1.00	0.45	0.32	0.29	0.52	0.50	0.49
ACI-d	1.51	1.62	1.66	0.38	0.39	0.33	0.98	1.02	1.10
AASHTO	1.76	1.78	1.76	0.22	0.23	0.23	1.26	1.30	1.23
EC2	1.51	1.44	1.41	0.29	0.31	0.28	0.89	0.82	0.78
prEN1	1.44	1.41	1.42	0.23	0.24	0.24	1.05	1.04	1.03
prEN2	1.49	1.39	1.38	0.29	0.30	0.29	0.95	0.86	0.81
prEN3	1.64	1.50	1.50	0.29	0.30	0.29	1.06	1.03	0.98
prEN4	1.39	1.30	1.30	0.26	0.26	0.25	0.96	0.90	0.85
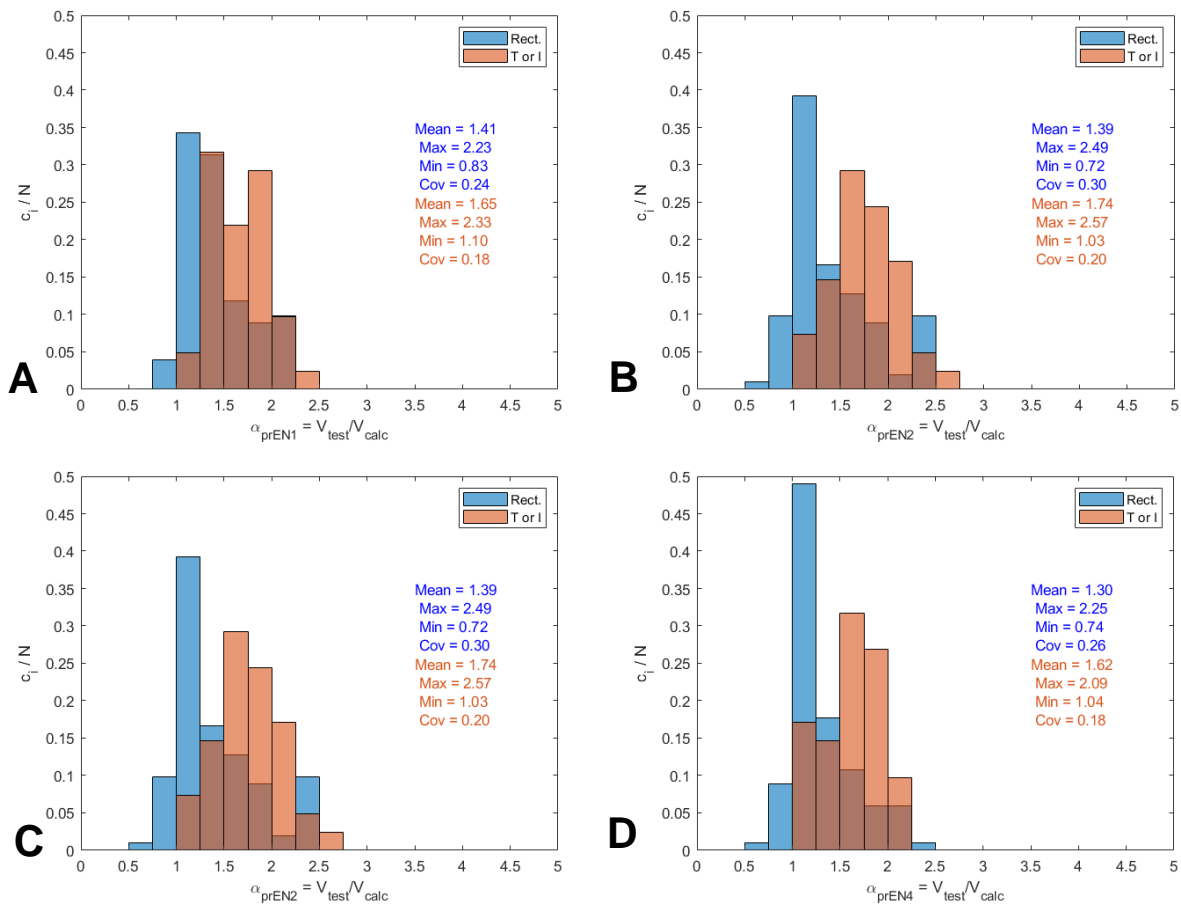
*c_i/N: refers to the number of tests within the bin (c_i) over the total number of elements (N)

Figure 5-8 Histograms comparing results obtained using subset 1 and x_f=a-d, for beams with rectangular cross-section and beams with I- or T-shape cross-section. (A) prEN1 (B) prEN2. (C) prEN3 and (D) prEN4

As in the previous chapter, one can compare the shear strength estimated within subset 1 for rectangular beams and I/T shape beams. One expectation is that the rectangular beams group obtains better accuracy than I/T beams group. Also, may be expected the underestimation of the shear strength of I/T beams group due to the assumed constant inner lever arm equal to $z = 0.9d$. This can be validated with the histograms presented in Figure 5-8, comparing the mean values of the shear strength ratios (V_{test}/V_{calc}) of the different alternatives are shown.

It can be seen that the accuracy is improved for all alternatives for the rectangular beam groups (prEN1: 1.44 to 1.41, prEN2: 1.49 to 1.39, prEN3: 1.64 to 1.50, prEN4: 1. 39 to 1.30) and for I/T beam groups, the accuracy is decreased with much higher mean values (prEN1: 1.44 to 1.65, prEN2: 1.49 to 1.74, prEN3: 1.74 to 1.74, prEN4: 1.39 to 1.62).

What is being learned at this point is that if one wants to consider different cross-section shapes into the different alternatives for the new Eurocode, one should include the influence of the actual gross cross-section area at least in the inner lever arm estimation to do not obtain such conservative results. Figure 5-5 shows the assumed rectangular cross-section for the calculation of the moment of equilibrium of a cross-section for prEN1992 approaches, from that point is where other assumptions should be given to have a formula that fits the different cross-section shapes. It could be keeping the inner lever arm term z without any assumptions until the end and trying to simplify it in the final expression, it is a work that can be done in another research.

Something interesting that can also be seen with the histograms shown in Figure 5-9 is the evolution of the performance of the alternatives within the different defined subsets. One can see that the mode tends to accentuate around 1 progressively from histogram for subset 1 to histogram for subset 3.
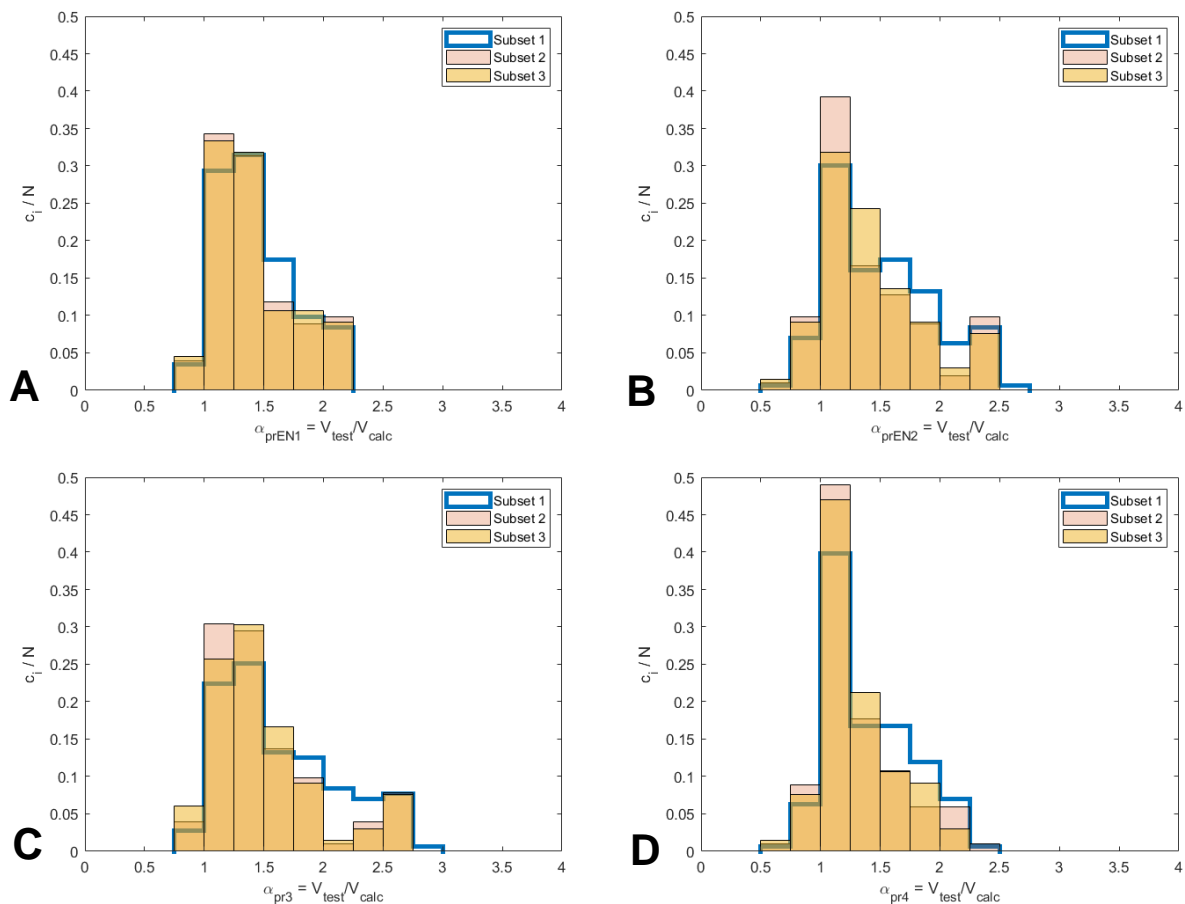
*c_i/N: *refers to the number of tests within the bin* (c_i) *over the total number of elements* (N)

Figure 5-9 Histograms for comparison levels of design codes with experimental data at x_i=a-d. (A) prEN1 and (B) prEN2, (C) prEN3 and (D) prEN4

As was done in chapter 4, the performance of the different alternatives for the new Eurocode proposal can be evaluated in terms of precision, safety and accuracy assuming different critical locations. Figure 5-10, Figure 5-11 and Figure 5-12 show the evolution of the mean value the COV and the 5th percentile lower bound of the shear strength ratio $\alpha = V_{test}/V_{calc}$ for the different critical locations assumed.

The new proposals that are added have varying accuracy and precision depending on the critical location assumed. Making a general evaluation at the most representative critical location $x_r = a - d$, and taking the criteria established in Table 4-5 for the relative assessment of the statistical indicators obtained, it can be said that:

- prEN1 for all the defined subsets obtains a COV in the range 0.23-0.24, which indicates a good precision of the results obtained. This is the best performance in terms of precision between the 4 alternatives proposed for the new Eurocode. The 5th percentile lower bound value indicates conservative results with values between 1.03 to 1.05.
- prEN2 obtains COV in the range 0.29-0.30 indicating that the results have reasonable precision, and the 5th percentile lower bound values in the range 0.81—0.95 indicate good levels of safety.
- prEN3 similar to prEN2 obtains COV in the range 0.29-0.30 indicating reasonable precision for the results, but the 5th percentile lower bound values are between 0.98-1.06 denoting more conservative results than prEN2.
- prEN4 is the best linearized proposal that obtains COV in the range 0.25-0.26 indicating results with reasonable precision, and the 5th percentile lower bound values are in the range 0.85-0.96 indicating good levels of safety.

In terms of accuracy comparing with test results, the alternative prEN4 has the best results (mean= 1.30-1.39) followed by prEN1 (mean= 1.41-1.44) and prEN2 (mean= 1.38-1.49). prEN3 is the less accurate approach from the alternatives for the prEN1992 with mean values in the range 1.50 to 1.64.

Comparing the proposal for the new Eurocode with the current EC2, it can be seen in Figure 5-10, Figure 5-11 and Figure 5-12, that there is an improvement in terms of accuracy with prEN1, prEN2 and prEN4. In terms of precision all the alternatives improve the precision obtained with EC2 and in terms of safety prEN4 and prEN2 improve safety as necessary, but prEN1 and prEN3 become somewhat conservative.
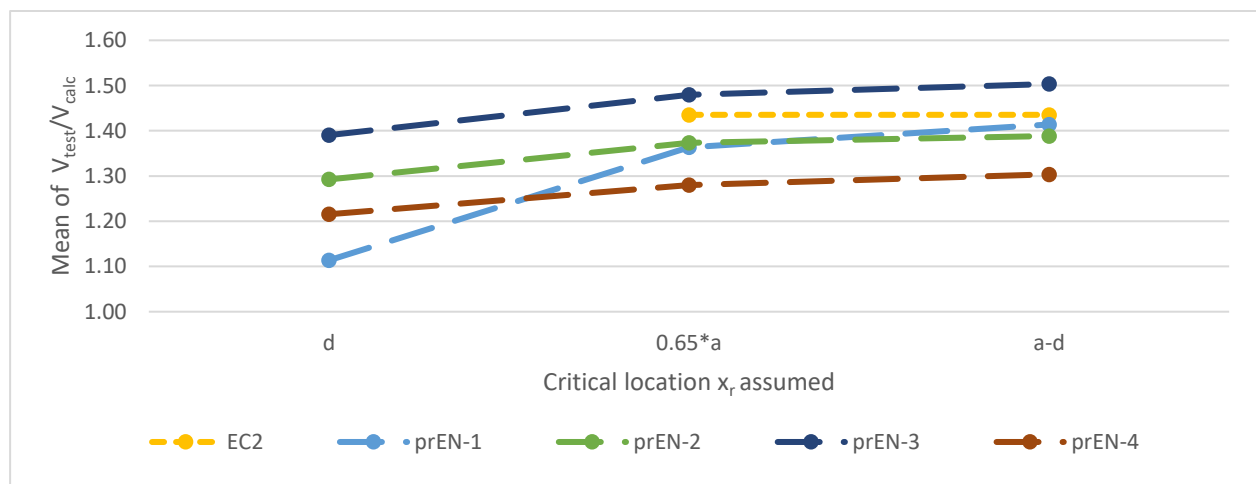
Figure 5-10 Subset 2, mean values for comparison of V$_{test}$/V$_{calc}$ as function of the critical location for EC2 and prEN1992 proposals.
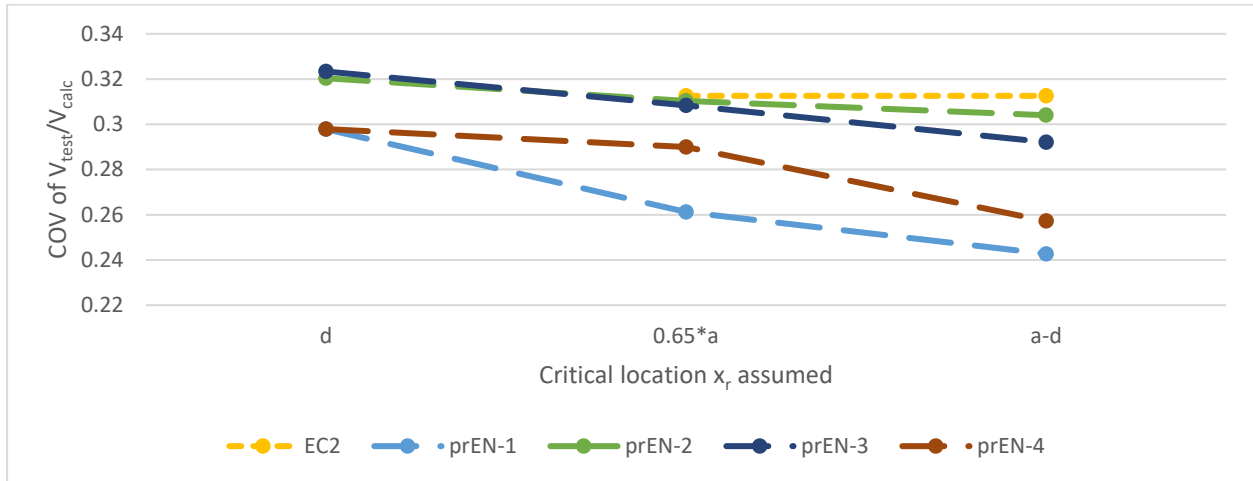
Figure 5-11 Subset 2, coefficients of variation for comparison of V_test/V_calc as function of the critical location for EC2 and prEN1992 proposals.
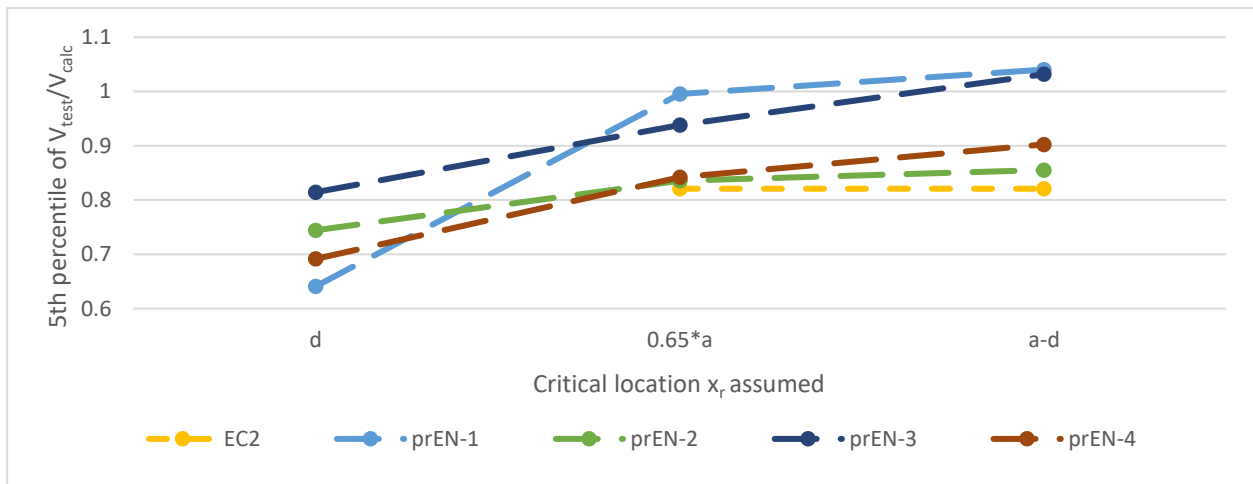
Figure 5-12 Subset 2, 5th percentile lower bound of V_test/V_calc as function of the critical location for EC2 and prEN1992 proposals

5.3.1 Assessment of the alternatives proposed for the new Eurocode

The 4 alternatives presented in this chapter for the estimation of the shear strength of prestressed concrete members without shear reinforcement will be examined comparing results and assumptions between them.

The main discussion is around the results obtained by adding prestressing within a model dependent on the estimated longitudinal strain of the longitudinal reinforcement that affects the crack width of the critical shear crack and consequently the estimated shear strength of concrete.

The initial approach prEN1, has been extensively tested for reinforced concrete beams, so it is expected to work for prestressed concrete beams if the correct terms are modified to consider the total effect of the normal loads applied on the beam. The concepts handled by prEN1 and prEN4 are very similar, and both consider that the effect of the prestressing force, which by definition is preload, is already considered in the effective shear span term (a_v), which considers the ratio between the acting bending moment (M_{Ed}) and acting shear force (V_{Ed}). So, both assume that it remains to consider the axial/normal loads applied in the neutral axis of the cross-section resulting from prestressing. This can be shown by the moment of equilibrium of a cross-section assumed to derive the prEN1 approach shown in Figure 5-5. prEN1 modified the derivation of its approach from there to include the effect of normal loads through the k_{vp} factor that modifies the effective shear span a_v. prEN4 simplifies the original approach through a linearization that ends up adding to the mean shear stress (τ_0) (which considers M_{Ed} and V_{Ed}) a term that includes the effect of the

axial stresses generated as a function of the ratio d/a_v. The expressions of prEN1 and prEN4 are shown below again.

$$\tau_1 = 0.66 \cdot \left(100\rho \cdot f_{ck} \cdot \frac{d_{dg}}{a_v \cdot \left(1 + \frac{N_E}{|M_E|} \cdot \frac{d}{3}\right)} \right)^{1/3} \quad [MPa]$$

$$\tau_4 = 0.66 \cdot \left(100\rho \cdot f_{ck} \cdot \frac{d_{dg}}{a_v} \right)^{1/3} - 0.17 \frac{d}{a_{cs}} \cdot \frac{N_E}{A_c} = \tau_0 - 0.17 \frac{d}{a_{cs}} \sigma_{cp} \ [MPa]$$

One notices that the final expression for prEN4 ends up being very similar to the current expression for EC2, only that instead of the empirical factor $k_1 = 0.15$ there is one dependent on the ratio d/a_v. This makes it much easier to make it accepted in terms of usability, since the effect of the normal loads on the shear strength can also be appreciated.

prEN2 and prEN3 are a linearization of the original approach as prEN4, but they include the eccentricity of tendons (e_p) in the factor that affects the influence of normal stresses on the shear resistance. This is questionable since it would be doubly considering the effect of the eccentricity of the tendons in the approach since this eccentricity is implicitly immersed in the acting bending moment and acting shear force. The expressions of prEN2 and prEN3 are shown below too.

$$\tau_2 = 0.66 \cdot \left(100\rho_l \cdot f_{ck} \cdot \frac{d_{dg}}{d_{nom}} \right)^{\frac{1}{3}} - k_1 \cdot \sigma_{cp} = \tau_0 - \frac{1.4}{\gamma_V} \cdot \left(0.07 + \frac{e_p}{4 \cdot d} \right) \sigma_{cp}$$

$$\tau_3 = 0.66 \cdot \left(100\rho_l \cdot f_{ck} \cdot \frac{d_{dg}}{d_{nom}} \right)^{\frac{1}{3}} - k_1 \cdot \sigma_d = \tau_0 - 0.67 \cdot \frac{e_p + \frac{d}{3}}{a_{cs}} \sigma_{cp} = \tau_0 - \left(0.22 \frac{d}{a_{cs}} + 0.67 \frac{e_p}{a_{cs}} \right) \sigma_{cp}$$

The main difference between prEN2 and prEN3 is the fixed $a/d = 4$ assumed for prEN2, and both approaches assume the influence of the eccentricity of the resultant axial prestress force into the moment of equilibrium of the cross-section. This last assumption could only be successful in the case of separating the effect of the prestressing force on the ultimate load, which extends the procedure much further and is detrimental to ease of use, and therefore initially, it is not considered.

Based on the alternatives proposed, a comparison was made based on the consideration of axial stress in the shear resistance. The linearized alternatives prEN2, prEN3 and prEN4 were compared with the alternative prEN1 and the following scatterplots were obtained as shown in Figure 5-13, Figure 5-14 and Figure 5-15.
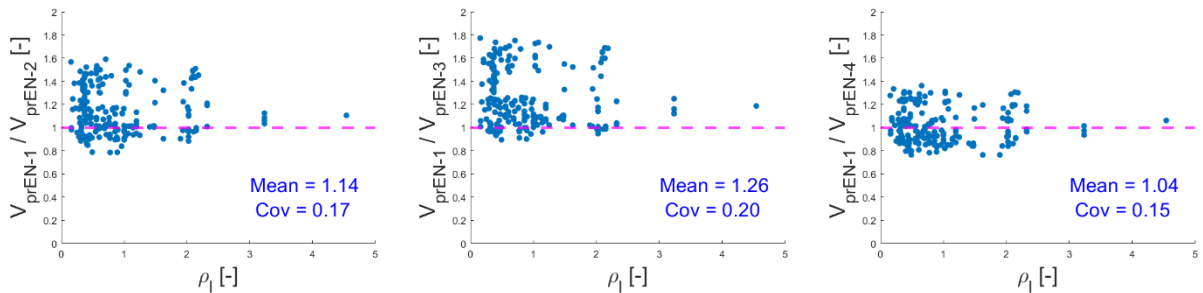
Figure 5-13 Shear strength ratio $\left(V_{prEN-1}/V_{calc}\right)$ versus longitudinal reinforcement ratio (ρ_l) for subset 1 from ACI-DAfStb-PC database
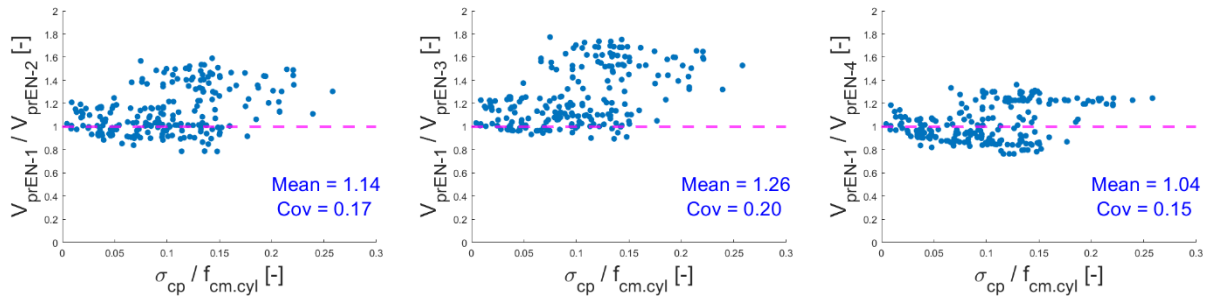
Figure 5-14 Shear strength ratio $\left(V_{prEN-1}/V_{calc}\right)$ versus dimension-free axial force $\left(\sigma_{cp}/f_{cm}\right)$ for subset 1 from ACI-DAfStb-PC database
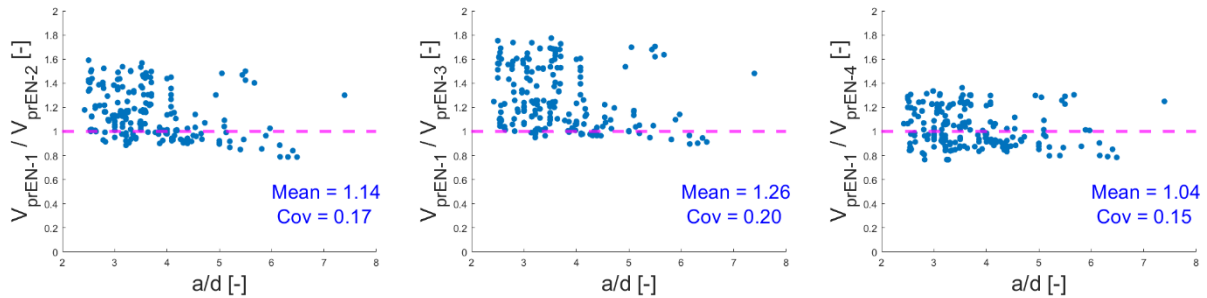
Figure 5-15 Shear strength ratio $\left(V_{test}/V_{calc}\right)$ versus shear span-to-effective depth ratio $\left(a/d\right)$ for subset 1 from ACI-DAfStb-PC database

The mean value of the shear strength ratio for the different alternatives compared to prEN1 shows that prEN4 is the most similar to prEN1 in terms of accuracy and precision, noting that the mean value of 1.04 for V_{prEN1}/V_{prEN4} denotes that the results for prEN4 are on the safe side. The precision is also the best of all with COV=0.15 which is considered a very good value.

The other alternatives obtain mean values of the shear strength ratio equal to 1.14 for prEN2 and 1.26 for prEN3, and the precision is not as good as prEN4, with COV=0.17 for prEN2 and COV=0.20 for prEN3.

The scatterplots shown in Figure 5-14 can initially show us the comparative results in terms of the considered axial stress, where one ends up including extra shear strength with alternatives prEN2 and prEN3 specially to members with high dimension-free axial force values. This is reflected in the evaluation of the other scatterplot shown in Figure 5-13, and Figure 5-15 where for all the ranges of a/d and ρ_l one can appreciate certain overestimation of the shear strength by prEN2 and prEN3 comparing with the results presented by prEN1.

The solution to correct these overestimated values for prEN2 and prEN3 could be the consideration by separate terms of the ultimate bending moment (M_u), ultimate shear force (V_u), prestress bending moment (M_p), and prestress shear force (V_p), excluding from the effective shear span (a_v) the incidence of prestressing, thus from the mean shear stress (τ_0). This complicates the procedure by lengthening it and questions the concept of prestressing as preload, so it is convenient to keep the concept established for prestressing and carry out a derivation as it is done with the alternatives prEN1 and prEN4.

5.4 DISCUSSION AND CONCLUSIONS

- If discussing the need for more alternatives over the two already existing alternatives in the draft document for the new Eurocode, one should point out that both alternatives result in a significant change compared to the current Eurocode. Several parameters and conditionals are added, and this initially creates displeasure. Therefore, it is suggested that this procedure be user-friendly to be quickly adopted in everyday practice. For this purpose, other procedures that try to avoid the calculation of more parameters or provide a straightforward interpretation of the effect of the prestressing forces on the shear strength of the member are proposed.

- The assumptions and simplifications made for the alternatives also were evaluated on how they incorporate the effect of normal forces on the longitudinal strain calculation. Considering that prestress is preload, one cannot consider eccentric forces since one would be doubly considering the effect of the prestressing force. In this case, the normal load, resultant from the prestressed forces applied at the centroid, will be the remaining external load to be considered in the calculations of the equivalent longitudinal strain.

- The procedures derived for all alternatives are based on the assumption of a rectangular cross-section to estimate the location of the compression resultant with respect to the neutral axis. If the shear strength estimation for I or T section beams needs to be improved, the contribution of the remaining part of the beam flanges to the concrete compression resultant should be included by another factor affecting the location of the concrete compression resultant.

- Considering that the suggested critical locations are at a distance d from the support of point load, results obtained comparing the shear strength ratio V_{test}/V_{calc} show that from the linearized alternatives prEN4 is the best if accuracy and precision are evaluated, followed by alternative prEN and prEN3 respectively. Furthermore, it must be said that the derivation of the final equation for prEN4 is more transparent and more concise, which makes it much easier to be used and interpreted in practice. Besides, following the logic mentioned earlier on considering normal forces, it is the alternative that best follows this concept.

- Alternatives prEN2, prEN3 and prEN4, which are based on the linearization of the failure criterion, take into account a second term that adds the effect of the prestressing force multiplying the axial concrete stress with a factor derived through a simplification procedure and assumptions mentioned in the document. It has been found that this factor is the one that can most influence the precision and accuracy that the alternative will acquire. Therefore, the procedure involved in its derivation is transcendental to try to improve the estimated shear strength for each alternative.
  - o Based on the above, it has been found that alternative prEN4 could consider part of the cross-section influence into the shear strength by maintaining the gross cross-section area term from [Eq. 5-45], obtaining the following expression:

$$\tau_4 = \tau_0 - 0.2 \cdot \frac{V_E}{M_E} \frac{A_c}{b_w} \sigma_{cp} = \tau_0 - 0.2 \cdot \frac{A_c}{a_{cs} \cdot b_w} \sigma_{cp}$$

It should be noted that in case any of the alternatives obtains a value of $a_{cs} > 4$, the shear capacity would be obtained directly without the need of an iterative process, since a_{cs} would be equal to d.

- In deriving an approach based on CSCT, the estimated longitudinal strain should be considered the most relevant factor since it rules over the estimated crack width and shear strength. Flexural-shear capacity depends on the contribution of the shear-transfer actions, which are affected by the applied prestressing as mentioned in section 2.2 due to the decrease of the crack width and crack angle. According to the Eurocode definition, prestressing is considered preload, so it affects the acting bending moment and acting shear force, which causes the decrease of the principal stresses acting on the longitudinal axis of the beam. Following this definition, the moment of equilibrium of the cross-section should simply include the resultant normal load applied on the neutral axis. Not following this definition creates problems in the effective shear span given since it relates the acting bending moment to the acting shear force. This is the problem faced by the alternatives prEN2 and prEN3 to calculate the total prestressing contribution to the shear strength, it is not possible without separating the acting forces of prestressing in another effective shear span. This creates more extensive terms to calculate and is detrimental to the ease of use. prEN1 and prEN4 following the initially stated concepts are similar approaches with the difference that prEN4 is more conservative than prEN1 because prEN4 is a linearization of the failure criterion.

6 DESIGN EXAMPLES FOR SHEAR STRENGTH

In this section all design procedures will be applied for typical design cases, the shear strength will be verified in critical locations and the differences in the easy-of-use will be highlighted. Design codes require efficient procedures, since engineering professionals have time as their most valuable resource.

The cases to be evaluated will be 2, the first one for the design of a new structure, a deck slab of a cut-and-cover tunnel and the second the assessment of an existing structure, in this case a bridge slab that is going to be evaluated under the condition of simple supported and continuous bridge deck.

The procedure to follow is well know at this point, referencing section 2.4, and considering for the design codes applied in Europe the partial safety factor for shear $\gamma_V = 1.4$, for concrete $\gamma_c = 1.5$, and for steel $\gamma_s = 1.15$. The failure criterion compares the design value of the applied shear force with the calculated shear resistance, requiring the condition ($V_{Ed} \leq V_{Rd.c}$) to be met to satisfy the demand.

In case of the codes typically applied in America, the shear strength calculated has to be multiplied with a shear strength reduction factor, then this value can be compared with the ultimate shear force. In case of ACI318-19M the shear strength reduction factor value is $\Phi = 0.75$. The conditional stated below, must be met to satisfy the demand.

$$V_u < \Phi V_c = 0.75 \cdot V_c \qquad \text{[Eq. 6-1]}$$

For AASHTO-LRFD the resistance factor for shear is $\Phi_V = 0.9$ for members with bonded strands. This factor is multiplied with the resultant of the factored shear strength of the concrete plus the component of prestressing force in the direction of the shear force. The result then is compared with the ultimate shear to verify the conditional stated below.

$$V_u < \Phi_V \cdot V_n = \Phi_V \cdot \left(V_c + V_p \right) \qquad \text{[Eq. 6-2]}$$

Another essential consideration is calculating the demand according to the different design codes. The safety is ensured not only by strength reduction factors; load factors are used to increase the amount of applied load on a structure to account for possible load increments during the structure's life span.

The design codes address different safety, reliability, and operational level criteria according to the parameters established for each region where the design codes are applied. A comparison between Eurocodes and AASHTO-LRFD for shear evaluation of slab bridges is shown in reference [55], and it was found that AASHTO-LRFD can generate shear stresses similar to Eurocodes at the support at different safety levels. However, the underlying safety requirements, indicated by the demanded reliability index, are considerably different. So, to briefly summarize, it should be noted that the safety requirements underlying the design code procedures are different.

The examples presented in the following sections related to highway structures assume that AASHTO-LRFD predominates over ACI318-19, which prevails for buildings. The factored load combinations for the Eurocodes and the one corresponding to AASHTO-LRFD are shown in Table 6-1.

Table 6-1 Common factored load combinations for the studied design codes

Common Factored Load Combination	
EN1990 (6.10b), Consequence class 3 (CC3). Also, for prEN1992.	$\xi\gamma_G G + \gamma_Q Q + \gamma_p P = 1.25G + 1.5Q + 1.0P$ G: Dead load, Q: Live load, P: Prestress load
AASHTO-LRFD – Strength I	$1.25w_{DL} + 1.75w_{LL}$ DL: Dead load, LL: Live load

The deck slab of a cut-and-cover tunnel will assume a uniform design load for all the design codes. This will allow us to see what happens in case the same design load is assumed, keeping in mind that there are significant variations in the safety requirements of each code.

Finally, for the analysis of bridge deck slabs, there are different traffic loads for the Eurocodes and for AASHTO-LRFD as detailed in section 6.2.

6.1 DESIGN OF DECK SLAB OF A CUT-AND-COVER TUNNEL

Figure 6-1 presents the section of the tunnel, where the frame structure has two spans of 10.55 meters between axes, and there is a deck that is part of it that forms the roof of the tunnel. The thickness of the slab is 700 mm, the concrete used is C30/37 ($f_{ck} = 30 \ [MPa], \ \lambda = 1$), the steel reinforcement used is grade B500S ($f_{yk} = 500 \ [MPa]; E_s = 200 \ [GPa]$) and the distributed dead and imposed loads are considered through a factored load of $q_d = 80 \ [kN/m^2]$.

The slab incorporated prestressing strands to improve its shear resistance. Four strands with 150 mm^2 ($\phi_p = 15.7 \ [mm], E_p = 196 \ [GPa]$) in a flat duct every 800mm are placed ($a_p = 750 \ mm^2/m$). The nominal yield stress is $f_{p0.1k} = 1500 \ [MPa]$, and the stress in the strands after friction losses reported is $f_{p.0} = 1275 \ [MPa]$. The losses due to creep, shrinkage and relaxation are assumed to be 22%, resulting in an effective prestress of $f_{p.\infty} = 994.5 \ [MPa]$.

The non-prestressed longitudinal steel reinforcement area is $a_s = 1340 \ [mm^2/m]$ ($\phi 16 @ 150 \ mm$), applied at $d_s = 0.64 \ [m]$ for both faces of the deck.

For the specified compressive strength, the relationship stated in section 4.1.1 was assumed ($f'_c = 31.6 \ [MPa]$). The maximum size and lower limit of aggregates were also assumed as $a_g = 40 \ [mm]$ and $D_{lower} = 20 \ [mm]$ respectively.

Figure 6-1 Geometry and cross-sectional dimensions of tunnel [dimensions in [m]; (Design example adapted from [56]) with details of intermediate support

The prestressing tendon profile is defined like in Figure 6-2, assuming the points of contraflexure at $x = [1.16, 7.42, 13.68, 19.94] \ [m]$, being x the distance from one of the support axis. With this

information is possible to calculate the prestressing shear and bending moment applied to the deck. The values obtained with half-meter intervals are shown in Figure 6-3.

$$e_A = 0.10 \text{ m}, e_S = e_B = 0.27 \text{ m}$$

Figure 6-2 Prestressing tendons profile

With this information is possible to calculate the acting shear and bending moment (V_{Ed}, M_{Ed}) shown in Figure 6-3. The lateral and axial stiffness of the walls has been considered for this calculation, and the results are obtained in units per meter.

With these values, the European design codes can verify if the demand is greater than the estimated shear design resistance at each interval, assuming a constant effective prestress along the length of the deck. These results are shown in Figure 6-4.

For the design codes used in America, the applied load by self-weight is required to be calculated separately, then it's assumed the concrete density equal to $24 \ [kN/m^3]$ that results in a distribute load of $16.8 \ [kN/m^2]$. The shear and bending moment due to self-weight is calculated along the length of the deck and with this information the shear resistance can be estimated by ACI318-19 and AASTHO-LRFD. The results obtained can be seen in Figure 6-5.
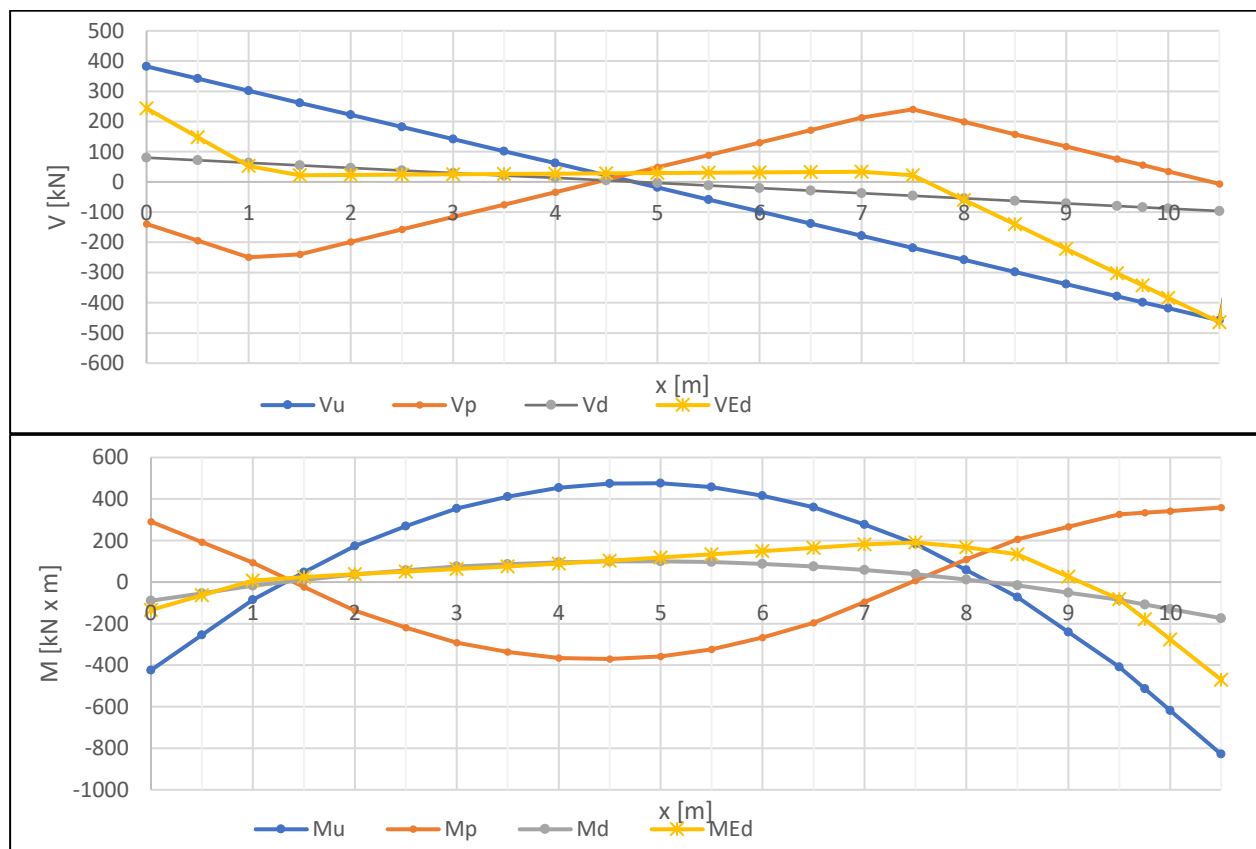
Figure 6-3 Moment and shear force diagrams for half of deck slab of tunnel

Different points of interest can be chosen to verify the shear resistance by analyzing the shear and bending forces illustrated in the last figure. When there is a uniform distributed load, the critical points to analyze are located near supports or near the points of contraflexure, as it is a continuous beam. Generally, one should consider a control section near static or geometric discontinuities, as mentioned in section 2.4.2 in the procedure state for the new Eurocode proposal (prEN1992).

The results obtained for all approaches show the critical location near the intermediate support (at a distance equal to the effective depth d approximately) as expected since this region has the highest moment and shear force. Among the European codes, alternative 1 (prEN1) gives the least conservative estimate of shear resistance if we compare the results obtained with the acting design shear. Considering the critical location at $x = L - d \approx 9.75 \, [m]$, the estimated shear force by prEN1 is $V_{Rd,c}(x = 9.75 \, m) = 428.20 \, [kN]$ in relation with the acting design shear equal to $V_{Ed}(x = 9.75 \, m) = 342.9 \, [kN]$.

Evaluating the results at the same critical location ($x_r = 9.75 \, [m]$) and defining a unity check factor $UC = \left(V_{Ed}/V_{Rd,c} \, [-] \right)$ some observations could be made to the different approaches for this design case. For the approaches applied in Eurocodes the unity check factors (UC) calculated for EC2, prEN1, prEN2, prEN3 and prEN4 have values of 0.97, 0.80, 0.93, 0.93 and 0.90 respectively. By carrying out the same procedure to analyze the American codes this time ($UC = V_u/V_c$), it is obtained that ACI318-19 with his approximate method obtains the least conservative estimation of the shear resistance with a $UC = 0.37$, then the AASHTO-LRFD obtains a $UC = V_u/V_n = 0.60$, and the ACI318-19 with his detailed method obtains a $UC = 0.92$.

As a result, it can be said that among the alternatives for the new Eurocode prEN1 is the least conservative for the assumed critical location $x_r = 9.75 \, [m]$, followed by prEN4 in this case because prEN2 and prEN3 assumed a limit for their factor influencing the axial stress contribution ($k_1 < 0.15$), otherwise the shear strength estimated by these two alternatives will be greater and less conservative, obtaining an $UC = 0.9$ for prEN2 and $UC = 0.6$ for prEN3, being as conservative as prEN4 in the case of prEN2, and much less conservative than prEN4 or prEN1 in the case of prEN3.

The results obtained in the practical design cases then follow the trend shown in comparison with the tests (section 4.6.3), with prEN4 being the method that is mainly on the safe side. prEN2 and prEN3, as explained in the previous paragraph, can obtain more conservative values than prEN4 in regions where certain limits have been set for them.

For a step-by-step verification of the results obtained, in Appendix D is presented the spreadsheet that was used as a basis for the calculation of the shear strength according to all the design codes proposed in this thesis. There one can follow the calculations done to estimate the shear strength of concrete for the critical location assumed at $x_r \approx 9.75 \, [m]$.
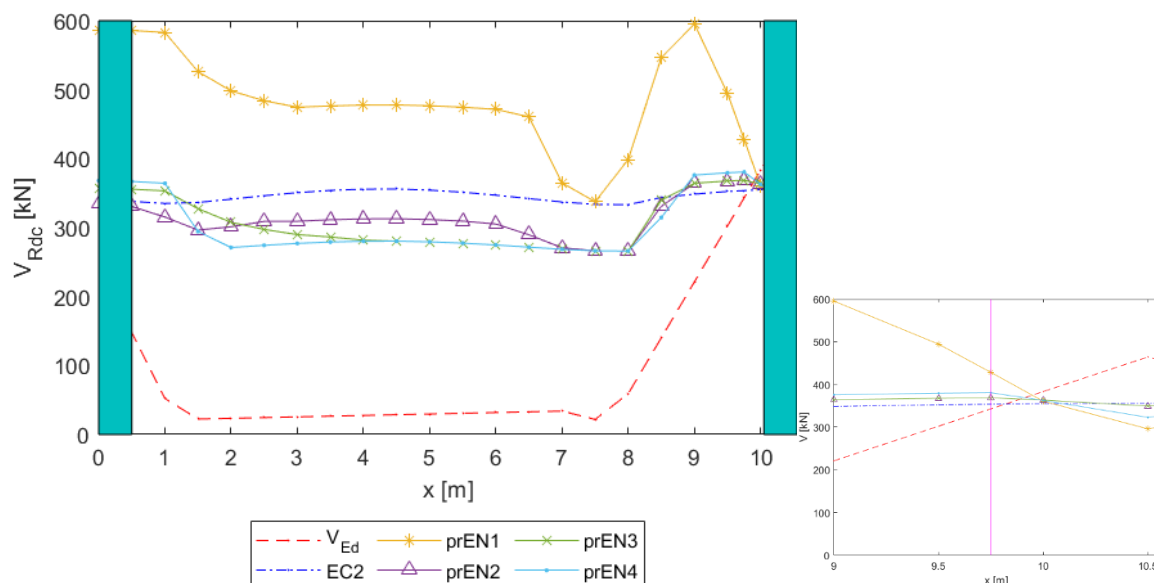
Figure 6-4 Shear resistance along the deck slab according to design codes applied in Europe
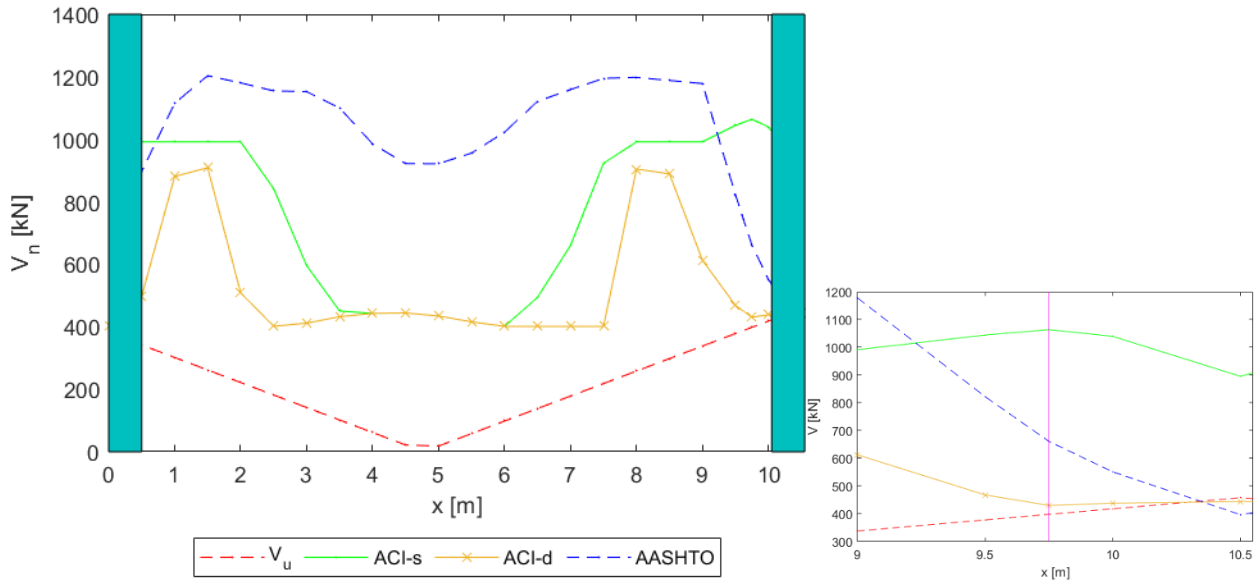
Figure 6-5 Shear resistance along the deck slab according to design codes applied in America

Analyzing Figure 6-5, one can question the results obtained by AASHTO-LRFD, which are much more conservative in this case than those obtained by ACI318-19M. As seen in section 4.6.4, the ACI318-19M detailed method considers only part of the longitudinal reinforcement ratio (ρ_l) influence because it doesn't include this parameter in its formulation. Then, the results can be more similar by varying the prestressing level, as will be done in the next section 6.3.2.2 to verify this hypothesis, using the load combinations, and live load corresponding to each design code.

6.2 TRAFFIC LOADS

For Eurocodes a generic model is defined as load model 1. A design truck defined with a tandem system which is combined with a uniformly distributed load called design lane load. The tandem system has an axle load of $\alpha_{Q1} \times 300\ kN$ for the first lane, $\alpha_{Q2} \times 200\ kN$ in the second lane and $\alpha_{Q3} \times 100\ kN$ in the third lane. The α_{Qi} terms are parameters determined by each nation to tailor the Eurocode load model to local traffic loading situation, but the recommended value is 1. The uniformly distributed load applied over the full lane's width is $\alpha_{qi} \times 9\ kN/m^2$ for the first lane and $\alpha_{q1} \times 2.5\ kN/m^2$ for all other lanes, with α_{qi} for bridges with three or more notional lanes $\alpha_{q1} = 1.15$ and $\alpha_{qi} = 1.4$. The separation between axle loads is 1.2 meters and the transverse separation is 2 meters.

For AASHTO-LRFD, the combination is between a design truck or design tandem with a design lane load. The design truck has three axle loads, one of 35 kN and two of 145 kN, with a longitudinal separation of 4.3 meters between the minor and intermediate axle and a variable separation between 4.3 and 9 meters between the major axles of 145 kN. The design tandem consists of two 110 kN axles separated 1.2 meters apart. The transverse separation for both cases is 1.8 meters and a dynamic load allowance (IM) of 33% is considered for both too. The design lane load of 9.3 N/mm uniformly distributed in the longitudinal direction, and transversely distributed over a 3 meters width, smaller than the full lane width of 3.6 meters.

Considering the definitions given above Figure 6-6 illustrates the traffic loads considered for the analysis of the bridge decks assessed in the next section.
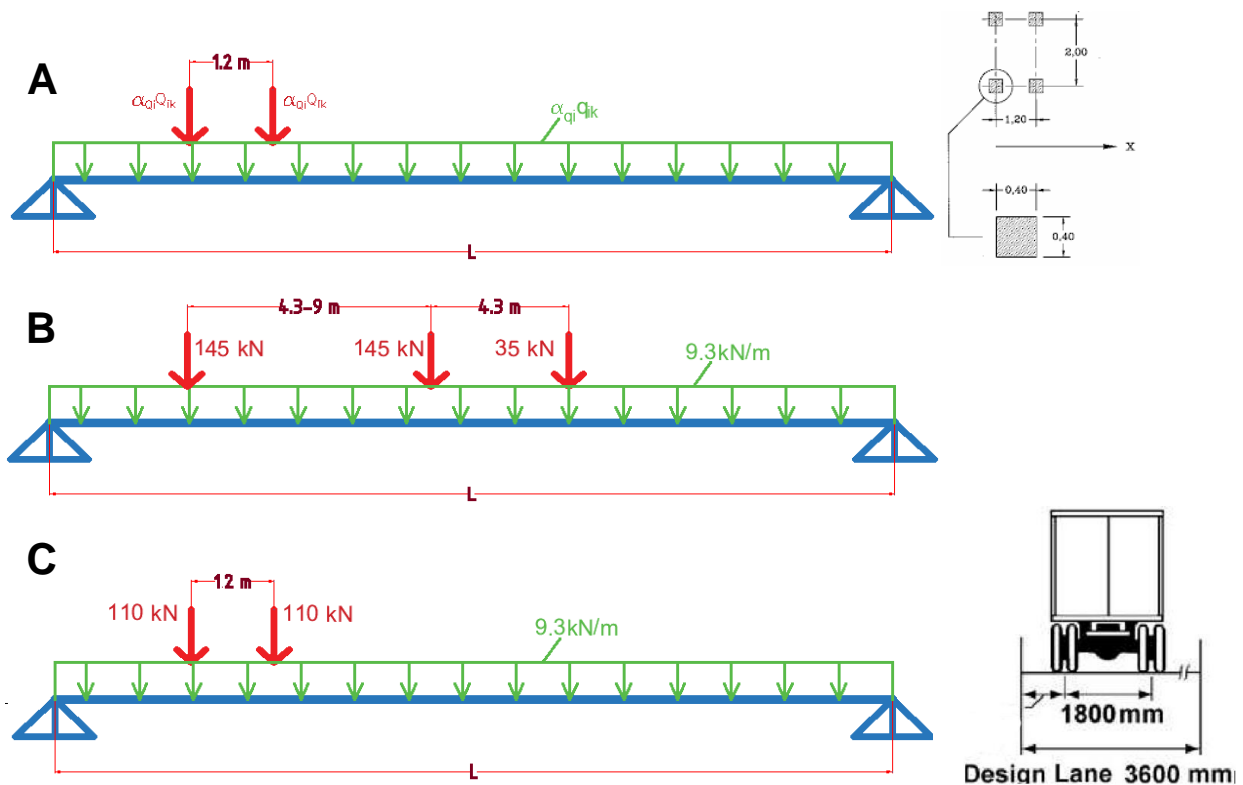
Figure 6-6 Traffic load according to Eurocodes (A) and AASHTO-LRFD for combination 1 (B) and combination 2 (C)

6.3 BRIDGE DESIGN EVALUATION

Based on the analysis contained in the report "Shear resistance of prestressed members without shear reinforcement according to prEN1992/D7 by Hageman", case studies on two bridges that are assumed to have been built in the Netherlands will be evaluated. The load combinations and critical load analysis are obtained from this report where the traffic load was analyzed at different positions to obtain the critical value. It will be assumed that the design of both bridges was carried out following the guidelines of the current Eurocode (EN1992-1-1:2004).

Then, having the shear $\left(V_{Ed}, V_u, V_p\right)$ and bending $\left(M_{Ed}, M_u, M_p\right)$ acting on the beam, the next step is to perform the design with the different alternatives studied in this document to make a comparative analysis of the results.

6.3.1 Prestressed concrete simple supported bridge deck

The first case is a simple supported bridge deck illustrated in Figure 6-7, the information required for the analysis of this problem can be found in Table 6-2. The analysis focuses on the assumed critical location near the supports, since distributed loads are applied. Then the region from 0 to 6 meters from the support axis will be assessed.
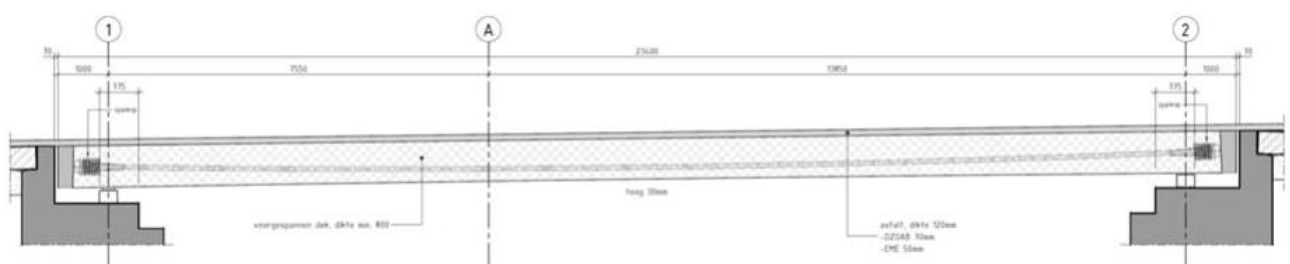
Figure 6-7 Side view of prestressed bridge deck

Table 6-2 Simple supported bridge deck parameters

Dimensions	$L = 21.4 \, [m]; \ b = 1 \, [m]; \ h = 0.8 \, [m]$
Concrete C35/45	$f_{ck} = 35 \, [MPa]; f_c' = 36.6 \, [MPa]; E_c = 28.4 \, [GPa]; \lambda = 1$ $a_g = 40 \, [mm]; D_{lower} = 20 \, [mm]$
Prestressed steel (Y1860S). 64 cables, 12φ15.7mm	$\phi_p = 15.7 \, [mm]; A_p = 4000 \, [mm^2]; E_p = 196 \, [GPa]$ $f_{pu} = 1860 \, [MPa]; f_{pd} = 1455.65 \, [MPa]; f_{se} = 1092.01 \, [MPa]$
Reinforcement steel B500, φ16-200	$d_s = 722 \, [mm]; A_s = 1005 \, [mm^2]; f_y = 500 \, [MPa]; E_s = 200 \, [GPa]$

6.3.1.1 Load cases and load combinations

In the Hageman report cited above, it is reported that a FEM was configured for the analysis of this problem. The critical location obtained is the called "location 2" (Figure 6-8) with about 36% higher design shear forces than the rest of the slab deck.
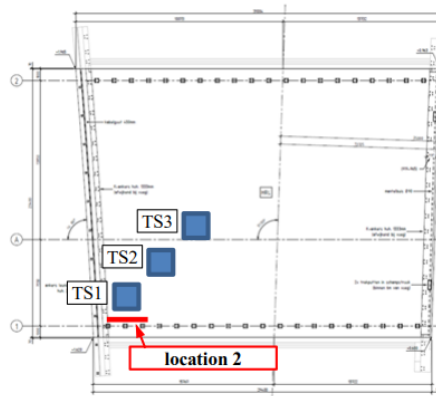
Figure 6-8 Considered critical load case for simple supported bridge deck

The load cases and load combination applied are detailed in Table 6-3.

Table 6-3 Load cases and load combinations for simple supported bridge deck

Load cases	
Self-weight	$p = h \cdot \gamma_{conc} = 0.8 \cdot 25 = 20 \, [kN/m^2]$
Asphalt	$p = d_{asphalt} \cdot \gamma_{asphalt} = 0.14 \cdot 23 = 3.2 \, [kN/m^2]$
Prestress	$p = 16 \, [kN/m^2]$ upwards, after losses, from design calculation)
Traffic load EC2	$p = 1.4 \cdot 2.5 = 3.5 \, [kN/m^2]$ over the entire bridge deck $p = 1.15 \cdot 9.0 - 3.5 = 6.85 \, [kN/m^2]$ extra for lane 1 $TS1 \rightarrow 2 \cdot 300 = 600 \, [kN]$ $TS2 \rightarrow 2 \cdot 200 = 400 \, [kN]$ $TS3 \rightarrow 2 \cdot 100 = 200 \, [kN]$
Common Factored Load Combination	
EN1990 (6.10b), Consequence class 3 (CC3). Also, for prEN1992.	$\xi \gamma_G G + \gamma_Q Q + \gamma_p P = 1.25G + 1.5Q + 1.0P$ G: Dead load, Q: Live load, P: Prestress load

The design bending moment and shear force due to traffic load (UDL and TS) were determined with a FEM-model with the results summarized in the report and presented in Figure 6-9. The tandem system TS1 is placed at a distance d from the considered control section, with a minimum of $2d$ from the support according to the specifications of the calculations done. Applying the different load combinations, the following Figure 6-9 summarize the load cases for Eurocodes.
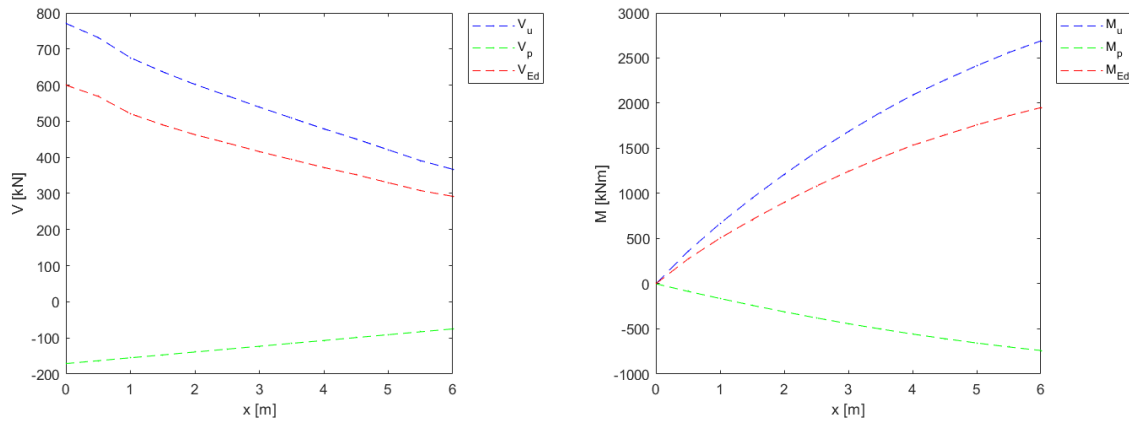
Figure 6-9 Shear and bending moment acting on simple supported bridge deck

Considering that only Eurocode traffic loads were taken into account in the configured FEM, it is only suitable for estimating the shear strength of concrete for prEN1992 and EC2 approaches as shown in Figure 6-10 below.

All alternatives for the new Eurocode (prEN1992), except alternative prEN4, indicate that the flexural-shear failure is verified in all the control sections established every half meter. The results obtained for alternatives prEN1, prEN3, and prEN4 have a similar trend, decreasing the estimated shear strength for control sections moving away from the support. On the other hand, prEN2 and EC2 tend to increase the estimated shear strength for control sections moving away from the support.
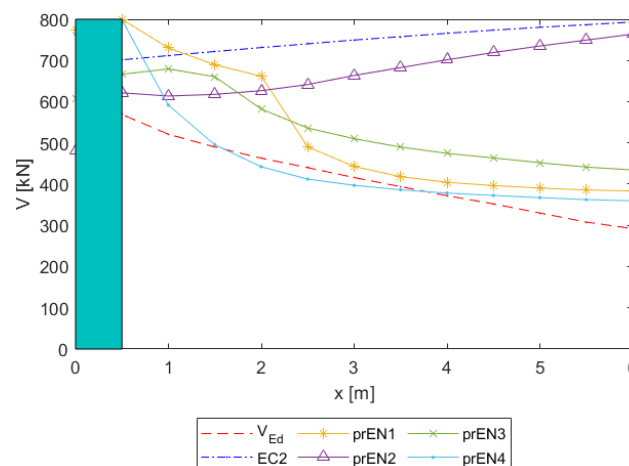
Figure 6-10 Shear resistance $(V_{Rd,c})$ along a simple supported bridge deck according to design codes applied in Europe

Suppose the most vulnerable location defined as the point where the unity check $UC = (V_{Ed}/V_{Rd,c} \ [-])$ is the highest. In that case, the vulnerable location marked by alternative 1 (prEN1) is at approximately 3.5 meters ($\approx 5d$) with an $UC = 0.942$. Alternative 4 (prEN4) marks a range between 2 meters ($\approx 3d$) and 3.5 meters ($\approx 5d$) as the most vulnerable region with $UC = [1.047, 1.067, 1.047, 1.02]$ for $x = [2.0, 2.5, 3.0, 3.5] \ [m]$ respectively, being the critical location at $x = 2.5 \ m$ the most critical. The other codes mark the assumed critical location at $x = d$ with $UC = 0.811$ for EC2, $UC = 0.915$ for prEN2, and $UC = 0.854$ for prEN3

However, what is desired is to assess the codes applied in America too, which is complicated by applying the FEM results from the Hageman report without configuring another FEM with the traffic loads corresponding to AASHTO-LRFD. To overcome this problem, a conservative approach has been assumed by converting the traffic loads (defined in section 6.2) into equivalent distributed loads, as detailed in Appendix E.

For the Eurocodes, the equivalent load for the critical lane has been calculated, obtaining an equivalent distributed live load of $q_{ll.EC} = 27.78\ kN/m$. For AASHTO-LRFD [37] specification for Slab-Type Bridges given in §4.6.2.3 have been used, obtaining the equivalent strip width and the equivalent distributed load $q_{ll.AASH} = 11.61\ kN/m$. Combined with the information already provided for dead loads and prestressed loads, the design loads according the load combination defined in Table 6-1 were calculated and the results are shown in Figure 6-11.
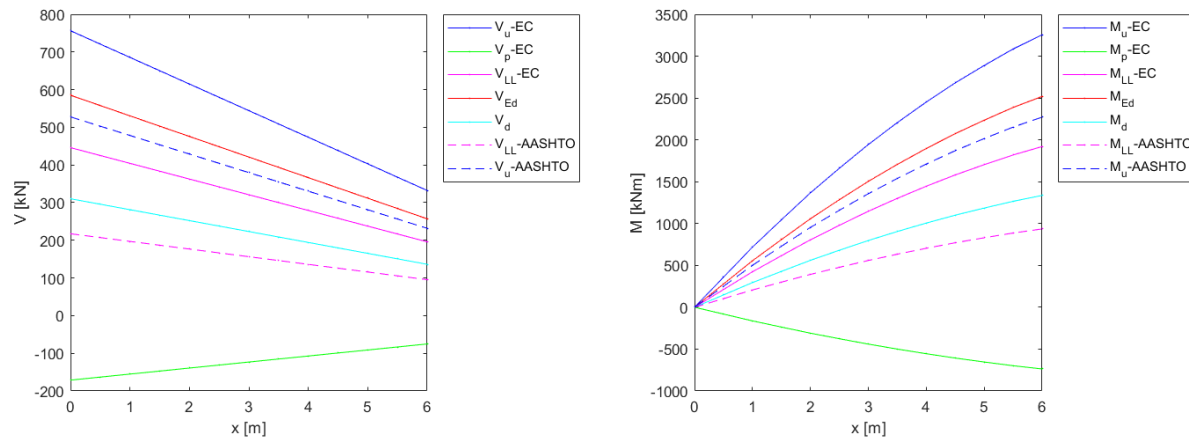
Figure 6-11 Shear forces and bending moments for simple supported bridge in region near support

The shear resistances applying the Eurocodes are presented in Figure 6-12, and applying AASHTO-LRFD and ACI318-19M in Figure 6-13. The shear strength is plotted from the assumed critical location equal to the effective depth (d).
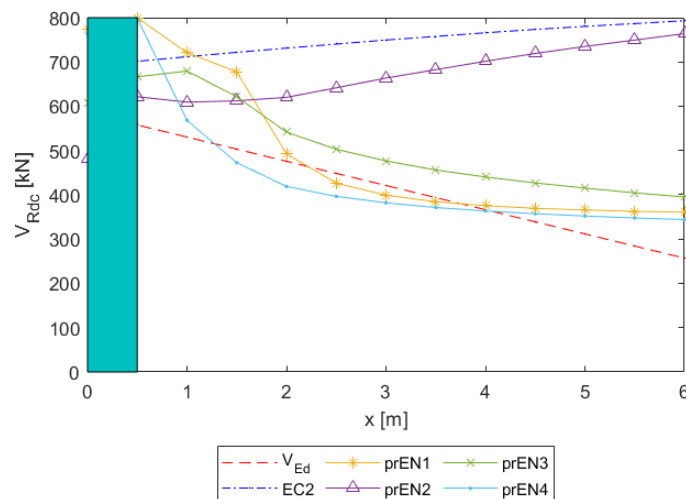
Figure 6-12 Shear resistance along a simple supported bridge deck according to design codes applied in Europe

With this conservative approach prEN4 marks a vulnerable region in the range between 1.5 and 4 meters $(\approx 2d\ to\ 6d)$ with a unity check $UC = [1.06, 1.14, 1.13, 1.10, 1.06, 1.01]$ for $x = [1.5, 2.0, 2.5, 3.0, 3.5, 4.0]$ respectively. In case of prEN1 now there is vulnerable region between 2.5 and 3.5 meters approximately $(\approx 3d\ to\ 5d)$ wit $UC = [1.05, 1.05, 1.02]$ for $x = [2.5, 3.0, 3.5]$. the other alternatives comply with the verification with unity checks less than 1, of which prEN3 marks the most vulnerable location at 2.5 meters $(\approx 3d)$ with UC=0.89, the others mark the critical

location at the beginning, at a distance d from the support with UC=0.89 for prEN2 and UC=0.79 for EC2.
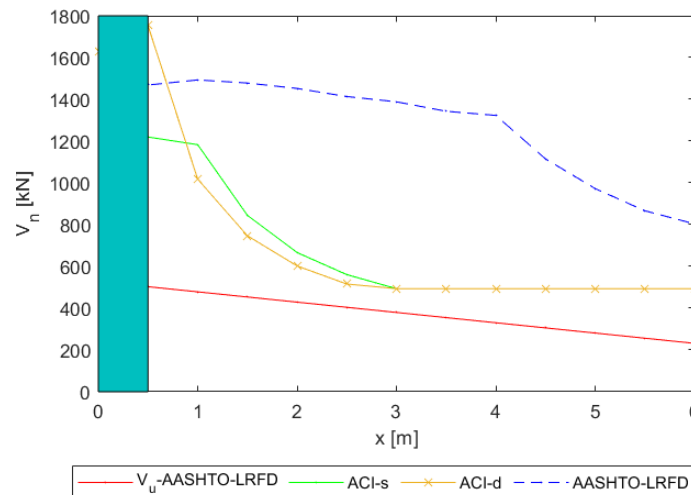
Figure 6-13 Shear resistance along a simple supported bridge deck according to design codes applied in America

Following the same logic of vulnerable locations, but now analyzing the results obtained by ACI318-19, one can observe that between 2.5 and 3 meters ($\approx 3d \ and \ 4d$) from the support axis, the locations with the highest unity check values ($UC = V_u/V_n$) can be found, with $UC = 0.77$ at x=2.5 meters for the approximate method and $UC = 0.78$ at x=3 meters for the detailed method. One can remark that this range contains the critical locations highlighted by prEN4 and prEN1 before.

On the other hand, AASHTO-LRFD marks its most vulnerable location at 6 meters ($\approx 8.5d$), the farthest of all with an $UC = 0.29$. Here, like the last design case presented in Figure 6-5, for a continuous deck slab, one questions the highly conservative values obtained by AASHTO-LRFD. In this case for a simply supported bridge, where near supports the probability of flexural-shear failure is lower due to the low flexural stresses present in this region. It is also presumed that AASHTO-LRFD considers the total effect of the prestressing force, and that ACI318-19 considers only a part of it as was noted in section 4.6.4. A detailed study is done in the following section 6.3.2.2 to evaluate the results obtained by AASHTO-LRFD.

6.3.2   Prestressed concrete continuous bridge deck

This case study for a continuous bridge with a variable deck height of 0.67 to 1 meter (Figure 6-14). The critical locations near the end and intermediate support are of interest, because distributed loads are the dominant again. So, the results are obtained for a range of 0 to 6 meters from the support axis. The parameters required to calculate the shear strength are detailed in Table 6-4, and the shear resistances obtained applying codes from Europe and America are presented in Figure 6-16 for region near end support and Figure 6-18 for region near middle support.
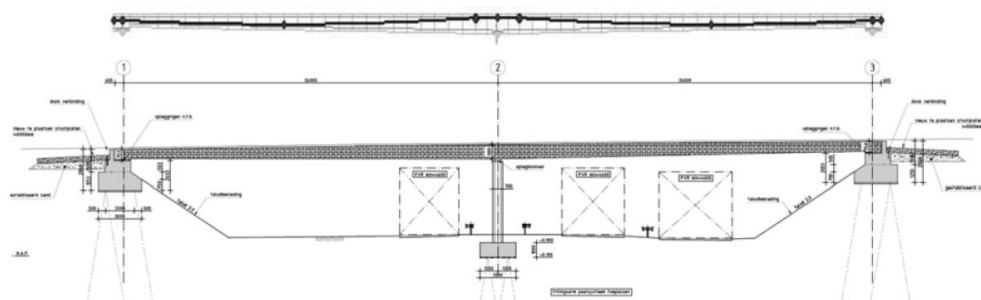
Figure 6-14 Side view of bridge deck with schematic prestress tendon profile

Table 6-4 Prestressed concrete continuous bridge parameters

Dimensions	$L = 2\ x\ 26.0\ [m];\ b = 5.49\ [m];\ h = 0.67 - 1\ [m]$
Concrete C55/67	$f_{ck} = 55\ [MPa];\ f_c' = 56.6\ [MPa];\ E_c = 35.4\ [GPa];\ \lambda = 1$ $a_g = 40\ [mm];\ D_{lower} = 20\ [mm]$
Prestressed steel (Y1860S). 7 cables, 19φ15.7mm	$\phi_p = 15.7\ [mm];\ A_p = 3634\ [mm^2];\ E_p = 196\ [GPa]$ $f_{pu} = 1860\ [MPa];\ f_{pd} = 1455.65\ [MPa];\ f_{se} = 1187.42\ [MPa]$
Reinforcement steel B500, φ16c200	$d_s = h - 200\ [mm];\ A_s = 1340\ [mm^2];$ $f_y = 500\ [MPa];\ E_s = 200\ [GPa]$

6.3.2.1 Load cases and load combinations

The report with the results mentions that the study was calibrated with the previously available FEM-model because of the relatively small deck width. The calibration was done using effective width smaller than the width of the deck. Using for bending effective widths equal to the deck width, but for shear using effective widths equal to the width of the tandem system $(2(m + d))$.

The load cases and load combination applied are the following:

Table 6-5 Load cases and load combinations for simple supported bridge deck

Load cases	
Self-weight	$q = h \cdot \gamma_{conc} \cdot b_{deck} = (0.67\ to\ 1.0) \cdot 25 \cdot 5.49 = 92\ to\ 137.3\ [kN/m]$
Asphalt + edge load	$q = 21\ [kN/m]$, from design calculation
Prestress	After losses, from design calculations Upwards along 11.2 m: $q = 81.6 \cdot 0.91 = 74.2\ [kN/m]$ Upwards along 13.3 m: $q = 94.3 \cdot 0.91 = 85.8\ [kN/m]$ Downwards along 1.5 m: $q = 842.6 \cdot 0.91 = 766.8\ [kN/m]$ Same in second span (vice-versa)
Traffic load	$q = 9 \cdot 3 + 2.5 \cdot 2 = 32\ [kN/m]$ $TS1 \rightarrow 2 \cdot 300 = 600\ [kN]$
Traffic load AASHTO-LRFD	$q = 9.3\ [kN/m]$ $HL - 93 \rightarrow 2x145\ [kN] + 35\ [kN]$ $TD \rightarrow 2x110\ [kN]$

The results in Hageman report specify the effective width considered for each of the loads, which facilitates the consideration of other live loads in the analysis. For the end support analysis, in case of Eurocodes, the UDL ($q = 32\ kN/m$) applied only in one span, and the TS1 load of 600 kN at variable locations close to the support was considered, capturing the envelope. The same was done for the AASHTO-LRFD distributed load, design truck and design tandem, where the critical case envelope was captured.

For the intermediate support analysis, using Eurocode traffic loads, the UDL was applied to both spans, and the distance of TS1 from the middle support was varied to capture the envelope. In the case of AASHTO-LRFD, 90 percent of the distributed load was applied to both spans, and two HL-93 design truck loads were applied 15 meters apart equidistant from the middle support, thus capturing the moment and shear for the problem.

After this analysis of live loads and obtaining the envelopes, the values of bending moment and shear force equivalent to a strip of 1 meter were obtained. For the Eurocodes, the defined effective

widths were applied, and for AASHTO-LRFD, the equivalent strip width calculated as detailed at the end of appendix E was used ($E_i = 3.34 \ [m]$).

Applying the different load combinations, the following Figure 6-15 and Figure 6-17 summarize the load cases for Eurocodes, ACI318-19M and AASHTO-LRFD for the regions near the end and mid support

6.3.2.2   End support
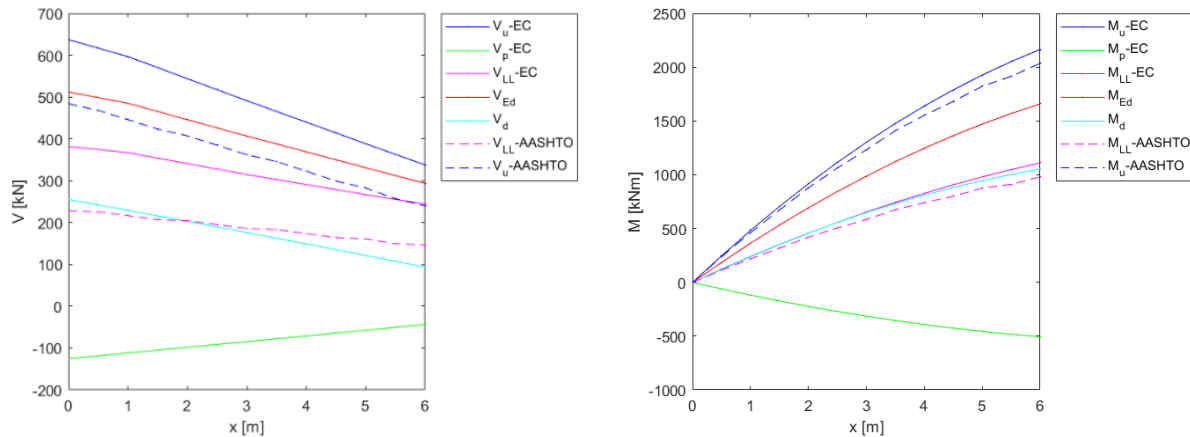
Figure 6-15 Ultimate and acting shear and bending moment for continuous bridge in region near end support

With this information one can estimate the design shear resistance according to the different design codes as follow, for the region near the end support.
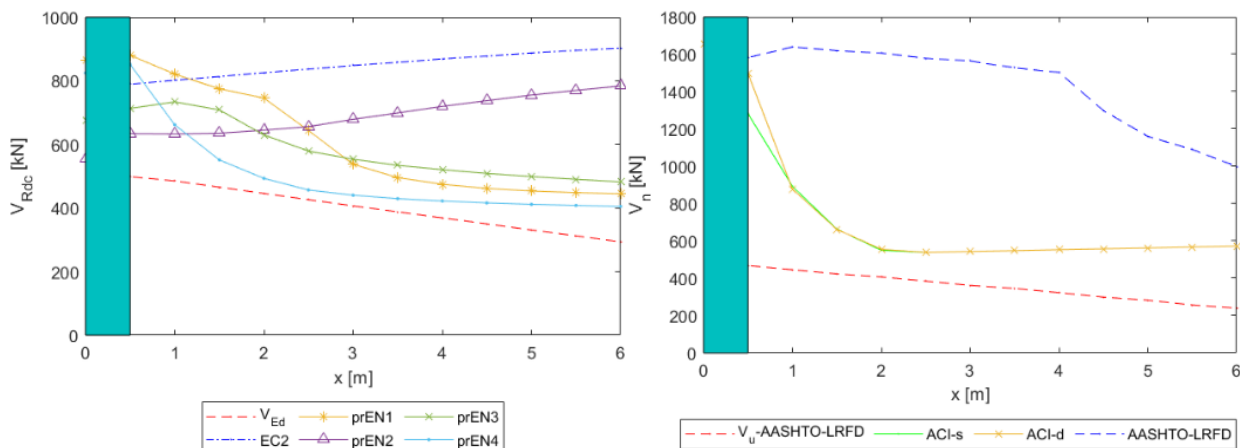
Figure 6-16 Shear resistance near end support of a continuous bridge deck according to design codes applied in Europe and America

The behavior of all the design codes is identical to that described in the previous section with the case of the simply supported deck. Here one can interpret the high values obtained for AASHTO-LRFD again due to the influence of the low bending moment, which apparently is not enough to generate considerable longitudinal strains in the region being analyzed since it is a region near a simple support where the bending moments are the lowest of the whole span. AASHTO-LRFD, which depends on the principal stresses, recognizes low longitudinal strain values in this region, then high shear strength values are generated.

But in order to analyze now this observation in detail, it is necessary to review the assumptions made in the formulation of the SMCFT to simplify the procedure stated by the MCFT, to obtain the approach used for AASHTO-LRFD.

The SMCFT [45] uses the "strain effect factor" ($4.8/(1 + 750\varepsilon_s)$) and the "size effect factor" ($1300/(1000 + s_{xe})$) as independent factors, suppressing their interdependence stated in the MCFT for the calculation of the factor that represents the ability of the shear crack to transmit tension and shear (β). The authors were able to simplify the calculation of this last factor (β) by observing the results obtained with the MCFT, assuming different values for the cracking space parameter (s_{xe}). With this analysis, the "size effect factor" expression was stated like the expression detailed before, and the final expression for β resulted in [Eq. 2-31]:

$$\beta = \frac{4.8}{1 + 750\varepsilon_s} \cdot \frac{1300}{1000 + s_{xe}}$$

With this "size effect factor" approximation, the authors observed that for very low values of longitudinal strain with low crack separation parameters, conservative values are produced by this simplified expression of β. This is related with the case of slender prestressed concrete members without shear reinforcement where the crack spacing parameter tends to be low, as the crack spacing parameter without the influence of aggregate size (s_x) is assumed to be equal to the effective shear depth (d_v), explaining in some way the conservative results obtained by this approach.

This tendency to generate conservative values can be partly analyzed by varying the amount of prestressing applied to the same problem, and this will help to check the different hypotheses that have been made about the results obtained by ACI318-19 compared with AASHTO-LRFD. In Appendix C, the same input data used for this problem, for the region near end support, has been used but considering different cases with only 50%, 25%, and 0% of the prestressing force applied.

Figure 0-2 of the appendix C shows that by reducing the prestressing by 50%, AASHTO-LRFD already starts to obtain more conservative shear strength values along the span. Figure 0-4 of the appendix C shows that reducing the prestressing by 25%, AASHTO-LRFD obtains more conservative shear strength values than ACI318-19M at critical locations at a distance of approximately $4d$ from the support, and obtains intermediate values between ACI318-19 approximate and detailed method at critical locations close to the support. Figure 0-6 of the appendix C shows that suppressing the prestress, AASHTO-LRFD obtains more conservative values than ACI318-19 approximate method at a distance of approximately $4d$ from the support and obtains intermediate values between ACI318-19 approximate and detailed method for distances less than $2d$ from the support.

Based on what has been observed in this brief analysis of the influence of prestressing on the estimation of shear strength of prestressed concrete members without shear reinforcement, one can point out that two factors influence AASHTO-LRFD to estimate very high values compared to ACI318-19.

> Firstly, the inclusion of the parameter taking into account the longitudinal reinforcement ratio effect is demonstrated in the parameter analysis of section 4. Second, the tendency related with the size effect factor to generate conservative values in members with low longitudinal strain and crack spacing parameter values.

Also, it is necessary to point out the debate that exists regarding the interpretation of the factor called *"Modulus of elasticity of prestressing steel multiplied by the locked-in difference in strain between the prestressing steel and the surrounding concrete"* (f_{po}) that directly influences the calculated longitudinal strain (ε_s), some authors such as [50] refer to different ways of interpreting this parameter.

Finally, taking advantage of the various figures generated in appendix C, one can also appreciate the close relationship between prEN1 and prEN4 with different levels of prestressing, prEN4 being constantly on the safe side. It can also be seen that the dependence of the alternatives for prEN1992 on a/d now demarcates critical zones not recognized in principle by the current EC2 and that prEN1 and prEN4, in this design case, obtain more conservative values than EC2 for different critical locations more distant from the support.

6.3.2.3 Mid support
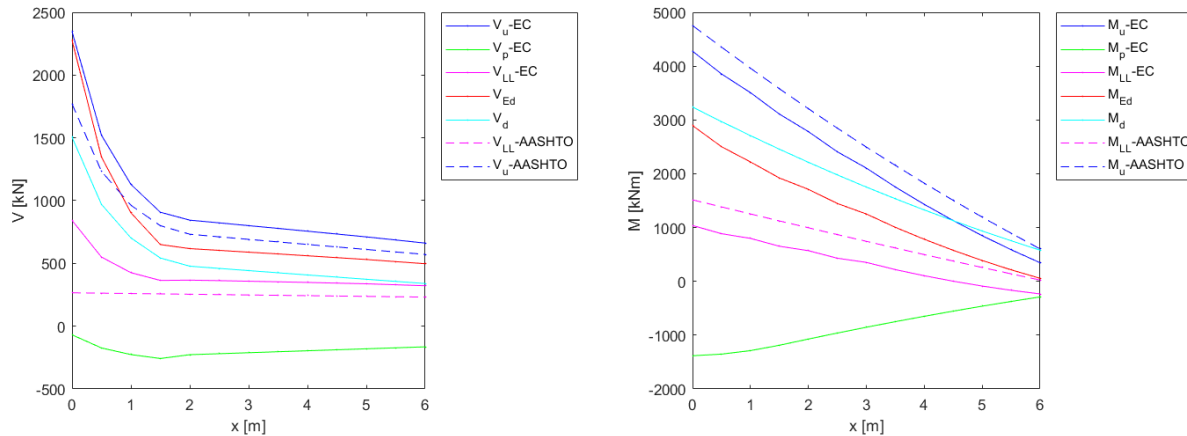
Figure 6-17 Ultimate and acting shear and bending moment for continuous bridge in region near mid support

With this information one can estimate the design shear resistance according to the different design codes as follow, for the region near the mid support.
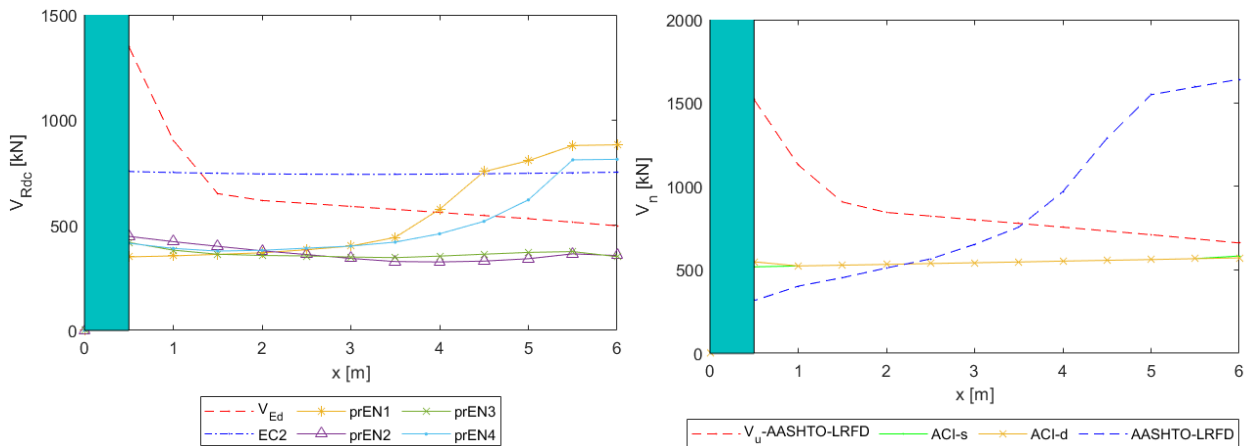
Figure 6-18 Shear resistance near middle support of a continuous bridge deck according to design codes applied in Europe

Near the intermediate support, there is a combination of high bending moments with high shear forces, then as in case of the slab deck for a tunnel in section 0, it is expected to have the critical location near the support .

Following the same logic of vulnerable locations according to the values of unity check ($UC = V_{Ed}/V_c$ $[-]$) described in the previous sections, comparing the difference between the estimated strength and the design shear, approaches applied in Europe mark the vulnerable locations at $x \approx 1.5d$ to $2d$ for the current Eurocode, EC2 with $UC = 1.2$ at x=1 meter from support. prEN1 results that does not meet the unit check a region 4 meters from the middle support and prEN4 a region 4.5 meters from the middle support. All other alternatives are below demand along the studied region. The highest unity check for all the alternatives for the new Eurocode is located at a distance d from middle support with a value of $UC = 3.8$ approx.

The same logic applied for ACI318-19 and AASHTO-LRFD denotes the vulnerable region for AASHTO-LRFD from the middle support until $x \approx 5d$, and ACI318-19 does no comply with the unity check in the whole region. The highest unity check in all cases is for $x = d$ from the support with $UC = 3.9$ for AASHTO-LRFD and $UC = 2.37$ for ACI318-19.

Here, again one must comment the influence of the magnitude of the bending moment for AASHTO-LRFD results, so the principal stresses and the longitudinal strain emulates the flexural-shear failure case, otherwise the longitudinal strain obtained is not enough to derive in a shear failure.

6.4 DISCUSSION AND CONCLUSIONS

- For the verification that is carried out for each design code, different distances at which the critical cross-section is located are indicated. ACI318-19 indicates locations at a distance $h/2$ from the support axis, AASHTO-LRFD at $0.5d_v \cot(\theta)\ or\ d_v$ from the face of the support, and prEN1992 indicates critical locations at a distance $d/2$ from geometric discontinuities, supports, point loads or contraflexure points. The current Eurocode (EC2) as it doesn't depend on the acting shear or bending moment will result in in a constant value over the whole span.

- To compare the design standards from Europe and America, it is necessary to distinguish the differences in the concept for the demanded resistance. Because as prestress is preload for Eurocodes, the acting shear force (V_{Ed}) that is the demanded resistance will not be equal to the demanded shear resistance for AASTHO-LRFD and ACI318-19, that is the ultimate shear load (V_u) which doesn't consider the prestressing influence.

- The two alternatives proposed for the new Eurocode, prEN3 and prEN4 have similar performances except for regions close to intermediate supports from continuous beams. This is because the eccentricity of the tendon considered for alternative prEN3 increases the estimated shear resistance calculated although its magnitude is limited by the upper bound stated for the factor k_1.

- To evaluate the different methods in terms of usability, one has to take into account the number of parameters used and the ease of interpreting intermediate results.
  - ○ ACI318-19, has two practical methods, at first according to the results obtained in chapter 3 with a very accurate approximate method apparently, but with a safety level below the desired one. It does not take into account the influence of the prestressing force at any time within the approach, which negates the interpretation of results based on the applied prestressing.
    The detailed method solves this drawback and considers composite and non-composite sections cleverly, making it easy to use and easy to interpret when comparing the two types of shear failure that can occur in beams of any shape.
  - ○ AASHTO-LRFD is a laborious but worthwhile method to develop for a detailed analysis of the influence of the prestressing force, the intermediate factors like the longitudinal strain or crack spacing parameter, give important details of the behavior of the structure and give further clues of the influence of different parameters on the final shear strength calculated.
  - ○ EC2, is the most straightforward method and the parameters are not too complicated to verify or obtain. This empirical formulation doesn't depend on external loads and the influence of prestressing is taken into account by a separated term that allow us to easily estimate the contribution of prestress for shear resistance.

- o The alternatives for the new Eurocode 2, 3 and 4 are similar, but prEN4 is the one that interprets the role of the initial shear stress τ_0 in a correct way. The alternative prEN1 is the one that maintains the structure of the initially proposed approach based on the CSCT, and the others are linearized simplifications of the main failure criterion. The disadvantage of alternative 1 is the visualization of the normal load contribution in the shear resistance.

- Evaluating the new proposals suggested (prEN3 and prEN4) in terms of easy-of-use, and the assumptions made in the derivation prEN4 is the best option, because it is easy to distinguish the influence of the normal load and it is not required to calculate any other additional term. The assumptions and the derivation based on theory is closely related with the assumption of prestressed as preload applied for Eurocodes, letting the normal force be the only one influencing shear strength.

- In the different design cases of continuous beams, the intermediate supports concentrating a high shear force and bending moment produced by a uniformly distributed load indicate the critical location close to the support, as suggested in most design codes, except EC2, which assumes a constant value for the shear span. This is also verified by results obtained in chapters 4 and 5, where the critical location indicated with higher precision is the one closest to the point load, which in this case is created by the intermediate support. In the case of distributed loads on simply supported beams, the critical locations are displaced further away from the supports, making it necessary to calculate the estimated shear strength at various intermediate points of the beam span to verify that it meets the demand.
- The shear strength of prestressed concrete elements without shear reinforcement according to AASHTO-LRFD can be much higher than that of ACI318-19M due to the inclusion of the complete influence of the longitudinal reinforcement ratio on concrete shear strength. In addition, there is a tendency produced by the "size effect factor" to generate conservative values in elements with low values of longitudinal strain and low crack spacing parameters.

7 CONCLUSIONS AND RECOMMENDATIONS

First of all, a set of general conclusions that were reached in the process will be presented. These are related to the most relevant findings along the intermediate steps established to answer the research question. Then, the research questions formulated will be answered based on the results obtained. Observations and recommendations for future works are given at the end.

7.1 GENERAL CONCLUSIONS

The performance of various design codes for calculating the flexural-shear resistance of prestressed concrete members without shear reinforcement has been evaluated. Semi-empirical approaches (ACI318-19M and EC2), MCFT-based approaches (AASHTO-LRFD), and CSCT-based approaches (prEN199) were studied. The proposal of the new Eurocode (prEN1992) contains two alternatives (prEN1 and prEN2) that are evaluated with other two approaches proposed (prEN3 and prEN4), in order to eventually choose the most suitable expression, with a solid theoretical basis and good performance compared to experimental results.

The ACI-DAfStb-PC/2015 database (214 tests) for prestressed concrete members without shear reinforcement, contains tests with beams of different cross-section shapes and failure modes, and some approaches of the design codes focus on only one type of failure or cross-section shape. Therefore, it was convenient to divide the database into 3 subsets defined as follow:

- Subset 1 (143 tests): Capturing tests from ACI-DAfStb-PC/2015 with flexural-shear failure regardless of cross-section shape (I/T/rectangular).
- Subset 2 (102 tests): Only rectangular beams from subset 1.
- Subset 3 (66 tests): Only tests that comply with the assessment for flexural and anchorage failure. The latter considered conservative.

- In this way, it is expected to correctly relate the failure mode considered by the approaches and the one undergone by the tests to obtain representative comparative values. In this way, for the different statistical indicators such as the coefficient of variation (COV), a range of values is given, indicating the minimum and maximum value obtained analyzing the 3 subsets.

The comparison carried out in Chapters 4 and 5 of the shear strengths estimated by ACI318-19M, AASHTO-LRFD, EC2, and prEN1992, with the experimental results presented in the ACI-DAfStb-PC/2015 database for slender prestressed concrete members without shear reinforcement, concludes that:

- AASHTO-LRFD is the most precise approach for evaluating flexural-shear capacity in simply supported slender prestressed beams without shear reinforcement with equidistant point loads applied, with COV=0.22-0.23 values at the critical location closest to the point load. This approach is followed by prEN1 with COV=0.23-0.24, which is still considered a good precision. In third place comes prEN4 with COV=0.25-0.26, which is at the limit of a good and reasonable level of precision. The approaches EC2 (COV=0.28-0.31), prEN2 (COV=0.29-0.30), and prEN3 (COV=0.29-0.30) obtain reasonable levels of precision, and finally, ACI318-19M with its detailed and approximate method obtains in most of the cases a poor level of precision with COV=0.29-0.45.

- In terms of safety, it can be highlighted that EC2, prEN2, and prEN4 obtain good safety levels according to the 5th percentile lower bound value obtained, which is in the range between 0.8-1. prEN1, AASHTO-LRFD, and ACI318-19 detailed method tend to be conservative with 5th percentile lower bound values greater than 1 obtained with a range between 0.98 to 1.06 for prEN3, 1.03 to 1.05 for prEN1, and 1.23 to 1.30 for AASHTO-LRFD being the most conservative of all. The ACI318-19 approximate method tends to a lower than desirable level of safety with 5th percentile lower bound values less than 0.7 in the range 0.49-0.52.

Based on the analysis of the parameters taken into account in the different design codes (section 4.6.4 and 5.3.1), it was noted that:

- Concrete shear strength (V_c) according ACI318-19 approximate method depends on few parameters (f_c', d_p, V_u, M_u, b_w, d) in which prestressing is not included, and of which f_c' has the greatest influence. The detailed method does not consider the total contribution of the longitudinal reinforcement ratio, although it implicitly includes it through the effective prestress applied. For the current approach used by ACI318-19M, the size effect factor for prestressed concrete members has not yet been included, although all other design codes studied have already included it, recognizing its relevance.

- AASHTO-LRFD tends to obtain less conservative values than ACI318-19 in slender beams without shear reinforcement with high levels of prestressing because it considers the total contribution of the longitudinal reinforcement ratio and has a tendency produced by the "size effect factor" to generate conservative values in elements with low values of longitudinal strain and low crack spacing parameters.

- EC2 current expression does not consider the shear span-to-effective depth ratio, thus a constant shear strength of concrete is obtained commonly for the entire span for beams with straight tendons. The alternatives for prEN1992 modify this by including the effective shear span parameter that relates the acting bending moment to the acting shear force to identify the most likely zones for critical shear crack formation. It should be noted that critical shear crack formation is dependent on the structural configuration of the element and that the alternatives for the new Eurocode (prEN1992) based on the CSCT only focus on flexural-shear cracks.

By solving the design cases presented in chapter 6, it was shown that:

- AASHTO-LRFD is the most laborious method, but it provides information about the shear behavior of the beam and the influence of the prestressing on the longitudinal strain. An iterative process must be performed to calculate the nominal flexural moment in a detailed calculation, but the code also offers simplified procedures for rectangular and I/T cross-section shape beams.

- ACI318-19 and EC2 are semi-empirical approaches that are easy to use and help make quick estimates of the shear strength of concrete. ACI318-19 detailed method is a more conservative method that takes the lowest value between the web-shear and flexural-shear strength as the final value.

- prEN1992 approaches start from a non-linear relationship such as prEN1, which estimates the least conservative values. The alternatives that linearize the main failure criterion as prEN2, prEN3, and prEN4 are approaches that estimate more conservative design values than prEN1 and that, compared with the current EC2, obtain similar values in the cases of design near supports that concentrate high shear forces and bending moments. However, in the case of simply supported beams with distributed loading, the new proposals indicate

critical locations further away from the supports that EC2 does not recognize. This is produced because the new alternatives (prEN1992) are sensitive to the effective shear span (a_{cs}) value obtained, which tends to reduce the concrete shear strength for high values of bending moment over shear force.

Analyzing the four alternatives for the new Eurocode proposal, there are two groups of alternatives. prEN2 and prEN3 that erroneously incorporate eccentric axial loads in the moment of equilibrium of the cross-section, thus considering doubly the applied prestressing, since it was implicitly included with the acting shear force and bending moment (V_{Ed}, M_{Ed}).

The other group (prEN1 and prEN4), noticing that the effect of prestressing was implicitly considered, only include the normal load in at the neutral axis as shown in Figure 5-5 presented again below. This difference turns out to be the break point between the two groups of alternatives.
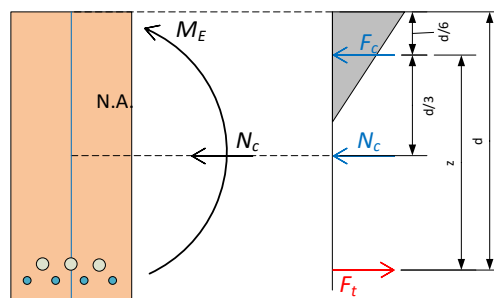
From prEN1 and prEN4, which are the most reliable alternatives, prEN4 is a more conservative alternative than prEN1, and it is handy for quick estimations showing the effect of normal loads by a term dependent on the ratio d/a_{cs} multiplied by the concrete axial stress (σ_{cp}) considering that the effect of prestressing is implicitly immersed in the effective shear span factor (a_v).

7.2 **RESEARCH QUESTION**

The research question stated is:

> *How can **prestressing force influence** be taken into account to estimate the **flexural-shear resistance** of **members without shear reinforcement** in a straightforward way, with an approach based on **Critical Shear Crack Theory (CSCT)**?*

The answer to the research question is:

> Alternative 4 (prEN4) estimates the flexural-shear resistance of prestressed concrete members without shear reinforcement using a CSCT-based method derived consistently to evaluate rectangular beams or one-way slabs. prEN4 adds to the concrete shear strength the contribution of the normal stresses dependent on the shear span (a_{cs}) and effective depth (d) assuming that prestressing is implicitly incorporated through the acting shear force and acting bending moment as prestressing is considered preload. Comparing this approach with tests results is the most precise from all the linearized alternatives for prEN1992 and the estimation of the shear strength is on the safe side comparing with the non-linearized expression that presents prEN1. prEN4 is also much easier to use than the other alternatives since it is an expression very similar to that used in the current EC2, replacing the empirical factor $k1$ by a value dependent on the d/a_{cs} ratio.

7.3 **FUTURE WORK**

- The critical location or the critical shear crack location is significant in the CSCT-based alternatives, so it is necessary to increase the number of tests for prestressed beams that

contain this information varying the structural configuration like the type of loads since there is not much information available for cases with distributed loads..

- The number of tests or reports on prestressed continuous concrete beams is still limited compared to those on simply supported beams, and the scale of the tests could be increased to better study the size effect factor.

- It is suggested to study in more detail the value to consider for the f_{po} factor used in AASHTO-LRFD when there are high prestress losses and the influence of the called "size effect factor", included in the derivation of the SMCFT, to verify its influence in the calculation of the shear strength of slender prestressed concrete members without shear reinforcement.

- The size effect factor has been incorporated into the ACI318-19M for reinforced concrete members with axial loads, but the method for prestressed beams remains unchanged. Remembering that prestressed is considered as capacity by ACI318-19, it is recommended to evaluate the influence of the effective depth on the shear carrying mechanics for beams without shear reinforcement.

- The estimation of the flexural-shear resistance for rectangular beams or one-way slabs is possible through the expression proposed for prEN4 [Eq. 5-47], but it is possible to include beams with different cross-section maintaining the gross cross-section area in expression presented in [Eq. 5-46]. Therefore, it is suggested to evaluate this variation in alternative 4 to include beams of different cross-section by comparing the estimated shear strength of this formula with the experimental results available for this group.

- The motivation of this thesis was the theoretical and experimental comparison of the different approaches estimating the flexural-shear resistance, but in the case of design for the comparison of the different design codes, more things must be considered as a detailed investigation of the probabilistic background of each code, as each region has different criteria for durability, reliability, safety, and affordability of their structures, e.g.

Bibliography

[1]   A. M. Neville, *Properties of concrete*, vol. 4. London: Longman, 1995.

[2]   K.-H. Reineck, E. C. Bentz, B. Fitik, D. A. Kuchma, and O. Bayrak, "ACI-DAfStb Database of Shear Tests on Slender Reinforced Concrete Beams without Stirrups.," *ACI Structural Journal*, vol. 110, no. 5, 2013.

[3]   D. Dunkelberg, L. H. Sneed, K. Zilch, and K.-H. Reineck, "The 2015 ACI-DAfStb database of shear tests on slender prestressed concrete beams without stirrups—Overview and evaluation of current design approaches.," *Structural Concrete*, vol. 19, no. 6, pp. 1740–1759, 2018, doi: 10.1002/suco.201700216.

[4]   E. G. Nawy, *Prestressed Concrete - A fundamental approach*, 5th. The State University of New Jersey, 2009.

[5]   M. A. Roosen, "Shear failure of prestressed girders in regions without flexural cracks," Ph.D Thesis, TU Delft, 2021.

[6]   Y. Yang, J. Walraven, and J. den Uijl, "Shear behavior of Reinfoced Concrete beams without transverse reinfocement based on critical shear displacement," *Journal of Structural Engineering*, vol. 143, no. 1, p. 04016146, 2017, doi: 10.1061/(ASCE)ST.1943-541X.0001608.

[7]   L. Xie, "The Influence of Axial Load and Prestress on The Shear Strength of Web-Shear Critical Reinforced Concrete Elements," University of Toronto, 2009.

[8]   M. Sozen, E. Zwoyer, and C. Siess, "Investigation of prestressed concrete for highway bridges: Part I strength in shear of beams without web reinforcement," Urbana Champaign, 1959.

[9]   A. Muttoni and M. F. Ruiz, "Shear Strength of Members without Transverse Reinforcement as Fucntion of Critical Shear Crack Width," *ACI Structural Journal*, vol. S17, no. 105, pp. 163–172, 2008.

[10] M. Fernández Ruiz, A. Muttoni, and J. Sagaseta, "Shear strength of concrete members without transverse reinforcement: A mechanical approach to consistently account for size and strain effects," *Engineering Structures*, vol. 99, pp. 360–372, 2015, doi: 10.1016/j.engstruct.2015.05.007.

[11] A. D. Sousa and E. O. L. Lantsoght, "One-way shear strength of wide reinforced concrete members without stirrups," *Structural Concrete*, vol. 22, no. 2, pp. 968–992, 2021, doi: 10.1002/suco.202000034.

[12] F. Cavagnis, "Shear in reinforced concrete without transverse reinforcement: from refined experimental measurements to mechanical models," Ph.D Thesis, École Polytechnique Fédérale de Lausanne, 2017.

[13] A. Muttoni and M. Fernández Ruiz, "From experimental evidence to mechanical modeling and design expressions: The Critical Shear Crack Theory for shear design," *Structural Concrete*, vol. 20, no. 4, pp. 1464–1480, 2019, doi: 10.1002/suco.201900193.

[14] P. Huber, T. Huber, and J. Kollegger, "Shear transfer actions in reinforced and prestressed beams with no stirrups or a small number of stirrups," *fib bulletin 85, Towards a rational understanding of shear in beams and slabs*, vol. 85, pp. 33–48, 2016.

[15] P. Huber, T. Huber, and J. Kollegger, "Influence of loading conditions on the shear capacity of post-tensioned beams with low shear reinforcement ratios," *Engineering Structures*, vol. 170, no. February, pp. 91–102, 2018, doi: 10.1016/j.engstruct.2018.05.079.

[16] G. N. J. Kani, "The Riddle of Shear Failure and its Solution," *ACI Journal*, vol. 61, no. 4, pp. 441–468, 1964, doi: 10.14359/7791.

[17] J. C. Kim, K. K. Choi, and G. T. Truong, "Shear design for prestressed concrete beams based on compression zone failure mechanism," *Proceedings of the Institution of Civil Engineers: Structures and Buildings*, vol. 174, no. 7, pp. 561–580, 2021, doi: 10.1680/jstbu.17.00196.

[18] R. Sarkhosh, J. A. den Uijl, C. R. Braam, and J. C. Walraven, "Shear Capacity of Concrete Beams without Shear Reinforcement under Sustained Loads," Delft, The Netherlands, 2010.

[19] J. . Walraven, "Aggregate Interlock: A theoretical and experimental analysis," Ph.D Thesis, TU Delft, Delft, The Netherlands, 1980.

[20] Y. Yang, "Shear Behaviour of Reinforced Concrete Members without Shear Reinforcement A New Look at an Old Problem.," Ph.D Thesis, Technische Universiteit Delft, 2014.

[21] R. H. Evans and M. S. Marathe, "Microcracking and Stress-Strain Curves for Concrete in Tension," *Materials and Structures*, vol. 1, no. 1, pp. 61–64, 1968.

[22] M. M. Hillerborg and P.-E. Petersson, "Analysis of crack formation and crack growth in concrete by means of fracture mechanics and finite elements," *Cement and Concrete research*, vol. 6, pp. 773–782, 1976.

[23] G. N. J. Kani, "Basic Facts Concerning Shear Failure," *Journal of the American Concrete Institute*, vol. 63, no. 6, pp. 675–692, 1966.

[24] J. Hegger, A. Karakas, E. Pelke, and U. Schölch, "Zur Querkraftgefährdung bestehender Spannbetonbrücken Teil I: Grundlagen," *Beton- und Stahlbetonbau*, vol. 104, no. 11, pp. 737–746, 2009, doi: 10.1002/best.200900039.

[25] M. Zink, *Zum Biegeschubversagen schlanker Bauteile aus Hochleistungsbeton mit und ohne Vorspannung*. Leipzig: Springer Gachmedien Wiesbaden GmbH, 199AD.

[26] G. N. J. Kani, "How safe are our large reinforced concrete beams?," *ACI Journal*, vol. 64, no. 12, pp. 128–141, 1967.

[27] M. Hebrand, "Shear Strength Models for Reinforced and Prestressed Concrete Members," Ph.D Thesis, RWTH Aachen University, 2017.

[28] F. J. Vecchio and M. P. Collins, "Modified Compression-Field Theory for Reinforced Concrete Elements Subjected To Shear.," *Journal of the American Concrete Institute*, vol. 83, no. 2. pp. 219–231, 1986, doi: 10.14359/10416.

[29] A. Muttoni, M. F. Ruiz, and J. T. Simões, "Recent improvements of the critical shear crack theory for punching shear design and its simplification for code provisions," *FIB 2018 - Proceedings for the 2018 fib Congress: Better, Smarter, Stronger*. FIB, pp. 116–129, 2019.

[30] F. Cavagnis, M. Fernández Ruiz, and A. Muttoni, "A mechanical model for failures in shear of members without transverse reinforcement based on development of a critical shear crack," *Engineering Structures*, vol. 157, no. February 2017, pp. 300–315, 2018, doi: 10.1016/j.engstruct.2017.12.004.

[31] V. Sadeghian and F. J. Vecchio, "The Modified Compression Field Theory: Then and now," *ACI Structural Journal*, vol. 3, no. 1, pp. 3.1-3.20, 2018.

[32] M. P. Collins, E. C. Bentz, E. G. Sherwood, and L. Xie, "An adequate theory for the shear strength of reinforced concrete structures," *Magazine of Concrete Research*, vol. 60, no. 9, pp. 635–650, 2008, doi: 10.1680/macr.2008.60.9.635.

[33] SIA Zurich, *SIA 262:2013*. 2013.

[34] Canadian Standards Association, *CSA A23.3-04*. Ontario, Canada, 2004.

[35] European Committee for Standarization, "Eurocode 2: Design of concrete structures - Part 1-1 : General rules and rules for buildings Eurocode (EN 1992-1-1:2004)," no. 2004. Brussels, 2010.

[36] American Concrete Institute, "ACI 318-19: Building code requirements for structural concrete and commentary." Farmington Hills, MI 48331, 2019, doi: 10.14359/51716937.

[37] American Association of State Highway and Transportation Officials, *AASHTO LRFD Bridge Design Specifications*, 8th. Washington, DC, 2017.

[38] European Committee for Standarization, "prEN1992-1-1-D7: 2020, Draft of Eurocode 2: Design of concrete structures Part 1–1: General rules and rules for buildings, bridges and civil engineering structures," vol. 7. pp. 1–455, 2020.

[39] C. Walraven and R. Braam, *Prestressed concrete*. Delft, The Netherlands: Delft University of Technology, 2019.

[40] G. Konig and J. Fischer, "Model Uncertainties concerning Design Equations for the Shear Capacity of Concrete Members without Shear Reinforcement," Federation internationale du beton (fib), Darmstadt, Germany, 1995.

[41] P. E. Regan, A. Al-Hussaini, K.-E. Ramdane, and H.-Y. Xue, "Behaviour of High Strength Concrete Slabs," *Concrete 2000*, vol. 1, pp. 761–773, Sep. 1993.

[42] D. A. Kuchma, S. Wei, D. H. Sanders, A. Belarbi, and L. C. Novak, "Development of the One-Way Shear Design Provisions of ACI 318-19 for Reinforced Concrete," no. 116, pp. 285–296, 2019, doi: 10.14359/51716739.

[43] B. J. G. Macgregor and J. M. Hanson, "Proposed Changes in Shear Provisions for Reinforced and Prestressed Concrete Beams*," *ACI Journal Proceedings*, vol. 66, no. 4, pp. 276–288, 1969, doi: 10.14359/7360.

[44] ACI-ASCE committee 326, "Shear and diagonal tension," 1962.

[45] E. C. Bentz, F. J. Vecchio, and M. P. Collins, "Simplified modified compression field theory for calculating shear strength of reinforced concrete elements," *ACI Structural Journal*, vol. 103, no. 4, pp. 614–624, 2006, doi: 10.14359/16438.

[46] E. Nakamura, "Shear Database for Prestressed Concrete Members," MSc. Thesis, University of Texas at Austin, 2011.

[47] D. A. Kuchma and B. Fitik, "Extended databases with shear tests on structural concrete beams without and with stirrups for the assessment of shear design procedures," 2010.

[48] K. H. Reineck, D. A. Kuchma, K. S. Kim, and S. Marx, "Shear database for reinforced concrete members without shear reinforcement," *ACI Structural Journal*, vol. 100, no. 2, pp. 240–249, 2003, doi: 10.14359/12488.

[49] C. W. Dolan, *Prestressed Concrete. Building, Design, and Construction*. Laramie, WY, USA: Springer Nature Switzerland AG 2019, 2019.

[50] A. E. Naaman, *Prestressed concrete Analysis and Design*, 2nd. Editi. Ann Arbor, Michigan, USA: Quality Books, Inc., 2004.

[51] N. L. Tran, "A mechanical model for the shear capacity of slender reinforced concrete members without shear reinforcement," *Engineering Structures*, vol. 219, no. June, p. 110803, 2020, doi: 10.1016/j.engstruct.2020.110803.

[52] and M. National Academies of Sciences, Engineering, *Simplified Shear Design of Structural Concrete Members Appendixes*. Washington, DC, 2005.

[53] A. Muttoni, M. Fernández Ruiz, and F. Cavagnis, "Shear in members without transverse reinforcement: from detailed test observations to a mechanical model and simple expressions for codes of practice." fib bulletin 85, Towards a rational understanding of shear in beams and slabs, Zurich, Switzerland, pp. 17–32, 2016.

[54] F. Cavagnis, J. T. Simões, M. F. Ruiz, and A. Muttoni, "Shear strength of members without transverse reinforcement based on development of critical shear crack," *ACI Structural Journal*, vol. 117, no. 1, pp. 103–118, 2020, doi: 10.14359/51718012.

[55] E. O. L. Lantsoght, C. Van Der Veen, A. De Boer, and J. C. Walraven, "Using Eurocodes and Aashto for assessing shear in slab bridges," *Proceedings of the Institution of Civil Engineers: Bridge Engineering*, vol. 169, no. 4, pp. 285–287, 2016, doi: 10.1680/jbren.14.00022.

[56] V. Sigrist *et al.*, "Background to the fib Model Code 2010 shear provisions - Part I: Beams and slabs," *Structural Concrete*, vol. 14, no. 3, pp. 195–203, 2013, doi: 10.1002/suco.201200066.

LIST OF FIGURES

LIST OF TABLES

APPENDIX A

Derivation of Concrete contribution according to ACI 318-19 [43]

The derivation of concrete contribution expression used in ACI code starts by looking at an infinitesimal element located directly at the top of a flexural-shear crack.
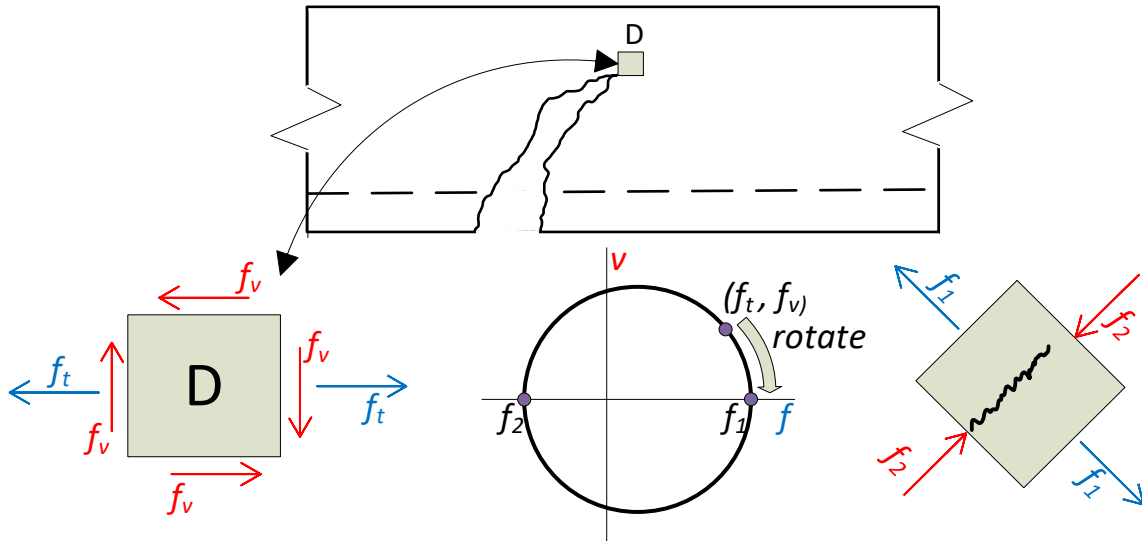

Figure 0-1 Stress state at infinitesimal level, principal stresses

The maximum tensile stress acting on the element can be found with Mohr's circle as follow:

$$f_{max} = \frac{f_t}{2} + \sqrt{\left(\frac{f_t}{2}\right)^2 + f_v^2} \quad \textbf{(a)}$$

[Eq. 0-1]

Assuming the shear stress equal to:

$$f_v = \frac{V_n \cdot Q}{I \cdot b} = k_1 \frac{V_n}{b \cdot d} \quad \textbf{(b)}$$

[Eq. 0-2]

And estimating the tensile stresses from flexure as follow:

Stablishing a relation between the nominal flexural moment with the steel stress as shown below.

$$M_n = A_s f_y \left(d - \frac{\beta c}{2}\right) \rightarrow f_{steel} \propto \frac{M_n}{A_s d}$$

[Eq. 0-3]

Transforming steel stresses to concrete stresses:

$$f_t \propto \frac{E_c}{E_s} f_{steel}$$

[Eq. 0-4]

Assuming the modulus of elasticity of concrete can be approximated by:

$$E_c = 4700\sqrt{f_c'} \; [MPa]$$

[Eq. 0-5]

Combining expressions [Eq. 0-3], [Eq. 0-4], and [Eq. 0-5] one can obtain:

$$f_t \propto \frac{4700\sqrt{f_c'}}{E_s} \cdot \frac{M_n}{\rho \cdot b \cdot d^2}$$

which parameterized is equal to:

$$f_t = \frac{k_4}{E_s} \cdot \left(\frac{\sqrt{f_c'}}{\rho}\right) \cdot \frac{M_n}{b \cdot d^2} \quad \text{(c)}$$

Finally, the maximum stress can be assumed as a function of another parameter:

$$f_{max} = k_5\sqrt{f_c'} \quad \text{(d)}$$

Then, one can combine all the expression replacing [Eq. 0-2], [Eq. 0-7], and [Eq. 0-8] into [Eq. 0-1] to obtain:

$$k_5\sqrt{f_c'} = \frac{1}{2}\frac{k_4}{E_s}\left(\frac{\sqrt{f_c'}}{\rho}\right)\left(\frac{M_n}{b \cdot d^2}\right) + \sqrt{\left[\frac{1}{2}\frac{k_4}{E_s}\left(\frac{\sqrt{f_c'}}{\rho}\right)\left(\frac{M_n}{b \cdot d^2}\right)\right]^2 + \left[k_1\frac{V_n}{b \cdot d}\right]^2}$$

Solving the last expression for normalized shear stress:

$$\left[\frac{k_5\sqrt{f_c'}}{V_n} - \frac{1}{2}\frac{k_4}{E_s}\left(\frac{\sqrt{f_c'}}{\rho}\right)\left(\frac{M_n}{V_n \cdot b \cdot d^2}\right)\right]^2 = \left[\frac{1}{2}\frac{k_4}{E_s}\left(\frac{\sqrt{f_c'}}{\rho}\right)\left(\frac{M_n}{V_n \cdot b \cdot d^2}\right)\right]^2 + \left[k_1\frac{1}{b \cdot d}\right]^2$$

$$\left[\frac{k_5\sqrt{f_c'} \cdot b \cdot d}{V_n} - \frac{1}{2}\frac{k_4}{E_s}\left(\frac{\sqrt{f_c'}}{\rho}\right)\left(\frac{M_n}{V_n \cdot d}\right)\right]^2 = \left[\frac{1}{2}\frac{k_4}{E_s}\left(\frac{\sqrt{f_c'}}{\rho}\right)\left(\frac{M_n}{V_n \cdot d}\right)\right]^2 + k_1{}^2$$

$$\frac{V_n}{b \cdot d \cdot \sqrt{f_c'}} = \frac{k_5}{\frac{1}{2}\frac{k_4}{E_s}\left(\frac{\sqrt{f_c'}}{\rho}\right)\left(\frac{M_n}{V_n \cdot d}\right) + \sqrt{\left[\frac{1}{2}\frac{k_4}{E_s}\left(\frac{\sqrt{f_c'}}{\rho}\right)\left(\frac{M_n}{V_n \cdot d}\right)\right]^2 + k_1{}^2}}$$

To simplify the last expression, variables can be defined as follow:

- Independent variable: $x = \frac{V_n \cdot d}{M_n} \cdot \frac{\rho}{\sqrt{f_c'}}$; case prestressed member ρ is suppressed.
- Dependent variable: $y = \frac{V_n}{b \cdot d \cdot \sqrt{f_c'}}$

and according to what was defined above, the following expression is obtained

$$y = \frac{k_5 E_s}{\frac{1}{x} + \sqrt{\left[\frac{1}{x}\right]^2 + k_1{}^2}}$$

This expression is the theoretically correct one and the constants k_5 and k_1 could be calibrated using the collected experimental results. But for the ACI things were simplified even further linearizing the last expression as $y = Ax + B$ resulting in the known first 2 expressions for the simplified procedure for ACI 318-19M (refer to section 2.4.3 of this document):

$$\frac{V_{c.a}}{b_w d\sqrt{f_c'}} = 0.05\lambda + 4.8\frac{V_u d_p}{M_u\sqrt{f_c'}} \, [MPa] \xrightarrow{\lambda=1} y = 0.05 + 4.8x$$

The last expression used in ACI318-19M approximate method defines the that the linear relationship is defined for one segment only that is delimited by upper and lower limits as shown in Figure 0-2.
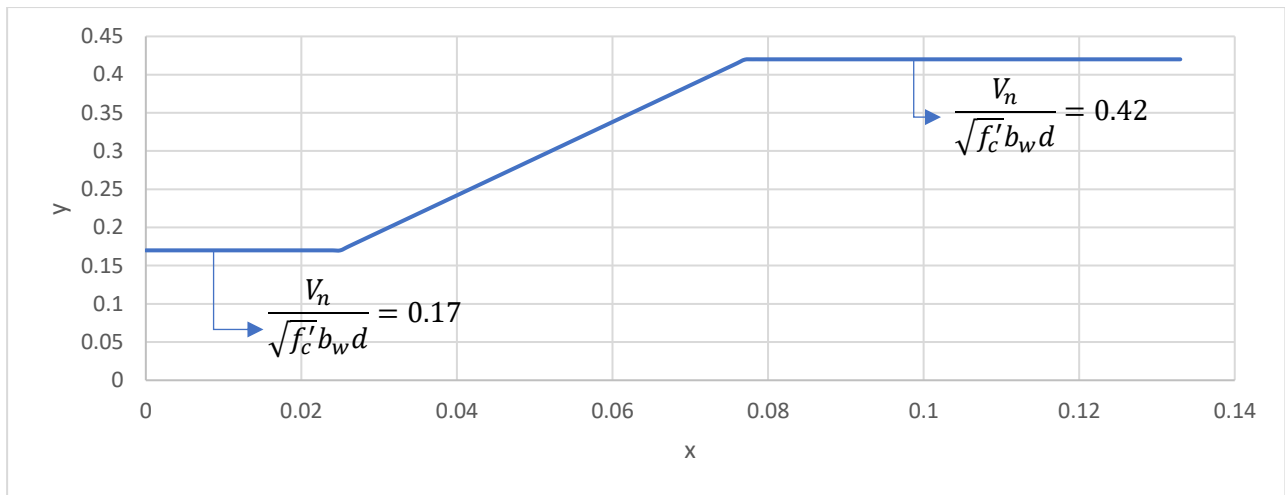

Figure 0-2 ACI318-19M approximate method graphical relation of parameters

APPENDIX B

Main criteria for data selection and sorting

The main filters applied to the gross ACI-DAfStb-PC/2015 database are shown in the following Table 0-1, considering the definitions corresponding to:

- Uniaxial compressive strength of concrete: $f_{1c} = 0.95 \cdot f_{cm,cyl}$
- Mechanical reinforcement Ratio of tension chord: $\omega_l = \frac{A_s \cdot f_{sy}}{b \cdot d \cdot f_{1c}} + \frac{A_{pbot} \cdot f_{py}}{b \cdot d \cdot f_{1c}}$
- Factor for depth of compression zone: $\xi_{test} = 2 \cdot \left(1 - \frac{z_{test}}{d}\right)$; where z_{test} is the inner lever arm.
- Longitudinal reinforcement type of bars used f_r: ribbed bars, plain bars, not reported
- Longitudinal prestressed reinforcement type of tendon f_{rp}: ribbed, plain.
- Assessment of flexural failure β_{flex} and anchorage failure β_{lb} (section 3.5 document)

Table 0-1 Main filters (kon_i) applied to the ACI-DAfStb-PC/2015 gross database.

kon_1	$f_{1c} > 12 \ [MPa]$
kon_2	$f_{1c} < 100 \ [MPa]$
kon_3	$b_w > 50 \ [mm]$
kon_4	$h \geq 70 \ [mm]$
kon_5	$a/d > 2.89$
kon_6	$2.4 \leq a/d \leq 2.89$
kon_7	$\omega_l \neq 0 \rightarrow \xi_{test} \leq 0.5$
kon_8	$\beta_{flex} = \mu_u/\mu_{flex} < 1.0$
kon_81	$1.0 \leq \beta_{flex} \leq 1.1$
kon_10	$f_r \ OR \ f_{rp} = ribbed \ bars; AND \ P_{method} = "Post"$
kon_11	$\beta_{lb} = l_{b,req}/l_{b,av} < 1.0$
kon_15	Other failure type

Some experiments did not specify explicitly the value of the beam height, so the following conditional (auxiliary filter) was devised where a beam height is assumed based on the effective depth of the non-prestressed longitudinal reinforcement equal $h = d_s/0.9$, for the group of beams complying with the length and width conditions as specified in the following Table 0-2.

Table 0-2 Composed conditional kon_34

kon_31	$50 \leq b_w \leq 100 \ [mm]$
kon_4	$h \geq 70 \ [mm]$
kon_41	$(h = 0) \cdot \left(70 \leq \frac{d_s}{0.9} < 150\right) OR \ (70 \leq h < 150)$
kon_34	$kon_{41} \cdot kon_{31} = \left[(h = 0) \cdot \left(70 \leq \frac{d_s}{0.9} < 150\right) OR \ (70 \leq h < 150)\right] \cdot (50 \leq b_w \leq 100)$

The combination of conditionals mentioned before in different ways end up forming the filters KON_A4 and KON_A5 detailed in the following Table 0-3. The sum of the tests captured by these filters end up forming the database used.

ACI-DAfSTb-PC = KON_A4 + KON_5

Table 0-3 Breakdown of the filters used, KON_A4 and KON_A5

KON_A4	$KON_{A2} \cdot kon_{34}$
KON_A2	KON_{A21} or KON_{A22}
	$KON_{A21a} \cdot kon_{11}$
	$KON_{A0} \cdot kon_5 \cdot kon_8$
KON_A21	$kon_1 \cdot kon_3 \cdot kon_4 \cdot kon_7 \cdot kon_{10} \cdot kon_{15} \cdot kon_5 \cdot kon_8 \cdot kon_{11}$
	$KON_{A22a} \cdot kon_{11}$
	$KON_{A0} \cdot kon_5 \cdot kon_{81}$
KON_A22	$kon_1 \cdot kon_3 \cdot kon_4 \cdot kon_7 \cdot kon_{10} \cdot kon_{15} \cdot kon_5 \cdot kon_{81} \cdot kon_{11}$

KON_A5	$KON_{A3} \cdot kon_{34}$
KON_A3	KON_{A31} or KON_{A32}
KON_A31	$kon_1 \cdot kon_3 \cdot kon_4 \cdot kon_7 \cdot kon_{10} \cdot kon_{15} \cdot kon_6 \cdot kon_8$
KON_A32	$kon_1 \cdot kon_3 \cdot kon_4 \cdot kon_7 \cdot kon_{10} \cdot kon_{15} \cdot kon_6 \cdot kon_{81}$

Calculation of the ultimate bending moment of prestressed concrete beams.

The factors used, the notation, and the procedures are based on the base document for the ACI-DAfStb-PC database [47].
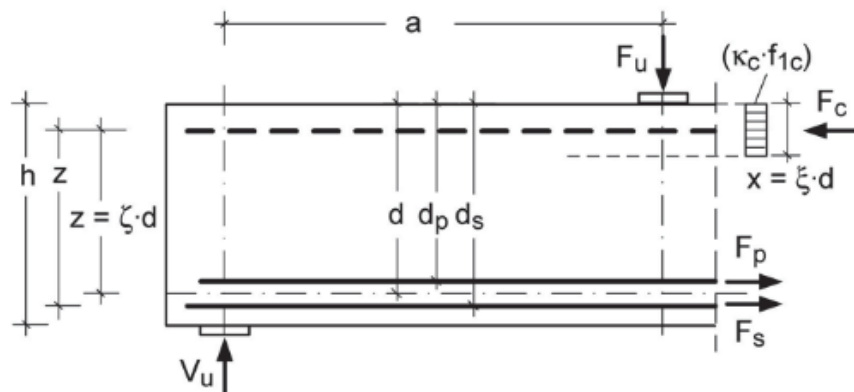

Figure 0-1 Free-body diagram and parameters to calculate the ultimate bending moment of prestressed concrete beams [47]

When $\omega_l > \omega_{lim} = \kappa_c \cdot \frac{0.4 \cdot d_s}{d}$ the tensile force of reinforcing steel (F_s), the tensile force of prestressing steel (F_p), and the compressive force of concrete (F_c) are defined as:

$$F_s = A_s \cdot \varepsilon_s \cdot E_s \ [N] \qquad \text{[Eq. 0-1]}$$

$$F_p = A_p \cdot (\Delta\varepsilon_p + \varepsilon_{pp}) \cdot E_p \ [N] \qquad \text{[Eq. 0-2]}$$

$$F_c = \kappa_c \cdot f_c \cdot \xi \cdot b \cdot d \ [N] \qquad \text{[Eq. 0-3]}$$

Where:

Cross-section area of reinforcing steel: $A_s \ [mm^2]$
Cross-section area of prestressing steel: $A_p \ [mm^2]$
Strain of reinforcing steel: $\varepsilon_s \ [-]$

Additional strain in prestressing steel: $\Delta\varepsilon_p$ $[-]$

Strain in prestressing steel due to prestress: $\varepsilon_{pp} = \frac{\sigma_{pp}}{E_p} = \frac{P}{E_p \cdot A_p}$ $[-]$

Young modulus in steel: $E_s; E_p$ $[MPa]$

Effective depth: $d = \frac{A_p \cdot f_{py} \cdot d_p + A_s \cdot f_{sy} \cdot d_s}{A_p \cdot f_{py} + A_s \cdot f_{sy}}$ $[mm]$

Stress block coefficient according to CEB-FIP MC 90: $\kappa_c = 1 - \frac{f_c}{250}$ $[-]$

Coefficient to locate the neutral axis: ξ $[-]$

And when $\omega_l < \omega_{lim}$

$$F_s = A_s \cdot f_{sy} \ [N] \qquad \text{[Eq. 0-4]}$$

$$F_p = A_p \cdot f_{py} \ [N] \qquad \text{[Eq. 0-5]}$$

To have handy expressions the mechanical reinforcement ratios for prestressing steel (ω_p), and for non-prestressed steel reinforcement (ω_s) are defined as.

$$\omega_p = \frac{A_p \cdot f_{py}}{b \cdot d \cdot f_c} \ [-] \qquad \text{[Eq. 0-6]}$$

$$\omega_s = \frac{A_s \cdot f_{sy}}{b \cdot d \cdot f_c} \ [-] \qquad \text{[Eq. 0-7]}$$

And to have a general term of analysis, in cases where both prestressed and non-prestressed longitudinal reinforcement are used or not, the mechanical reinforcement ratio of the tension chord is defined as.

$$\omega_l = \omega_s + \omega_p \ [-] \qquad \text{[Eq. 0-8]}$$

In order to determine the ultimate flexural moment, the procedure explained below is applied.

- When $\omega_l < \omega_{lim}$ is true, where the limit of reinforcement ratio

  By the equilibrium of horizontal forces one can estimate the coefficient for the neutral axis as follow

  - $\sum H = 0$: $\xi = \frac{A_p \cdot f_{py} + A_s \cdot f_{sy}}{\kappa_c \cdot b \cdot d \cdot f_c} = \frac{1}{\kappa_c} \cdot (\omega_s + \omega_p) = \frac{\omega_l}{\kappa_c}$ $[-]$

  And by the equilibrium of moments using the inner lever arm equal to the distance between the resultant of total compression force and resultant of tension force from prestressed and non-prestressed steel, one can estimate the ultimate bending moment in this case equal to:

  - $\sum M$: $M = F_c \cdot z = (\kappa_c \cdot b \cdot d \cdot f_c \cdot \xi) \cdot z$
    Where
    Inner lever arm: $z = \zeta \cdot d$
    Coefficient for inner lever arm: $\zeta = 1 - \frac{1}{2}\xi$

  In order to calculate a dimension-free ultimate flexural moment the following definition is established.

  $$\mu_{flex,1} = \frac{M}{b \cdot d^2 \cdot f_c} = \frac{F_c \cdot z}{b \cdot d^2 \cdot f_c} = \frac{\kappa_c \cdot f_c \cdot \xi \cdot b \cdot d_s \cdot \zeta \cdot d}{b \cdot d^2 \cdot f_c} = \kappa_c \cdot \xi \cdot \zeta = \omega_l \cdot \zeta \qquad \text{[Eq. 0-9]}$$

  Only applicable for pure bending, without consideration of the compressive reinforcement and when the upper limit for the concrete strain is $\varepsilon < 3.5/1000$

- If $\omega_l > \omega_{lim}$

  The horizontal equilibrium of forces is equal to

  $$\sum H = 0: \quad \kappa_c \cdot b \cdot d \cdot f_c \cdot \xi = A_p \cdot \left(\Delta\varepsilon_p + \varepsilon_{pp}\right) \cdot E_p + A_s \cdot \varepsilon_s \cdot E_s$$

  Where, from the strain distribution follows that:

  $$\xi = \frac{\varepsilon_c}{\varepsilon_s + \varepsilon_c}$$

  [Eq. 0-10]

  $$\Delta\varepsilon_p = \frac{d_p}{d} \cdot (\varepsilon_c + \Delta\varepsilon) - \varepsilon_c$$

  [Eq. 0-11]

  $$\varepsilon_s = \frac{d_s}{d} \cdot (\varepsilon_c + \Delta\varepsilon) - \varepsilon_c$$

  [Eq. 0-12]

  Considering $\Delta\varepsilon$ the additional strain at level of effective depth d.

  After substitution of last equation into the equilibrium condition the following equation can be solved for $\Delta\varepsilon$.

  $$\left(\frac{\omega_p}{\varepsilon_{py}} \cdot \frac{d_p}{d} + \frac{\omega_s}{\varepsilon_{sy}} \cdot \frac{d_s}{d}\right) \cdot \Delta\varepsilon^2 + \left(\frac{\omega_p}{\varepsilon_{py}} \cdot \left(2 \cdot \varepsilon_c \cdot \frac{d_p}{d} - \varepsilon_c + \varepsilon_{pp}\right) + \frac{\omega_s}{\varepsilon_{sy}} \cdot \varepsilon_c \cdot \left(2 \cdot \frac{d_s}{d} - 1\right)\right) \cdot \Delta\varepsilon$$
  $$+ \frac{\omega_p}{\varepsilon_{py}} \cdot \varepsilon_c \cdot \left(\frac{d_p}{d} \cdot \varepsilon_c - \varepsilon_c + \varepsilon_{pp}\right) + \frac{\omega_s}{\varepsilon_{sy}} \cdot \varepsilon_c^2 \cdot \left(\frac{d_s}{d} - 1\right) - \kappa_c \cdot \varepsilon_c = 0$$

  [Eq. 0-13]

  Where $\frac{\omega_p}{\varepsilon_{py}} = \frac{\rho_p \cdot E_p}{f_c}$ and $\varepsilon_{py} = \frac{f_{py}}{E_p}$ for prestressed steel, $\frac{\omega_s}{\varepsilon_{sy}} = \frac{\rho_s \cdot E_s}{f_c}$ and $\varepsilon_{sy} = \frac{f_{sy}}{E_s}$ for non-prestressed longitudinal reinforcement.

- For members with non-prestressed longitudinal reinforcement, where $\omega_s \neq 0; \frac{d_p}{d} < 1$ and $\Delta\varepsilon = \Delta\varepsilon_p$, the calculated ultimate flexural moment will be

  $$\sum M: \quad M = F_p \cdot \left(d_p - \frac{1}{2} \cdot \xi \cdot d\right) + F_s \cdot \left(d_s - \frac{1}{2} \cdot \xi \cdot d\right) [-]$$

  [Eq. 0-14]

  And the non-dimensional flexural moment is equal to:

  $$\mu_{flex,2} = \frac{M}{b \cdot d^2 \cdot f_c} = \frac{F_p \cdot \left(d_p - \frac{1}{2} \cdot \xi \cdot d\right) + F_s \cdot \left(d_s - \frac{1}{2} \cdot \xi \cdot d\right)}{b \cdot d^2 \cdot f_c}$$
  $$= \frac{\omega_p}{\varepsilon_{py}} \cdot \left(\Delta\varepsilon_p + \varepsilon_{pp}\right) \cdot \left(\frac{d_p}{d} - \frac{1}{2} \cdot \xi\right) + \frac{\omega_s}{\varepsilon_{sy}} \cdot \varepsilon_s \cdot \left(\frac{d_s}{d} - \frac{1}{2} \cdot \xi\right)$$

  [Eq. 0-15]

- For members without non-prestressed longitudinal reinforcement, follow that $\omega_s = 0; \frac{d_p}{d} = 1$ and $\Delta\varepsilon = \Delta\varepsilon_p$, and the non-dimensional flexural moment is equal to:

  $$\mu_{flex,2} = \frac{\omega_p}{\varepsilon_{py}} \cdot \left(\Delta\varepsilon_p + \varepsilon_{pp}\right) \cdot \zeta$$

  [Eq. 0-16]

Inner lever-arm at shear failure calculation

The contribution of steel in compression is not considered in the approach proposed by [47]. It is assumed that their contribution is minimal and a conservative result is obtained too.
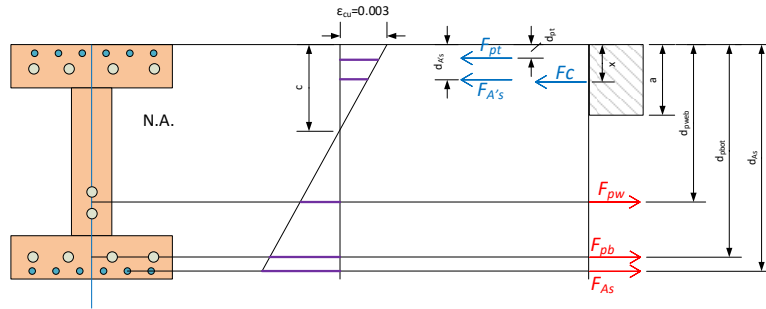
Figure 0-2 Free-body diagram, notation and parameters considered for calculating the ultimate bending moment for prestressed concrete beams.

Prestressed concrete beams without reinforcing steel

In this case it is not necessary to consider a resultant for the tensile force by non-prestressed longitudinal steel reinforcement.

From equilibrium of horizontal forces, results in:

$$\sum H = 0: \quad \xi = \frac{A_p \cdot \sigma_p}{\kappa_c \cdot b \cdot d \cdot f_c} = \frac{\omega_p \cdot \sigma_p}{\kappa_c \cdot f_{py}} \, [-]$$

In this case $d = d_p$

With, $\sum M: F_c \cdot z = F_p \cdot z$, using non-dimensional flexural moment results in:

$$\mu_u = \frac{M_u}{b \cdot d^2 \cdot f_c} = \frac{F_c \cdot z}{b \cdot d^2 \cdot f_c} = \frac{\kappa_c \cdot f_c \cdot \xi \cdot b \cdot d \cdot (\zeta \cdot d)}{b \cdot d^2 \cdot f_c} = \kappa_c \cdot \xi \cdot \left(1 - \frac{\xi}{2}\right) \qquad \text{[Eq. 0-17]}$$

Where:

Coefficient for inner lever arm: $\zeta = 1 - \frac{1}{2} \cdot \xi \, [-]$

Solving for ξ, it is obtained that:

$$\xi = 1 - \sqrt{1 - 2 \cdot \frac{\mu_u}{\kappa_c}} \, [-] \qquad \text{[Eq. 0-18]}$$

And subsequently, can be determined the following reltaion:

$$\sigma_p = \frac{\kappa_c \cdot f_{py}}{\omega_p} \cdot \xi \leq f_{py} \, [MPa] \qquad \text{[Eq. 0-19]}$$

For prestressed concrete beams with longitudinal non-prestressed steel reinforcement

Considering the collaboration by non-prestressed longitudinal steel reinforcement.

From equilibrium of horizontal forces $\sum H = 0$ results that:

$$F_c = F_s + F_p \rightarrow \kappa_c \cdot f_c \cdot \xi_{test} \cdot d \cdot b = A_p \cdot \Delta\sigma_p + A_s \cdot \varepsilon_s \cdot E_s \qquad \text{[Eq. 0-20]}$$

Then, taking the coefficient to locate the neutral axis as one of the variables to find.

$$\xi_{test} = \frac{\omega_p \cdot E_p}{\kappa_c \cdot f_{py}} \cdot \left(\Delta\varepsilon_p + \varepsilon_{pp}\right) + \frac{\omega_s \cdot E_s}{\kappa_c \cdot f_{sy}} \cdot \varepsilon_s = \frac{\omega_p \cdot \varepsilon_{pp}}{\kappa_c \cdot \varepsilon_{py}} + \frac{\omega_p \cdot \Delta\varepsilon_p}{\kappa_c \cdot \varepsilon_{py}} + \frac{\omega_s \cdot \varepsilon_s}{\kappa_c \cdot \varepsilon_{sy}} \qquad \text{[Eq. 0-21]}$$

Where:

Mechanical reinforcement ratio of reinforcing steel: $\omega_s = \frac{A_s \cdot f_{sy}}{b \cdot d \cdot f_c}$

Mechanical reinforcement ratio of prestressing steel: $\omega_p = \frac{A_p \cdot f_{py}}{b \cdot d \cdot f_c}$

Yield strain of reinforcing steel: $\varepsilon_{sy} = f_{sy}/E_s$

Yield strain of prestressing steel: $\varepsilon_{py} = f_{py}/E_p$

One can use the theorem of intersecting lines to find the relation between strains.

$$\frac{\Delta\varepsilon_p}{\varepsilon_s} = \frac{d_p - x}{d_s - x} \xrightarrow{\text{with } x=\xi \cdot d} \Delta\varepsilon_p = \left(\frac{d_p - \xi \cdot d}{d_s - \xi \cdot d}\right)\varepsilon_s \qquad \textit{[Eq. 0-22]}$$

Combining [Eq. 0-21] and [Eq. 0-22], results that

$$\xi_{test} = \frac{\omega_p \cdot \varepsilon_{pp}}{\kappa_c \cdot \varepsilon_{py}} + \frac{\omega_p \cdot \varepsilon_s}{\kappa_c \cdot \varepsilon_{py}} \cdot \left(\frac{d_p - \xi \cdot d}{d_s - \xi \cdot d}\right) + \frac{\omega_s \cdot \varepsilon_s}{\kappa_c \cdot \varepsilon_{sy}} \qquad \textit{[Eq. 0-23]}$$

Now, for $\sum M$ one obtains that:

$$\mu_u = \omega_s \cdot \frac{\varepsilon_s}{\varepsilon_{sy}} \cdot \left(\frac{d_s}{d} - \frac{x}{2 \cdot d}\right) + \omega_p \cdot \frac{\Delta\varepsilon_p}{\varepsilon_{py}} \cdot \left(\frac{d_p}{d} - \frac{x}{2 \cdot d}\right) + \omega_p \cdot \frac{\varepsilon_{pp}}{\varepsilon_{py}} \cdot \left(\frac{d_p}{d} - \frac{x}{2 \cdot d}\right) \qquad \textit{[Eq. 0-24]}$$

And inserting [Eq. 0-22] with [Eq. 0-24] the following relation is obtained.

$$\mu_u = \omega_s \cdot \frac{\varepsilon_s}{\varepsilon_{sy}} \cdot \left(\frac{d_s}{d} - \frac{x}{2 \cdot d}\right) + \omega_p \cdot \frac{\varepsilon_s}{\varepsilon_{py}} \cdot \left(\frac{d_p - \xi \cdot d}{d_s - \xi \cdot d}\right) \cdot \left(\frac{d_p}{d} - \frac{x}{2 \cdot d}\right) + \omega_p \cdot \frac{\varepsilon_{pp}}{\varepsilon_{py}} \cdot \left(\frac{d_p}{d} - \frac{x}{2 \cdot d}\right)$$

$$= \left(\frac{d_s}{d} - \frac{\xi_{test}}{2}\right) + \left[\omega_s \cdot \frac{\varepsilon_s}{\varepsilon_{sy}} + \omega_p \cdot \frac{\varepsilon_s}{\varepsilon_{py}} \cdot \left(\frac{d_p - x}{d_s - x}\right) \cdot \left(\frac{d_p - \frac{x}{2}}{d_s - \frac{x}{2}}\right) + \omega_p \cdot \frac{\varepsilon_{pp}}{\varepsilon_{py}} \cdot \left(\frac{d_p - \frac{x}{2}}{d_s - \frac{x}{2}}\right)\right] \qquad \textit{[Eq. 0-25]}$$

According to the background document of the ACI-DAfStb-PC [47], as the difference between d_p and d_s is small, and after an internal evaluation of the results obtained, the following equalities were established

$$\frac{d_p - \xi \cdot d}{d_s - \xi \cdot d} = 0.9578 \, [-] \qquad \textit{[Eq. 0-26]}$$

$$\frac{d_p - x/2}{d_s - x/2} = 0.9680 \, [-] \qquad \textit{[Eq. 0-27]}$$

Inserting [Eq. 0-23] into [Eq. 0-24] and subsequently using the relations established in [Eq. 0-26] and [Eq. 0-27], a relation to find the longitudinal strain of non-prestressed steel reinforcement results as follow:

$$\varepsilon_s = \frac{-b_{cal} - \sqrt{b_{cal}^2 - 4 \cdot a_{cal} \cdot c_{cal}}}{2 \cdot a_{cal}} \qquad \textit{[Eq. 0-28]}$$

Where:

$$a_{cal} = \left(\frac{\omega_s^2}{\varepsilon_{sy}^2} + 1.9680 \cdot 0.9578 \cdot \frac{\omega_s \cdot \omega_p}{\varepsilon_{sy} \cdot \varepsilon_{py}} + 0.9578^2 \cdot 0.9680 \cdot \frac{\omega_p^2}{\varepsilon_{py}^2}\right) [-]$$

$$b_{cal} = 2 \cdot \kappa_c \cdot \frac{d_s}{d} \cdot \left(\frac{\omega_s}{\varepsilon_{sy}} + 0.9578 \cdot 0.9680 \cdot \frac{\omega_p}{\varepsilon_{py}}\right) + 0.9680 \cdot \frac{\omega_s \cdot \omega_p}{\varepsilon_{sy} \cdot \varepsilon_{py}} \cdot \varepsilon_{pp} + 2 \cdot 0.9578 \cdot 0.9680 \cdot \frac{\omega_p^2}{\varepsilon_{py}^2} \cdot \varepsilon_{pp} \, [-]$$

$$c_{cal} = 0.9680 \cdot \frac{\omega_p^2}{\varepsilon_{py}^2} \cdot \varepsilon_{pp}^2 - 2 \cdot 0.9680 \cdot \kappa_c \cdot \frac{d_s}{d} \cdot \frac{\omega_p}{\varepsilon_{py}} \cdot \varepsilon_{pp} + 2 \cdot \kappa_c \cdot \mu_u \, [-]$$

Finally, with the longitudinal strain determined then, the coefficient to locate the neutral axis can be calculated from [Eq. 0-23] and the coefficient for inner lever arm ζ subsequently.

Anchorage failures at end support

In order to assess the anchorage capacity some input parameters are important, the width of the support (a_A) and the overhang of the beam behind the support axis (b_A) are some. In the report of the ACI-DAfStb-PC database [47], it is reported that some tests do not contain some information, so some assumptions were made in order not to discard too much information. These assumptions are listed below.

$$l_{b,prov} = 0.5 \cdot a_A + b_A - (h - d) \ [mm] \ if \ a_A > 0 \ and \ b_A > 0$$

$$l_{b,prov} = b_A \ [mm] \ if \ a_A = 0 \ and \ b_A > 0$$

$$l_{b,prov} = a_A + 0.1 \cdot d \ [mm] \ if \ a_A > 0 \ and \ b_A = 0$$

$$l_{b,prov} = 0.25 \cdot d \ [mm] \ if \ a_A = 0 \ and \ b_A = 0$$

Where d is the effective depth of the beam.

Assessment of anchorage for prestressed concrete beams without shear reinforcement.

Determination of the tension chord force

Using a truss with concrete struts inclined at an angle of 24 degrees ($\cot\theta = 2.20$) from the longitudinal axis and concrete ties inclined 66 degrees the force to be anchored was determined as follow.

$$F_{sA} = V_{u,Rep} \cdot \left(0.5 \frac{a_A}{z} + 2.20 \frac{h - d}{z} + 0.873 \right) \ [kN] \qquad \text{[Eq. 0-29]}$$

Where:

Shear force at failure: $V_{u,Rep} \ [kN]$

Associated stress: $\sigma_{pau} = \frac{F_{sA}}{A_p} \ [MPa]$

Assessment without consideration of non-tensioned reinforcement

The following equations apply for:

- Beams with 7-wire strands for prestressing steel

$$l_{b,req} = \frac{d_{sp}}{4 \cdot 0.55 \cdot f_{ctm,cal}} \cdot \left(0.5 \cdot \sigma_{pp} + 0.8 \cdot \sigma_{pau} \right) \ [mm] \qquad \text{[Eq. 0-30]}$$

- Beams with other types of prestressing steel

$$l_{b,req} = \frac{d_{sp}}{4 \cdot 0.641 \cdot f_{ctm,cal}} \cdot \left(0.7 \cdot \sigma_{pp} + 1.0 \cdot \sigma_{pau} \right) \ [mm] \qquad \text{[Eq. 0-31]}$$

- Post-tensioned beams, for all types of prestressing steel

$$l_{b,req} = \frac{\alpha_a \cdot d_{sp} \cdot \left(\sigma_p + \sigma_{pau} \right)}{9 \cdot f_{ctm,cal}} \ [mm] \qquad \text{[Eq. 0-32]}$$

Where:

Stress in prestressing steel due to prestress: $\sigma_{pp} = P/A_p \ [MPa]$
Prestressing steel cross-sectional area: A_p
If $a_A = 0$ it is assumed $a_A = 0.2 \cdot d$ instead
Type of anchorage dependent factor (hook 0.1; straight 1; anchor plate 0.01): $\alpha_a \ [-]$
Diameter of prestressing steel: d_{sp}

Calculated value of concrete tensile strength: $f_{ctm,cal}$

Assessment with consideration of non-prestressed reinforcement

The non-prestressed reinforcement is checked first, reviewing if it provides enough anchorage length. Therefore, the following ratio is calculated for the actual force to be anchored in relation to the yield force.

$$\alpha = \frac{F_{sA}}{A_s \cdot f_{sy}} \; [-]$$

[Eq. 0-33]

And according to this ratio the following conditions apply to calculate the first required length.

$$l_{b,req} = \frac{\alpha_a \cdot d_{st} \cdot \sigma_{slau}}{9 \cdot f_{ctm,cal}} \; [mm]; when \; \alpha < 1 \; with \; \sigma_{slau} = \frac{F_{sA}}{A_s} \; [MPa]$$

[Eq. 0-34]

$$l_{b,req} = \frac{\alpha_a \cdot d_{st} \cdot f_{sy}}{9 \cdot f_{ctm,cal}} \; [mm]; when \; \alpha > 1$$

[Eq. 0-35]

Then the anchorage length ratio is checked, and used to compute the required anchorage force ΔF_{sA} that the prestressing steel has to resist. Then if $\beta_{lb1} > 1$ for the non-prestressed steel, it means that prestressed steel needs to provide the remaining anchorage force that is calculated as stated below.

$$\Delta F_{sA} = F_{sA} - F_{sA,prov} \; [kN]$$

[Eq. 0-36]

Where: $F_{sA,prov} = \frac{F_{sA}}{\beta_{lb1}} \; [kN] \; if \; \alpha < 1; otherwise \; F_{sA,prov} = \frac{A_s \cdot f_{sy}}{\beta_{lb1}} \; [kN]$

So, the associated stress in prestressing steel reinforcement is equal to:

$$\sigma_{pau} = \frac{\Delta F_{sA}}{A_p} \; [MPa]$$

[Eq. 0-37]

And in this case the following equations apply for case of pretensioned members:

- For members with 7-wire strands as prestressing steel

$$l_{b,req} = \frac{d_{sp}}{4 \cdot 0.55 \cdot f_{ctm,cal}} \cdot (0.5 \cdot \sigma_{pp} + 0.8 \cdot \sigma_{pau}) \; [mm]$$

[Eq. 0-38]

- For members with other types as prestressing steel

$$l_{b,req} = \frac{d_{sp}}{4 \cdot 0.641 \cdot f_{ctm,cal}} \cdot (0.7 \cdot \sigma_{pp} + 1.0 \cdot \sigma_{pau}) \; [mm]$$

[Eq. 0-39]

- For post-tensioned beams

$$l_{b,req} = \frac{\alpha_a \cdot d_{sp} \cdot (\sigma_{pp} + \sigma_{pau})}{9 \cdot f_{ctm,cal}} \; [mm]$$

[Eq. 0-40]

Finally, the new anchorage ratio can be generated as follow.

$$\beta_{lb2} = \frac{l_{b,req}}{l_{b,prov}} \; [-]$$

[Eq. 0-41]

Appendix C

Analysis of region near end support for prestressed concrete continuous bridge deck, using only 50% of the prestressing force initially stated.
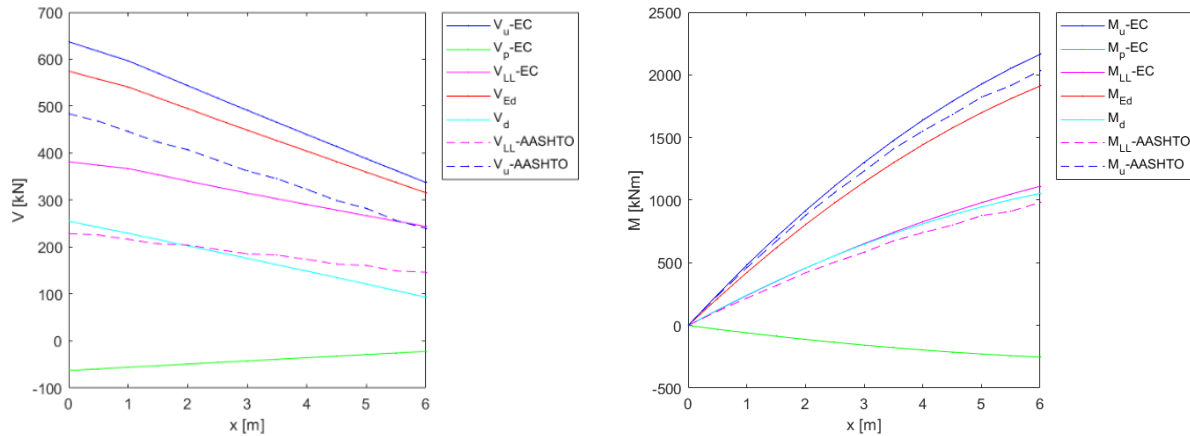

Figure 0-1 Ultimate and acting shear and bending moment for continuous bridge in region near end support, considering only 50% of the prestressing force initially stated
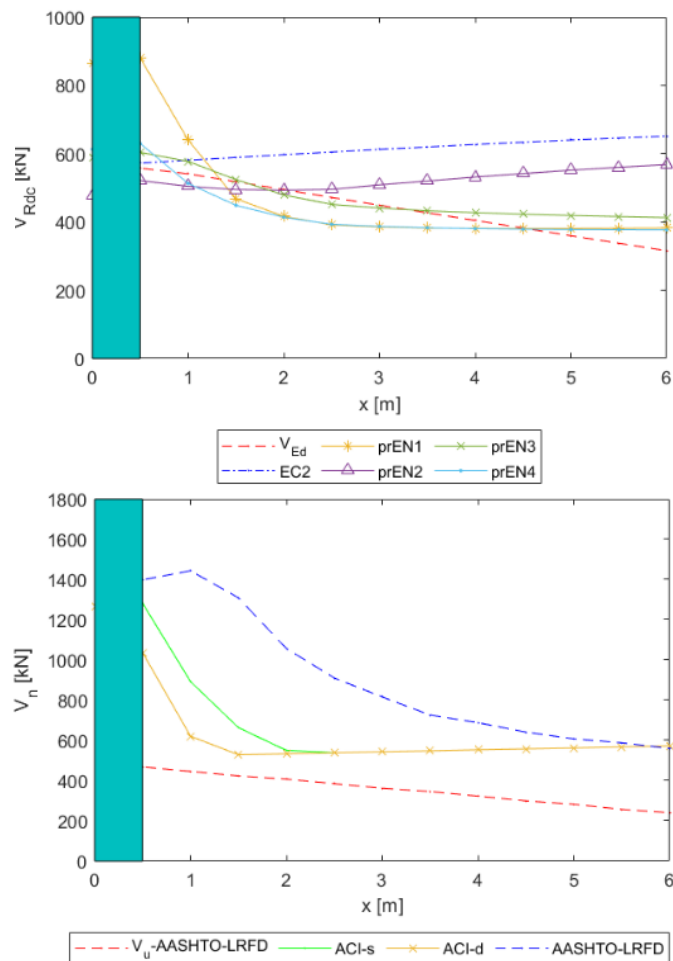

Figure 0-2 Shear resistance near end support of a continuous bridge deck according to design codes applied in Europe and America for the case applying only 50% of the prestressing force initially stated

Analysis of region near end support for prestressed concrete continuous bridge deck, using only 25% of the prestressing force initially stated.
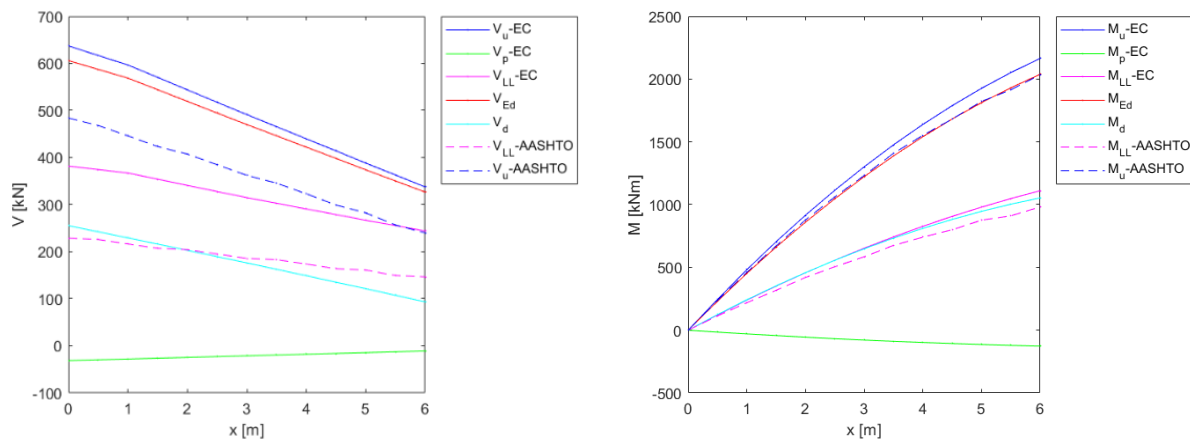

Figure 0-3 Ultimate and acting shear and bending moment for continuous bridge in region near end support, considering only 25% of the prestressing force initially stated
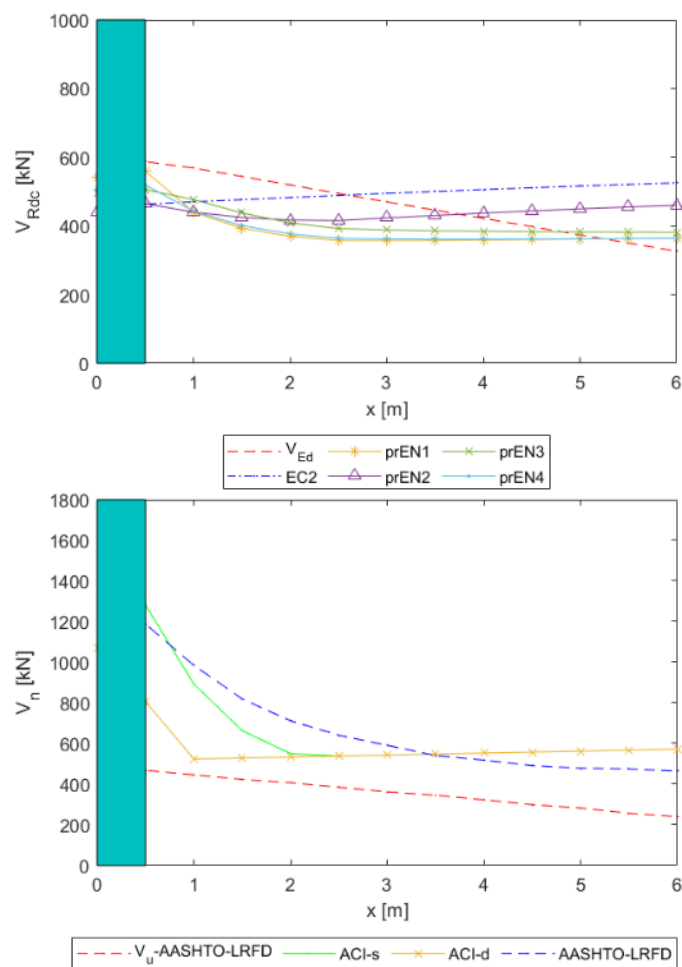

Figure 0-4 Shear resistance near end support of a continuous bridge deck according to design codes applied in Europe and America for the case applying only 25% of the prestressing force initially stated

Analysis of region near end support for prestressed concrete continuous bridge deck, using 0% of the prestressing force initially stated.
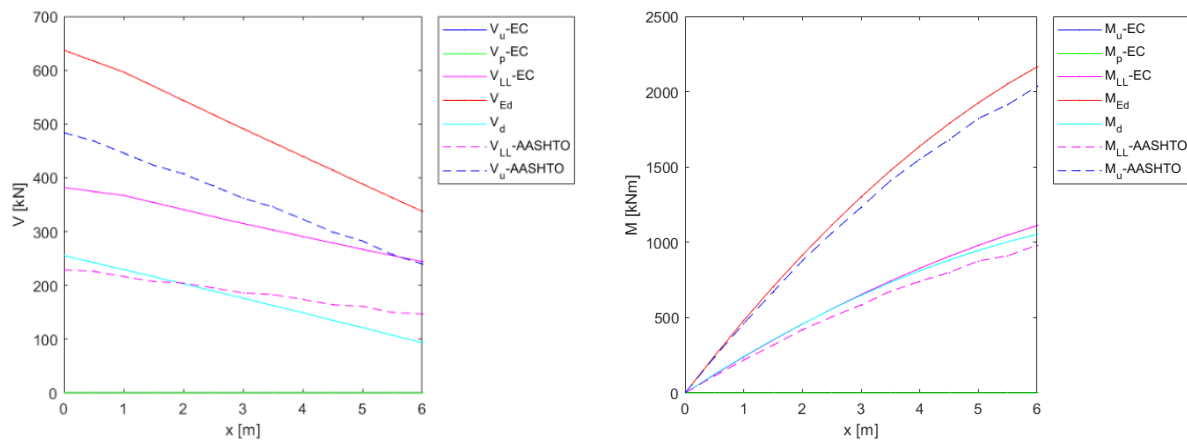

Figure 0-5 Ultimate and acting shear and bending moment for continuous bridge in region near end support, considering 0% of the prestressing force initially stated
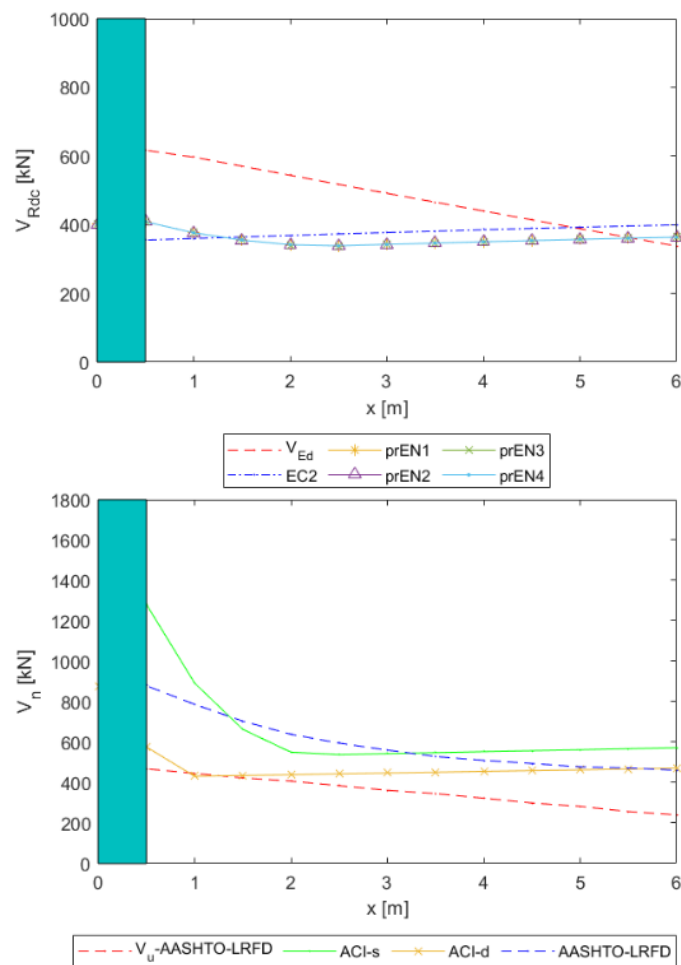

Figure 0-6 Shear resistance near end support of a continuous bridge deck according to design codes applied in Europe and America for the case applying 0% of the prestressing force initially stated

APPENDIX D

SHEAR DESIGN FOR CONTINUOUS DECK SLAB

Cross section dimensions

Total beam height $\qquad$ $h := 700\ mm$

Beam/flange width $\qquad$ $b := 1\ m$

Gross section properties

Distance centroidal axis from bottom $\qquad$ $y_t := \dfrac{h}{2} = 350\ mm$

Gross section area $\qquad$ $A_c := b \cdot h = 700000\ mm^2$

Momento of inertia $\qquad$ $I_{cs} := b \cdot \dfrac{h^3}{12} = 0.03\ m^4$

First moment of area above and about centroidal axis $\qquad$ $S := b \cdot \dfrac{h^2}{8} = 0.06\ m^3$ $\quad$ prEN1992

Area of the concrete on the flexural tension side of the member $\qquad$ $A_{ct} := \dfrac{A_c}{2} = 0.35\ m^2$ $\quad$ AASHTO

Steel longitudinal reinforcement B500

Steel yield strength $\qquad$ $f_y := 500\ MPa$

Steel young modulus $\qquad$ $E_s := 200 \cdot 10^3\ MPa$

Area of longitudinal reinf. $\qquad$ $A_s := 1340\ mm^2$

Distance compression face to centroid of rebars $\qquad$ $d_s := 0.64 \cdot m$

Long. compression reinf. $\qquad$ $A'_s := 1340\ mm^2$

Dist. to c.a. from compression rebar resultant $\qquad$ $d'_s := 0.64\ m$

Concrete C55/65

Mean concrete strength $\qquad$ $f_{ck} := 30\ MPa$

Specified compressive strength of concrete $\qquad$ $f'_c := f_{ck} + 1.6\ MPa = 31.6\ MPa$ ACI - AASHTO

Modulus of elasticity of concrete $\qquad$ $E_c := 4700 \cdot \sqrt{f'_c}\ MPa^{\frac{1}{2}} = 26.42\ GPa$

Maximum aggreate size $\qquad$ $a_g := 40\ mm$ $\quad$ AASHTO

Aggregate type factor $\qquad$ $\lambda := 1$ $\quad$ ALL

Smallest value of the upper sieve size D in an aggregate for the coarsest fraction of aggregates (EN 206) $\qquad$ $D_{lower} := 20\ mm$ $\quad$ prEN1992

Prestressing steel Y1860S7

Angle of tendon: $\qquad$ $\theta_p := 0.0575\ rad$

Nominal strand diameter $\qquad$ $\phi_p := 15.7\ mm$

Area of prestressed tendons $\qquad$ $A_p := 750\ mm^2$

Total area of prestressed tendons $\qquad$ $A_{ps} := A_p = 750\ mm^2$ $\quad$ AASHTO

Distance compression face to strands centroid $\qquad$ $d_p := h - 0.0992\ m = 600.8\ mm$

Modulus of Elasticity prestress $\qquad$ $E_p := 196\ GPa$

Eccentricity of tendons $\qquad$ $e_p := d_p - y_t = 250.8\ mm$

Partial factors for materials 4.3.3 (1) Concrete $\gamma_C := 1.5$

Reinforcing ans prestressing steel $\gamma_S := 1.15$

Shear and punching without shear reinforcement $\gamma_V := 1.4$

Nominal yield stress

$$f_{p.0.1k} := 1500 \ \textbf{MPa}$$

Especified tensile strength prestressing

$$\sigma_{pu} := \frac{f_{p.0.1k}}{0.9} = 1666.67 \ \textbf{MPa}$$

$$f_{pu} := \sigma_{pu} = 1666.667 \ \textbf{MPa} \quad \text{prEN1992}$$

Yield strength of prestressing steel

$$f_{py} := \frac{f_{p.0.1k}}{\gamma_S} = 1304.35 \ \textbf{MPa}$$

Initial stress after friction losses

$$\sigma_{p.0} := 1275 \ \textbf{MPa}$$

Effective prestress after all losses

$$\sigma_{p.inf} := \sigma_{p.0} \cdot 0.78 = 994.5 \ \textbf{MPa} \quad \text{EC2 - prEN1992}$$

Prestressing force after all losses

$$P_{p.inf} := \sigma_{p.inf} \cdot A_p = 745.88 \ \textbf{kN}$$

Effective stress in prestressed strand assumed after all losses (>0.5 fpu)

$$f_{pe} := \sigma_{p.inf} = 994.5 \ \textbf{MPa} \quad \text{ACI}$$

Load configuration

Critical section

$$x_r := 9.75 \ \textbf{m}$$

EC2 - prEN1992 General parameter

$$x := x_r$$

Distance between compression face and tensile resultant

$$d := \frac{d_s^2 \cdot A_s + d_p^2 \cdot A_p}{d_s \cdot A_s + d_p \cdot A_p} = 626.5 \ \textbf{mm}$$

Information from structural analysis

Prestress:

$$V_p := -55.41 \ \textbf{kN}$$

$$M_p := -334.18 \ \textbf{kN} \cdot \textbf{m}$$

Remember: When analyzing calculated negative moment, the calculated values change sign

Total Shear: $Vu := 398.29 \ \textbf{kN}$

Total Bending moment: $Mu := 513.64 \ \textbf{kN} \cdot \textbf{m}$

Design bending moment EC2: $M_{Ed} := Mu + M_p = 179.46 \ \textbf{kN} \cdot \textbf{m}$

Design shear EC2: $V_{Ed} := Vu + V_p = 342.88 \ \textbf{kN}$

Empirical formulation calibrated with experimental data through a statistical approach.
Shear strength of concrete given by:

Concrete properties according EN1992:

Design compressive and tensile strengths (3.1.6)

(3.15) Compressive strength definition
- Coefficient for long term effects and
unfavourable effects

$$\alpha_{cc} := 1$$

- **Design compressive strength**

$$f_{cd} := \alpha_{cc} \frac{f_{ck}}{\gamma_C} = 20 \ MPa$$

- Mean compressive strength

$$f_{cm} := f_{ck} + 8 \ MPa = 38 \ MPa$$

(3.16) Tensile strength definition
- Mean tensile strength

$$f_{ctm} := \mathbf{If}\left(f_{ck} \le 50 \ MPa , 0.3 \cdot f_{ck}^{\frac{2}{3}} \cdot MPa^{\frac{1}{3}} , 2.12 \cdot \ln\left(1 + \left(\frac{f_{cm}}{10 \ MPa}\right)\right) MPa \right) = 2.9 \ MPa$$

- Coefficient for long term effects and
unfavourable effects

$$\alpha_{ct} := 1$$

- **Design tensile strength**

$$f_{ctd} := \alpha_{ct} \frac{0.7 \cdot f_{ctm}}{\gamma_C} = 1.35 \ MPa$$

6.2.2 (1) Members not requiring design shear reinforcement. In cracked regions subjected to bending

Recommended values for coefficients and factors:

$$k := min\left(1 + \sqrt{\frac{200 \ mm}{d}} , 2\right) = 1.57$$

$$C_{Rd.c} := \frac{0.18}{\gamma_C} = 0.12$$

$$k_1 := 0.15$$

Reinf. ratio for longitudinal reinforcement

$$\rho_l := min\left(\frac{A_p + A_s}{b \cdot d} , 0.02\right) = 0.00334$$

Compressive stress in concrete from axial load or prestressing

$$\sigma_{cp} := min\left(\frac{P_{p.inf}}{A_c} , 0.2 \cdot f_{cd}\right) = 1.07 \ MPa$$

Minimum shear resistance

$$v_{min} := 0.035 \cdot k^{\frac{3}{2}} \cdot f_{ck}^{\frac{1}{2}} \cdot MPa^{\frac{1}{2}} = 0.38 \ MPa$$

$$V_{Rd.c.min} := \left(v_{min} + k_1 \cdot \sigma_{cp}\right) \cdot b \cdot d = 335.27 \ kN$$

Shear resistance

$$V_{Rd.c} := max\left(\left(C_{Rd.c} \cdot k \cdot \left(100 \cdot \rho_l \cdot f_{ck}\right)^{\frac{1}{3}} \cdot MPa^{\frac{2}{3}} + k_1 \cdot \sigma_{cp}\right) \cdot b \cdot d , V_{Rd.c.min}\right) = 353.69 \ kN$$

General parameters

8.2.1 (4)

- Ratio of tensile reinforcement in cross section

$$\rho_l := \frac{d_s \cdot A_s + d_p \cdot A_P}{b \cdot d^2} = 0.00333$$

- Size parameter describing failure zone roughness

$$d_{dg} := \text{if } f_{ck} > 60 \text{ } \textbf{MPa} \qquad\qquad = 36 \text{ } \textbf{mm}$$
$$\left\| 16 \text{ } \textbf{mm} + D_{lower} \cdot \left(\frac{60 \text{ } \textbf{MPa}}{f_{ck}}\right)^4 \right.$$
$$\text{else}$$
$$\left\| 16 \text{ } \textbf{mm} + D_{lower} \right.$$

(e) prEN 1992-1-1 D7

Parameters required:

Design compressive stregnth of concrete 5.1.6 (1)

Undisturbed compressive strength factor $\qquad \eta_{cc} := min\left(\left(\frac{40 \text{ } \textbf{MPa}}{f_{ck}}\right)^{\frac{1}{3}}, 1\right) = 1$

High sustained loads factor $\qquad\qquad k_{tc} := 0.85$

Design compressive strength $\qquad\qquad f_{cd} := \eta_{cc} \cdot k_{tc} \cdot \dfrac{f_{ck}}{\gamma_C} = 17 \text{ } \textbf{MPa}$

Tensile strength of strands Y1860 (Table 5.6)

$f_{pk} := f_{pu} = 1666.67 \text{ } \textbf{MPa}$
$f_{p0.1k} := f_{py} = 1304.35 \text{ } \textbf{MPa}$

Design tensile strength of strands $\qquad f_{pd} := \dfrac{f_{p0.1k}}{\gamma_S} = 1134.22 \text{ } \textbf{MPa}$

Steel reinf. B500

Design tensile strength $\qquad\qquad f_{yd} := \dfrac{f_y}{\gamma_S} = 434.78 \text{ } \textbf{MPa}$

8.2.1 (4) Minimum shear resistance:

Case of prestressed members without nonprestressed reinforcement, use difference between desing tensile strength and effective stress instead of yield strength

$$\tau_{Rdc.min} := \text{if } A_s = 0 \text{ } \textbf{cm}^2 \qquad\qquad = 0.4947 \text{ } \textbf{MPa}$$
$$\left\| \frac{11 \text{ } \textbf{MPa}}{\gamma_C} \cdot \sqrt{\frac{f_{ck}}{f_{pd} - \sigma_{p.inf}}} \cdot \frac{d_{dg}}{d} \right.$$
$$\text{else}$$
$$\left\| \frac{11 \text{ } \textbf{MPa}}{\gamma_V} \cdot \sqrt{\frac{f_{ck}}{f_{yd}}} \cdot \frac{d_{dg}}{d} \right.$$

8.2.2 Detailed verification for members not requiring design shear reinforcement

Detailed verification omitted for cross sections that are closer than d from the face of the support or from a significant concentrated load.

(3) **Effective shear span** with respect to the control section, (eq. 8.18). Conditional to replace dnom by factor av in regions with shear spans shorter than 4d.

$$a_{cs} := \max\left(\left|\frac{M_{Ed}}{V_{Ed}}\right|, d\right) = 626.5 \; \textbf{mm}$$

(4) **In presence of axial forces,** coefficient according to formula (eq. 8.20)

Factor as function of the applied effective prestressing load P_pinf. Note signs **(+) tensile, (-) compressive**

$$k_{vp} := \max\left(1 + \frac{-P_{p.inf}}{|V_{Ed}|} \cdot \frac{d}{3 \cdot a_{cs}}, 0.1\right) = 0.27$$

(3) Factor for short shear spans (eq. 8.18)

$$a_v := \begin{aligned} &\text{if } a_{cs} \leq 4 \cdot d \\ &\quad \left\| \min\left(\sqrt{\frac{a_{cs}}{4} \cdot d}, d\right) \right. \\ &\text{else} \\ &\quad \| d \end{aligned} \quad\quad = 313.25 \; \textbf{mm}$$

8.2.2 (2) Design value of shear stress resistance (eq. 8.16) and comparisson with lower boundary

$$\tau_{Rd.a} := \frac{0.66 \; \textbf{MPa}}{\gamma_V} \cdot \left(100 \cdot \rho_l \cdot \frac{f_{ck}}{\textbf{MPa}} \cdot \frac{d_{dg}}{a_v \cdot k_{vp}}\right)^{\frac{1}{3}} = 0.76 \; \textbf{MPa}$$

$$\tau_{Rd.c1} := \max\left(\tau_{Rd.a}, \tau_{Rdc.min}\right) = 0.76 \; \textbf{MPa}$$

Shear force capacity, approach ALTERNATIVE 1

$$V_{Rd.prEN1} := \tau_{Rd.c1} \cdot b \cdot 0.9 \cdot d = 428.2 \; \textbf{kN}$$

8.2.2 (5) Alternative approach considering the effect of compressive normal forces

Factor (eq. 8.22)

$$k_1 := \min\left(\frac{1.4}{\gamma_V} \cdot \left(0.07 + \frac{e_p}{4 \cdot d}\right), 0.15 \cdot \frac{1.4}{\gamma_V}\right) = 0.15$$

Axial stress

$$\sigma_{cp} := \min\left(\frac{-P_{p.inf}}{A_c}, 0.2 \cdot f_{cd}\right) = -1.07 \; \textbf{MPa}$$

For alternative approach (a), as the prestressing force is considered in the second term, the values of factors are recalculated without considering axial forces

$$\tau_{Rd.c2} := \max\left[\frac{0.66\ \boldsymbol{MPa}}{\gamma_V}\cdot\left(100\cdot\rho_l\cdot\frac{f_{ck}}{\boldsymbol{MPa}}\cdot\frac{d_{dg}}{a_v}\right)^{\frac{1}{3}} - k_1\cdot\sigma_{cp}, \tau_{Rdc.min}\right] = 0.65\ \boldsymbol{MPa}$$

Shear force capacity, approach ALTERNATIVE 2

$$V_{Rd.prEN2} := \tau_{Rd.c2}\cdot b\cdot 0.9\cdot d = 368.54\ \boldsymbol{kN}$$

ALTERNATIVE 3 (Fernandez)

Use of shear span conditionals (Eq. 8.18 and Eq. 8.19) expressions as stated for Alternative 1

Initial shear stress (without normal loads consideration)
$$\tau_{Rdc.0} := \frac{0.66\ \boldsymbol{MPa}}{\gamma_V}\cdot\left(100\cdot\rho_l\cdot\frac{f_{ck}}{\boldsymbol{MPa}}\cdot\frac{d_{dg}}{a_v}\right)^{\frac{1}{3}} = 0.49\ \boldsymbol{MPa}$$

Maximum shear stress
$$\tau_{max} := 0.33\cdot\frac{\sqrt{f_{ck}}\cdot\boldsymbol{MPa}^{0.5}}{\gamma_V} = 1.29\ \boldsymbol{MPa}$$

Factor accounting for normal loads effect
$$k_1 := \min\left(0.67\cdot\frac{e_p+\frac{d}{3}}{a_{cs}}, 0.15\right) = 0.15$$

Estimated shear stress:
$$\tau_{Rd.c3} := \max\left(\min\left(\tau_{Rdc.0} - k_1\cdot\sigma_{cp}, \tau_{max}\right), \tau_{Rdc.min}\right) = 0.65\ \boldsymbol{MPa}$$

$$V_{Rd.prEN3} := \tau_{Rd.c3}\cdot b\cdot 0.9\cdot d = 368.54\ \boldsymbol{kN}$$

Yuguang Proposal

Use of shear span conditionals (Eq. 8.18 and Eq. 8.19) expressions as stated for Alternative 1

Maximum shear stress
$$\tau_{Rdc.max} := 2.15\cdot\tau_{Rdc.0} = 1.06\ \boldsymbol{MPa}$$

Estimated shear stress:
$$\tau_{Rd.c4} := \max\left(\min\left(\tau_{Rdc.0} - 0.17\cdot\frac{d}{a_{cs}}\cdot\sigma_{cp}, \tau_{Rdc.max}\right), \tau_{Rdc.min}\right) = 0.67\ \boldsymbol{MPa}$$

$$V_{Rd.prEN4} := \tau_{Rd.c4}\cdot b\cdot 0.9\cdot d = 380.56\ \boldsymbol{kN}$$

Shear capacity using (a) ACI 318-19 Simplified, (b) ACI 318-19 Detailed

Distance between compression face and strands centroid (22.5.2.1)
$$d := \max\left(0.8\cdot h, d_p\right) = 600.8\ \boldsymbol{mm}$$

Information from structural analysis
Shear and moment due to UNFACTORED DEAD LOAD

Shear function: $Vd := 83.64\ \boldsymbol{kN}$

Bending moment function: $Md := 107.86\ \boldsymbol{kN\cdot m}$

Remember: When analyzing calculated negative moment, the calculated values change sign

Shear and moment due to EXTERNALLY APPLIED FACTORED LOADS

$$Vi := Vu - Vd = 314.65 \; kN \qquad Mmax := Mu - Md = 405.78 \; kN \cdot m$$

Prestress force Analysis

Effective stress in prestressed reinforcement (22.5.7.2)

$$f_{se} := f_{pe} = 994.5 \; MPa$$

Effective prestressing force applied

$$P_{p.se} := A_p \cdot f_{se}$$

Lower bound for reduced effective prestressing force (Area of stirrups = 0) (22.5.6.2)

$$P_{p.c} := 0.4 \cdot (A_p \cdot f_{pu}) = 500 \; kN$$

$$appr := \text{if } P_{p.se} \geq P_{p.c} \qquad = \text{``Good''}$$
$$\qquad \| \text{``Good''}$$
$$\text{else}$$
$$\qquad \| \text{``Below lower bound''}$$

The values for low prestress shall be verified according 22.5.7 (Vc for regions of reduced prestress force)

The simplified method within this range is limited by Vcw calculated using the reduced effective prestress force (Done at the end of the calculations)

(a) ACI 318-19. Approximate method for calculating Vc (22.5.6.2)

Minimum concrete shear resistance

$$V_{c.min} := 0.17 \cdot \lambda \cdot \sqrt{f'_c} \cdot MPa^{0.5} \cdot b \cdot d = 574.15 \; kN$$

Concrete Shear Resistance:

Case a:
$$V_{c.a} := \left(0.05 \cdot \lambda \cdot \sqrt{\frac{f'_c}{MPa}} + 4.8 \cdot \frac{|Vu| \cdot d_p}{Mu} \right) MPa \cdot b \cdot d = 1512.38 \; kN$$

Case b:
$$V_{c.b} := \left(0.05 \cdot \lambda \cdot \sqrt{\frac{f'_c}{MPa}} + 4.8 \right) MPa \cdot b \cdot d = 3052.71 \; kN$$

Case c:
$$V_{c.c} := \left(0.42 \cdot \lambda \cdot \sqrt{\frac{f'_c}{MPa}} \right) MPa \cdot b \cdot d = 1418.48 \; kN$$

Shear Resistance $V_{c.ACI.s} := \max \left(\min \left(V_{c.a}, V_{c.b}, V_{c.c} \right), V_{c.min} \right) = 1418.48 \; kN$

22.5.7.3 (c) within transfer length in region of reduced prestressed force the upper limit will be Vcw calculated using fpx. Presented in the last figure of this calculation sheet

(b) ACI 318-19. Detailed method for calculating Vc (22.5.6.3)

Cracking moment: Sum of all stress components in the bottom fiber and set them equal to the tensile strength of the concrete

Assuming tension positive, we have the following expression

Bottom fiber stress:
$$\frac{-P_p}{A} - \frac{P_p \cdot e_p}{s_b} + \frac{M_d}{s_b} + \frac{M_{cre}}{s_b} = 0.33 \cdot \lambda \sqrt{f'_c}$$

Section modulus for our section
$$s_b := \frac{I_{cs}}{y_t} = (8.17 \cdot 10^{-2}) \ m^3$$

Cracking moment

Prestress compression at bottom extreme fiber

Stresses at tension extreme fiber by different prestressed tendons

$$f_{pe.A} := \frac{P_{p.se}}{A_c} + \frac{P_{p.se} \cdot e_p}{s_b} = 3.36 \ MPa$$

Cracking moment due to external load (22.5.6.3.1d)

$$M_{cre} := \frac{I_{cs}}{y_t} \cdot \left(0.5 \ \lambda \cdot \sqrt{\frac{f'_c}{MPa}} \cdot MPa + f_{pe.A} - \frac{Md}{s_b} \right) = 395.76 \ kN \cdot m$$

1. Flexure-shear strength (22.5.6.3.1)

(22.5.6.3.1a)
$$V_{ci.a} := 0.05 \cdot \lambda \cdot \sqrt{\frac{f'_c}{MPa}} \cdot MPa \cdot b \cdot d + |Vd| + \frac{|Vi| \cdot M_{cre}}{Mmax} = 559.39 \ kN$$

(22.5.6.3.1b and c)
$$V_{ci.b} := \text{if } appr = \text{"Good"} \qquad\qquad = 574.15 \ kN$$
$$\left| \lambda \cdot 0.17 \cdot \sqrt{\frac{f'_c}{MPa}} \cdot MPa \cdot b \cdot d \right.$$
$$\text{else}$$
$$\left| \lambda \cdot 0.14 \cdot \sqrt{\frac{f'_c}{MPa}} \cdot MPa \cdot b \cdot d \right.$$

$$V_{ci} := \max \left(V_{ci.a}, V_{ci.b} \right) = 574.15 \ kN$$

2. Compressive stress in the concrete after allowance for all prestress losses, at centroid of cross section resisting externally applied loads or at junction of web and flange where the centroid lies within the flange. (**compression is positive**).

Compressive stress at centroidal axis
$$f_{pe} := \frac{P_{p.se}}{A_c} = 1.07 \ MPa$$

Vertical component of prestress load
$$V_p := P_{p.se} \cdot \sin(\theta_p) = 42.86 \ kN$$

Web-shear capacity (22.5.6.3.2)
$$V_{cw} := \left(0.29 \cdot \lambda \cdot \sqrt{\frac{f'_c}{MPa}} \cdot MPa + 0.3 \cdot f_{pe} \right) \cdot b \cdot d + V_p = 1214.34 \ kN$$

3. Concrete shear component as the minimum of the web-shear and flexure-shear capacity (22.5.6.3)

Concrete $\qquad V_{c.ACI.d} := min\ (V_{cw}, V_{ci}) = 574.15\ \textbf{kN}$

22.5.7.3 (c) upper limit for simplified method in regions of reduced prestress force

$$V_{c.ACI.s} := \text{if } appr = \text{"Good"} \qquad = 1418.48\ \textbf{kN}$$
$$\left\| V_{c.ACI.s} \right.$$
$$\text{else}$$
$$\left\| min\ (V_{c.ACI.s}, V_{cw}) \right.$$

(c) AASHTO LRFD - General procedure (units: mm, MPa)

General parameters

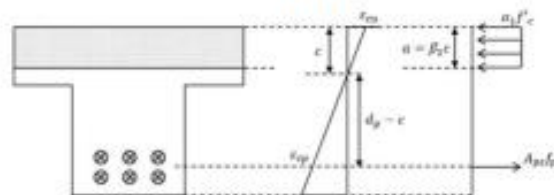### Stress block factors (5.6.2.2)

$$\alpha_1 := \textbf{if}\left(f'_c < 69\ \textbf{MPa}, 0.85, 0.85 - 0.02 \cdot \frac{f'_c - 69\ \textbf{MPa}}{7\ \textbf{MPa}}\right) = 0.85$$

$$\beta_1 := \textbf{if}\left(f'_c < 28\ \textbf{MPa}, 0.85, 0.85 - 0.02 \cdot \frac{f'_c - 28\ \textbf{MPa}}{7\ \textbf{MPa}}\right) = 0.84$$

Prestressing influence (5.6.3.1.1)

STRAIN COMPATIBILITY APPROACH

Concrete ultimate strain $\qquad \varepsilon_{cu} := \dfrac{3}{1000} = 3 \cdot 10^{-3}$

1) Locked-in Straind at time of Ultimate Loading:

Ultimate strain prestressing steel $\qquad \varepsilon_{pu} := \dfrac{35}{1000}$

Yield strain prestressing steel $\qquad \varepsilon_{py} := \dfrac{f_{py}}{E_p} = 6.65 \cdot 10^{-3}$

Ultimate strain reinf. steel $\qquad \varepsilon_{su} := \dfrac{45}{1000}$

Yield strain reinf. steel $\qquad \varepsilon_{sy} := \dfrac{f_y}{E_s} = 2.5 \cdot 10^{-3}$

Effective prestress $\qquad f_{pe} = 994.5\ \textbf{MPa}$

Effective strain $\qquad$ $\varepsilon_{pe} := \dfrac{f_{pe}}{E_p} = 5.07 \cdot 10^{-3}$

Effective prestress force $\qquad$ $P_e := f_{pe} \cdot A_{ps} = 745.88 \ \textbf{kN}$

Decompression strain $\qquad$ $\varepsilon_d := \dfrac{P_e}{A_c \cdot E_c} + \dfrac{P_e \cdot e_p^{\ 2}}{I_{cs} \cdot E_c} = 1.02 \cdot 10^{-4}$

Tension:

| **Bottom prestressing tendon** | **Nonprestressed tension steel** |

$\Delta\varepsilon_{bot}(ca) := \dfrac{d_p - ca}{ca} \cdot \varepsilon_{cu}$ $\qquad$ $\varepsilon_s(ca) := \dfrac{d_s - ca}{ca} \cdot \varepsilon_{cu}$

$\varepsilon_{ps}(ca) := \varepsilon_d + \varepsilon_{pe} + \Delta\varepsilon_{bot}(ca)$ $\qquad$ $f_{sy}(ca) := \text{if } \varepsilon_s(ca) < \varepsilon_{sy}$
$\qquad\qquad\qquad\qquad\qquad\qquad\qquad\qquad \left\| E_s \cdot \varepsilon_s(ca) \right.$

$f_{ps}(ca) := \text{if } \varepsilon_{ps}(ca) < \varepsilon_{py}$ $\qquad\qquad\qquad$ else
$\qquad \left\| E_p \cdot \varepsilon_{ps}(ca) \right.$ $\qquad\qquad\qquad\qquad \left\| f_y \right.$
$\qquad$ else
$\qquad \left\| \dfrac{f_{pu} - f_{py}}{\varepsilon_{pu} - \varepsilon_{py}} \cdot (\varepsilon_{ps}(ca) - \varepsilon_{py}) + f_{py} \right.$ $\qquad$ $F_{sy}(ca) := A_s \cdot f_{sy}(ca)$

$F_p(ca) := A_p \cdot f_{ps}(ca)$

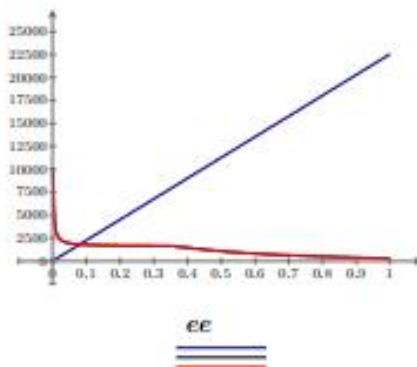## TOTAL TENSION RESULTANT $\qquad F_T(ca) := F_p(ca) + F_{sy}(ca)$

Compression:

Concrete compressive force resultant

$\alpha_1 = 0.85 \qquad \beta_1 = 0.84$
$a(ca) := \beta_1 \cdot ca$
$F_c(ca) := \alpha_1 \cdot f'_c \cdot a(ca) \cdot b$
$X_{na}(ca) := \dfrac{a(ca)}{2}$

TOTAL COMPRESIVE RESULTANT $F_{COM}(ca) := F_c(ca)$

$\dfrac{F_{COM}(ee \cdot m) \ (\textbf{kN})}{}$

$\dfrac{F_T(ee \cdot m) \ (\textbf{kN})}{}$

$F_T(ee \cdot m) \ (\textbf{kN})$

ee

Guess Values $\qquad ca := 140 \ \textbf{mm}$

Constraints $\qquad F_T(ca) = F_{COM}(ca)$

Solver $\qquad ca := \text{find}(ca) = 80.67 \ \textbf{mm}$

Verification if strain is less than ultimate strains for steel

$$\text{if } \varepsilon_{ps}(ca) > \varepsilon_{pu} \vee |\varepsilon_s(ca)| > \varepsilon_{su} \quad = \text{"OK"}$$
$$\quad \text{"Greater than ltimate strain!"}$$
$$\text{else}$$
$$\quad \text{"OK"}$$

Equilibrium: $\quad F_T(ca) = 1819.52 \ \textbf{kN}$ $\qquad\qquad F_{COM}(ca) = 1819.52 \ \textbf{kN}$

Nominal flexural resistance (5.6.3.2.2-1)

Moment by prestressed tendons: $\qquad\qquad f_{ps}(ca) = 1532.69 \ \textbf{MPa}$

$$M_{n.p} := A_p \cdot f_{ps}(ca) \cdot (d_p - X_{na}(ca)) = 651.7 \ \textbf{kN} \cdot \textbf{m}$$

Nominal flexural resistance

$$M_n := M_{n.p} + A_s \cdot f_{sy}(ca) \cdot (d_s - X_{na}(ca)) = 1057.8 \ \textbf{kN} \cdot \textbf{m}$$

Effective shear depth (5.7.2.8)

(C5.7.2.8-1)
$$d_v := \frac{M_n}{A_s \cdot f_{sy}(ca) + A_{ps} \cdot f_{ps}(ca)} = 581.36 \ \textbf{mm}$$
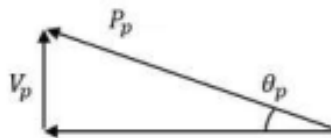
(5.7.2.8-2)
$$d_e := \frac{A_{ps} \cdot f_{ps}(ca) \cdot d_p + A_s \cdot f_{sy}(ca) \cdot d_s}{A_{ps} \cdot f_{ps}(ca) + A_s \cdot f_{sy}(ca)} = 615.23 \ \textbf{mm}$$

$$d_v := \max(d_v, 0.9 \cdot d_e, 0.72 \cdot h) = 581.36 \ \textbf{mm}$$

Vertical component of prestressing (5.9.4.3.2): AASHTO uses fps to find prestressing force, different from ACI that uses effective prestress fse

Vertical prestress force component (5.7.3.3)

Angle possitive if prestressed vertical resultant resist shear

$$V_p(ca) := A_{ps} \cdot f_{ps}(ca) \cdot \sin(\theta_p)$$

If it doesn't contribute to resistance then it's negative

Modulus of elasticity of prestressing tendons multiplied by the locked-in difference in strain between the prestressing tendons and surrounding concrete **(5.7.3.4.2)**

Assumed by AASHTO for post- and pre-tensioned members

$$f_{po} := \left(f_{pe} + \frac{P_e}{A_c} \cdot \frac{E_p}{E_c}\right) = 1002.4 \ \textbf{MPa}$$

fpo --> Should increase linearly within transfer length from zero at the location where bond between strands and concrete starts to its full value at the end of the transfer length

Factored moment at the section (5.7.3.4.2)

$$Mu := \mathbf{if}\left(Mu \geq \left\|Vu\right| - V_p(ca)\right| \cdot d_v, Mu, \left\|Vu\right| - V_p\right| \cdot d_v\right) = 513.64 \; \mathbf{kN \cdot m}$$

Axial load applied (not prestress, as it's not preload) (5.7.3.4.2)

$N_u := 0 \; \mathbf{kN}$ (+) tensile, (-) compressive

Net longitudinal tensile strain in the section at the centroid of tension reinforcement
(5.7.3.4.2-4)

Tensile strain $\varepsilon_{s.t} := \min\left(\dfrac{\dfrac{\left|Mu\right|}{d_v} + 0.5 \cdot N_u + \left\|Vu\right| - V_p(ca)\right| - A_{ps} \cdot f_{po}}{E_s \cdot A_s + E_p \cdot A_{ps}}, 6.0 \cdot 10^{-3}\right) = 1.12 \cdot 10^{-3}$

If compression, modifiying the denominator for the tensile strain

$$\varepsilon_{s.c} := \max\left(-0.4 \cdot 10^{-3}, \dfrac{\dfrac{\left|Mu\right|}{d_v} + 0.5 \cdot N_u + \left\|Vu\right| - V_p(ca)\right| - A_{ps} \cdot f_{po}}{E_s \cdot A_s + E_p \cdot A_{ps} + E_c \cdot A_{ct}}\right) = 4.8 \cdot 10^{-5}$$

Verify if the main assumption that tensile strain is governing, otherwise use modified
expression

$\varepsilon_s := \mathbf{if} \; \varepsilon_{s.t} < 0 = 1.12 \cdot 10^{-3}$
$\qquad \left\| \varepsilon_{s.c} \right.$
$\quad$ else
$\qquad \left\| \varepsilon_{s.t} \right.$

Crack spacing parameter
(5.7.3.4.2-7)
$\qquad s_{xe} := \max\left(300, \min\left(d_v \cdot \dfrac{35}{a_g + 16 \; \mathbf{mm}}, 2000\right)\right) = 363.35$

Concrete effectiveness factor
(5.7.3.4.2-2)
$\qquad \beta := \dfrac{4.8}{1 + 750 \cdot \varepsilon_s} \cdot \dfrac{1300}{1000 + s_{xe}} = 2.49$

Concrete shear component
(5.7.3.3-3)
$\qquad V_{c.AA} := 0.083 \cdot \beta \cdot \sqrt{\dfrac{f'_c}{\mathbf{MPa}}} \cdot \mathbf{MPa} \cdot b \cdot d_v = 675.3 \; \mathbf{kN}$

Total shear resistance (5.7.3.3-1)
$V_{c.AASHTO}(ca) := \min\left(V_{c.AA} + V_p(ca), 0.25 \cdot f'_c \cdot b \cdot d_v + V_p(ca)\right)$ $V_{c.AASHTO}(ca) = 741.36 \; \mathbf{kN}$
$\qquad\qquad\qquad\qquad\qquad\qquad\qquad\qquad\qquad\qquad\qquad\qquad\qquad V_p(ca) = 66.06 \; \mathbf{kN}$

Second value ensures that we don't have crushing of the concrete as dominant failure
before shear

Design values applying safety factors for ACI and AASHTO

$Vu = 398.29$ **kN** Ultimate shear force

$0.75\ V_{c.ACI.a} = 1063.86$ **kN** $UC_{ACI.a} := \dfrac{Vu}{0.75\ V_{c.ACI.a}} = 0.37$ ACI318-19 approximate method

$0.75\ V_{c.ACI.d} = 430.61$ **kN** $UC_{ACI.d} := \dfrac{Vu}{0.75\ V_{c.ACI.d}} = 0.92$ ACI318-19 detailed method

$0.9\ V_{c.AASHTO}(ca) = 667.23$ **kN** $UC_{AASHTO} := \dfrac{Vu}{0.9\ V_{c.AASHTO}(ca)} = 0.6$ AASHTO-LRFD

Design values obtained for EC2 and prEN1992

$V_{Ed} = 342.88$ **kN** Acting shear force

$V_{Rd.c} = 353.69$ **kN** $UC_{EC2} := \dfrac{V_{Ed}}{V_{Rd.c}} = 0.97$ EN1991-1-1 (EC2)

$V_{Rd.prEN1} = 428.2$ **kN** $UC_{prEN1} := \dfrac{V_{Ed}}{V_{Rd.prEN1}} = 0.8$ Alternative 1 for prEN1992

$V_{Rd.prEN2} = 368.54$ **kN** $UC_{prEN2} := \dfrac{V_{Ed}}{V_{Rd.prEN2}} = 0.93$ Alternative 2 for prEN1992

$V_{Rd.prEN3} = 368.54$ **kN** $UC_{prEN3} := \dfrac{V_{Ed}}{V_{Rd.prEN3}} = 0.93$ Alternative 3 for prEN1992

$V_{Rd.prEN4} = 380.56$ **kN** $UC_{prEN4} := \dfrac{V_{Ed}}{V_{Rd.prEN4}} = 0.9$ Alternative 4 for prEN1992

APPENDIX E

Load distribution for traffic loads:

Notional lanes (EC2-2 4.2.3):

Carriageway width

$$w := 30.55 \ \boldsymbol{m}$$

Number and width of notional lanes:

$$n_l := \text{round}\left(\frac{w}{3 \ \boldsymbol{m}}\right) = 10$$

Lane width

$$w_l := 3 \ \boldsymbol{m}$$

Remain area width

$$w_r := w - 3 \cdot w_l = 21.55 \ \boldsymbol{m}$$

Vertical loads - Load Model 1 (EC 2-2 4.3.2):

A double-axle load (Tandem System: TS) is applied in each traffic line. At the same time an uniformly distributed load (UDL System). Assuming the following factors

$$Q_k := \begin{bmatrix} 300 \\ 200 \\ 100 \\ 0 \end{bmatrix} \boldsymbol{kN} \quad \alpha_Q := \begin{bmatrix} 1 \\ 1 \\ 1 \\ 1 \end{bmatrix} \quad q_k := \begin{bmatrix} 9 \\ 2.5 \\ 2.5 \\ 2.5 \end{bmatrix} \frac{\boldsymbol{kN}}{\boldsymbol{m^2}} \quad \alpha_q := \begin{bmatrix} 1.15 \\ 1.4 \\ 1.4 \\ 1.4 \end{bmatrix}$$
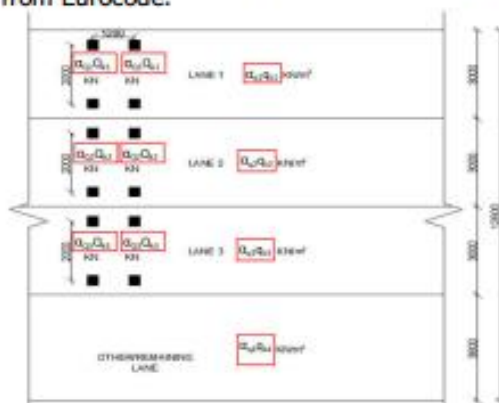
$$\alpha_{Q_1} \cdot Q_{k_1} = 300 \ \boldsymbol{kN} \qquad \alpha_{q_1} \cdot q_{k_1} = 10.35 \ \frac{kN}{m^2}$$

$$\alpha_{Q_2} \cdot Q_{k_2} = 200 \ \boldsymbol{kN} \qquad \alpha_{q_2} \cdot q_{k_2} = 3.5 \ \frac{kN}{m^2}$$

$$\alpha_{Q_3} \cdot Q_{k_3} = 100 \ \boldsymbol{kN} \qquad \alpha_{q_3} \cdot q_{k_3} = 3.5 \ \frac{kN}{m^2}$$

$$\alpha_{Q_4} \cdot Q_{k_4} = 0 \ \boldsymbol{N} \qquad \alpha_{q_4} \cdot q_{k_4} = 3.5 \ \frac{kN}{m^2}$$

The following figure shows the load distribution obtained according to the Load Model 1 from Eurocode.
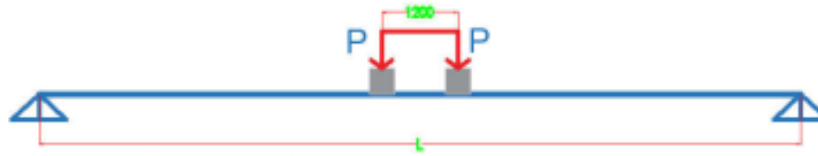

Now, a conservative approach is going to be developed to obtain the load carried by one beam considering the total load distributed over an effective width as following:

Load on one beam due to Double-axle concentrated loads:

Longitudinal Direction:

The maximum bending moment in longitudinal direction with the following configuration is:

Span: $L_s := 21.4\ m$

$$M_{P1} := P \cdot \left(\frac{L_s}{2} - \frac{1.2\ m}{2}\right) \rightarrow P \cdot (-0.6 \cdot m + 10.7 \cdot m)$$

Equivalent UDL can be estimated with:

$$8 \cdot \frac{M_{F1}}{L_s^2} \rightarrow \frac{0.17643462311118875011 \cdot P}{m} \qquad q_{eq.a}(P) := 8 \cdot \frac{10.1\ m \cdot P}{L_s^2} \rightarrow \frac{0.1764346231111887501}{m}$$
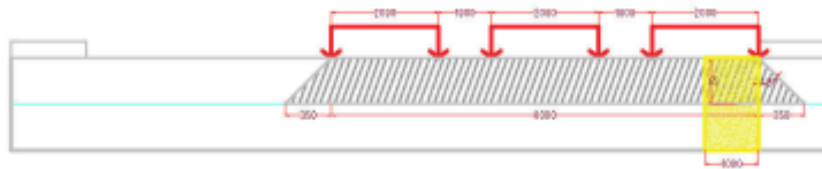
Transversal Direction:

To obtain the equivalent force per beam that we need to calculate the equivalent UDL for axle load we follow this procedure:

The model is splited in three parts assigning the same load to the different lanes.

Tendon load: $\qquad F_w := \alpha_{Q_s} \cdot Q_{k_s} \cdot 0.5 = 50\ kN$

Height of deck: $\qquad h := 0.8\ m$

Unitary width for deck slab: $\qquad b_1 := 1\ m$

Puntual loads case 1: $\qquad F_1 := 6 \cdot F_w = 300\ kN$

Effective width case 1: $\qquad w_{eff_1} := 0.35\ m \cdot 2 + 8\ m = 8.7\ m$

Equivalent load per meter: $\qquad F_{eq_1} := q_{eq.a}\left(F_1\right) \cdot \frac{b_1}{w_{eff_1}} = 6.084\ \frac{kN}{m}$

Puntual loads case 2: $\qquad F_2 := 4 \cdot F_w = 200\ kN$

Effective width case 2: $\qquad w_{eff_2} := 0.35\ m \cdot 2 + 5\ m = 5.7\ m$

Equivalent load per meter: $\qquad F_{eq_2} := q_{eq.a}\left(F_2\right) \cdot \frac{b_1}{w_{eff_2}} = 6.191\ \frac{kN}{m}$

Puntual loads case 3:	$F_3 := 2 \cdot F_w = 100 \ \mathbf{kN}$
Effective width case 3:	$w_{eff_3} := 0.35 \ \mathbf{m} \cdot 2 + 2 \ \mathbf{m} = 2700 \ \mathbf{mm}$
Equivalent load per meter:	$F_{eq_3} := q_{eq.a}(F_3) \cdot \dfrac{b_1}{w_{eff_3}} = 6.535 \ \dfrac{\mathbf{kN}}{\mathbf{m}}$
Maximum load on one beam from axle load:	$q_{axle} := \displaystyle\sum_{i=1}^{3} F_{eq_i} = 18.809 \ \dfrac{\mathbf{kN}}{\mathbf{m}}$

Load on one beam due to UDL:

With load case 1 of Eurocode we have the following configuration for UDL:

This is going to be divided in two cases that are going to be superimposed later in order to make simpler the calculation with effective widths:

UDL over whole deck:	$q_r := \alpha_{q_3} \cdot q_{k_3} = 3.5 \ \dfrac{\mathbf{kN}}{\mathbf{m}^2}$
Effective width:	$w_r := 0.35 \ \mathbf{m} \cdot 2 + w = 31.25 \ \mathbf{m}$
Equivalen UDL per beam:	$UDL_r := q_r \cdot b_1 \cdot \dfrac{w}{w_r} = 3.422 \ \dfrac{\mathbf{kN}}{\mathbf{m}}$
UDL over slow lane:	$q_s := \alpha_{q_1} \cdot q_{k_1} - \alpha_{q_3} \cdot q_{k_3} = 6.85 \ \dfrac{\mathbf{kN}}{\mathbf{m}^2}$
Effective width:	$w_s := 0.35 \ \mathbf{m} \cdot 2 + 3 \ \mathbf{m} = 3.7 \ \mathbf{m}$
Equivalen UDL per beam:	$UDL_s := q_s \cdot \dfrac{w_l}{w_s} \cdot b_1 = 5.554 \ \dfrac{\mathbf{kN}}{\mathbf{m}}$
Maximum load on one beam from UDL:	$q_{UDL} := UDL_r + UDL_s = 8.976 \ \dfrac{\mathbf{kN}}{\mathbf{m}}$
MAX. TOTAL TRAFFIC LIVE LOAD ON ONE BEAM :	$q_{Lt} := q_{axle} + q_{UDL} = 27.785 \ \dfrac{\mathbf{kN}}{\mathbf{m}}$

Equivalent Strip Width for Slab-Type Bridges (4.6.2.3)

Table 4.6.2.3-1—Typical Schematic Cross-section

Supporting Components	Type of Deck	Typical Cross-Section
Cast-in-place Concrete Slab or Voided Slab	Monolithic	(a)

Span: $L := 21.4\ m = 70.21\ ft$

Width: $w_b := 30.55\ m = 100.23\ ft$

Number of Design Lanes (3.6.1.1): $\dfrac{w_b}{12\ ft} = 8.352$ $\qquad N_L := 8$

Modifie span length: $L_1 := min\,(L,\,60\ ft) = 60\ ft$

Modified edge-to-edge width of bridge taken $\qquad W_1 := min\,(w_b,\,30\ ft) = 9.144\ m$

Physical edge-to-edge width of bridge $\qquad W := w_b = 100.23\ ft$

Equivalent width (in) of longitudinal strips per lane for shear and moment width one lane, i,e,, two lines of wheels, loaded:

$$E_{i1} := \left(10 + 5 \cdot \sqrt{\dfrac{L_1}{ft} \cdot \dfrac{W_1}{ft}}\right) \cdot in = 5.642\ m$$

Equivalent width (in) of longitudinal strips per lane for shear and moment width more than one lane loaded:

Modified edge-to-edge width of bridge taken $\qquad W_1 := min\,(w_b,\,60\ ft) = 18.288\ m$

$$E_{i2} := \left(min\left(84 + 1.44 \cdot \sqrt{\dfrac{L_1}{ft} \cdot \dfrac{W_1}{ft}},\ 12 \cdot \dfrac{\dfrac{W}{ft}}{N_L}\right)\right) \cdot in = 3.819\ m$$

Equivalent width of interior strip for live load

$$E_i := min\,(E_{i1},\,E_{i2}) = 3.819\ m$$

Live load analysis:

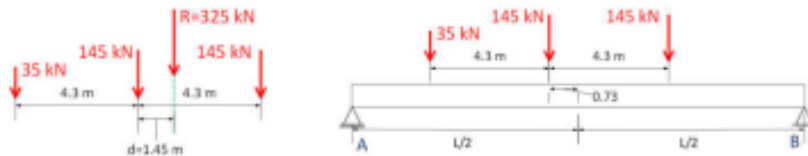Impact factor for all other limit states $\qquad IM := 1.33$

Distributed Lane Load

Design lane load: $w_{ln} := 9.3 \ \dfrac{kN}{m}$

Maximum bending moment: $M_{ln} := w_{ln} \cdot \dfrac{L^2}{8} = 532.379 \ kN \cdot m$

Maximum shear force: $V_{ln} := w_{ln} \cdot \dfrac{L}{2} = 99.51 \ kN$

Design truck HL-93:

Finding the maximum bending moment on a simple supported beam

$$R_B := \dfrac{145 \ kN \cdot \left(\left(\dfrac{L}{2} - 0.73 \ m\right) + \left(\dfrac{L}{2} + 3.57 \ m\right)\right) + 35 \ kN \cdot \left(\dfrac{L}{2} - 5.03 \ m\right)}{L} = 173.516 \ kN$$

$$R_A := 145 \ kN \cdot 2 + 35 \ kN - R_B = 151.484 \ kN$$

Maximum bending on intermediate 145kN point load

$$M_{HL93} := R_B \cdot \left(\dfrac{L}{2} + 0.73 \ m\right) - 145 \ kN \cdot 4.3 \ m = 1359.79 \ kN \cdot m$$

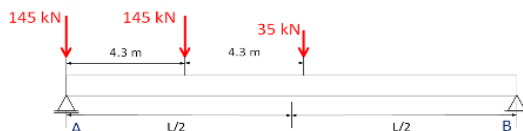**Total maximum bending moment:** $M_{LL.IM} := \dfrac{M_{HL93} \cdot IM + M_{ln}}{E_i} = 613.002 \ kN \cdot \dfrac{m}{m}$

Equivalent distributed load: $q_{ss.m} := M_{LL.IM} \cdot \dfrac{8}{L^2} = 10.708 \ \dfrac{1}{m} \cdot \dfrac{kN}{m}$
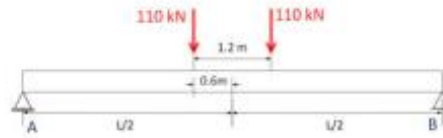
Maximum shear on support. 145kN axle locate on support

$$V_{A.max} := \dfrac{35 \ kN \cdot (L - 4.3 \ m \cdot 2) + 145 \ kN \cdot ((L - 4.3 \ m) + (L))}{L} = 281.799 \ kN$$

Total maximum shear force: $V_{LL} := \dfrac{V_{A.max} \cdot IM + V_{ln}}{E_i} = 124.204 \ \dfrac{kN}{m}$

Equivalent distributed load: $q_{ss.v} := V_{LL} \cdot \dfrac{2}{L} = 11.608 \ \dfrac{1}{m} \cdot \dfrac{kN}{m}$

Design Tandem:

$$R_B := \frac{220 \; kN \cdot \dfrac{L}{2}}{L} = 110 \; kN$$

$$R_A := 110 \; kN \cdot 2 - R_B = 110 \; kN$$

Maximum bending moment at midspan:

$$M_{TD} := R_A \cdot \frac{L}{2} - 110 \; kN \cdot 0.6 \; m = 1111 \; kN \cdot m$$

Total maximum bending moment:
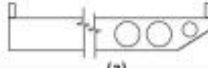$$M_{LL.IM} := \frac{M_{TD} \cdot IM + M_{ln}}{E_i} = 526.352 \; kN \cdot \frac{m}{m}$$

Equivalent distributed load:
$$q_{ss.m} := M_{LL.IM} \cdot \frac{8}{L^2} = 9.195 \; \frac{kN}{m} \cdot \frac{1}{m}$$

CASE OF CONTINUOUS BRIDGE DECK
Equivalent Strip Width for Slab-Type Bridges (4.6.2.3)

Table 4.6.2.3-1—Typical Schematic Cross-section

Supporting Components	Type of Deck	Typical Cross-Section
Cast-in-place Concrete Slab or Voided Slab	Monolithic	 (a)

Span: $\quad L := 26 \; m = 85.302 \; ft$

Width: $\quad w_b := 5.49 \; m = 18.012 \; ft$

Number of Design Lanes (3.6.1.1): $\quad \dfrac{w_b}{12 \; ft} = 1.501 \qquad N_L := 1$

Modifie span length: $\quad L_1 := min(L, 60 \; ft) = 60 \; ft$

Modified edge-to-edge width of bridge taken $\quad W_1 := min(w_b, 30 \; ft) = 5.49 \; m$

Physical edge-to-edge width of bridge $\quad W := w_b = 18.012 \; ft$

Equivalent width (in) of longitudinal strips per lane for shear and moment width one lane, i,e,, two lines of wheels, loaded:

$$E_{i1} := \left(10 + 5 \cdot \sqrt{\frac{L_1}{ft} \cdot \frac{W_1}{ft}}\right) \cdot in = 4.429 \; m$$

Equivalent width (in) of longitudinal strips per lane for shear and moment width more than one lane loaded:

Modified edge-to-edge width of bridge taken $\quad W_1 := min(w_b, 60 \; ft) = 5.49 \; m$

$$E_{i2} := \left(min\left(84 + 1.44 \cdot \sqrt{\frac{L_1}{ft} \cdot \frac{W_1}{ft}}, 12 \cdot \frac{\dfrac{W}{ft}}{N_L}\right)\right) \cdot in = 3.336 \; m$$

Equivalent width of interior strip for live load

$$E_i := min(E_{i1}, E_{i2}) = 3.336 \; m$$